ANALYTICA CHIMICA ACTA

International monthly devoted to all branches of analytical chemistry
Revue mensuelle internationale consacrée à tous les domaines de la chimie analytique
Internationale Monatsschrift für alle Gebiete der analytischen Chemie

ELSEVIER PUBLISHING COMPANY
AMSTERDAM

Anal. Chim. Acta, Vol. 54, No. 2, 189–380, April 1971
Published monthly

Publication Schedule for 1971

In the interests of rapid publication it has been found necessary to schedule 5 volumes for appearance in 1971. Since monthly publication will be maintained, this implies that 2 of the volumes will each consist of three issues, while 3 of the volumes will each consist of only 2 issues. The following provisional schedule applies:

Vol. **53**, No. **1**	January 1971	
Vol. **53**, No. **2**	February 1971	**(completing Vol. 53)**
Vol. **54**, No. **1**	March 1971	
Vol. **54**, No. **2**	April 1971	
Vol. **54**, No. **3**	May 1971	**(completing Vol. 54)**
Vol. **55**, No. **1**	June 1971	
Vol. **55**, No. **2**	July 1971	**(completing Vol. 55)**
Vol. **56**, No. **1**	August 1971	
Vol. **56**, No. **2**	September 1971	
Vol. **56**, No. **3**	October 1971	**(completing Vol. 56)**
Vol. **57**, No. **1**	November 1971	
Vol. **57**, No. **2**	December 1971	**(completing Vol. 57)**

Subscription price: $17.50 or Dfl. 63.— per volume plus postage. Total subscription price for 1971: $87.50 or Dfl. 315.— plus postage. Additional cost for copies by airmail available on request. For subscribers in the U.S.A. and Canada, 2nd class postage paid at New York, N.Y. For advertising rates apply to the publishers.

Subscriptions should be sent to:

ELSEVIER PUBLISHING COMPANY P.O. Box 211, Amsterdam, The Netherlands

GENERAL INFORMATION

Languages

Papers will be published in English, French or German.

Submission of papers

Papers should be sent to:	or to:
PROF. PHILIP W. WEST, Coates Chemical Laboratories, College of Chemistry and Physics, Louisiana State University, Baton Rouge 3, La. 70803 (U.S.A.)	DR. A. M. G. MACDONALD, Department of Chemistry, The University, P.O. Box 363 Birmingham B15 2TT (Great Britain)

Reprints

Fifty reprints will be supplied free of charge. Additional reprints (minimum 100) can be ordered at quoted prices. They must be ordered on order forms which are sent together with the proofs.

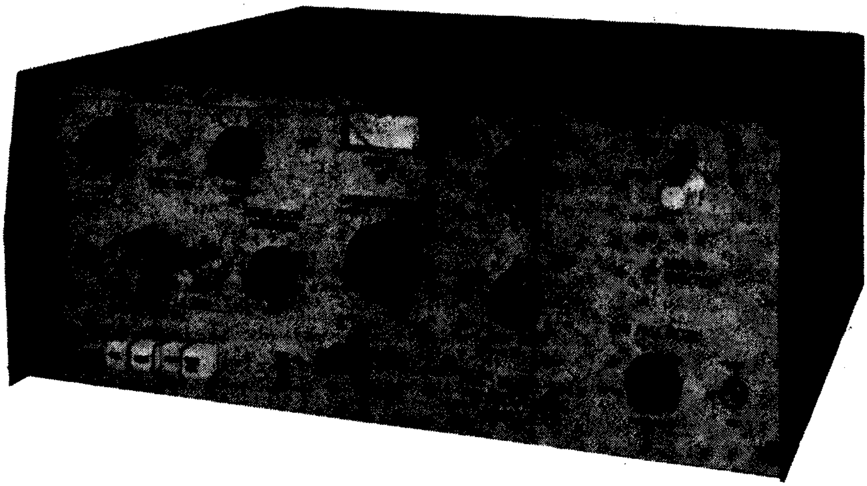

Journal of Mass Spectrometry and Ion Physics

Editors:
J. FRANZEN (Dortmund)
A. QUAYLE (Chester)
H.J. SVEC (Ames, Iowa)

the journal has 6 issues per volume and approx. two volumes appear per year. Subscription price per volume Dfl. 90.00 plus Dfl. 18.00 postage or equivalent US$25.00 plus US$5.00

Subscriptions may be placed with your usual supplier or direct with the publisher

Elsevier Publishing Company

P.O. BOX 211,
AMSTERDAM, THE NETHERLANDS

CONTENTS VOLUME 5 NO. 1/2

A new single-stage mass spectrometric method for studying charge transfer reactions (D.L. Smith, Salt Lake City, Utah, U.S.A. and L. Kevan, Detroit, Mich., U.S.A.)
General method for computing the statistics of charge amplification in particle and photon detectors used for pulse counting (L.A. Dietz, (Schenectady, N.Y., U.S.A.)
Computer analysis of low resolution mass spectra. Correction for natural abundance of ^{13}C, ^{2}H, ^{15}N, ^{17}O and ^{18}O (B. Boone, R.K. Mitchum and S.E. Scheppele Stillwater, Okla., U.S.A.)
Ion-optical properties of magnetic prisms with axially symmetric r^{-1} fields and spiral main paths (D. Ioanoviciu, Cluj, Romania)
Calculation of sector-shaped mass spectrometric analysers with curvilinear boundaries (A.A. Sysojev and G.A. Samsonov, Moscow, U.S.S.R.)
Calculation of the current - voltage characteristics of a field ion microscope (V.A. Nazarenko, Kiev, U.S.S.R.)
Ionization, attachement and ion-molecule reactions in oxygen (P.R. Kinsman and J.A. Rees, Liverpool, Great Britain)
Relative sensitivities of twenty elements in the iron matrix for spark-source mass spectrometry (J.M. McCrea, Monroeville, Pa., U.S.A.)
Ionisation and dissociation of carbonyl fluoride and trifluoromethyl hypofluorite by electron impact (J.C.J. Thynne and K.A.G. MacNeil, Edinburgh, Great Britain)
Study of ion-neutral reactions with a time-of-flight double mass spectrometer (J.F. Paulson, F. Dale and S.A. Studniarz, Bedford, Mass., U.S.A.)
Mass-spectrometric observations of uranium and plutonium monohydrides formed by ion-molecule reaction (P.E. Moreland, Jr., D.J. Rokop and C.M. Stevens, Argonne, Ill., U.S.A.)
A study of Penning ionization reactions using a single-source mass spectrometer (E.G. Jones and A.G. Harrison, Toronto, Ontario, Canada)
Ionization potentials of pentaborane(9) derivatives by electron impact and molecular orbital calculations (C.B. Murphy, Jr., Syracuse, N.Y., U.S.A. and R.E. Enrione, Cincinnati, Ohio, U.S.A.)
Electron impact excitation by the SF_6 scavenger technique. II. Benzene and ethylene (M.-J. Hubin-Franskin and J.E. Collin, Liege, Belgium)
Short Communications
Resonant charge transfer reactions in neon, argon and krypton (E.G. Jones and A.G. Harrison, Toronto, Ontario, Canada)
Comment on the rule concerning rearrangement peaks in field ionization mass spectra (H.D. Beckey, Bonn, Germany)

CONTENTS VOLUME 5 NO. 3/4

Current-voltage characteristics and angular distribution of the ions in field ionization (I.V. Goldenfeld and V.A. Nazarenko, Kiev, U.S.S.R.)
Theoretical analysis of a cylindrical time-of-flight mass spectrometer with radial ion paths (M.F. Zabielski, H.T. Diem and B.R.F. Kendall, University Park, Pa., U.S.A.)
A multiple trajectory ion beam analyzer (J.D. Stein and F.A. White, Troy, N.Y., U.S.A.)
Magnet and controller for a fast scanning mass spectrometer (G. Haertel, J.D. Morrison and J.F. Smith, Bundoora, Vic., Australia)
A proposed technique for signal multiplexing in mass spectrometry (C.J. Eckhardt and M.L. Gross, Lincoln, Nebr., U.S.A.)
The interpretation of double resonance signals in ion cyclotrom resonance mass spectrometry (G.C. Goode, A.J. Ferrer-Correia and K.R. Jennings, Sheffield, Great Britain)
On-line acquisition of ionization efficiency data (R.A.W. Johnstone, F.A. Mellon and S.D. Ward, Liverpool, Great Britain)
Multiply charged cluster ions of nitrogen (W. Henkes and G. Isenberg, Karlsruhe, Germany)
Electron impact excitation by the SF_6 scavenger technique. III. Carbon monoxide (M.-J. Hubin-Franskin and J.E. Collin, Liege, Belgium)
Hochempfindlicher Nachweis metastabiler Ein- und Zweistufenzerfälle (U. Löhle und Ch. Ottinger, Freiburg, Deutschland)
Kinetische Energie von Produktionen aus Ionen-Molekül-Reaktionen bei thermischen Energien (P.-J. Bauer und H.-J. Drewitz, Braunschweig und Berlin, Deutschland)
Cryogenic mass spectrometry of reactive fluorine-containing species. I. The mass spectra of sulfur hexafluoride, chlorine trifluoride, chlorine monofluoride, nitrosyl fluoride and tetrafluorohydrazine. II. Applications to synthesis via pyrolysis, photolysis and microwave discharge (S.S. Cristy and G. Mamantov, Knoxville, Tenn., U.S.A.)
Ionisation of tetrafluoroethylene by electron impact (J.C.J. Thynne and K.A.G. MacNeil, Edinburgh, Great Britain)
Short Communications
Determination of background-to-signal ratio in a molecular-beam sampling system (A. Tessier and W. Forst, Quebec, Canada)
Threshold ionization of acetylene by monoenergetic electron impact (F.P. Lossing, Ottawa, Canada)
Bimolecular reactions of trapped ions. II. Reactions in vinyl fluoride (N.A. McAskill and A.G. Harrison, Toronto, Ontario, Canada)
Announcements

Kodak

For a copy of the new Eastman Catalog (No. 46)

or for any of the 6,000 chemicals it contains, contact one of these laboratory supply houses. EASTMAN Organic Chemicals are stocked locally in the continental U.S.A. by:

B&A
CURTIN
FISHER
HOWE & FRENCH
NORTH-STRONG
PREISER
SARGENT-WELCH
WILL/VW&R

For EASTMAN Organic Chemicals service elsewhere:

ARGENTINA
Cientifica Comercial
Argentina S.A.C.I.
Buenos Aires

AUSTRALIA
H. B. Selby and Co., Pty., Ltd.
Adelaide Melbourne
Brisbane Perth
Hobart Sydney
Ramsay Surgical Limited
Victoria

BELGIUM
s. a. Belgolabo
Overijse

BRAZIL
Atlantida Representacoes
e Importacoes, Ltda.
Rio de Janeiro
Tennant Quimica S.A.
Sao Paulo

CANADA
Fisher Scientific Co., Ltd.
Edmonton Toronto
Montreal Vancouver
Ottawa
Sargent-Welch Scientific of
Canada, Ltd.
Vancouver Weston

DENMARK
H. Struers Chemiske
Laboratorium
Copenhagen K

FINLAND
Havulinna Oy
Helsinki

FRANCE
Touzart & Matignon
Paris

W. GERMANY
Serva International
Chemie-Handels GmbH & Co.
Heidelberg

GREECE
P. Bacacos S.A.
Athens

GUATEMALA
F. Krafka and Co., Ltd.
Emaoa

INDIA
Kodak Limited
Bombay

ISRAEL
Landseas Israel
Tel Aviv

ITALY
Prodotti Gianni, s.r.l.
Milan

JAPAN
Muromachi Kagaku Kogyo
Kaisha, Ltd.
Tokyo
Nagase and Co., Ltd.
Tokyo

KOREA
The Sang Chung
Commercial Co., Ltd.
Seoul

MEXICO
Alfonso Marhx, S.A.
Mexico 1, D. F.
Hoffmann-Pinther and
Bosworth, S.A.
Mexico 1, D. F.

NETHERLANDS
N. V. Holland-Indie
Agenturen Mij, HIAM
Amsterdam C

NEW ZEALAND
Kempthorne, Prosser & Co's.
New Zealand Drug Co., Ltd.
Wellington-Dunedin

NORWAY
Nerliens Kemisk Tekniske
Aktieselskap
Oslo

PORTUGAL
Soquimica, Sociedad de
Representacoes de Quimica
Lisbon

PUERTO RICO
Fisher Scientific Co.
Santurce

REPUBLIC OF CHINA
San Ho Instrument Co.
Taipei, Taiwan
Teh Ying Co., Ltd.
Taipei, Taiwan

REPUBLIC OF MALAWI
Baird and Tatlock
(International) Ltd.
Blantyre

REPUBLIC OF SOUTH AFRICA
Baird and Tatlock S.A., Pty.
Johannesburg

REPUBLIC OF ZAMBIA
Baird and Tatlock (Zambia) Ltd.
Ndola

SWEDEN
KEBO AB
Stockholm 6

SWITZERLAND
Dr. Bender and Dr. Hobein AG
Zurich 6

UNITED KINGDOM
Kodak Limited
Kirkby, Liverpool

VENEZUELA
Equipos Cientificos y
Educativos S.A.
Caracas

The catalog may also be obtained from:
Dept. 412L, Eastman Organic Chemicals,
Eastman Kodak Company, Rochester, N.Y. 14650, U.S.A.

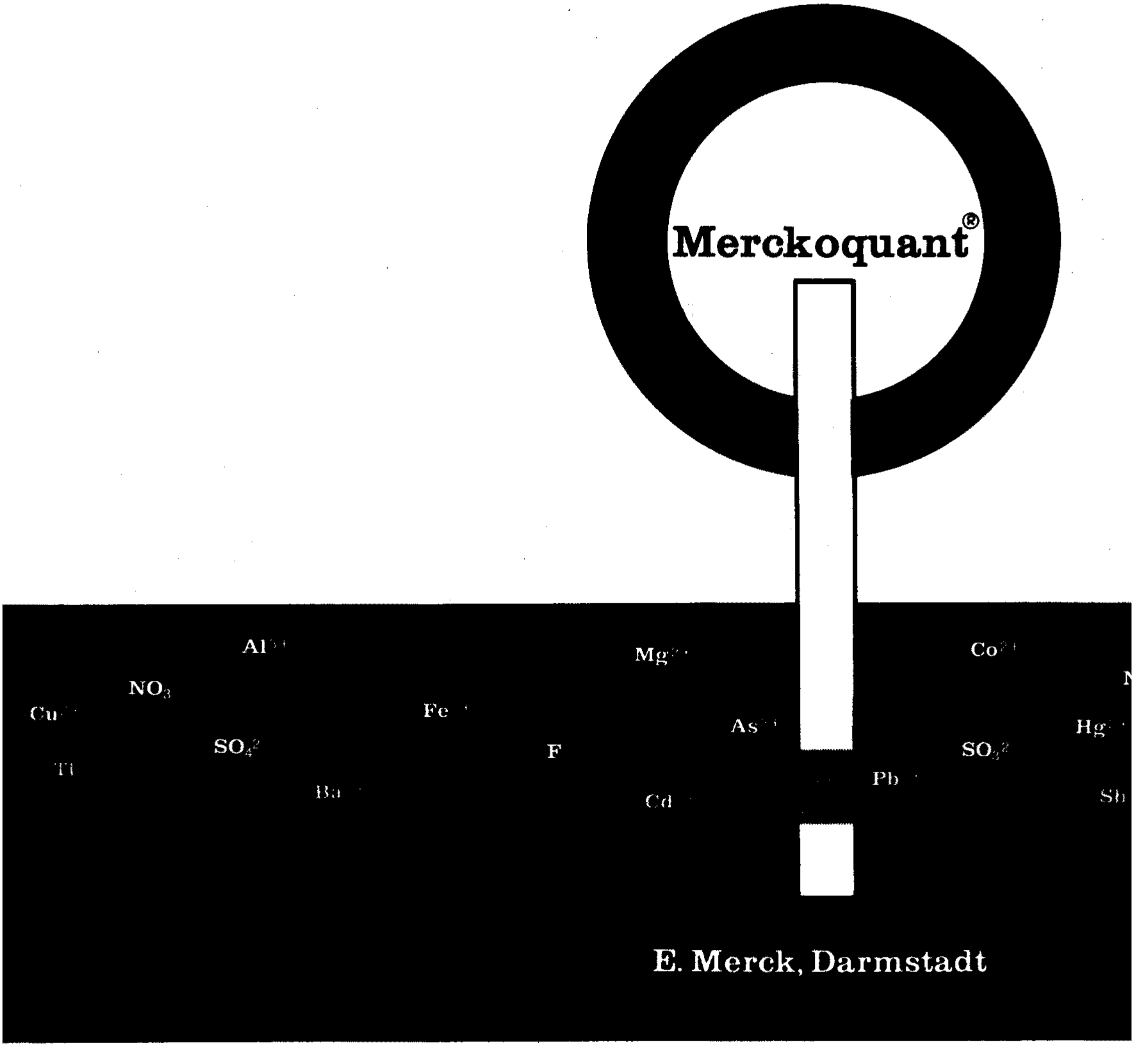
Merckoquant®
Al
NO_3
Cu
SO_4
Ti
Ba
Fe
F
Mg
Cd
As
Pb
Co
SO_4
Hg
Sb

Analytica Chimica Acta
Elsevier Publishing Company, Amsterdam
Printed in The Netherlands

SENSITIVITY OF THE FLUORIDE-SELECTIVE ELECTRODE BELOW THE MICROMOLAR RANGE

ELIZABETH W. BAUMANN

Savannah River Laboratory, E. I. du Pont de Nemours and Company, Aiken, S. C. 29801 (U.S.A.)

(Received 2nd November 1970)

The past few years have witnessed wide application of the lanthanum fluoride electrode[1] as a sensitive, highly selective device for determining free fluoride ion in solution. The lower limit of theoretical response is generally accepted[2] to be *ca.* 10^{-6} *M*, a limit considered inherent to the electrode because dissolution of the lanthanum fluoride membrane crystal contributes a fluoride background. In the work described below, it was found that the presence of cations that complex fluoride extends the range of theoretical response from one to three decades below the quoted limit.

This extended sensitivity was encountered during recent determinations of stability constants of thorium fluorides[3]. Similar capability was suggested when Lingane[4] showed the sensitivity limit is a decade lower in 0.1 *M* hydrochloric acid than in 0.1 *M* sodium nitrate. Further, Norén[5] used the electrode to determine HF in his investigation of the thorium–fluoride system in 4 *M* perchloric acid at free fluoride concentration which is estimated to be *ca.* 10^{-8} *M*. He concluded that "the fluoride membrane electrode functions properly" because he obtained fair agreement between stability quotients from electrode and solvent extraction measurements.

This paper reports work done to validate that the measured potential at these low concentrations can be theoretically interpreted as free fluoride and to inquire into the nature of the limitation in sensitivity. The response of the electrode below 10^{-6} *M* fluoride was systematically determined by comparing free fluoride concentrations measured with a calibrated electrode with those calculated from published stability quotients for zirconium–, thorium–, lanthanum–, and hydrogen–fluoride systems. Because the behavior at the limit suggests fluoride contamination in the system, the reagents and the electrode were also assessed as contributors to the fluoride background.

EXPERIMENTAL

Reagents

Reagent-grade chemicals and deionized water were used throughout. Sodium fluoride (0.1 *M*) was prepared from the oven-dried salt, and its concentration confirmed by titration with standard lanthanum nitrate solution. Solutions of zirconyl perchlorate, thorium nitrate and lanthanum nitrate were standardized by EDTA titration. The ionic strength of each metal ion solution was the same as that of the experimental system, *e.g.* 0.05 M thorium nitrate was used in the system with an ionic strength of 0.5 M.

HZO-1 (hydrous zirconium oxide; Bio-Rad Laboratories, Richmond, Calif.) was eluted with 1 M ammonia solution and washed with water to eliminate an acidic component that otherwise was leached into the solution.

Equipment

The potentials were measured to ±0.1 mV by an Orion Digital pH Meter, Model 801 (Orion Research Incorporated, Cambridge, Mass.). The fluoride-selective electrode was Orion Model 94-09, and the reference electrode was the Orion double junction reference electrode, Model 90-02, with the outer compartment filled with 3.5 M sodium chloride. A glass electrode (Beckman 40498, Beckman Instrument Company, Fullerton, Calif.) was also in the solution to ascertain acidity during each experiment.

Experimental solutions were maintained at 25° by partially immersing the polypropylene titration beaker in a constant temperature water bath. Solutions were stirred at a constant rate by a Teflon (DuPont Co.) stirring bar, rotated by a water-driven stirrer in the bath.

Procedures

Extended sensitivity experiments. In each experiment, first the calibration point was established by measuring the potential of the fluoride-selective electrode and reference electrode in 50 ml of the supporting electrolyte solution containing 5–100 μM sodium fluoride. Then portions of 0.5 M perchloric acid were added, and the stability constant of HF was verified from the measured potentials. Serial additions of the metal ion solution were made to this solution, and the potential was measured after each addition. The range of concentrations of total fluoride, metal, and hydrogen ions in the experimental solutions is given in Table I.

In the zirconium system, where the supporting electrolyte was 2 M perchloric acid, fluoride calibration was made in 2 M sodium perchlorate. The stability quotient

TABLE I

COMPOSITION OF EXPERIMENTAL SOLUTIONS IN EXTENDED SENSITIVITY MEASUREMENTS

Complexing cation	*Range of concentration (mM)*			*Ionic strength (M)*	*Supporting electrolyte*
	F_T	M_T	H_T		
Zr^{4+}	0.49–0.48	0.10–0.29	2000	2	$HClO_4$
	0.97–0.94	0.20–0.39	2000	2	$HClO_4$
Th^{4+}	0.005–0.1	0.095–2.3	1.0 –0.95	0.5	$NaClO_4$
	0.099–0.079	0.94 –8.3	0.98–0.78	0.5	$NaClO_4$
	1.08 –1.03	1.16 –11.1	1.98–1.90	0.5	$NaClO_4$
La^{3+}	0.005–0.001	0.81–61.3	0	0.5	$NaClO_4$
	0.002–0.0005	0.82–61.2	0	0.5	$NaClO_4$
H^+	0.005 –0.003	0	1.0 –1.64	0.5	$NaClO_4$
	0.005 –0.0045	0	0.20–11.3	0.5	$NaClO_4$
	0.0045–0.0038	0	13.1–178	0.5	$NaClO_4$
Standard curve	0.001–0.193	0	0	0.5	$NaClO_4$

for HF, which was not available at the ionic strength of 2 *M*, was determined from potential measurements of sodium fluoride in 2 *M* perchloric acid.

Potentials were allowed to stabilize for about 1 h during the calibration, and again after initial addition of the metal ion solution. With this procedure, the electrode responded promptly to further additions of metal ion, and reasonably stable potentials were reached within 15 min. Drift, which was toward a more positive potential, was less than 0.1 mV every 3 min at the time the reading was recorded.

Solubility measurements by neutron activation analysis. A polished single crystal of europium-doped lanthanum fluoride[1] about 8 mm in diameter and 5 mm thick, removed from the early model (white barrel) of the Orion fluoride-specific electrode, was submerged in about 25 ml of water or 100 μM thorium nitrate for several days at 25° in a continuously rotated container. At intervals, about 5 ml of solution was removed, and its lanthanum content determined by neutron activation analysis.

For this analysis, aliquots of samples and standards were evaporated on aluminum foils and were irradiated to an integrated dose of about $3 \cdot 10^{19}$ neutrons cm^{-2}. About three days after irradiation, the radioactivity was assayed by γ-spectrometry with a coaxial Ge(Li) detector and a 4096-channel pulse-height analyzer. The 487, 815, and 1596-keV γ-rays from 40.2-h ^{140}La were used for the determination.

Solubility measurements by electrode. The lanthanum fluoride single crystal used in the neutron activation experiments, a crushed crystal from the later, thin-window model of the Orion electrode, and an intact fluoride-selective electrode were maintained at room temperature for several days in separate polypropylene beakers containing 50 ml of 0.5 *M* sodium perchlorate. Each solution was slowly stirred by Teflon-covered stirring bars that remained in the solutions throughout the experiment; these were presumed to make no contribution to the fluoride content.

At intervals, the test solution was equilibrated at 25°, and the potential determined for 1 h with a fluoride-reference electrode pair that had been calibrated in 9.85 μM sodium fluoride in 0.5 *M* sodium perchlorate immediately before the measurement. During early stages of the test, when the fluoride content was low, potentials after 1 h were still drifting upward at the rate of about 0.5 mV every 5 min. The highest reading was used to calculate the fluoride content. Later when more fluoride was present, the reading was steady within the hour of measurement.

Background fluoride in reagents. The fluoride-reference electrode pair was calibrated by 9.85 μM sodium fluoride in 0.1, 0.5, or 2 *M* sodium perchlorate, whichever corresponded to the test solution. The limiting potential of the pure electrolyte was then determined by taking measurements in successive portions of solution. When the potential values were reasonably consistent after 15 min, measurement was extended to 1 h. With the first portion or two of test solution after calibration, the potential was frequently low (*e.g.* 190 mV), which suggests fluoride contamination in the system. After the test solution had been replaced several times (same beaker and stirring bar), a higher potential (*e.g.* 220 mV) was consistently obtained.

INTERPRETATION OF DATA

Experimental fluoride ion concentrations, F_{E}, were calculated from the calibration point established at the beginning of each experiment, E_{std} for a concentration

F_{std}. The Nernst equation was assumed to apply, and junction potentials and activity coefficients were assumed constant to give at 25° :

$$E_{std} - E_E = 59.16 \log (F_E/F_{std}) \tag{1}$$

The ionic strength of the initial calibration was maintained throughout the experiment.

The fluoride concentration, F_k, was calculated from the equation

$$\begin{aligned} & F_T + [F_T(k_1+\kappa) - M_T k_1 - H_T \kappa - 1] F_k \\ & \quad + [F_T(k_2 + k_1 \kappa) - M_T(2k_2 + k_1 \kappa) - (k_1 + \kappa) - H_T k_1 \kappa] F_k^2 \\ & \quad + [k_2 \kappa (F_T - H_T) - 2\, M_T k_2 \kappa - k_1 \kappa - k_2] F_k^3 - k_2 \kappa F_k^4 = 0 \end{aligned} \tag{2}$$

which results from combining the stability quotients

$$k_1 = \frac{(\mathrm{MF})}{(\mathrm{M})(\mathrm{F})} \tag{3}$$

$$k_2 = \frac{(\mathrm{MF_2})}{(\mathrm{M})(\mathrm{F})^2} \tag{4}$$

$$\kappa = \frac{(\mathrm{HF})}{(\mathrm{H})(\mathrm{F})} \tag{5}$$

and the material balance expressions

$$F_T = \mathrm{F} + (\mathrm{MF}) + 2(\mathrm{MF_2}) + (\mathrm{HF}) \tag{6}$$

$$M_T = \mathrm{M} + (\mathrm{MF}) + (\mathrm{MF_2}) \tag{7}$$

$$H_T = \mathrm{H} + (\mathrm{HF}) \tag{8}$$

where F_T, M_T, or H_T is total concentration of fluoride, metal, or hydrogen ion; F, M, or H is concentration of free fluoride, metal, or hydrogen ion; and (MF), (MF_2), or (HF) is concentration of the complex.

Only complex species that are present in significant amounts below micromolar

TABLE II

STABILITY QUOTIENTS OF FLUORIDE COMPLEXES

Complexing cation	*Electrolyte*	*Stability quotients (±% relative uncertainty)*			
		$k_1 (M^{-1})$	$k_2 (M^{-2})$	$\kappa (M^{-1})$	*Reference*
Zr^{4+}	2 M $HClO_4$	$4.04 \cdot 10^8$ (±14%)	$5.35 \cdot 10^{15}$ (±20%)	640[a] (±10%)	7
Th^{4+}	0.5 M $NaClO_4$	$3.65 \cdot 10^7$ (±12.5%)	$1.93 \cdot 10^{13}$ (±14%)	813 (±6%)	8
La^{3+}	0.5 M $NaClO_4$	480 (±7%)	—	—	9
H^+	0.5 M $NaClO_4$	—	—	813 (±6%)	10

[a] This work.

concentrations of free fluoride were taken into account. From Goldstein[6] these are MF and MF_2 for the thorium and zirconium systems. By similar reasoning, only MF need be considered in the lanthanum and hydrogen systems. In the zirconium measurements, the contribution of HF, which is not entirely negligible with 2 M perchloric acid as supporting electrolyte, was also included.

The published stability quotients for the systems investigated are given in Table II. Relative precision of each quotient was derived from the uncertainty estimated by the original investigator. With these precisions, the range of each calculated free fluoride concentration was established.

In the solubility measurements by neutron activation, the apparent free fluoride concentration in the thorium solution was calculated from eqn. (2), with F_T equal to three times the measured lanthanum concentration and H_T equal to zero.

RESULTS AND DISCUSSION

Extended sensitivity experiments

In Fig. 1, the extended sensitivity of the electrode is dramatically illustrated by a Nernst plot of normalized measured potentials and log F_k, the free fluoride concentration calculated from the stability quotients by eqn. (2). The straight line has the theoretical Nernst slope of 59.2 mV per decade of fluoride ion concentration. Each system conforms well with the theoretical line until at the lower fluoride concentrations the measured potential falls below the line, *i.e.*, the electrode indicates too much fluoride.

A more quantitative view of the difference between the measured and calculated fluoride concentrations is presented in Fig. 2. The relative error of the measured

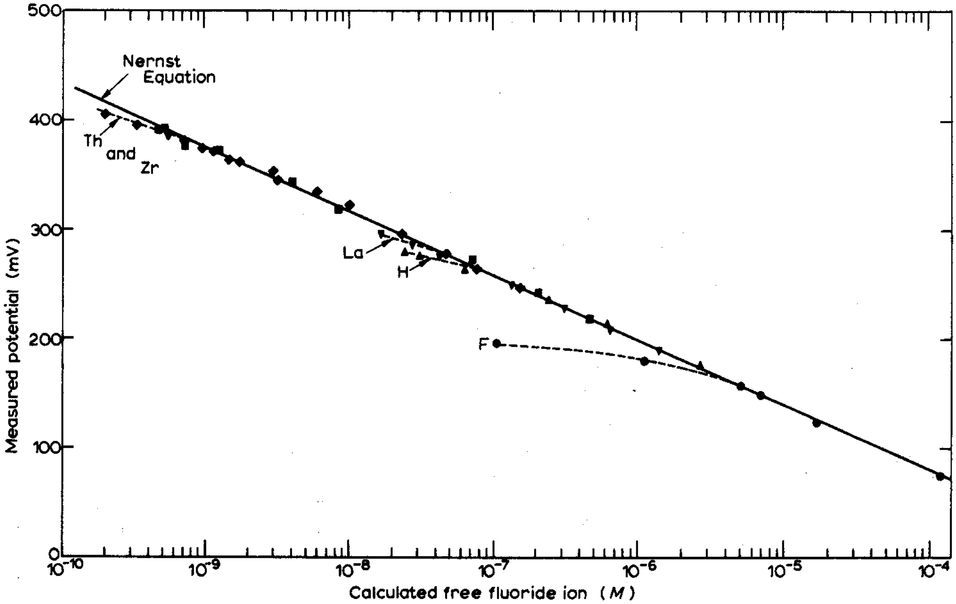

Fig. 1. Nernst plot of measured potential and calculated fluoride: (■) $NaF+HClO_4+ZrO(ClO_4)_2$, (◆) $NaF+HClO_4+Th(NO_3)_4$, (▼) $NaF+La(NO_3)_3$, (▲) $NaF+HClO_4$, (●) NaF only.

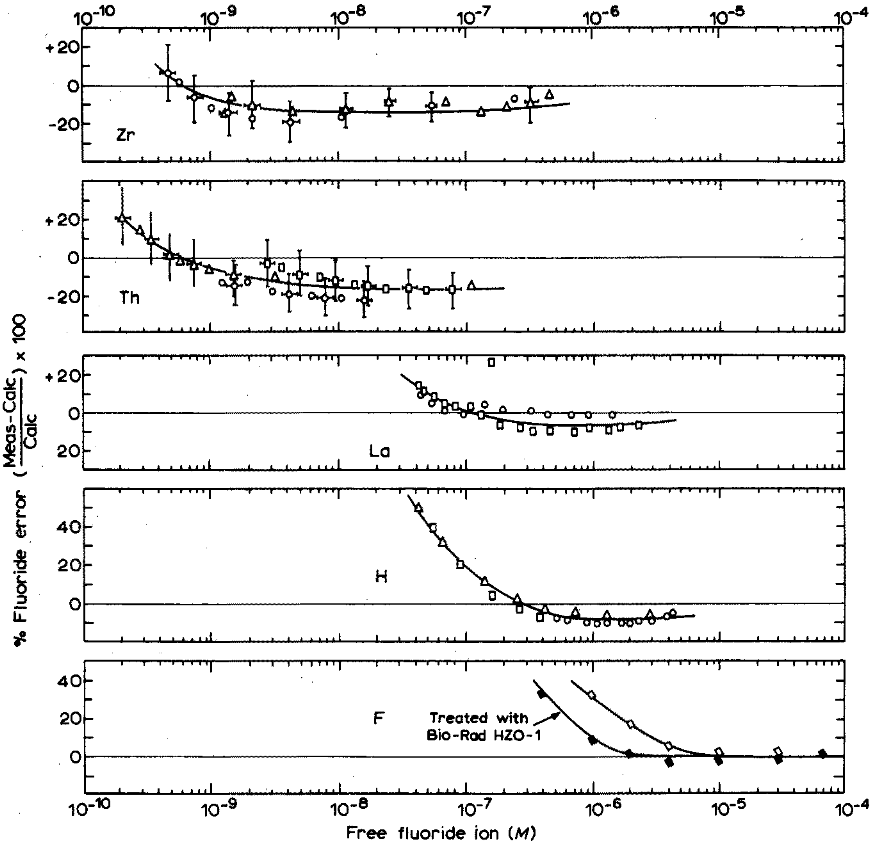

Fig. 2. Comparison of measured and calculated fluoride concentrations.

value F_E, calculated with respect to F_k, is presented as a function of F_k. Lines through the data points indicate the general trend. Flags on selected data points in the zirconium and thorium systems represent the extreme values that could be obtained from the quoted uncertainties in the published stability constants.

Relative errors at the higher concentrations of fluoride in the thorium and zirconium systems (where the electrode is presumed to be operating within its limitations) are generally less than 20%, but they have a negative bias. The magnitude of the bias is outside the range derived from the estimated uncertainties of the stability quotients. Thus, either the stability quotients determined by other methods are too low, or there is a bias in the electrode measurement at these low concentrations. The explanation for the discrepancy is not evident at this time. It is interesting to note, however, that the k_1 values of Norén[5] in the thorium fluoride system show the same trend: the stability quotient from the fluoride electrode measurements is 15% higher than that from solvent extraction measurements. The agreement between the present calculated and measured values is quite good, however, considering the low concentration levels and the distance of extrapolation from the standard.

The inversion of sensitivity limits of hydrogen and lanthanum fluoride systems

(Fig. 2) points to the lanthanum fluoride crystal as a source of fluoride background. Because $k_{HF} > k_{LaF}$, one would predict that the hydrogen system would have the lower sensitivity limit. The fact that the reverse is true suggests the source of background fluoride has been affected by the lanthanum, *i.e.*, the presence of lanthanum ion has suppressed the solubility of the lanthanum fluoride crystal.

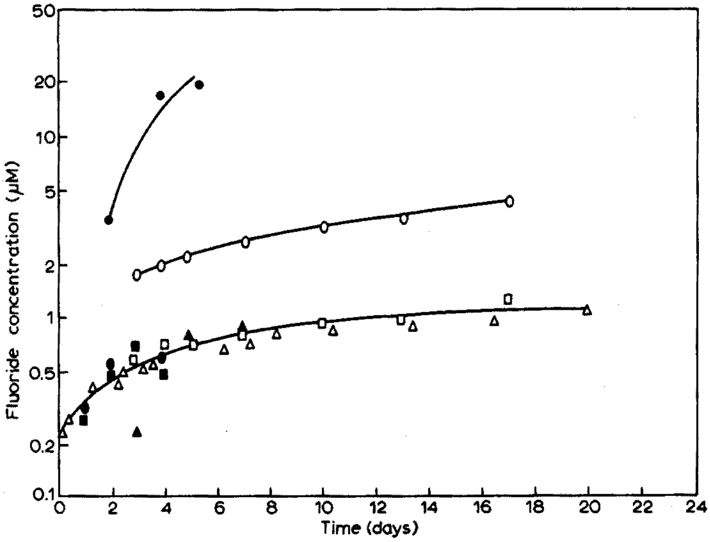

Fig. 3. Dissolution of crystalline lanthanum fluoride from Orion fluoride-selective electrodes: (■, ⬮, ▲) single crystal in deionized H_2O, (●) single crystal in 100 μM $Th(NO_3)_4$, (all black signs) La detected by neutron activation (data points represent 3 × La concentration); (△) electrode in 0.5 *M* $NaClO_4$, (□) single crystal in 0.5 *M* $NaClO_4$, (0) crushed crystal in 0.5 *M* $NaClO_4$, (all open signs) F^- concentration measured with F electrode.

Solubility of lanthanum fluoride

Contribution of fluoride to the bulk solution from progressive dissolution of lanthanum fluoride crystals taken from fluoride-selective electrodes is shown in Fig. 3. Dissolution experiments in pure water and in thorium nitrate solution, with dissolved lanthanum determined by neutron activation analysis, provide a measurement independent of electrode response or fluoride background. However, activation analyses could not conveniently be performed in the 0.5 *M* sodium perchlorate supporting electrolyte of the extended sensitivity experiments; therefore, the apparent contribution of fluoride in this medium was measured by a calibrated fluoride electrode. Values of solubility monitored by activation analysis and electrode measurements agree well. Exact agreement would not be expected because solubility is affected by the presence of other solutes.

The fluoride contributions in 0.5 *M* sodium perchlorate from the electrode and from the crystal were similar, which rules out leakage of fluoride through the membrane or its seal as a source of fluoride. Dissolution of the crushed crystalline lanthanum fluoride was much more rapid than that of the single crystal.

The presence of 100 μM thorium nitrate increases the amount and the rate of dissolution of the single crystal. Most of the fluoride released is complexed by the thorium so that the corresponding free fluoride concentration is very low; for example, the last point in Fig. 3, which indicates 19 μM total fluoride, corresponds to a calculated free fluoride concentration of only 0.00053 μM.

Neutron activation measurements show that fluoride contribution to the bulk solution from the electrode would account satisfactorily for the background fluoride the electrode seems to indicate. The limiting solubilities found for the single crystals produce a calculated solubility product of the order of 10^{-24}, the maximum value consistent with electrode response as estimated by Butler[2]. This solubility product is somewhat higher than the initial estimate of 10^{-28} made by Frant and Ross[1], but is considerably lower than the 10^{-19} measured by Lingane[4] for freshly precipitated lanthanum fluoride.

Background fluoride in reagents

The limiting concentration of fluoride indicated by the calibrated electrode in 0.1, 0.5, and 2.0 M sodium perchlorate was determined to assess fluoride contribution from the reagent. Precision of measurements was poor, but the apparent fluoride indicated by the potential was 0.1 to 0.4 μM, with no clear relationship to the concentration of the salt. Thus the reagent salt was evidently not a prime fluoride contributor. The solvent, deionized water, is regarded as an unlikely source of fluoride.

In Fig. 2, the curve for fluoride in 0.5 M sodium perchlorate that was treated with hydrous zirconium oxide shows a lower limit of sensitivity than in the untreated sodium perchlorate. This could mean the treatment removed fluoride but it could also mean that the solution became slightly contaminated with zirconium. The analytical methods did not suffice to confirm possible zirconium contamination, which would be $<10^{-7}$ M.

The help of Dr. S. F. Peterson, who performed the neutron activation analyses, is gratefully acknowledged.

SUMMARY

In the presence of fluoride-complexing cations, the lanthanum fluoride electrode responds theoretically to free fluoride one to three decades below 10^{-6} M, the accepted limit in non-complexing solutions. Experimentally determined fluoride concentrations were compared with values calculated from literature stability quotients for the thorium, zirconium, lanthanum, and hydrogen systems. The limit suggests the presence of background fluoride. Dissolution of the lanthanum fluoride crystal, determined by neutron activation analyses and electrode measurements, could supply the required level of background fluoride in bulk solution. Contribution of fluoride from reagents was not significant.

RÉSUMÉ

L'électrode au fluorure de lanthane, en présence de cations complexant les fluorures, répond théoriquement au fluorure libre, une à trois décades en dessous de 10^{-6} M. Les concentrations en fluorure, déterminées expérimentalement, sont comparées avec les valeurs calculées à partir des coefficients de stabilité trouvés dans la littérature pour les systèmes thorium, zirconium, lanthane et hydrogène.

ZUSAMMENFASSUNG

In Gegenwart von Kationen, die mit Fluorid Komplexe bilden, spricht die Lanthanfluorid-Elektrode theoretisch auf freies Fluorid ein bis drei Dekaden unterhalb 10^{-6} *M* an, der in nichtkomplexierenden Lösungen angenommenen Grenze. Experimentell bestimmte Fluoridkonzentrationen wurden mit Werten verglichen, die aus Stabilitätsquotienten der Literatur für die Systeme mit Thorium, Zirkonium, Lanthan und Wasserstoff berechnet worden waren. Die Grenze deutet auf das Vorliegen eines Fluorid-Untergrundes hin. Die Auflösung des Lanthanfluoridkristalls, die durch Neutronenaktivierungsanalysen und durch Elektrodenmessungen bestimmt worden war, konnte die geforderte Höhe des Fluoriduntergrundes in der ganzen Lösung liefern. Der Fluoridbeitrag der Reagenzien war unbedeutend.

REFERENCES

1 M. S. Frant and J. W. Ross, Jr., *Science*, 154 (1966) 1553.
2 R. A. Durst (Editor), *Ion Selective Electrodes*, National Bureau of Standards Special Publication No. 314, November, 1969.
3 E. W. Baumann, *J. Inorg. Nucl. Chem.*, 32 (1970) 3823.
4 J. J. Lingane, *Anal. Chem.*, 40 (1968) 935.
5 B. Norén, *Acta Chem. Scand.*, 23 (1969) 931.
6 G. Goldstein, *Anal. Chem.*, 36 (1964) 243.
7 R. E. Connick and W. H. McVey, *J. Amer. Chem. Soc.*, 71 (1949) 3182.
8 H. W. Dodgen and G. K. Rollefson, *J. Amer. Chem. Soc.*, 71 (1949) 2600.
9 J. W. Kury, Z. Z. Hugus, Jr. and W. M. Latimer, *UCRL-3678*, 1957.
10 R. E. Connick, L. G. Hepler, Z. Z. Hugus Jr., J. W. Kury, W. M. Latimer and Maak-Sang Tsao, *J. Amer. Chem. Soc.*, 78 (1956) 1827.

Analytica Chimica Acta
Elsevier Publishing Company, Amsterdam
Printed in The Netherlands

POTENTIOMETRIC DETERMINATION OF ACIDS AND BASES WITH A SILICONE RUBBER-BASED GRAPHITE ELECTRODE AS INDICATING ELECTRODE

ÉVA SZEPESVÁRY* AND ERNÖ PUNGOR
Institute for General and Analytical Chemistry, Technical University, Budapest (Hungary)

(Received 9th November 1970)

The determination of acids and bases by automatic titrations, both in aqueous and in non-aqueous solutions is still rather limited, for certain difficulties are encountered in constructing an appropriate potentiometric measuring cell. Glass electrodes, which have a high input resistance in aqueous solutions, could advantageously be applied as sensors of appropriate time-constants, but in the titration the dynamic behaviour of the measuring cell must also be considered. Because of the rather large time-constant, the rate of the titration must be decreased, and because of the high input resistance, a simple potentiometer cannot be utilised. In non-aqueous solutions, a further difficulty is encountered in establishing the appropriate surface structure of a glass electrode.

It is known that for the end-point detection of acid–base titrations, any electrode showing a hydrogen-ion function is appropriate, and that a theoretical response of the electrode to changes in pH (59 mV/pH) is unnecessary.

In addition to glass electrodes, hydrogen, quinhydrone or metal–metal oxide electrodes can also be used as acid–base indicator electrodes. Furthermore, molybdenum, tungsten and bright platinum electrodes, which behave as an oxygen-gas electrode, can also be applied for this purpose. In the presence of irreversible redox systems such as MnO_4^-/Mn^{2+}, $Cr_2O_7^{2-}/Cr^{3+}$, etc., owing to the pH-dependence of the redox equilibrium, the platinum electrode shows an advantageous pH-function.

In recent years, the analytical applicability of graphite electrodes has been widely studied. In 1960 Berčik[1] was the first to use wax-impregnated graphite electrodes as indicator electrodes in potentiometric acid–base titrations. This type of electrode was earlier suggested for voltammetric purposes by Lord and Rogers[2] and by Gaylor *et al.*[3,4]. Before use, the electrodes were soaked in distilled water. By measuring the correlation between electrode potential and pH in buffer solutions of different pH values, it was found, that the electrode potential changed with pH linearly. Berčik found that the potential jump at the end-point was about 70 mV when 0.1 *M* sodium hydroxide was titrated with 0.05 *M* sulphuric acid solution. The change was even higher when so-called "activated" electrodes were used; these electrodes were pretreated by immersion for several minutes in an aqueous solution of a suitable oxidant,

---

* Department of Analytical Chemistry, University of Chemical Industries, Veszprém.

e.g. potassium bromate, dichromate or permanganate. Thus when permanganate was used, the potential jump was nearly ten times higher than in the previous case. The potential of the graphite electrode, activated with permanganate, also changed linearly with the pH, *i.e.* by about 70 mV per pH unit. According to Berčik, in the course of the activation process, a quinone–hydroquinone redox system is formed from the coal on the surface of the graphite, the redox potential of which depends on the pH.

Berčik and Hladky[5] have titrated a series of strong and weak acids and bases with the help of activated graphite indicator electrodes. Graphite electrodes activated with potassium permanganate dissolved in sulphuric acid, could be used for acid–base titrations, both in aqueous and non-aqueous solutions: the electrode was found to be suitable as an indicator electrode in anhydrous acetic acid medium[6]. Activated graphite electrodes have been used for acid–base titrations by Berčik *et al.*[7,8] in methyl ethyl ketone, and by Berčik and Hladky[9] in anhydrous pyridine medium.

Miller[10] used pyrolytic graphite[11] as the indicator electrode for potentiometric acid–base titrations. The potential of the electrode measured in solutions of different pH value was found to change linearly with pH; this change was about 50 mV per pH unit in the pH ranges 1–4 and 11–13. With the pyrolytic graphite indicator electrode in titrations of 0.1 N hydrochloric or sulphuric acid and sodium hydroxide solutions, potential jumps of about 100 mV were obtained at the end-point. The electrodes could also be applied in non-aqueous media.

Doležal and Štulik[12] carried out acid–base titrations with the so-called glassy-carbon[13] as indicator electrode. The electrode potential changed by about 20 mV per pH unit. In the titration of 0.1 M sodium hydroxide with 0.1 M hydrochloric acid a potential jump of about 180 mV was found at the equivalence point. The presence of anionic oxidants was again found to increase the magnitude of the potential jump. According to Doležal and Štulik, the electrode behaves as an oxygen electrode; this was confirmed by the fact that when oxygen in the test solution was removed by nitrogen gas, the electrode showed no pH dependence.

The silicone rubber-based graphite electrode[14] is of similar nature to the above-mentioned electrodes. Among its advantageous features, it is important to note, with respect to voltammetry, that the end-groups of the silicone rubber cover the distance existing in the direction of the C-axis in the graphite crystals; consequently, this type of electrode does not show any "memory" effect. It seemed worthwhile to examine this electrode to establish if it could be used for the detection of the hydrogen ion concentration analogously to the other graphite electrodes. In this paper, the experimental results obtained are described.

EXPERIMENTAL

Instrumentation and electrodes

An expanded-scale pH meter (Model OP 205 Radelkis, Budapest) was used for all measurements. A silicone rubber-based graphite electrode[14] was used as indicator electrode; a saturated calomel electrode, and, for certain measurements, a silicone rubber-based chloride-selective electrode were used as reference electrodes. The sensor part of the indicator electrode was a membrane layer with a surface area of 0.25 cm^2, which consisted of graphite embedded in silicone rubber; this was glued to one end of a glass tube. In some tests, so-called microelectrodes were also used; the graphite-filled rubber layer was glued to glass tubes of 0.5–1.0 mm diameter. Mercury was poured into the glass tubes to ensure electrical contact in all cases. All the chemicals used were of *pro analysi* grade.

pH Sensitivity of electrodes

First the pH sensitivity of the silicone rubber-based graphite electrode was examined. For these studies in aqueous media, calibration curves were obtained from buffer solutions of different pH values, and titration curves of strong acids and bases as well as of weak acids were recorded. With due consideration of the concentrations of the solutions, the titration curves were evaluated on the basis of the correlation between the equilibrium pH values calculated for every point of the titration curve and the mV values measured.

The equilibrium pH values were calculated by means of a computer, the dissociation constants of acids, bases, salts and water being used with a program based on exact concentration values.

Evaluation of both calibration and titration curves showed that the pH–mV correlation of these graphite electrodes has an average slope of 30 mV. This value is in good agreement with literature data.

The situation changed when the electrode was placed before measurement in an oxidizing medium. In such cases – in agreement with earlier data – the electrode became more sensitive ("activated"), showing a higher potential change per pH unit. Depending on the oxidant used, this behaviour was maintained for varying times.

The activation was carried out by soaking the electrodes in a solution of an oxidant for several minutes. Hydrogen peroxide, cerium(IV) sulphate, potassium dichromate, and acidic potassium permanganate solutions of different concentrations were used. The treatment with cerium(IV) did not alter the pH dependence of the electrode, whereas treatment with hydrogen peroxide and potassium dichromate increased the pH sensitivity by 5–10 mV/pH and 20–25 mV/pH, respectively.

The slope of the pH *vs.* mV function increased significantly when the activation was carried out with potassium permanganate solution, and the electrode retained its activity for a longer period of time than when other oxidants were used. When the electrode was immersed in 0.1 *N* permanganate solution for 1–3 min before use, the electrode potential changed, giving an average value of 60 mV/pH unit. The concentration of the sulphuric acid used in the activation had no significant effect on the slopes obtained, but the permanganate concentration was of importance. When the activation of the electrode was done with 1 *N* potassium permanganate solution in 1 *N* sulphuric acid, even a slope of 70–90 mV/pH could be obtained. The results obtained are shown in Fig. 1.

Since the electrode is pH-sensitive and the electrode potential becomes constant quickly (in 2–3 sec), it was hoped that it could be used as indicator electrode to acid–base titrations.

TITRATION CURVES FOR ACIDS AND BASES

Various strong acids and bases as well as weak acids were titrated in different concentrations. The potentiometric determinations were carried out with both non-activated and activated graphite electrodes. For calibrations, measurements were also

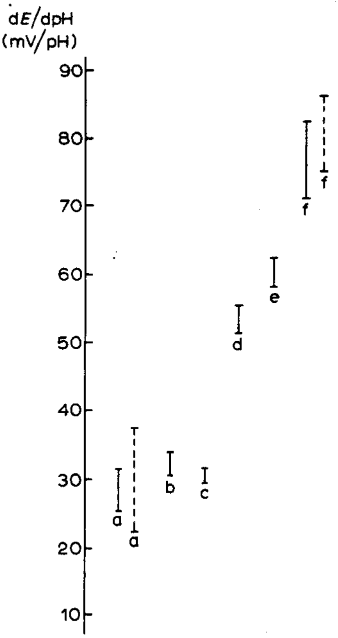

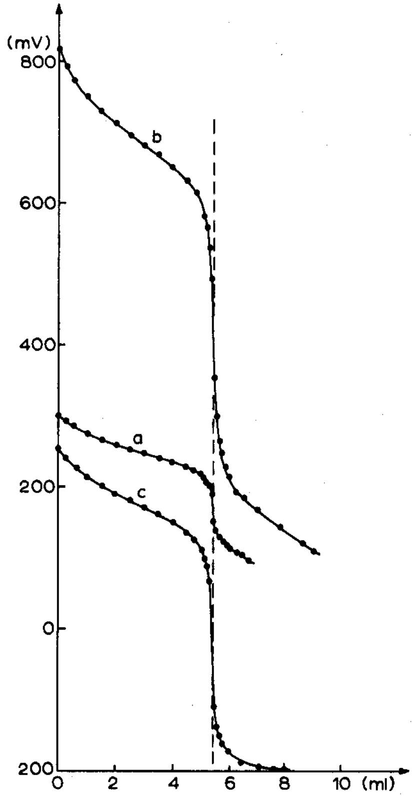

Fig. 1. pH sensitivity of graphite electrodes activated with different oxidants. (——) Values measured in buffer solutions; (------) values obtained from titrations. Oxidants: (a) no oxidant; (b) H_2O_2; (c) Ce(IV); (d) $K_2Cr_2O_7$; (e) 0.1 *N* $KMnO_4$; (f) 1 *N* $KMnO_4$.

Fig. 2. Titration of 0.102 *N* acetic acid with 0.094 *N* sodium hydroxide. Indicator electrode used: (a) non-activated graphite; (b) activated graphite (treated with 1 *N* $KMnO_4$); (c) glass electrode.

made with glass electrodes, and classical titrations were also applied. It was established that the end-point of the titrations was correctly indicated by both the non-activated and activated electrodes.

Figure 2 shows the titration curves of acetic acid with sodium hydroxide, for activated and non-activated graphite indicator electrodes, as well as a glass electrode.

As was mentioned earlier, activation with permanganate is advantageous, because several titrations can be carried out without further activation, although the magnitude of the potential jump (pH sensitivity of the electrode) decreases from titration to titration. Figure 3 shows a case when the electrode had been activated only before the first titration. The measurements were repeated after 4, 5, 20 and 30 days, the electrode being stored in distilled water between titrations. As can be seen, the pH sensitivity of the electrode continuously decreased, until the pH/mV slope reached that of a non-activated electrode.

Virtually superimposable titration curves were obtained, when the electrode was soaked in permanganate solution of the same concentration for a short time be-

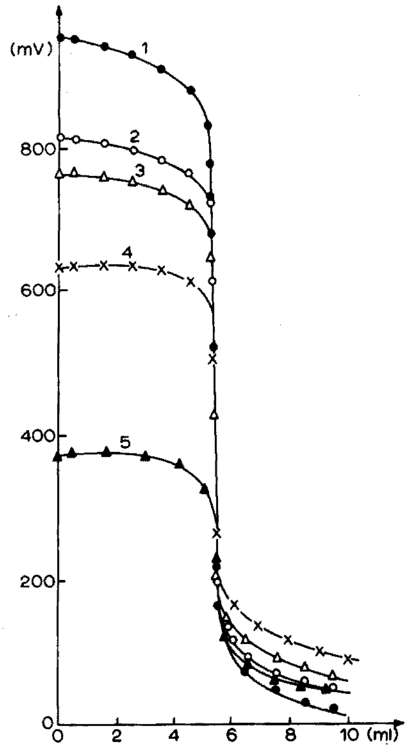

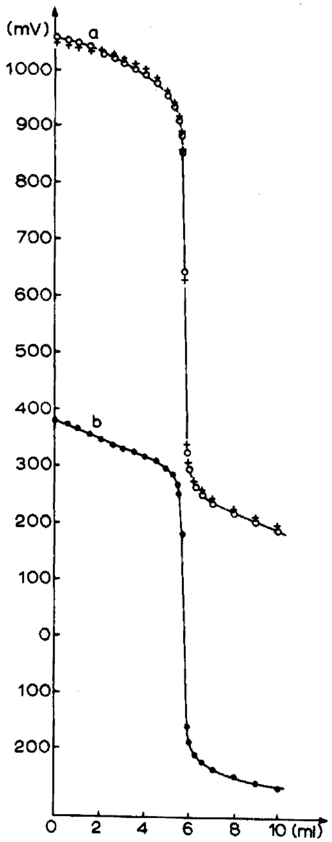

Fig. 3. Titration of 0.102 N hydrochloric acid with 0.095 N sodium hydroxide. (1) Electrode activated with N $KMnO_4$–N H_2SO_4 before use. The titration was then repeated without further activation after 4 days (2), 5 days (3), 20 days (4), and 30 days (5).

Fig. 4. Titration of 0.112 N hydrochloric acid with 0.097 N sodium hydroxide. Indicator electrode used: (a) activated graphite; (b) glass electrode. Repeat titrations with the graphite electrode are indicated by + and ○.

fore each titration. Figure 4 shows the titration curves of hydrochloric acid twice repeated with an electrode which was activated by 1 N permanganate in N sulphuric acid solution before every measurement.

Micro-titrations

Experiments were also carried out to examine the behaviour of micrographite electrodes of small surface area (1–3 mm^2). On decreasing the electrode surface, the reproducibility of the titration curves increased, and under exactly the same conditions of pretreatment, titration curves overlapping one another were obtained.

With the measuring sensor of small surface area, titrations were carried out in a maximum of 2 ml of solution and the smallest amount of substance determined was 10^{-5} mol. Figure 5 shows the titration of 1 ml of 10^{-3} N sodium hydroxide with 10^{-2} N perchloric acid.

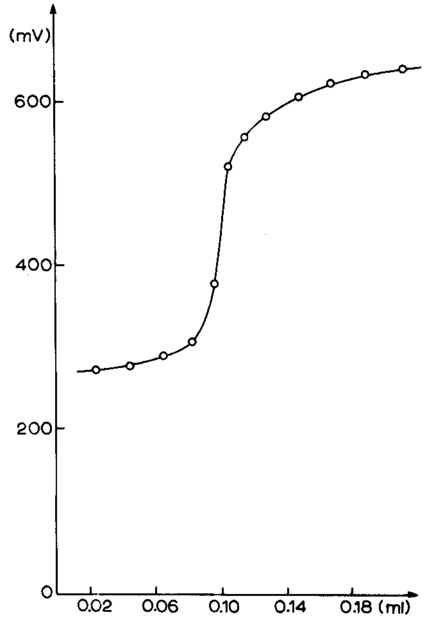

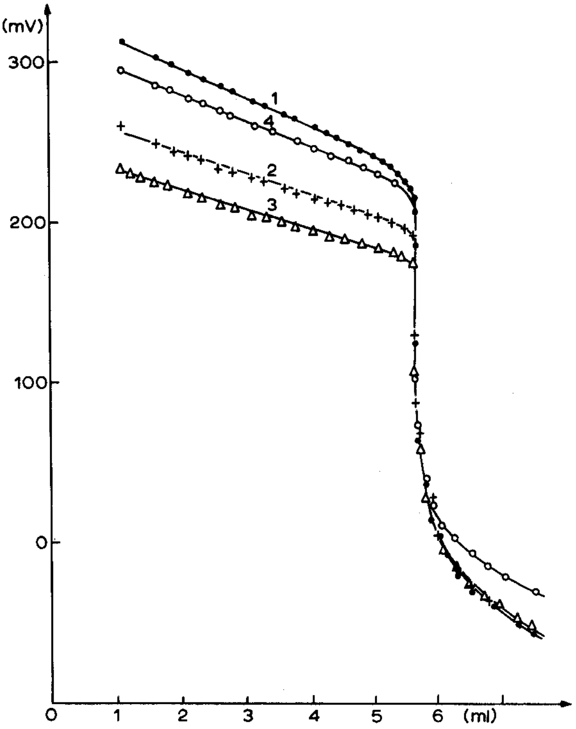

Fig. 5. Titration of $0.9 \cdot 10^{-3}$ N sodium hydroxide with $1.1 \cdot 10^{-2}$ N perchloric acid. Indicator electrode, activated micrographite.

Fig. 6. Titration of 0.1 N benzoic acid with 0.089 N sodium hydroxide in acetone. Indicator electrode, non-activated graphite.

In order to decrease further the size of the measuring cell, a silicone rubber-based chloride-selective electrode of similarly small electrode surface (1–3 mm^2) was applied as reference electrode, in solutions of high chloride ion concentration. In this way, the diffusion potential could be eliminated even when different solvents were used. This measuring cell with the small electrodes could be used even for solutions with volumes less than 1 ml. Table I summarizes the results obtained in titrations under these conditions.

Titrations in non-aqueous media

The silicone rubber-based graphite electrodes also appeared to be useful as indicator electrodes in acid–base titrations in non-aqueous media.

Figure 6 shows the potentiometric titration curves obtained for benzoic acid in acetone. A non-activated silicone rubber-based graphite indicator electrode was used. As can be seen, repeated determinations showed the end-point of the titration to be readily reproducible, although the potential of the indicator electrode shifted. However, when the electrode was soaked between two titrations for a period of time in water exposed to the atmosphere, then the electrode took up nearly the original potential value (curve 4, Fig. 6).

Figure 7 shows the titration curves for benzoic acid and hydrochloric acid in the presence of each other. The measurement was carried out in acetone with a non-activated graphite indicator electrode.

TABLE I

RESULTS OF TITRATIONS WITH MICRO-ELECTRODES

(Indicator electrode: silicone rubber-based graphite electrode. Reference electrode: chloride-selective membrane electrode)

Solution titrated	*Titrant*	*Consumed (ml)*		*Relative error (%)*[a]
		Calcd.	*Found*	
0.1 *N* H_2SO_4	0.1 *N* NaOH	2.32	2.34	+0.86
		2.32	2.34	+0.86
		4.20	4.23	+0.71
		4.20	4.22	+0.47
		4.20	4.23	+0.71
0.01 *N* H_2SO_4	0.01 *N* NaOH	2.169	2.156	−0.60
0.1 *N* CH_3COOH	0.1 *N* NaOH	2.15	2.15	0.0
		2.15	2.15	0.0
0.01 *N* CH_3COOH	0.01 *N* NaOH	2.149	2.152	+0.14
		2.149	2.154	+0.23
		2.149	2.151	+0.09
0.1 *N* citric acid	0.1 *N* NaOH	2.149	2.185	+1.68
		2.149	2.147	−0.09
0.01 *N* citric acid	0.01 *N* NaOH	2.238	2.220	−0.80
		2.238	2.235	−0.13
0.1 *N* oxalic acid	0.1 *N* NaOH	1.544	1.522	−1.41
		1.544	1.540	−0.26
0.01 *N* oxalic acid	0.01 *N* NaOH	1.540	1.564	+1.56
		1.540	1.572	+2.10
0.1 *N* tartaric acid	0.1 *N* NaOH	2.160	2.145	−0.70
0.1 *N* benzoic acid (in abs. methanol)	0.1 *N* KOH (in abs. methanol)	2.088	2.151	+3.02
		2.088	2.080	−0.38

[a] From the calculated value.

Figure 8 shows the potentiometric titration curves of 10^{-2} *N* sulphuric acid. The solution to be titrated was only 1 ml and its methanol content was varied between 0 and 90% (v/v); a 0.1 *N* potassium hydroxide solution in absolute methanol served as titrant, and a micrographite electrode, which had been activated before every measurement by soaking for 1 min in 1 *N* permanganate solution containing 1 *N* sulphuric acid, served as indicator electrode.

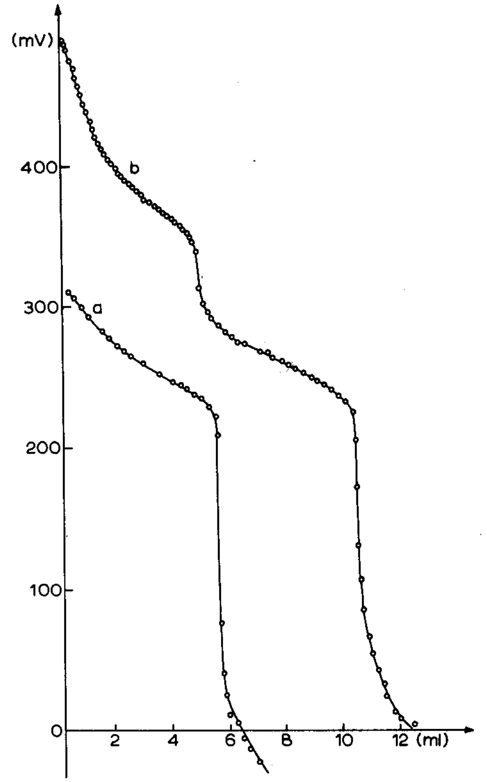

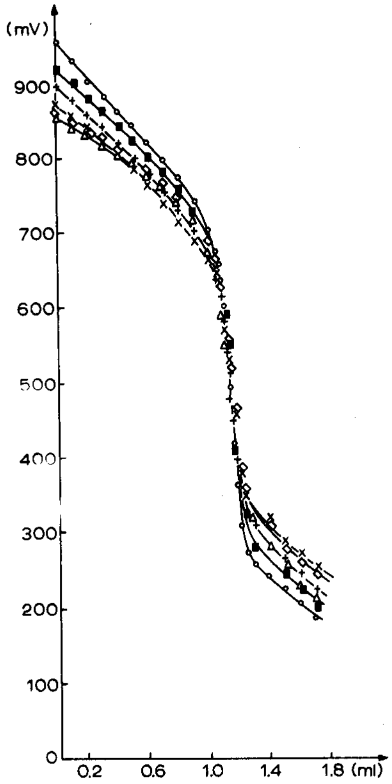

Fig. 7. (a) Titration of benzoic acid with sodium hydroxide in acetone; (b) titration of hydrochloric acid and benzoic acid in the presence of each other with sodium hydroxide in acetone medium. Indicator electrode, non-activated graphite.

Fig. 8. Titration of 0.0128 *N* sulphuric acid with 0.1123 *N* potassium hydroxide in absolute methanol, in the presence of different percentages (by volume) of methanol. (○) 0%, (■) 20%, (+) 40%, (×) 60%, (◇) 80%, (△) 90%. Indicator electrode, activated micrographite.

DISCUSSION

The experimental results prove that silicone rubber-based graphite electrodes whether activated or non-activated, are pH-sensitive. The potential of the non-activated electrode changes by an average of 30 mV per pH unit. If the electrode is soaked for a few minutes before the measurement in a suitable oxidant solution, the pH sensitivity of the electrode is increased. For activation, aqueous solutions of hydrogen peroxide, cerium(IV) sulphate, potassium dichromate and potassium permanganate were tested, and acidic permanganate solutions proved to be the most effective. For permanganate-activated electrodes, the electrode potential changed by 70–90 mV per pH unit, *i.e.* the mV change was about 20–25% greater than that obtained with the glass electrode or any other conventional pH-sensitive electrode.

The electrodes, both activated and non-activated, were used as indicator electrodes for potentiometric acid–base titrations. Various strong acids and bases as well as weak acids were titrated in different concentrations; measurements were made with the same accuracy as for glass electrodes, but the potential jump at the end-point of the titration was greater when the activated graphite indicator electrodes were used. This effect is particularly favourable for the titration of weak acids and bases.

This type of graphite electrode can be used in aqueous or non-aqueous solutions. The small resistance, ease of handling and durability, are further advantages of the electrode. When non-aqueous solvents are used—in contrast to glass electrodes—there is no need for pretreatment of the electrodes.

A measuring cell consisting of a silicone rubber-based graphite indicator electrode of small surface area and a silicone rubber-based chloride-selective reference electrode of similar size, can be applied also to micro-scale acid–base titrations. If the measuring cell must have a small input resistance, then the silicone rubber-based graphite electrode must be combined with an appropriate calomel or other electrode of the second kind.

In the course of these studies, some interpretations for the mechanism of the electrode reaction have been found, and these will be reported at a later date after further investigations.

SUMMARY

Silicone rubber-based graphite electrodes have been used as indicator electrodes in potentiometric acid–base titrations. The pH sensitivity of the electrodes is increased by pretreatment with various oxidants, acidic permanganate solutions being most suitable. When electrodes "activated" in this way are used, the potential jumps at the end-point are greater than those obtained with conventional electrodes, which is favourable for the titration of weak acids and bases. These electrodes can be used in aqueous or non-aqueous media. A measuring cell consisting of a silicone rubber-based graphite electrode of small surface area and an appropriate silicone rubber-based ion-selective reference electrode, is suitable for acid–base titrations in volumes less than 1 ml.

RÉSUMÉ

On propose des électrodes silicone–graphite comme électrodes indicatrices dans des titrages potentiométriques acide–base. Leur sensibilité au pH est accrue par prétraitement avec divers oxydants; des solutions acides de permanganate conviennent le mieux. Ces électrodes peuvent être utilisées en milieu aqueux ou non aqueux, et permettent des titrages avec des volumes inférieurs à 1 ml.

ZUSAMMENFASSUNG

Graphit-Elektroden auf Silikonkautschuk-Basis wurden als Indikatorelektroden bei potentiometrischen Säure–Base-Titrationen verwendet. Die pH-Empfindlichkeit der Elektroden wird durch Vorbehandlung mit verschiedenen Oxidationsmitteln grösser, wobei saure Permanganat-Lösungen sich am besten eignen. Bei so "aktivierten" Elektroden sind die Potentialsprünge am Endpunkt grösser als jene bei konventionellen Elektroden, was für die Titration schwacher Säuren und Basen

besonders günstig ist. Diese Elektroden können in wässrigen oder nichtwässrigen Lösungen angewendet werden. Eine Messzelle, die aus einer Graphitelektrode mit kleinem Oberflächenbereich und aus einer besonderen ionenselektiven Vergleichselektrode ebenfalls auf Silikonkautschuk-Basis besteht, eignet sich für Säure–Base-Titrationen in Volumina kleiner als 1 ml.

REFERENCES

1 J. Berčik, *Chem. Zvesti*, 14 (1960) 372.
2 S. S. Lord and L. B. Rogers, *Anal. Chem.*, 26 (1954) 284.
3 V. F. Gaylor, A. L. Conrad and J. H. Landerl, *Anal. Chem.*, 29 (1957) 224.
4 V. F. Gaylor, A. L. Conrad and J. H. Landerl, *Anal. Chem.*, 29 (1957) 228.
5 J. Berčik and Z. Hladky, *Proc. Anal. Chem. Conf. Budapest*, 1966, p. 99.
6 J. Berčik and Z. Hladky, *Chem. Zvesti*, 17 (1963) 95.
7 J. Berčik and M. Čakrt, *Chem. Zvesti*, 22 (1968) 755.
8 J. Berčik, M. Čakrt and K. Derzsiová, *Chem. Zvesti*, 22 (1968) 761.
9 J. Berčik and Z. Hladky, *Chem. Zvesti*, in press.
10 F. J. Miller, *Anal. Chem.*, 35 (1963) 929.
11 F. J. Miller and H. E. Zittel, *Anal. Chem.*, 35 (1963) 1866.
12 J. Doležal and K. Štulik, *J. Electroanal. Chem.*, 17 (1968) 87.
13 H. E. Zittel and F. J. Miller, *Anal. Chem.*, 37 (1965) 200.
14 E. Pungor and É. Szepesváry, *Anal. Chim. Acta*, 43 (1968) 289.

Analytica Chimica Acta
Elsevier Publishing Company, Amsterdam
Printed in The Netherlands

THE STANDARD POTENTIAL OF HETEROGENEOUS PRECIPITATE-BASED MEMBRANE ELECTRODES

A. MARTON AND E. PUNGOR*
Department of Analytical Chemistry, University of Chemical Industries, Veszprém (Hungary)

(Received 25th November 1970)

Research on ion-selective silicone-rubber membrane electrodes has been directed mainly to examinations of reversible electrode function[1], selectivity[2,6], response time[3] and various applications of ion-selective electrodes[4]. However, a full understanding of the behaviour of these electrodes also requires a detailed study of the standard electrode potential. In this connection, the thermodynamic basis of the reactions on which the electrode activity depends, needed further investigation.

Thus, the values of the standard electrode potentials of the silver iodide-based membrane electrodes and their dependence on temperature have been examined; the results are summarized in this paper.

EXPERIMENTAL

For all the measurements, unless otherwise specified, the silicone-rubber silver halide membrane electrodes used had the inner electrical contact ensured by mercury and a platinum wire, *i.e.* no internal reference solution was used.

Since earlier investigations have shown that the potential of a membrane electrode can be interpreted most easily by comparing it with the potential of an appropriate electrode of the second kind, the measurements were carried out in measuring cells with an electrode of the second kind as reference electrode. The electrodes of second kind were prepared as described by Ives and Janz[5]. The measuring cell used was as follows:

$$\text{Pt Hg}\,\Big|\,\text{AgX}\,\Big|\,\overset{\text{AgNO}_3}{\underset{\text{KX}}{}}\,(10^{-1}\text{–}10^{-5}\,M)\,\Big|\,\text{AgX}\,\Big|\,\text{Ag}$$

$$(\text{X} = \text{Cl}^-, \text{Br}^-, \text{I}^-)$$

The measurements were carried out in silver nitrate or in potassium chloride, bromide or iodide solutions, at 25° with a precision pH-meter (type OP 205, Radelkis, Budapest).

The temperature dependence of the electrode potential was measured in the range 13–75°. A Radiometer K-901 electrode of the second kind of known temperature coefficient, served as reference electrode.

Measurements were carried out in serial dilutions of potassium chloride, bro-

---

* Present address: Institute for General and Analytical Chemistry, Technical University, Budapest.

mide and iodide solutions. The concentration ranged between 10^{-1} and 10^{-5} *M*. The ionic strength (J) of the solutions was adjusted to 1 with potassium nitrate; thus, in the calculations, it was not necessary to consider any change in the activity coefficient.

RESULTS

The standard potentials of ion-selective electrodes

The measurements were carried out with AgCl-, AgBr- and AgI-based membrane electrodes and corresponding electrodes of the second kind.

It is known that the potential of these membrane electrodes, similarly to electrodes of second kind, changes with the ionic activity of the solution according to the Nernst equation[1,2,6]. Since the electrode investigated and the reference electrode employed actually are two identical reversible indicator electrodes, the e.m.f. measured is equal to the difference of the standard electrode potentials of the two electrodes.

In the course of the measurements, it was found that the measured e.m.f. differed considerably from zero. The deviation was nearly characteristic for the quality of the precipitate. However, electrodes of identical standard potentials could not be

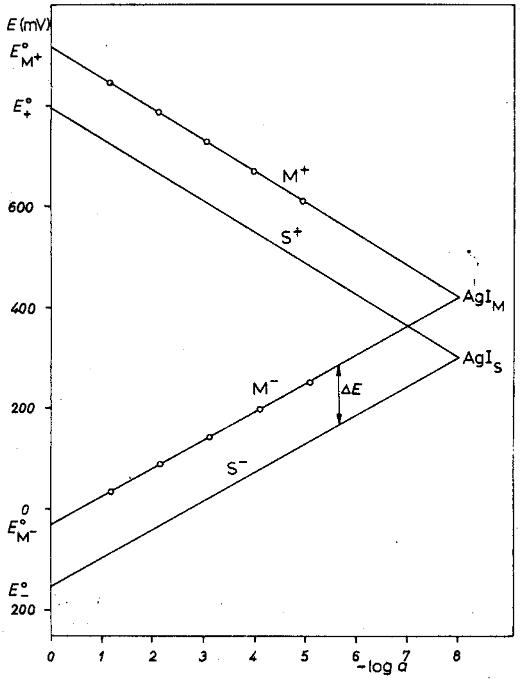

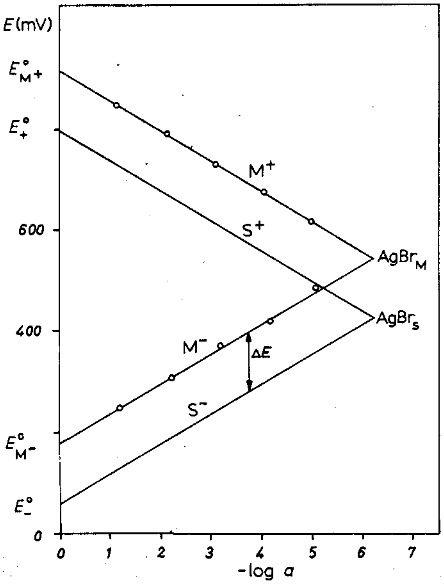

Fig. 1. Comparison between the function of a silver iodide electrode of the second kind (AgI_s) and the function of a silver iodide membrane electrode (AgI_M).

Fig. 2. Comparison between the function of a silver bromide electrode of the second kind and the function of a silver bromide membrane electrode.

made even from precipitates prepared in exactly the same way. It was also found that the standard potentials of the membrane electrodes, depending on the conditions of the preparation of the precipitates incorporated in the membrane, were always more positive than the standard potential of the corresponding electrode of the second kind.

In Figure 1, the potentials corresponding to the cation and anion reversible function of a silver iodide membrane electrode and a silver iodide electrode of the second kind are plotted against the negative logarithm of the iodide activity. It can be seen clearly that the straight lines (M) which represent the cation and anion reversible functions of the membrane electrodes, lie well above the lines (S) which are characteristic for the behaviour of electrodes of the second kind. Thus, in solutions of the same concentrations, there is a well defined difference (ΔE) in the potentials of the two kinds of electrodes. (Membrane potentials for concentrations higher than 10^{-1} M or lower than 10^{-5} M were extrapolated.) The same phenomenon was observed in comparisons of the standard potentials of silver bromide and silver chloride membrane electrodes with those of the appropriate electrodes of the second kind (Figs. 2 and 3).

Since it seemed that the magnitudes of the ΔE potential differences were related to the chemical composition of the precipitate included in the membrane, the electrochemical behaviour of membrane electrodes made of precipitates of different composition was examined systematically.

TABLE I

EFFECT OF EXPOSURE TIME ON THE DIFFERENCES BETWEEN THE POTENTIALS OF MEMBRANE ELECTRODES AND ELECTRODES OF THE SECOND KIND

Membrane electrode	*Exposure time (min)*	ΔE *(mV)*
AgCl	5	80
	10	72
	20	60
AgBr	5	157
	10	139
	20	131
	30	73
AgI	10	177
	20	151
	30	104

In the case of silver halide crystals, the easiest way to alter their composition is to expose the crystals to ultraviolet light for various times. The processes that occur are identical to the formation of the so-called latent picture in photography. Under the effect of light silver specks separate out in the crystal, so that the phase composition is altered.

For further measurements membrane electrodes prepared of such precipitates which had been exposed to ultraviolet light for different times were used. Measurements were carried out in a dark room.

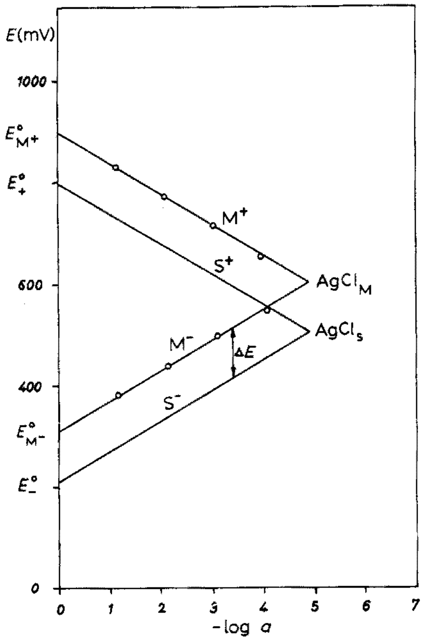

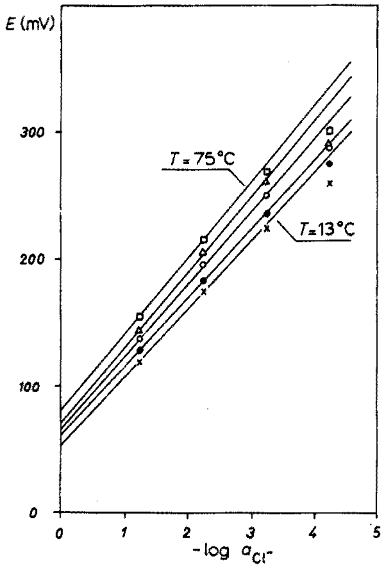

Fig. 3. Comparison between the function of a silver chloride electrode of the second kind and the function of a silver chloride membrane electrode.

Fig. 4. Temperature dependence of the potential of a silver chloride membrane electrode (T = 13, 30, 45, 60 and 75°).

Table I shows the potential values of the silver halide membrane electrodes measured in a silver nitrate solution as a function of the exposure time.

Dependence of the standard electrode potentials on temperature

The temperature dependence of the standard potential of the chloride-, bromide- and iodide-selective membrane electrodes was examined in the temperature range 13–75° by measuring the calibration curves in the appropriate 10^{-1}–10^{-5} *M* potassium halide solutions.Figures 4, 5 and 6 show the membrane potentials measured with the three membrane electrodes at different temperatures as functions of the activity of the individual ions.

EVALUATION OF THE RESULTS

On the basis of the results presented in Figs. 1–3 it is clear that the standard potentials of the electrodes of the second kind and of the analogous silver halide membrane electrodes are not the same. The potential difference established between the two types of electrode (ΔE) is always different for chloride-, bromide- and iodide-selective membrane electrodes, and it can even differ for the same type of electrode, depending on the preparative conditions.

In further investigations, an attempt was made to correlate the composition of the solid electrode phase and the electrochemical behaviour observed.

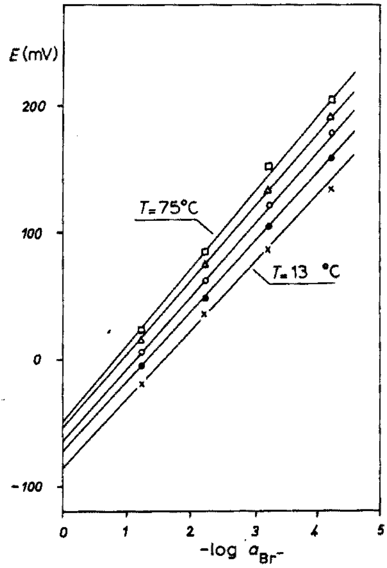

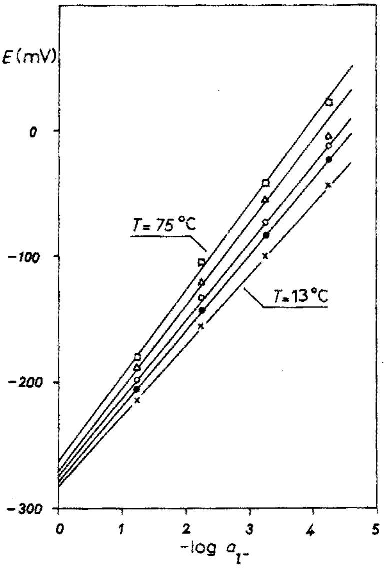

Fig. 5. Temperature dependence of the potential of a silver bromide membrane electrode (T = 13, 30, 45 60 and 75°).

Fig. 6. Temperature dependence of the potential of a silver iodide membrane electrode (T = 13, 30, 45, 60 and 75°).

The theoretical basis of the behaviour of precipitate-based membrane electrodes has already been considered by Pungor[6]. The electrode potential is considered to be the result of a rapid reversible ion-exchange reaction between the ions in the membrane precipitate and the ions in the solution. The selectivity of the electrodes depends on the fact that a preferential ion-exchange reaction will occur with those ions which are identical with the ions in the precipitate itself. At equilibrium when the electrochemical potentials in the solution and membrane phase are equal, the following equation describes the electrode potential:

$$E = E^0 + (RT/zF) \ln (a)_s/(a)_c \tag{1}$$

The symbols used in the following paragraphs are defined in Table II. M_jX_i represents the composition of the precipitate contained in the membrane, where M is the metal ion, and X is the halide ion; both cation and anion are in fact univalent.

On the basis of eqn. (1), the membrane potentials belonging to the reversible functions of the cation (E_1) and anion (E_2) are as follows:

$$E_1 = E^0_+ + (RT/iF) \ln (a_{M^+})_s/(a_M)_c \tag{2}$$

and

$$E_2 = E^0_- + (RT/jF) \ln (a_{X^-})_s/(a_X)_c \tag{3}$$

where

$$E^0_+ = (iF)^{-1} [\mu^0(M^+)_s - \mu^0(MX)_c] \tag{4}$$

$$E^0_- = (jF)^{-1} [\mu^0(X^-)_s - \mu^0(MX)_c] \tag{5}$$

TABLE II

LIST OF SYMBOLS

E	electrode potential measured
ΔE	difference in the potentials of a membrane electrode and the corresponding electrode of the second kind
E^0_+	standard potential of the ion-function indicated by the subscript
$E^0_{M^+}$	standard potential of the cation-reversible function of the membrane electrode
$E^0_{M^-}$	standard potential of the anion-reversible function of the membrane electrode
ε^0	characteristic membrane potential defined by eqn. (9)
R, F, z	general electrochemical constants
T	absolute temperature
ΔG^0	standard free enthalpy change
K_s and K_c	equilibrium constants
$\mu^0\,(M^+)_s$	standard chemical potential of the component in parentheses in the phase marked
s and c	subscripts referring to solution and crystal phases
i	charge of the metal ion (+1)
j	charge of the halide ion (−1)
n_X	mole fraction of the component indicated by the subscript in the crystal phase
$\vert\,\vert$	symbol of the absolute value

Equations (4) and (5) are based on the following potential-forming reactions:

$$[M]_c \rightleftharpoons [M^+]_s \quad MX - e \rightleftharpoons M^+ + X \tag{6}$$

$$[X]_c \rightleftharpoons [X^-]_s \quad MX + e \rightleftharpoons M + X^- \tag{7}$$

If the solution is saturated with the MX compound, then the potentials E_1 and E_2 are equal, and a general equation can be deduced which is valid for both ions when the sum of potentials E_1 and E_2 is divided by two.

$$E_{1,2} = \varepsilon^0 + \frac{RT}{2ijF} \ln \{[(a_M)_c^{|j|}/(a_{M^+})^{|j|}] \cdot [(a_{X^-})_s^{|i|}/(a_X)^{|i|}]\} \tag{8}$$

where

$$\varepsilon^0 = \tfrac{1}{2}[E^0_+ + E^0_-] \tag{9}$$

The potential defined by eqn. (9) is called the characteristic membrane potential.

The term in brackets in eqn. (8) corresponds to the product of the activities of the positive and negative ions, partly in the solution phase and partly the activity of the elements composing the compound in the precipitate phase.

The product of the activities of the ions in the solution which are in equilibrium with the precipitate, is simply the solubility product of the precipitate, *i.e.* the equilibrium constant which can be calculated from the standard free enthalpy changes of the following reaction:

$$MX \rightleftharpoons M_s^+ + X_s^- \tag{10}$$

$$RT \ln K_s = \Delta G^0 = \mu^0(M^+)_s + \mu^0(X^-)_s - \mu^0(MX)_c \tag{11}$$

$$K_s = (a_{M^+})_s (a_{X^-})_s \tag{12}$$

Similarly to the equilibrium established between solution and precipitates, a strict quantitative relation exists for the equilibrium between compound and its components, which, for the solid phase, is identical with the activity product (K_c), *i.e.* the equilibrium constant which can be calculated from the standard free enthalpy change of the following reaction:

$$\mathrm{MX} \rightleftharpoons \mathrm{M}+\mathrm{X} \tag{13}$$

$$-RT \ln K_c = \Delta G^0 = \mu^0(\mathrm{M})+\mu^0(\mathrm{X})-\mu^0(\mathrm{MX}) \tag{14}$$

where $K_c = (a_\mathrm{M})_c(a_\mathrm{X})_c$ (15)

The substitution of eqns. (12) and (15) into eqn. (8) yields equations which describe the cation- and anion-reversible functions of the membrane electrode, depending on whether the activity of the positive or negative ions is expressed by the constants K_s or K_c. This substitution followed by the appropriate simplifications, yields the following equation for the reversible cation function of a silver halide membrane electrode:

$$E_1 = \varepsilon^0-(RT/F)\ln\left[(K_s/K_c)^{\frac{1}{2}}(a_\mathrm{M})_c\right]+(RT/F)\ln(a_{\mathrm{M}^+})_s \tag{16}$$

In the same way, a similar relationship can be deduced for the potential of a membrane electrode made of MX compound in a solution containing X^- ions:

$$E_2 = \varepsilon^0+(RT/F)\ln\left[(K_s/K_c)^{\frac{1}{2}}(a_\mathrm{X})_c\right]-(RT/F)\ln(a_{\mathrm{X}^-})_s \tag{17}$$

If the factors independent of concentration are combined, eqns. (16) and (17) become, respectively,

$$E_1 = E^0_{\mathrm{M}^+}+(RT/F)\ln(a_{\mathrm{M}^+})_s \tag{18}$$

where

$$E^0_{\mathrm{M}^+} = \varepsilon^0-(RT/F)\ln\left[(K_s/K_c)^{\frac{1}{2}}(a_\mathrm{M})_c\right] \tag{19}$$

and

$$E_2 = E^0_{\mathrm{M}^-}-(RT/F)\ln(a_{\mathrm{X}^-})_s \tag{20}$$

where

$$E^0_{\mathrm{M}^-} = \varepsilon^0+(RT/F)\ln\left[(K_s/K_c)^{\frac{1}{2}}(a_\mathrm{X})_c\right] \tag{21}$$

According to eqns. (18) and (20), the potential of the membrane electrode changes with the ionic activity of the solution in exactly the same way as that of electrodes of the second kind, but the standard potentials differ.

For the calculation of the standard potential relating to the cation- and anion-reversible function of membrane electrodes, the following values must be known: the characteristic membrane potential ε^0, the constants K_s and K_c, and the activity values $(a_\mathrm{M})_c$ and $(a_\mathrm{X})_c$.

The value of ε^0 can be calculated on the basis of eqns. (4), (5) and (9), while K_s and K_c can be determined from eqns. (11) and (14), respectively.

Table III shows the ε^0, K_s and K_c values for silver halide membrane electrodes. (For the calculations, data published by Latimer[7] were used.)

However, with the exception of two limiting cases, values of $(a_\mathrm{M})_c$ and $(a_\mathrm{X})_c$ cannot be exactly calculated in advance. The change in the activity of the components can be obtained by means of the correlation valid for the phase-equilibrium of the binary system formed by the components M and X[8]; more exactly, with the aid of μ–n curves, it is possible to estimate the range within which the activity of the compo-

TABLE III

VALUES OF THE CONSTANTS ε^0, K_s AND K_c OF THE SILVER HALIDE MEMBRANE ELECTRODES

Electrode examined	ε^0 (*mV*)	K_s	K_c
AgCl	1079	$2.8 \cdot 10^{-10}$	$1.5 \cdot 10^{-21}$
AgBr	932	$5.0 \cdot 10^{-13}$	$1.3 \cdot 10^{-17}$
AgI	667	$8.5 \cdot 10^{-17}$	$2.2 \cdot 10^{-12}$

nents of a certain compound can change.

The relationships can be demonstrated most easily by means of a Gibbs diagram of free enthalpy *vs.* composition; the diagram for compound MX is shown schematically in Fig. 7. For the construction of the diagram, the composition of the compound phase existing in the 0–1 mole fraction region was assumed to be MX; since the composition of compounds—in contrast to that of mixtures—is characterized by a strict weight-proportion of the components, the curve in Fig. 7 representing the formation of the compound, extends in practice to a very narrow region of the composition. As can be seen, the compound symbolized by the formula MX shows a certain variation around the stoichiometric composition within a small mole fraction range. As is known, in the case of a compound of given composition, the partial molar free enthalpy of the components can be obtained graphically as the ordinate intercept of the tangent drawn to a given point of the curve.

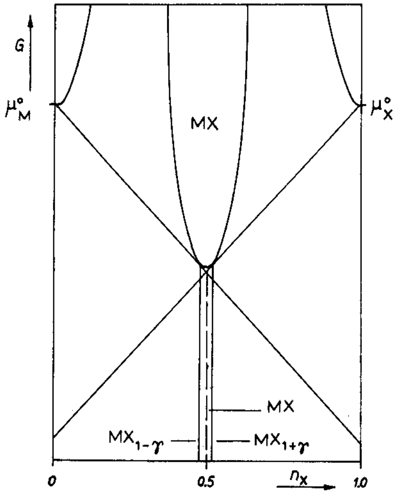

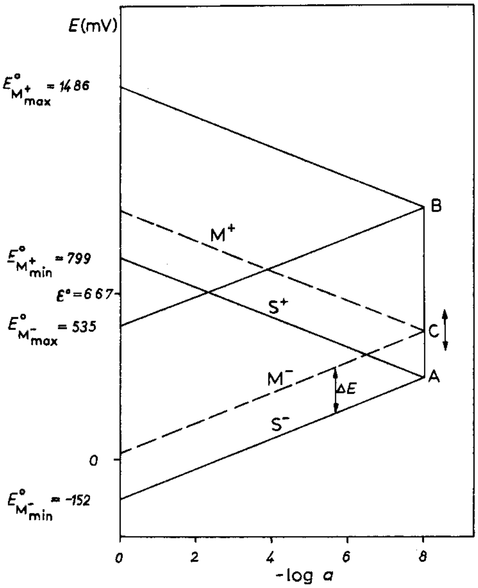

Fig. 7. Free enthalpy *vs.* composition diagram of the MX compound according to Gibbs.

Fig. 8. With increase of the silver activity of the electrode phase, the intersection points C of the straight-line couples representing the function of the AgI membrane electrode, are shifted in the direction of point A.

Although the deviation from the stoichiometric composition is infinitesimally small, and has no significant effect on the free enthalpy of the crystal itself, these small changes strongly affect the partial molar free enthalpy of the crystal components[9]. This point must always be considered when the components themselves take part in the chemical or electrochemical processes.

In Fig. 7, moving to the right from the 0.5-mole fraction—which represents the stoichiometric composition—raises the amount of X; for composition $MX_{1+\gamma}$, the compound maintains near equilibrium with the pure X component, *i.e.* its activity in the compound phase is $(a_X)_c = 1$, while according to eqn. (15), the activity of the M component is $(a_M)_c = K_c$. Moving to the left from the 0.5-mole raises the quantity of M until the compound is in equilibrium with the pure M component, and the point $MX_{1-\gamma}$ of the composition is reached. In such cases the activity of the metal in equilibrium with the compound is $(a_M)_c = 1$; while according to eqn. (15), $(a_X)_c = K_c$.

Accordingly, in the crystalline solid electrode phase, the activity of the electropositive component can decrease from $(a_M)_c = 1$ to K_c, whereas the activity of the electronegative component can increase from $(a_X)_c = K_c$ to 1.

However, for the activity product of the two components, eqn. (15) is always valid. The characteristic membrane potential ε^0 is the common standard potential belonging to both the cation and anion function of the membrane electrode, when the activities of the both components are equal to each other in the membrane phase. With the knowledge of the two possible extreme limits of the change in composition, the maximal and minimal values of the standard potential, *i.e.* the values between which the standard potential can change depending on the actual composition of the crystalline phase, can be calculated on the basis of eqns. (19) and (21). Table IV shows the relevant values for the two kinds of electrode functions of the silver halide membrane electrodes.

Figure 8 shows the diagram constructed on the basis of eqns. (16) and (17); the potentials of the silver iodide membrane electrode referred to the normal hydrogen electrode are plotted as a function of the negative logarithm of the activity. The intersection point of the straight lines representing the reversible cation and anion function can vary between points A and B depending on the composition and conditions of preparation of the silver. The dotted lines were plotted on the basis of potentials measured by the silver iodide membrane electrodes. On the basis of eqn. (16), it can also be seen (Fig. 8) that when the silver activity of the electrode phase is raised, the potential of the intersection point (C) is shifted in the direction of point (A) while

TABLE IV

MAXIMAL AND MINIMAL VALUES OF THE STANDARD POTENTIALS OF MEMBRANE ELECTRODES

Electrode examined	$E^0_{M^+}$ *(mV)*		$E^0_{M^-}$ *(mV)*	
	Max	*Min*	*Max*	*Min*
AgCl	+1936	+799	+1359	+222
AgBr	+1793	+799	+1065	+ 71
AgI	+1486	+799	+ 535	−152

an increase in the iodide activity shifts the potential of the intersection point in the direction of point (B).

The data presented in Table I indicate that as the time of exposure to u.v. light increases, the silver activity of the electrode phase also increases. The difference between the potentials of the membrane electrode in question and the corresponding electrode of the second kind then decreases. This observation is in accordance with the conclusions drawn from the equation mentioned previously.

The measurements regarding the temperature dependence of the potential of membrane electrodes are in very good agreement with the observations regarding the standard potential. Figures 4–6 show the change in potential of membrane electrodes as a function of both activity and temperature.

From eqn. (20) it can be easily realized that if the membrane potential values relating to activity $(a_{X^-})_s = 1$ are plotted against temperature, then the temperature dependence of the membrane standard potential value defined by eqn. (21) is obtained.

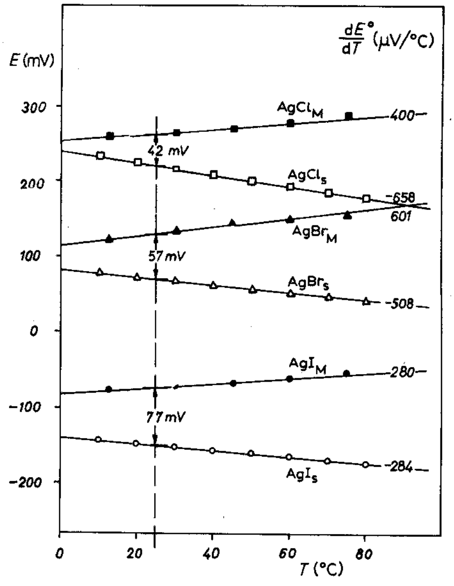

Fig. 9. Effect of temperature on the standard potential of the membrane electrode and the electrode of the second kind.

Figure 9 shows the temperature dependence of the standard potential values of the chloride-, bromide- and iodide-selective membrane electrodes, as well as electrodes of the second kind. It should be noticed that the temperature coefficients of the two types of electrode differ in sign. However, it must be emphasized that the temperature coefficients given for these precipitate-based membrane electrodes are not characteristic parameters for such electrodes, for the temperature coefficients will certainly depend on the composition of the precipitate, similarly to the standard potentials. It is worth noting that Ives and Janz[10] found in connection with the standard potential of sulphide electrodes of the second kind, that the measured temperature coefficient value was not equal to the dE^0/dT value calculated from thermodynamic data. Probably the reason for this phenomenon also lies in the alteration of the composition of the metal sulphide precipitate.

SUMMARY

The standard potentials of silicone-rubber, silver halide membrane electrodes and their temperature dependence have been studied. The value of the standard potential of these electrodes depends on the actual composition of the silver halide crystals. A theoretical explanation of this finding is discussed. The temperature coefficient of the standard potential of the halide-selective membrane electrodes differs in sign from that of the corresponding electrode of the second kind.

RÉSUMÉ

Une étude est effectuée sur les potentiels standards des électrodes à membrane silicone–halogénure d'argent, en fonction de la température. La valeur de ces potentiels dépend de la composition de l'halogénure d'argent.

ZUSAMMENFASSUNG

Die Standardpotentiale von Silikonkautschuk–Silberhalogenid-Membranelektroden und deren Temperaturabhängigkeit wurden untersucht. Der Wert des Standardpotentials dieser Elektroden hängt von der tatsächlichen Zusammensetzung des Silberhalogenid-Kristalls ab. Eine theoretische Deutung dieses Befundes wird erörtert. Der Temperaturkoeffizient des Standardpotentials der halogenidselektiven Membranelektroden unterscheidet sich im Vorzeichen von dem der korrespondierenden Elektrode zweiter Art.

REFERENCES

1 E. PUNGOR, K. TÓTH AND J. HAVAS, *Mikrochim. Acta*, (1964) 565; *Acta Chim. Acad. Sci. Hung.*, 48 (1966) 17; J. HAVAS, E. PAPP AND E. PUNGOR, *Acta Chim. Acad. Sci. Hung.*, 58 (1968) 9; E. PUNGOR AND K. TÓTH, *Hung. Sci. Instr.*, 14 (1968) 15.
2 E. PUNGOR AND K. TÓTH, *Estratto de Chronache di Chimica*, N. 22, Dicembre, 1968; *Anal. Chim. Acta*, 47 (1969) 291.
3 E. PUNGOR AND K. TÓTH, *Hung. Sci. Instr.*, 18 (1970) 1.
4 D. KÜTTEL, Ö. SZABADKA, J. HAVAS AND E. PUNGOR, *Magy. Kem. Folyoirat*, 75 (1969) 181; E. PAPP AND E. PUNGOR, *Kiserl. Orvostud.*, 21 (1969) 333; *Z. Anal. Chem.*, 246 (1969) 26.
5 D. J. G. IVES AND G. J. JANZ, *Reference Electrodes*, Academic Press, New York, 1961.
6 E. PUNGOR, *Anal. Chem.*, 39, No. 13 (1967) 67A.
7 W. M. LATIMER, *The Oxidation States of the Elements and their Potentials in Aqueous Solutions*, 2nd Edn., Prentice-Hall, New York, 1950.
8 W. ALBERS, in M. AVEN AND J. S. PRENER, *Physics and Chemistry of II–VI Compounds*, North Holland Amsterdam, 1967, p. 167.
9 F. A. KRÖGER, *The Chemistry of Imperfect Crystals*, North Holland, Amsterdam, 1964, p. 516.
10 D. J. G. IVES AND G. J. JANZ, *Reference Electrodes*, Academic Press, New York, 1961, p. 379.

Analytica Chimica Acta
Elsevier Publishing Company, Amsterdam
Printed in The Netherlands

NEUE MÖGLICHKEITEN DER VERWENDUNG VON MEMBRANEN IN DER VOLTAMMETRIE

H. BERGE UND S. KUNKEL
Sektion Chemie, Universität Rostock, Rostock (D.D.R.)

(Eingegangen den 16. November 1970)

In dieser Arbeit wird eine für analytische Untersuchungen vielseitig verwendbare voltammetrische Messanordnung vorgestellt. Die Indikatorelektrode wird von einer stationären Quecksilbermembranelektrode gebildet. Als Membranen werden Celluloseacetatmembranen (CAM) der Firma Membranfilter GmbH Sartorius, Göttingen, und eine monofunktionelle Ionenaustauschermembran mit Iminodiessigsäure-Ankergruppen* verwendet.

Bei der von Clausen *et al.*[1] vorgestellten stationären "mercury frit electrode" wird das als Elektrodenmaterial dienende Quecksilber durch eine Borosilikatglasfritte von der Elektrolytlösung getrennt. Diese Quecksilber-Frittenelektrode kann als Membranelektrode angesehen werden, in der die Dicke der Membran (Fritte) die Dicke der Diffusionsschicht zu jeder Zeit darstellt. Die durch Voltammetrie** an dieser Indikatorelektrode erhaltenen idealen Peakvoltammogramme weisen auf völlige Abwesenheit von natürlicher oder/und künstlicher Konvektion der Lösung an der Elektrodenoberfläche hin. D.h., an der Quecksilberoberfläche stellt sich ein stationärer Zustand ein.

Bowers und Wilson[3] benutzten für ihre voltammetrischen Untersuchungen eine Cellophanmembran, die die bewegte Lösung von der ruhenden Quecksilberelektrode trennt.

Lässt man nach Braunwalder *et al.*[4] Quecksilber durch eine angeschliffene Kapillare an einem mit Depolarisator und Trägerelektrolyt getränkten Stück Filterpapier vorbeifliessen, so kann man bei genügend raschem Spannungsvorschub dieselben Stromstufen erhalten wie in der Polarographie der freien Elektrolytlösungen. Diese sogenannte Oberflächenpolarographie soll für Gleich- und Wechselspannungsverfahren geeignet sein.

Das Prinzip der quecksilberdurchflossenen Kapillare wird von Bersier *et al.*[5] beibehalten. Sie benutzen für ihre voltammetrischen Untersuchungen mit Picein befestigte Aluminiumoxid-Deckschichten, arbeiten jedoch mit stehendem Quecksilber und ruhender Lösung.

Das Ankleben der Membran wird von Gerber *et al.*[6] durch ein Andrücken an den quecksilberdurchflossenen Kanal ersetzt. Die Methode wird zur Untersuchung

---

* Herrn Prof. Dr. R. Hering (Pädagogische Hochschule, Güstrow) danken wir für die freundliche Bereitstellung dieser Ionenaustauschermembran.

** Als Voltammetrie wird die Betrachtung von Strom–Spannungs- und Strom–Zeit-Beziehungen unter stationären Bedingungen an stromdurchflossenen Elektroden bzw. elektrochemischen Zellen bezeichnet[2].

von Diffusionsprozessen in Membranen (z.B. Ionenaustauschermembranen) und kolloidalen Systemen eingesetzt.

In der vorgestellten Messanordnung werden die Vorzüge der stationären Quecksilberelektrode, das leichte Auswechseln der Membran, das Einsetzen bereits vorbereiteter Membranen und die Verwendung für verschiedene Untersuchungsmethoden (Gleich- und Wechselspannungsverfahren, inversvoltammetrische Methoden) vereinigt.

MESSANORDNUNG

Als Messzelle dient ein aus Piacryl angefertigtes zylinderförmiges Gefäss (Abb. 1). In dem Deckel aus PVC sind Bohrungen für das Ein- und Ableiten des inerten Spülgases (Wasserstoff oder Argon), für einen KPG-Rührer und eine Elektrolytbrücke angebracht. Nach unten hat diese Zelle eine trichterförmige Öffnung.

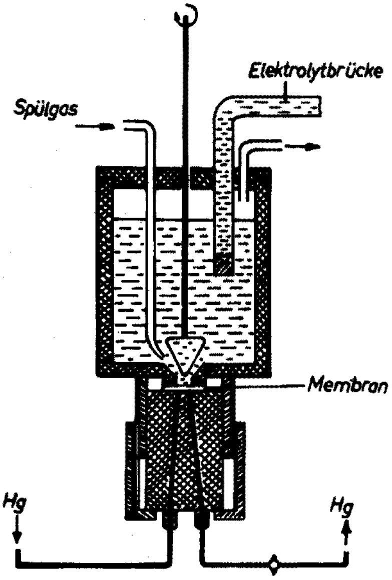

Abb. 1. Darstellung der Messanordnung.

Sie wird von einem festanzuziehenden Stempel mit darauf liegender Membran und Dichtungsring verschlossen. Der Stempel enthält zwei ungefähr 1-mm starke, am oberen Ende zusammenlaufende Kapillaren. An deren Berührungsstelle ist der Stempel so weit angeschliffen, dass das durch die Kapillaren fliessende Quecksilber hier in Berührung mit der Membran steht. Der Quecksilberfluss kann sowohl durch die Höhe des Quecksilberniveaugefässes als auch durch eine am Abfluss vorgeschaltete Kapillare geregelt werden. Über die Elektrolytbrücke (0.5 *M* KNO_3) ist die zu messende Lösung mit der als Bezugselektrode dienenden gesättigten Kalomelelektrode verbunden.

Die runden Membranen werden in einer Grösse von 1 cm Durchmesser verwendet. Die wirksame Membranfläche beträgt *ca.* 10 mm^2. Die Anordnung mit er CAM hat einen Widerstand von etwa 3500 Ohm. Die Elektrolytlösungen werden ur Entfernung des Sauerstoffs mit Elektrolytwasserstoff (nach Reinigen über Platin-sbestkontakt bei 300°) oder Schweissargon gespült. Ein Vorteil der Messanordnung esteht darin, dass vorbehandelte Membranen, d.h. Membranen, die sich im Gleich-ewicht mit dem Trägerelektrolyten befinden oder mit einer Ionenart beladen sind, erwendet werden können. Es entfallen so Wartezeiten bis zur Einstellung dieser Gleichgewichte, die viele dieser voltammetrischen Verfahren sehr zeitaufwendig gestalten.

Die Messanordnung gestattet, Untersuchungen sowohl in ruhender und bewegter Lösung als auch mit stehendem oder fliessendem Quecksilber auszuführen.

BETRACHTUNG DER UNTERSUCHUNGSERGEBNISSE MIT DER CELLULOSEACETATMEMBRAN

Gleichspannungsvoltammetrische Untersuchungen

Die CAM erweist sich als eine Matrix, die den permeierenden Stoffen aufgrund des grossen Porenvolumens und der Porengrösse nur einen geringen Widerstand entgegensetzt. Die Wandladungskonzentration (= Festionenkonzentration) ist bei diesem Membrantyp so niedrig, dass sie die Messungen nicht beeinflusst und somit vernachlässigt werden kann. Erscheinungen, die auf eine Adsorption an der Membran schliessen lassen, werden nicht beobachtet.

Das Eintreten und die Wanderung von Ionen in der CAM können mit den bestehenden Konzentrationsgradienten an der Phasengrenze Elektrolyt/Membran und innerhalb der Membran erklärt werden. Die innere Diffusion wird durch das angelegte elektrische Feld noch verstärkt. Permeabilitätsunterschiede für einzelne Ionen bestehen an der CAM nicht, so dass mit der voltammetrischen Methode mit angelegter Gleichspannung grundsätzlich alle die Ionen erfasst werden, deren Halbstufenpotential im Messbereich der Anordnung liegen, und die an der Quecksilberelektrode bestimmbar sind.

Eine Konvektion der Lösung beeinflusst die Transportvorgänge in der Membran nicht. Durch mechanisches Rühren oder Einleiten von Gas wird die Diffusionsschichtdicke an der Elektrode so weit herabgesetzt, bis sie schliesslich durch die Dicke der Membran gegeben ist. Der geschwindigkeitsbestimmende Schritt für die Elektrodenreaktion ist dann die Diffusion der Teilchen durch die Membran. Der Einfluss der Rührgeschwindigkeit auf die Höhe des Diffusionsstromes ist nach Erreichen dieser minimalen Diffusionsschichtdicke äusserst gering. Eine Erhöhung der Rührgeschwindigkeit um 200 U min^{-1} macht sich in diesem Bereich (340 U min^{-1}) nur mit etwa 1–2% in der Diffusionsstromhöhe bemerkbar. Dagegen bewirkt eine Erhöhung der Rührgeschwindigkeit vor Erreichen des Grenzzustandes von 100 auf 300 U min^{-1} einen um mehr als 50% höheren Diffusionsstrom.

Durch das Registrieren von Strom–Spannungskurven wird das Gleichgewicht, das sich zwischen Elektrolyt und Porenflüssigkeit eingestellt hat, gestört. Dieser Gleichgewichtzustand kann sich durch Rückdiffusion des am Quecksilber abgeschiedenen Metalls (durch Hydrolyse des Amalgams) und durch Nachdiffusion aus der Lösung an der Membran neu einstellen. Bei fliessendem Quecksilber (2 mg Hg sec^{-1}) reicht schon eine Zeit von 30 sec aus, um das gesamte mit der Membran in Berührung stehende Quecksilber zu erneuern. Beim Registrieren einer Strom–Spannungskurve wird das gebildete Amalgam laufend abtransportiert und durch neues Quecksilber ersetzt. Nach Abschluss der Messung genügen die schon erwähnten 30 sec, um das restliche Amalgam zu entfernen.

Wenn eine Rückdiffusion aus dem Amalgam erfolgt, muss sich diese bei der Abhängigkeit des Diffusionsstromes vom Zeitintervall zwischen den einzelnen Messungen durch Zunahme des Stromes mit der Wartezeit bemerkbar machen. Da dieses Anwachsen des Diffusionsstromes jedoch nicht beobachtet wird, kann eine Rückdiffusion des abgeschiedenen Metallions aus dem Amalgam heraus für die Gleichgewichtseinstellung an der Membran ausgeschlossen werden. Die Neueinstellung des Gleichgewichts kann deshalb nur durch Nachdiffusion der elektroaktiven Substanz erfolgen. Da Wartezeiten zwischen 1 und 10 Min gleichbleibend hohe Strom–Spannungskurven erreichen lassen, muss die Nachdiffusion und damit der Auffüllprozess relativ schnell erfolgen.

Der Einfluss der Potentialänderungsgeschwindigkeit auf die Höhe der Strom–Spannungskurven an der voltammetrischen Membranelektrode und der tropfenden Quecksilberelektrode (D.M.E.) ist gleich. In beiden Fällen nimmt beim Erhöhen der Geschwindigkeit v der Potentialänderung die Diffusionsstromhöhe mit der Wurzel aus v zu.

Die Nachdiffusion der Ionen spielt auch für die Kurvengestalt eine Rolle. Für niedrige Konzentrationen (10^{-5} bis etwa 10^{-4} M Lösungen) und langsame Potentialänderungen (125 mV min^{-1}) werden Strom–Spannungskurven erhalten, die den mit der D.M.E. registrierten Kurven, abgesehen von den fehlenden Oszillationen, sehr ähnlich sind. Mit Zunahme der Potentialänderungsgeschwindigkeit nimmt die Neigung zu Peakströmen zu. Ursache dieser Peakströme sind Verarmungseffekte an der Phasengrenze Membran/Elektrode, die auch bei Erhöhung der Metallionenkonzentration in Erscheinung treten. Zwischen Zunahme der Metallionenkonzentration und des registrierten Stromes wird eine sehr gute lineare Abhängigkeit im weiten Konzentrationsbereich (z.B. $6 \cdot 10^{-5}$ bis $1.5 \cdot 10^{-3}$ M Cd^{2+}) festgestellt. Die Konzentrationsproportionalität der Diffusionsströme wird für ein Ion durchgehend an einer Membran überprüft. Die Fliessgeschwindigkeit des Quecksilbers ist praktisch ohne Einfluss auf den Diffusionsstrom. Lediglich zwischen den am stehenden und fliessenden Quecksilber registrierten Strömen besteht ein geringer Unterschied. Das am Quecksilber abgeschiedene Metall verringert die freie Elektrodenoberfläche, wodurch nach jeder Elektrolyse niedrigere Diffusionsstromwerte erhalten werden als das am ständig nach jeder Elektrolyse erneuerten Quecksilber der Fall ist. Eine geringe Fliessgeschwindigkeit des Quecksilbers ist daher angebracht.

Die Durchtrittszeit für Cd^{2+}-, Cu^{2+}- und Pb^{2+}-Ionen beträgt an der mit Trägerelektrolyten getränkten, neu eingesetzten CAM etwa 40 Min. Nach Verstreichen dieser Zeit werden Strom–Spannungskurven erhalten, die sehr gut reproduzierbar sind.

Die Polarisations- und Messbereiche an der voltammetrischen Membranelektrode entsprechen denen an der D.M.E. Eine Abweichung ergibt sich jedoch in den Leitelektrolyten, die mit den Quecksilberionen reagieren (Cl^-, SO_4^{2-}). Im positiven Potentialbereich tritt dabei ein Peak auf, der durch die Niederschlags- und Filmbildung auf der Quecksilberelektrode bedingt ist. Eine Aufnahme von Strom–Spannungskurven ist in diesen Lösungen erst im negativen Potentialbereich möglich.

Bei der Voltammetrie mit Gleichspannung liegt die Nachweisgrenze für die Cu^{2+}- und Cd^{2+}-Ionen bei 10^{-5} M Lösungen. Die logarithmischen Kurvenanalysen sprechen für einen Zweielektronenübergang bei der Reduktion von Cu^{2+}- und Cd^{2+}-Ionen am Quecksilber und für einen reversiblen Reaktionsverlauf. Die Kurvenanalysen liefern ausserdem Halbstufenpotentiale, die in der Nähe der mit der D.M.E. erhaltenen Potentiale liegen.

Die Reproduzierbarkeit der gemessenen Stromwerte ist sehr gut. Die an einer Membran erhaltenen Messwerte weisen eine Standardabweichung von etwa 1.7% auf. Einmal mit einer Membran erhaltene Messwerte sind unter gleichen Bedingungen, d.h. nach gleicher Vorbehandlung der Membran und in gleicher Lösung, in ausreichendem Masse reproduzierbar. Mittels einer aufgenommenen Eichkurve können unbekannte Konzentrationen bestimmt werden.

Neben Metallionen, die unter Amalgambildung an der Quecksilbermembranelektrode reduziert werden, können auch nichtamalgambildende Substanzen nur durch einen Wertigkeitswechsel bestimmt werden. Die Schwierigkeit dieses Vorhabens liegt darin, dass das Reduktionsprodukt nicht in Form des Amalgams von der fliessenden Quecksilberelektrode abtransportiert wird, sondern in der Membran verbleibt bzw. aus der Membran wieder in die Lösung diffundiert. Es gelingt z.B., Eisen(III)-ionen (in 0.2 *M* Nitrilotriessigsäure und 0.4 *M* Acetat) zu Eisen(II)-ionen mit dieser Messanordnung zu reduzieren. Erst bei Zeitintervallen von 5 Min zwischen den einzelnen Messungen werden gleichbleibende Diffusionsstromwerte erhalten. Diese grössere Zeitspanne ist vermutlich nötig, damit sich zwischen dem Transport der Fe^{3+}-Ionen in Richtung zur Elektrodenoberfläche und dem Abtransport des Reduktionsproduktes (Fe^{2+}-Ionen) durch die Membran ein Gleichgewicht einstellt.

Voltammetrische Untersuchungen mit überlagerter Wechselspannung

Bei diesen Untersuchungen brauchen die Lösungen nicht mit Inertgas gespült zu werden, da Sauerstoff irreversibel reduziert wird und keinen Spitzenstrom gibt. Als Depolarisatoren werden Bi^{3+}-, Tl^{+}-, Pb^{2+}-, Cd^{2+}-, Cu^{2+}- und Zn^{2+}-Ionen eingesetzt. Zur Kontrolle werden gleichzeitig Wechselstrompolarogramme mit der D.M.E. registriert.

Abb. 2 zeigt eine Aufnahme einer Lösung, die jeweils $2 \cdot 10^{-4}$ Mol l^{-1} Bi^{3+}- und Tl^{+}-Ionen enthält. In 0.1 *M* Perchlorsäure als Leitelektrolyt werden an der Quecksilbermembranelektrode unter stationären Bedingungen gut ausgebildete Spitzenströme erhalten. Bei einer Wechselspannungsamplitude von 20 mV kann mit dem phasenselektiven Gleichrichter ein guter Grundstrom erhalten werden. Die Spitzenpotentiale kommen den entsprechenden Halbstufenpotentialen nahe.

Keine Spitzenströme werden erhalten für das Cu^{2+}-Ion im Konzentrationsbereich von 10^{-5} bis 10^{-3} Mol l^{-1} im neutralen wie auch im sauren Leitelektrolyten (0.1 *M* Acetatpuffer pH 5.6 bzw. 0.1 *M* $HClO_4$). Erst ab Konzentrationen von $2 \cdot 10^{-3}$ *M* Cu^{2+} kann das Auftreten von Spitzenströmen beobachtet werden. Dagegen entstehen an der D.M.E. schon ab 10^{-5} Mol l^{-1} Strompeaks. Ein ähnliches Verhalten wird auch beim Zn-Ion beobachtet. Es liegt die Vermutung nahe, dass die Irreversibilität der Elektrodenprozesse für diese Erscheinung verantwortlich gemacht werden kann. Wahrscheinlich wird die Irreversibilität der Cu- und Zn-Abscheidung durch das Vorhandensein der CAM noch verstärkt und dadurch das Auftreten von entsprechenden Strompeaks verhindert.

In Abb. 3 wird die Abhängigkeit der Spitzenstromwerte von der Konzentration an Cd^{2+}-Ionen dargestellt. Im Bereich von 10^{-5} bis 10^{-4} *M* Lösungen wird eine

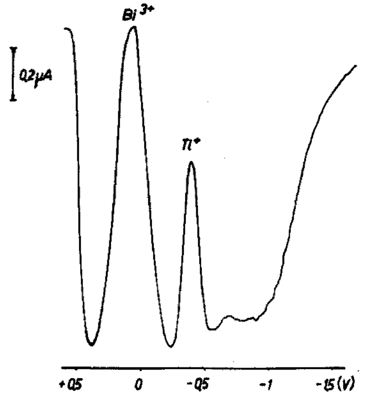

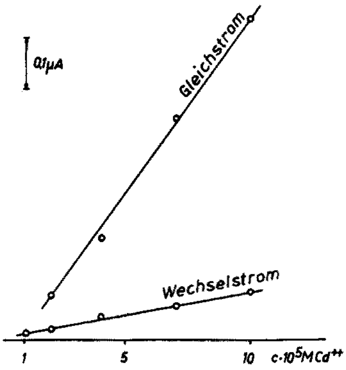

Abb. 2. Voltammetrie mit überlagerter Wechselspannung. Spitzenströme für Bi^{3+}- und Tl^{+}-Ionen. $2 \cdot 10^{-4}$ Mol l^{-1} Bi^{3+} und Tl^{+}, Amplitude 20 mV.

Abb. 3. Vergleichende Konzentrationsabhängigkeit für Voltammetrie mit Gleich- und überlagerter Wechselspannung. Cd^{2+} in 0.5 M KNO_3 + 1.3 M NH_4OH.

lineare Abhängigkeit erhalten. Mit einer Linearität über einen noch grösseren Bereich kann kaum gerechnet werden, weil die Gesamtimpedanz der Messanordnung gegenüber der Anordnung mit der D.M.E. relativ hoch ist.

In der gleichen Abbildung sind die Stromstärken für die mit Gleichspannung erhaltenen Strom–Spannungskurven eingezeichnet. Die Gerade für die Konzentrationsabhängigkeit der Gleichstromwerte verläuft wesentlich steiler als die Gerade für die Wechselstromwerte. Deshalb erscheint die Voltammetrie mit Gleichspannung für Konzentrationsbestimmungen geeigneter als die Methode mit überlagerter Wechselspannung.

Inversvoltammetrische Untersuchungen

Bei der inversen Polarographie und Voltammetrie wird das zu bestimmende Ion vor der Bestimmung an der Arbeitselektrode elektrolytisch angereichert. Die Anreicherung erfolgt bei der vorliegenden Quecksilbermembranelektrode durch die Membran hindurch an der stehenden Quecksilbersäule. Die Elektrolysespannung des Anreicherungsschrittes wählt man in der Regel 0.2 bis 0.4 V negativer als das polarographische Halbstufenpotential. Bei diesen Untersuchungen wird das Cu^{2+}-Ion bei −0.5 V und das Cd^{2+}-Ion bei −1 V gegen S.C.E. angereichert.

Der elektrochemische Bestimmungsschritt besteht in der Umkehrung des Anreicherungsvorganges. Durch Oxydation der kathodisch abgeschiedenen Metalle werden anodische Auflösungsströme erhalten. Wie am hängenden Quecksilbertropfen werden in Abhängigkeit von der Anreicherungszeit am Quecksilber typische Kurven für den Auflösungsstrom des Amalgams erhalten. In Abb. 4 ist das Ergebnis für eine 10^{-5} M Cu^{2+}-Lösung im 0.1 M Acetatpuffer vom pH 5.6 dargestellt. Zunächst nimmt der Auflösungsstrom mit der Anreicherungszeit linear zu, bis er schliesslich einen Grenzwert erreicht, wo eine grössere Anreicherungszeit keinen höheren Peakstrom mehr verursacht. In diesem Bereich der Kurve ist die Diffusion des Amalgams von der Oberfläche ins Innere des Quecksilbers so gross, dass sie die weiterhin

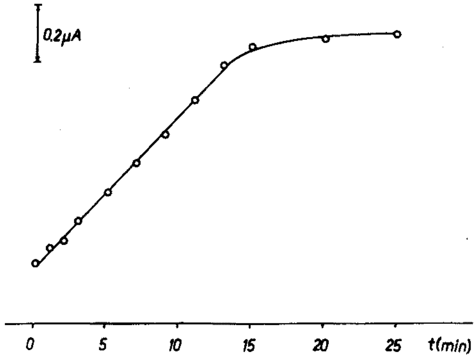

Abb. 4. Abhängigkeit des Auflösungsstromes i_p von der Elektrolysezeit t. 10^{-5} M Cu^{2+} in 0.1 M Acetatpuffer (pH 5.6).

erfolgende Konzentrationszunahme des Amalgams ausgleicht. Die inversvoltammetrische Bestimmung der Cu^{2+}-Ionen erfolgt nach einer Anreicherungszeit von 13 Min und die der Cd^{2+}-Ionen nach 5 Min.

Im Quecksilber erfolgt eine sehr schnelle Verteilung des gebildeten Amalgams. Diese bewirkt, dass beim anodischen Auflösungsvorgang nicht sämtliches Amalgam oxidiert wird. Bei mehrmaligem Anreichern an der gleichen Quecksilberoberfläche nimmt daher der Auflösungsstrom allmählich zu. Eine Erneuerung des mit der Membran in Berührung stehenden Quecksilbers ermöglicht dagegen, gleichbleibend hohe Auflösungsströme unter gleichen Bedingungen zu erzielen. Bei einer für die voraufgegangenen Untersuchungen verwendeten Quecksilberfliessgeschwindigkeit ist schon eine Zeitspanne von 30 sec für die Quecksilbererneuerung ausreichend.

Die Abhängigkeit des Auflösungsstromes i_p von der Metallionenkonzentration ergibt für das Cd^{2+}-Ion im Konzentrationsbereich von $3\cdot10^{-6}$ bis 10^{-4} Mol l^{-1} (im 0.1 M Acetatpuffer vom pH 4.6) eine ausgezeichnete Linearität. Sowohl für das Cd^{2+}- als auch für das Cu^{2+}-Ion liegt die Nachweisgrenze bei dieser Bestimmungsmethode bei $3\cdot10^{-6}$ Mol l^{-1}. Diese relative "Unempfindlichkeit" wird verursacht durch das ungünstige Verhältnis von Quecksilberoberfläche zu -volumen, das bei der D.M.E. wesentlich günstiger für die Elektrodenoberfläche ausfällt.

Sofern die Cd-Ionenkonzentration $3\cdot10^{-6}$ Mol l^{-1} und die Cu^{2+}-Ionenkonzentration $5\cdot10^{-6}$ Mol l^{-1} übersteigt, werden typische Peakvoltammogramme erhalten. Sonst werden Strom–Spannungskurven ohne Ausbildung von Peaks registriert.

Untersuchungen an der gefüllten Celluloseacetatmembran

Neben der reinen CAM wurden auch solche Membranen untersucht, die mit bestimmten Füllstoffen getränkt wurden, die dann durch Lösungswechsel (pH-Änderung, Lösungsmittelwechsel) in der Membran fixiert werden können. Zu diesem Zweck wurden als Komplexbildner 8-Hydroxychinolin und das 5,5-Methylen-bis-(8-Hydroxychinolin) und als Komplex das Cadmiumoxinat eingesetzt. Mit Hilfe dieser Füllstoffe müsste es möglich sein, bestimmte Ionen aus der Lösung zu binden, d.h., sie selektiv anzureichern. Bei anderer Zusammensetzung der Lösung (z.B. pH-Änderung) müssen sie jedoch aus der Membran wieder herausgelöst und am Quecksilber bestimmt werden können.

Prinzipiell gelingt es, Metalle am Komplexbildner (siehe Abb. 5) bzw. am schwachen Komplex unter Bildung eines stärkeren Komplexes in der Membran zu binden und zu bestimmen. Für quantitative Betrachtungen wie Abhängigkeit des Auflösungsstromes von der Metallionenkonzentration in der Lösung und der Anreicherungszeit des Metallions am Komplexbildner und Komplex sind diese gefüllten Membranen jedoch nicht geeignet. Ursache dafür ist ein mehr oder weniger starkes Verstopfen der Membranporen durch den Füllstoff, wodurch die Anreicherung am Füllstoff der Membran und das Ablösen des betreffenden Ions zwecks Anreicherung am Quecksilber stark behindert werden.

BETRACHTUNG DER UNTERSUCHUNGSERGEBNISSE MIT DER p.a. IMINODIESSIGSÄURE-HARZMEMBRAN

Von Hering und Mitarbeitern[7] liegen Untersuchungen vor über die Komplexbildung mit ein- und mehrwertigen Metallionen am monofunktionellen (p.a.) Iminodiessigsäure(IDE)-Harz. Für Trennungen von Metallionengemischen ist es am günstigsten, wenn der Austauscher in der Monoalkaliform, am besten in der Monokaliumform, vorliegt. Die Elution erfolgt mit einer Mineralsäure.

Die Chelonharzmembran mit p.a. IDE-Ankergruppen wurde im VEB Filmfabrik Wolfen in einer Schichtdicke von *ca.* 1 mm hergestellt.

An der vorliegenden Messanordnung ergibt sich für die Harzmembran in der H-Form in 0.1 *M* Perchlorsäure ein Polarisationsbereich von +0.4 bis −0.85 V gegen S.C.E. Dabei treten trotz Spülens mit Inertgas und negativen Polarisierens beide Sauerstoffstufen auf. Da die Elution wie bei den gefüllten CAM im sauren Medium erfolgt, muss wegen des störenden Auftretens der Sauerstoffstufen die inverse Voltammetrie als Bestimmungsmethode herangezogen werden.

Während am p.a. IDE-Harz eine ganze Reihe von Elementen adsorbiert und

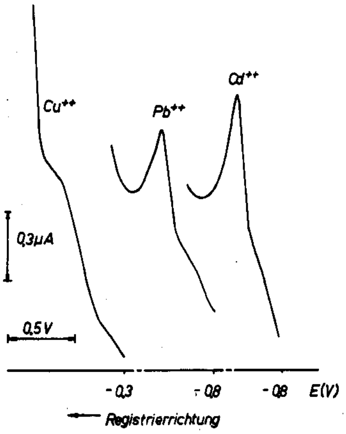

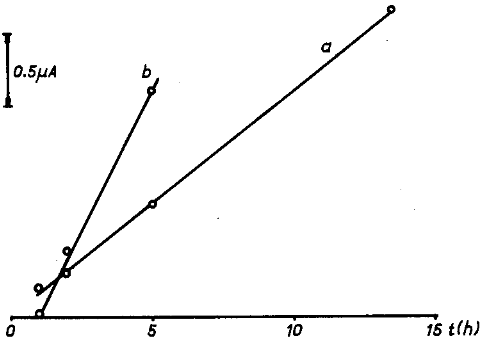

Abb. 5. Anreicherung an einer Oxinmembran. Inversvoltammetrische Bestimmung von Cu^{2+}, Pb^{2+} und Cd^{2+}, eingesetzte Konzentration 10^{-5} Mol l^{-1}, Anreicherungszeit 2 Std.

Abb. 6. Abhängigkeit der Spitzenströme von der Anreicherungszeit an der p.a. IDE-Harzmembran. 10^{-5} *M* Cd^{2+} in (a) $HClO_4$ (pH 4); (b) 0.1 *M* Acetatpuffer (pH 5.6). Elutionsmittel $3 \cdot 10^{-2}$ *M* $HClO_4$ in 0.1 *M* KNO_3.

verdrängungschromatographisch bestimmt werden können, lassen sich nur die Cu^{2+}-, Cd^{2+}- und Pb^{2+}-Ionen nach dieser Methode bestimmen, da die Halbstufenpotentiale oder Peakpotentiale der anderen Elemente ausserhalb oder am Rande des ermittelten Messbereiches für diese Anordnung liegen.

Die Strom–Zeit-Charakteristik für die p.a. IDE-Harzmembran ergibt für den Durchtritt des Cu^{2+}-Ions aus einer 10^{-5} *M* Cu^{2+}-Lösung in 1 *M* $HClO_4$, dass etwa 180 Min bis zum Erhalten konstanter Auflösungsströme benötigt werden. Für das Cd^{2+}-Ion liegen die Durchtrittszeiten bei etwa 240 Min in 0.1 *M* $NaClO_4$-Lösung. Diese Zeitspannen reduzieren sich bei der Elution der an der Chelonharzmembran schon angereicherten Metallionen auf 60 bis 120 Min.

Die Ursache für diese langen Durchtrittszeiten liegt im Aufbau der Membran begründet. Während die CAM eine Matrix ohne Festionen darstellt, besitzt die p.a. IDE-Harzmembran eine hohe Festionenkonzentration. Die Durchtrittszeit für ein Ion kann nur gemessen werden, indem eine Lösung eines Ions mit dem für dieses Ion zutreffenden Dekomplexierungs-pH-Wert verwendet wird. Der Durchtritt vollzieht sich dabei in Wechselwirkung mit den p.a. IDE-Ankergruppen, wodurch die längeren Durchtrittszeiten verursacht werden.

Die Abhängigkeit des Auflösungsstromes i_p von der Anreicherungszeit des Ions am Quecksilber in einer 10^{-4} *M* Cd^{2+}-Lösung (0.1 *M* $NaClO_4$) ergibt bei Anreicherungszeiten über 14 Min konstante Peakströme. Bis zu Anreicherungszeiten von 10 Min steigen die Stromwerte linear mit der Anreicherungszeit an. Bei den folgenden Untersuchungen werden alle Ionen stets 10 Min am Quecksilber angereichert, um für diese Ionen Vergleichsmöglichkeiten zu besitzen.

Die Anreicherungen von Metallionen erfolgen ausserhalb der Messzelle. Danach muss die Membran gründlich gewaschen werden, um ein vollständiges Herauswaschen von freien Ionen aus der Membran zu gewährleisten. Ausserdem ist so eine bessere Ausnutzung der Messanordnung möglich.

In acetatgepufferter Lösung werden im Vergleich zur ungepufferten Lösung höhere Spitzenströme erzielt. Gleichzeitig liegen aber auch grössere Zeitspannen zwischen Elutionsbeginn und dem Erhalten konstanter Peakströme. Diese Stabilitätserhöhung wird erklärt durch zusätzliche Koordination von Acetationen. Wegen des grösseren Zeitbedarfs werden die folgenden Anreicherungen in ungepufferten Lösungen vom pH 4 ($HClO_4$) durchgeführt.

In Abb. 6 ist die Abhängigkeit der Spitzenstromstärke von der Anreicherungszeit an der p.a. IDE-Harzmembranen in ungepufferter (*a*) und in gepufferter Lösung (*b*) dargestellt.

Die Untersuchung der Abhängigkeit des Auflösungsstromes von der zur Anreicherung an der p.a. IDE-Harzmembran eingesetzten Ionenkonzentration erfolgt durch Anreicherung über 2 Stunden aus Cd-Lösungen steigender Konzentrationen vom pH 4 ($HClO_4$). Eluiert wird mit Perchlorsäure (pH 1.5) im 0.1 *M* KNO_3-Leitelektrolyten. Im untersuchten Konzentrationsbereich von $3 \cdot 10^{-6}$ bis 10^{-4} Mol l^{-1} Cd^{2+} wird eine ausgezeichnete lineare Abhängigkeit des Auflösungsstromes von der Cd^{2+}-Ionenkonzentration beobachtet. Die Nachweisgrenze für das Cd^{2+}-Ion liegt unter diesen Bedingungen für diese Methode nahe unterhalb $3 \cdot 10^{-6}$ Mol l^{-1}. Die Verwendung acetatgepufferter Lösungen bei der Anreicherung ergibt jedoch eine Möglichkeit, dieses Verfahren noch empfindlicher zu gestalten.

Abb. 7 zeigt die Auflösungsströme, die für das Cu^{2+}-, Pb^{2+}- und Cd^{2+}-Ion

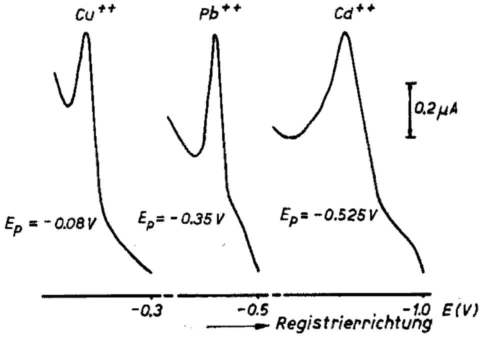

Abb. 7. Peakströme für Cu^{2+}, Pb^{2+} und Cd^{2+} nach Anreicherung an der p.a. IDE-Harzmembran. Konzentration je 10^{-5} Mol l^{-1}, Anreicherungszeit an der Membran 2 Std., am Quecksilber 10 Min.

nach zweistündiger Anreicherung an der Harzmembran aus 10^{-5} *M* Lösungen (pH 4) erhalten werden. Diese Peaks sind gut ausgebildet und lassen sich gut auswerten.

Neben der Anreicherung von nur einem Ion an der p.a. IDE-Harzmembran können auch mehrere Ionen zugleich (z.B. Cd^{2+} und Cu^{2+}) an den Festionen der Membran fixiert werden. Nach Elution mit einem gemeinsamen Elutionsmittel (1 *M* $HClO_4$) werden dann nacheinander die Peaks für die Auflösung des Cd- und des Cu-Amalgams erhalten. Die Höhe der Strompeaks stimmt dabei für die beiden Ionenarten sehr gut überein.

Um nach gemeinsamer Anreicherung an der Membran die Ionen getrennt zu eluieren, wird zunächst das schwächer gebundene Ion aus dem Harz herausgelöst und bestimmt. Danach erst erfolgt die Elution mit dem stärkeren Elutionsmittel. Als Anwendungsbeispiel für diese Möglichkeit dient die Trennung von Cu^{2+}- und Cd^{2+}-Ionen, wobei zunächst die Cd-Ionen mit $3 \cdot 10^{-2}$ *M* Perchlorsäure in 0.1 *M* KNO_3-Lösung dekomplexiert und bestimmt werden. Erst nach Elution mit 1 *M* Perchlorsäure erfolgt die Cu-Bestimmung. Die für die Cd- und Cu-Amalgamauflösung erhaltenen Peaks sind etwa gleich hoch.

Eine gemeinsame Dekomplexierung kann nach erfolgter Adsorption von Cu^{2+}- und Pb^{2+}-Ionen an der Harzmembran mit 1 *M* HNO_3 durchgeführt werden. Die Spitzenströme stimmen gut überein.

Nach der Anreicherung von zwei bestimmbaren Ionen an der Harzmembran wird weiter untersucht, ob Ionen, die an der Membran adsorbiert werden, mit der inversvoltammetrischen Methode aber nicht bestimmt werden können, die Bestimmung des Cu^{2+}- bzw. des Pb^{2+}-Ions stören. So erfolgt die gemeinsame Anreicherung folgender Ionen in einem Zeitraum von 2 Std. aus ihren 10^{-5} *M* Lösungen vom pH 4: Cu^{2+}/Co^{2+} (1), Cu^{2+}/Ni^{2+} (2), Cu^{2+}/Zn^{2+} (3), $Cu^{2+}/Co^{2+}/Ni^{2+}$ (4), $Cu^{2+}/Co^{2+}/Ni^{2+}/Zn^{2+}$ (5), Pb^{2+}/Zn^{2+} (6), und Pb^{2+}/Co^{2+} (7). Für die Kombinationen 1, 2 und 4 werden Spitzenströme für die anodische Auflösung des Cu- bzw. Pb-Amalgams registriert, die gut mit den in 10^{-5} *M* Cu^{2+}- und Pb^{2+}-Lösungen erhaltenen Werten übereinstimmen. In den anderen Fällen treten Störungen auf, die entweder auf eine störende Beeinflussung bei der Anreicherung an der p.a. IDE-Harzmembran oder (und) an der Quecksilberoberfläche zurückzuführen sind.

Eine weitere Möglichkeit zur Trennung von Ionen bilden die unterschiedlichen

DpH-Werten der gebildeten Komplexe. Wenn der pH-Wert der Lösung, in der die Anreicherung an der Membran erfolgen soll, weit genug unterhalb des DpH eines schwächer gebundenen Ions liegt, wird nur das fester fixierte Ion an der Harzmembran festgehalten. Auf diese Weise kann das Cu^{2+} selektiv aus einer Cu^{2+}/Cd^{2+}-Lösung (pH 1.5) an der p.a. IDE-Harzmembran angereichert werden. Eine Vortrennung erfolgt so auch in der $Cu^{2+}/Pb^{2+}/Cd^{2+}$-Lösung, aus der nur die Cu^{2+}- und Pb^{2+}-Ionen bei diesem pH-Wert am p.a. IDE-Harz gebunden werden. Die Trennung dieser beiden Ionenarten erfolgt dann nach gemeinsamer Elution mit 1 *M* Perchlorsäure am Quecksilber aufgrund ihrer unterschiedlichen Peakpotentiale.

Durch geeignete Wahl des pH-Wertes der Ausgangslösung, durch ein geeignetes Elutionsmittel und durch die unterschiedlichen Peakpotentiale für die Auflösung des Amalgams ergeben sich eine ganze Reihe von Möglichkeiten zur Auftrennung von Metallionengemischen.

ZUSAMMENFASSUNG

Es wird eine neue Membranelektrode für voltammetrische Messungen vorgeschlagen, bei der die Quecksilberelektrode durch eine Celluloseacetatmembran von der Lösung getrennt ist. Die Anordnung gestattet ein schnelles Auswechseln der Membranen. Polarographisch erfassbare Metallionen lassen sich in weitem Konzentrationsbereich von $6 \cdot 10^{-5}$ bis $1.5 \cdot 10^{-3}$ *M* durch konzentrationsproportionale Ströme mit Gleich- und Wechselstrompolarographen bestimmen. Inversvoltammetrische Anreicherungen geringer Konzentrationen sind ebenfalls möglich. Eine Füllung der Membranen mit Komplexbildnern zur stromlosen Anreicherung von Metallen bzw. mit Metallkomplexen zur Anreicherung unter Metallionenaustausch ist möglich, analytisch jedoch nocht nicht verwendbar. Dagegen lassen Ionenaustauschermembranen mit polyfunktionellen Ankergruppen selektive Anreicherungen von Metallionen mit folgender voltammetrischer Bestimmung zu.

SUMMARY

A new membrane electrode in which mercury is separated from the solution by a cellulose acetate membrane is suggested for voltammetric measurements. The arrangement allows a rapid exchange of the membranes. Polarographically active metal ions may be determined from the currents which are proportional to concentration in a wide range from $6 \cdot 10^{-5}$ to $1.5 \cdot 10^{-3}$ *M*. Lower concentrations may be detected by inverse-voltammetric measurements after accumulation on the mercury surface. The membranes may be filled with complexing agents for currentless accumulation of metal ions or with metal complexes for accumulation after an exchange reaction of the metals in the complex, but this is not yet applicable to analytical measurements. However, selective accumulations with subsequent voltammetric determination of small amounts of metal ions are possible by using membranes of ion-exchange resins with polyfunctional groups.

RÉSUMÉ

On propose une nouvelle électrode à membrane, avec séparation du mercure

d'avec la solution, par une membrane d'acétate de cellulose, pour des mesures voltammétriques. Ce système permet un échange rapide des membranes. Les ions métalliques polarographiquement actifs peuvent être dosés par mesure de courant, proportionnel à la concentration (de $6 \cdot 10^{-5}$ à $1.5 \cdot 10^{-3}$ *M*). Des concentrations inférieures peuvent être décelées par mesures voltammétriques inverses, après accumulation sur la surface du mercure. Des accumulations sélectives avec dosage voltammétrique successif de faibles quantités d'ions métalliques sont possibles en utilisant des membranes de résines échangeuses d'ions, avec des groupes polyfonctionnels.

LITERATUR

1 J. H. Clausen, G. B. Moss und J. Jordan, *Anal. Chem.*, 38 (1966) 1398.
2 P. Delahay und G. Charlot, *Anal. Chem.*, 32 (1960) 103A.
3 R. C. Bowers und A. M. Wilson, *J. Amer. Chem. Soc.*, 80 (1958) 2968.
4 A. Braunwalder, A. Grubenmann und F. Hügli, *Chimia (Aarau)*, 15 (1961) 461.
5 P. Bersier, J. Bersier und F. Hügli, *Helv. Chim. Acta*, 43 (1960) 478.
6 H. Gerber, R. Schaich und F. Hügli, *Chimia (Aarau)*, 19 (1965) 503.
7 Literatur in R. Hering, *Chelatbildende Ionenaustauscher*, Akademie-Verlag, Berlin, 1967.

Analytica Chimica Acta
Elsevier Publishing Company, Amsterdam
Printed in The Netherlands

A MICROWAVE-INDUCED ARGON PLASMA SYSTEM SUITABLE FOR TRACE ANALYSIS

K. M. ALDOUS, R. M. DAGNALL, B. L. SHARP AND T. S. WEST

Chemistry Department, Imperial College of Science and Technology, South Kensington, London, S.W.7 (England)

(Received 2nd November 1970)

In recent years there has been interest in the development of non-flame cells for spectroscopic analysis, *e.g.* the L'vov furnace[1], Massmann furnace[2], carbon filament atom reservoir[3] and platinum loop devices[4]. These have been shown to be valuable when the liquid sample available for analysis is too small for conventional pneumatic nebulising systems and when dilution results in concentrations below the detection limit. Non-flame cells, however, generally cannot be used for emission purposes because they lack the excitation energy necessary. In consequence, most emission studies have been concerned with the use of high-frequency or microwave-excited inert or diatomic gas plasmas[5-9] as an alternative to the use of flames. The main advantages of these systems are the high electronic excitation temperature (as high as 10,000°K) and the presence of an inert gas atmosphere which tends to preclude the formation of stable species such as metal oxides and hydroxides. However, in most instances, as with the use of flames, it is necessary to use conventional nebuliser systems for sample introduction, which reduces the detection limits obtained with most plasma systems.

The use of alternative methods of sample introduction has been suggested by Cooke *et al.*[10] and more recently by Runnels and Gibson[11], who both used low-powered, microwave-induced plasmas. In the former method, organic species eluted from a gas chromatographic column were introduced into the plasma cell; in the latter, excitation of mostly organometallic species was obtained in a plasma stream following volatilisation of a film of material from a heated platinum filament. However, the spectral measurements must be made through a quartz cell or tube which is subject to corrosion and plating-out of the elements of interest. In addition, we have found that when the procedure described by the latter workers is used, the plasma stability and analytical sensitivity depend on the solvent used.

The method described in this paper utilises a simple low-powered, microwave-induced argon plasma supported at the mouth of a quartz tube which is in turn connected to a platinum or tungsten loop[4] sample introduction device. The system provides a sensitive emission source for a wide range of elements and is suitable for very small sample volumes. In addition, a simple amplifier/integrator detection system is described which is capable of following the weak and transient emission signals received at the photomultiplier.

EXPERIMENTAL

Plasma system

The microwave-induced argon plasma system is depicted in Fig. 1. Microwave energy (2450±25 MHz) was derived from a "Microton 200"-microwave generator (Electro-Medical Supplies, Wantage, England) and coupling was via an Evenson type 1/4 λ resonant cavity (Electro-Medical Supplies 214 L). The radiation emitted from the plasma after sample volatilisation from the platinum or tungsten loop was viewed by means of a Unicam SP900 spectrophotometer with an EMI 9601B photomultiplier. The read-out unit normally incorporated in the instrument was by-passed in favour of the more rapid amplifier/integrator unit described below.

In the initial experiments a platinum loop was utilised to support the liquid sample and emission from cadmium (at 228.8 nm) was selected in order to optimise the various experimental parameters of the system.

Electronic read-out

Weak and transient light signals such as those obtained in the system outlined in this manuscript cannot be recorded by conventional d.c. amplification techniques common to most spectrophotometers. Normally the response time of the electronic

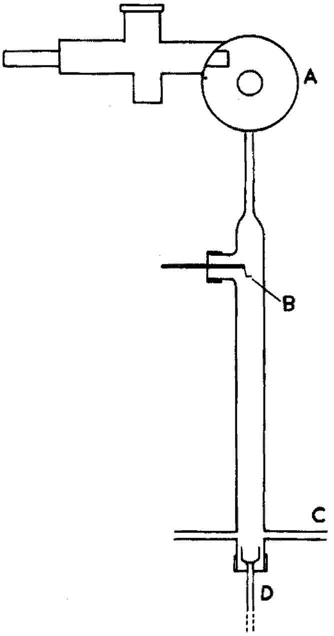

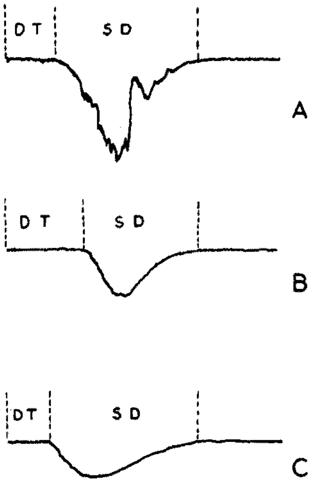

Fig. 1. Plasma cell and microwave cavity. (A) Microwave cavity, (B) platinum or tungsten loop, (C) gas inlets, (D) sample cup.

Fig. 2. Effect of argon flow rate on cadmium emission signal profile. Argon flow rate 2.5 l min^{-1} (A); 1.8 l min^{-1} (B); < 1.6 l min^{-1} (C). DT, delay time; SD, signal duration.

circuitry is high (approaching or even longer than the lifetime of the signal) which results in poor reproducibility and detection limits[12]. Figure 2 shows typical "pulses" of emission produced when a cadmium sample is vaporised from a platinum loop and is allowed to enter the plasma region. The radiation emitted at 228.8 nm was recorded via the spectrophotometer photomultiplier, the output of which was connected directly to a storage oscilloscope. These traces can be photographed and evaluated at a later date, but this is time-consuming and unnecessary. The emission signal is not always perfectly Gaussian in shape and integration of the total signal is the most obvious method. In such instances, the more commonly encountered spectroscopic apparatus utilising direct potentiometric recorder peak-height measurement would give poor reproducibility because of the relatively large response times of the recorder and amplifier circuits.

The rapid electronic amplifier/integrator described is capable of measuring this type of signal and the use of this or similar circuitry should be encouraged whenever transient signals or signals with a lifetime approaching that of the measuring system are encountered.

The dynode chain of the EMI 9601B photomultiplier present in the spectrophotometer was connected to negative EHT supply (*ca.* 1.0 kV) and the output was connected directly to the amplifier/integrator shown in Fig. 3, which was in turn connected to a Servoscribe potentiometric recorder.

Operating procedure

Allow about 20 min before making a series of measurements to permit stabilisation of supply and circuit. With switch S1 in position 1 (see Fig. 3), set up the first operational amplifier (OAl) for voltage and current trim. With the 5 kΩ potentiometer at the earth end of its track, adjust RV1 until there is 0 V at the output. (This can be determined with the Servoscribe recorder on the 2-mV range.) When this is achieved, the first operational amplifier is current-trimmed. Select the voltage trim ($R_{T_1}+R_{T_2}$) according to the value suggested by the manufacturer.

With S1 in position 2 and S2 in position 1, trim the second operational amplifier (OA2) as before·by adjusting the helipot RV2.

If the off-sets have been correctly adjusted, S1 can be moved now to position 3 with readjustment of any trims provided there is no input current. The unit now operates as an amplifier with a gain of × 100. With switch S2 in position 2, the unit integrates the input signal after a gain of × 10 (due to OA1). The capacitor in the feedback loop of the OA2 charges at a rate proportional to the input voltage such that

$$E_{\text{output}} = -(RC)^{-1}\int_0^t E_{\text{in}}\,\mathrm{d}t.$$

Thus for a 10-V output, 50 mV would have to be applied at the input for 1 sec.

The output voltage can be reset by pressing the reset button which discharges the capacitor.

Before each series of measurements the dark current from the photomultiplier tube must be offset. This is achieved by operating the OA1 in a differential mode and offsetting the positive input with the 5 kΩ preset such that with S1 in position 3 ans S2 in position 1 there is 0 V output. This means that the integrator, when S2 is in position 2, does not integrate the dark current, but only integrates the signal pulse. The zero can

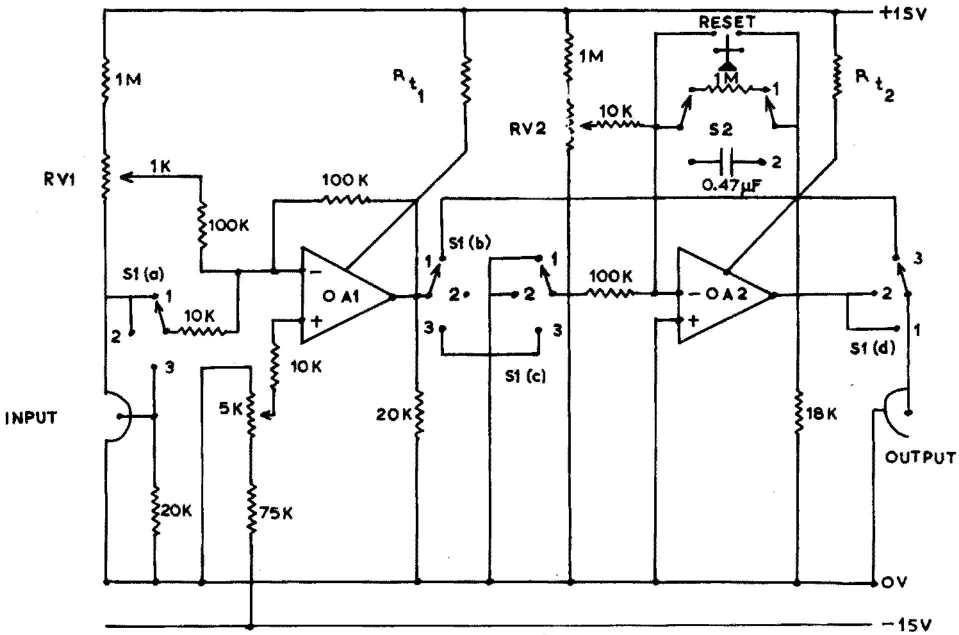

Fig. 3. Amplifier/integrator circuit:
OA1 = operational amplifier no. 1 } Philbrick PF85AU
OA2 = operational amplifier no. 2 }
S1 = switch no. 1—3 way 4 pole
S2 = switch no. 2—2 way 4 pole
RV1 = current off-set
RV2 = integrator off-set
Resistors, 0.5 W Hystab (Radiospares Ltd.)
Power supply, −15, 0, +15 V, Coutant OA10 stabilised supply unit.

be accurately trimmed before each reading by using the helipot RV2 to ensure integration is giving zero output. Once the radiation pulse has been recorded the output voltage is steady until the reset button is pushed.

The cost of the electronic system is very low, but the use of more expensive chopper-controlled operational amplifiers would eliminate many of the trimming and resetting operations described above.

The plasma cell

The plasma cell was constructed in transparent quartz from a piece of 8-mm (internal diameter) tubing *ca.* 10 cm in length with a jet fused into one end of it. The gas inlets were attached at the lower end, and a third part just below the fused jet allowed the platinum or tungsten loops to be introduced via a PVC plug. Dimensions were not found to be very critical except in the case of the jet which should be 2-mm internal diameter and sufficiently long to give laminar gas flow at the orifice. If the jet is too short, the plasma will be unstable and difficult to ignite. It was not possible to make the jet diameter equal to the diameter of the plasma (see below) because the gas velocity was then too great for the plasma to be ignited. Use of a 2-mm jet, however, caused the plasma to wander somewhat and hence change its position relative to the spectrophotometer slit. Because of the different rates of diffusion of ions and electrons, plasmas in general have a negative sheath and a positive core. It was hence possible to solve the problem by securing to the jet a 15-mm length of 1-mm steel rod such that it was opposite the centre of the slit and parallel to it. The plasma induces a positive region within the steel rod and is thus attracted to it and held parallel to the slit. A pyrex sample cup (minimum capacity 20 μl) was sealed onto a greased glass rod and mounted into the main tube via a PVC plug; this allows the cup to be slid up and down so that the sample solution may be supplied to the loop. The diameter of the cup must be small enough so that gas is allowed to pass in its raised position without quenching the plasma. Alternatively, the liquid sample may be introduced with a syringe.

The plasma

The main body of the plasma was formed above the jet orifice so that plating out and devitrification problems encountered when the plasma is operated within a quartz tube were eliminated. We have found this to be a particularly difficult problem which cannot readily be solved by other methods. Under the recommended experimental conditions (see below) a short section of the plasma (*ca.* 2 mm) remained in the tube whilst a stable plasma pencil some 20 mm in length and 1.0 mm in diameter extended beyond the orifice. The plasma was formed by first tuning the cavity to minimum reflected power (with a reflected power meter) and then by initiating with a "Tesla" vacuum tester.

Sample loops

For most of the studies reported here, loops were made from 10-mm lengths of 0.1-mm diameter platinum wire. The loops formed resembled an ellipse with a major axis of 0.86 mm and a minor axis of 0.62 mm.

It was found that such a loop when just dipped into aqueous solution picked up a sample volume of *ca.* 0.12 μl which is in the form of a surface tension film with reproducible dimensions. The measurement was made by taking ten samples from a solution containing 1000 μg Cd ml^{-1}, washing them into a 10-ml volumetric flask and analysing the resulting solutions by atomic absorption spectroscopy. Several loops were made and their sampling volumes were found to range between 0.1 and 0.15 μl.

The aqueous film was evaporated first by the passage of *ca.* 0.1 A d.c. (via a 4.5 V battery and variable resistance); during this process the plasma became less stable and shorter in length. Then the current was increased to *ca.* 1.9 A which caused the compound remaining on the loop to vaporise and pass into the plasma region. Tungsten loops formed from 0.1-mm tungsten wire were used when a higher volatilisation temperature than could be achieved with platinum was required.

Optimal operating conditions

Argon flow rate. Gas flow rate was found to be the most critical factor influencing plasma stability and therefore a careful examination of its effect was made. An oscilloscope with a storage facility was used to observe the signal profile obtained when a sample containing 10 μg Cd ml^{-1} was vaporised into the plasma at varying gas flow rates. Provision of a calibrated time base on this instrument also enabled the delay time (from the switch-on of the loop current to the beginning of the signal profile) and signal duration to be measured. With an argon flow rate of 2.95–2.10 l min^{-1}, the plasma was unstable owing to turbulence in the gas jet. Figure 2A shows a typical signal profile under these conditions; the shape is non-Gaussian in nature having a linear growth and exponential decay. The turbulence of the plasma is reflected in the positive and negative fluctuations superimposed on the main profile. In this instance the delay time was 75 msec and the signal duration 225 msec.

The plasma was stable when the argon flow rate was between 2.10 and 1.64 l min^{-1} and was easy to initiate. The profile obtained (Fig. 2B) is smoother than before and slightly flattened at the bottom. This indicates that the sample vaporisation rate and the rate at which the argon is carrying the vapour to the plasma are approximately equal. The delay time was again 75 msec and the signal duration was slightly longer at 250 msec.

Below 1.64 l min^{-1} the plasma rapidly decreased in length and was finally quenched at a flow rate of *ca.* 1.03 l min^{-1}. Plasmas in general are sensitive to the introduction of molecular species and the rate of sample introduction must be low to

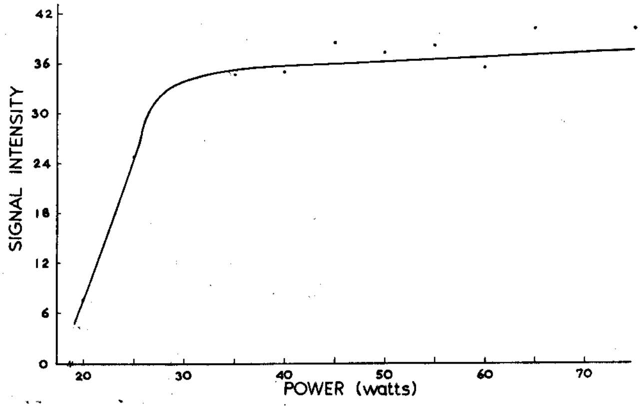

Fig. 4. Effect of microwave power on cadmium emission intensity.

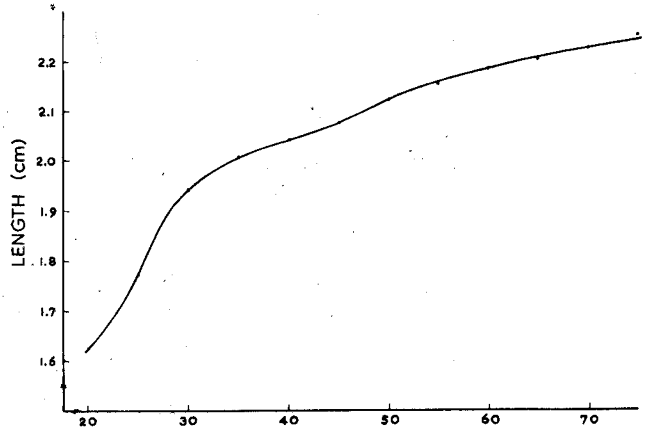

Fig. 5. Effect of microwave power on plasma length.

avoid quenching the plasma. In the system described here (Fig. 2C) a period of ca. 5 sec was required to evaporate the water under normal conditions; a much longer period was necessary at low argon flow rates. In this instance, the signal profile was very shallow along its bottom edge indicating a lower rate of sample introduction to the plasma. The delay time was 90 msec, but the signal duration remained at 250 msec. A flow rate of 1.85 l min^{-1} was chosen as optimum because it resulted in a stable plasma and a reproducible signal profile.

Optimal microwave power. The optimal microwave power was determined with the argon flow rate set at 1.85 l min^{-1}. A stable plasma could be maintained at microwave powers ranging from 20 to 75 W. Samples containing 0.1 μg Cd ml^{-1} were vaporised into the plasma at varying powers within this range and the resulting signals were recorded on a Servoscribe potentiometric recorder (Fig. 4). It was noted that the plasma increased in length with increasing microwave power; Fig. 5 shows a plot of microwave power *versus* plasma length. The graph shows that at about 35 W the length of the plasma reaches 20 mm and then just fills the entrance slit (20 mm long) of the spectrophotometer used. It was therefore concluded that the increase in plasma dimensions was responsible for the steep rise in the signal/power curve (Fig. 4) and not an increase in the translational or electronic excitation temperature. The coupling of the microwave energy to the plasma is not 100% efficient and therefore increasing the input power above the level required to give a stable plasma results in higher reflected powers and a slightly longer plasma, but no increase in the emission signal. The optimal microwave power was selected at 40 W because it represented a point on the plateau of the signal/power curve.

Occurrence of intensity antinodes in the plasma. The entrance slit was blocked except for a 2-mm square portion in the centre to view the plasma. The emission intensities of the argon background and of cadmium signals were then observed at different plasma heights. Identical curves were obtained for each, showing a large maximum opposite the central electrode and a much smaller and less pronounced maximum near the edge of the cavity approximately 9 mm below the first. It is thought that these maxima occur at positions where the electric field intensity within the cavity is greatest.

RESULTS

Analytical working curve for cadmium

Analytical-grade chemicals and deionised water were used in the preparation of all solutions. Ten samples at each concentration examined were vaporised into the plasma and the readings at 228.8 nm were averaged. The slope of the log/log curve (Fig. 6) is unity and the normal analytical working curve is linear over the concentration range 0.01–5.00 μg Cd ml^{-1}. It was not possible to study concentrations above 5.00 μg Cd ml^{-1}, because the capacitor used in the integrator was almost fully charged at this level. Normally this problem could be avoided by reducing the spectral band pass of the monochromator, but this also reduces the background radiation from the plasma, which necessitates changing the backing-off potentiometer in the amplifier system. Curves constructed without using the integrator were not of a reproducible shape and were non-linear, the signal increasing approximately 4-fold for a 1000-fold increase in concentration. The slit width was set at 0.1 mm for most of the experiments reported here. Solutions containing 0.002 μg Cd ml^{-1} were detected with the photo-

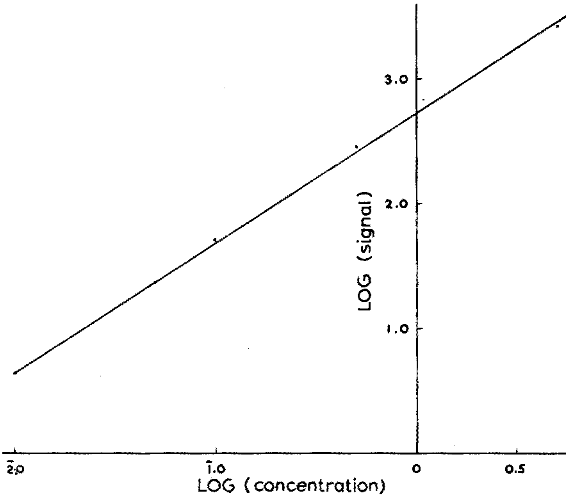

Fig. 6. Log–log analytical working curve for cadmium.

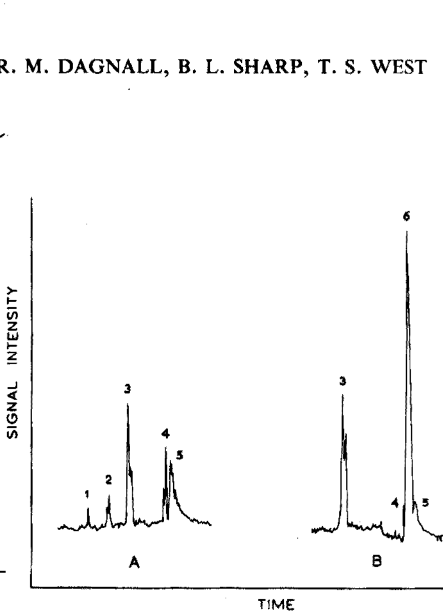

Fig. 7. Arsenic interference on cadmium emission. A: (1, 2, 3) Arsenic signal profiles at room temperatures, (4, 5) arsenic signal profiles with loop at red-heat. B: (3, 4, 5) As above in A, (6) cadmium signal profile with loop at red-heat.

multiplier EHT supply set to its maximum value of 1.2 kV. This represents an absolute detection limit for cadmium of $2 \cdot 10^{-13}$ g. Precision data were obtained by analysing thirty solutions containing 0.25 μg Cd ml^{-1}. The relative standard deviation obtained was 10% which can be attributed to three factors:

(I) drift by the operational amplifiers which were not chopper-stabilised,
(ii) variation in the quantity picked up by the loop, and
(iii) variation in the proportion of sample entering the plasma (the plasma pencil did not completely fill the 2.0-mm jet orifice).

It is thought that improvements with respect to factors (i) and (ii) in particular should considerably increase the precision of the method.

Interferences

Spectral interferences. Solutions containing 0.25 μg Cd ml^{-1} together with various other elements present in 1000-fold molar amounts were studied. The strongest spectral interference associated with cadmium comes from the 228.812-nm direct line emission from arsenic. The solutions of arsenic were prepared by dissolving arsenic trioxide in 20% (v/v) hydrochloric acid and then diluting to volume with water. When a sample containing both cadmium and arsenic was vaporised rapidly by switching the current directly to 1.9 A, a large positive interference was observed. However, it was found subsequently that emission peaks were observed without heating the loop and that further peaks could be obtained by increasing the current to its maximum (1.9 A) over a period of time. Figure 7 shows two traces (unintegrated) which illustrate the effect of adding arsenic to a cadmium solution. The ratio of concentrations was

TABLE I

LIMITS OF DETECTION FOR VARIOUS ELEMENTS

Element	*Wavelength (nm)*	*Loop material*	*Detection limit (g)*	*Detection limit (p.p.m.) for 0.12-µl sample*
Zinc	213.85	Pt	$8.0 \cdot 10^{-11}$	0.67
Antimony	252.85	Pt	$5.0 \cdot 10^{-10}$	4.60
Selenium	203.98	Pt	$4.0 \cdot 10^{-10}$	3.24
Arsenic	228.81	Pt	$4.2 \cdot 10^{-11}$	0.35
Lead	261.41	Pt	$1.2 \cdot 10^{-10}$	1.0
Cadmium	228.81	Pt	$2.0 \cdot 10^{-13}$	0.0017
Iron	248.32	Pt	$3.0 \cdot 10^{-10}$	2.5
Iodine	206.16	Pt	$1.2 \cdot 10^{-9}$	10.0
Copper	217.89	W	$1.2 \cdot 10^{-10}$	1.0
Boron	249.77	W	$1.2 \cdot 10^{-10}$	1.0
Beryllium	234.86	Pt	$1.2 \cdot 10^{-10}$	1.0
Mercury	253.65	Pt	$1.6 \cdot 10^{-11}$	0.13

chosen so that peaks caused by both arsenic and cadmium were easily discernible. When a solution containing 10 µg As ml^{-1} alone was placed on the loop peaks 1, 2 and 3 (Fig. 7A) were observed after *ca.* 40 sec. Then the current was increased steadily to its maximum of 1.9 A; peaks 4 and 5 were observed when the current reached 1.5 A and the loop was just below red-heat (*ca.* 500° K). The separation of peaks 1–2 and 2–3 is *ca.* 3 sec each, and the separation of peaks 3–4 and 4–5 depends on the rate at which the loop is heated. Figure 7B shows that cadmium is vaporised (peak 6) at a temperature between that of the arsenic species (represented by peaks 4 and 5). This investigation shows that under suitable conditions the system might be used not only for the determination of total concentration of an element, but also for the determination of the different species present.

No interference was observed from either cobalt or antimony, both of which exhibit emission close to 228.8 nm (Co at 228.781 nm and Sb at 228.898 nm) when present in a 1000-fold molar amount compared to cadmium. Cadmium solutions containing sodium ($\geq$ *ca.* 5000 µg ml^{-1}) distorted the integrated emission reading owing to a light leak in the spectrophotometer used. Under these conditions sodium emission was observed visually for several minutes after the cadmium signal was received and the precision of the measurement was decreased slightly.

Chemical interferences. The effects of phosphate, silicate, aluminium and vanadium when present in 1000-fold molar amounts compared to cadmium were also investigated. Only vanadium, present in the form of ammonium metavanadate, was found to interfere, giving a 40% reduction in the expected signal intensity.

Application to other elements

Table I shows the limits of detection obtained with platinum or tungsten loops (as indicated) for a range of elements. As can be seen, the system is applicable to elements which are well known to form stable refractory oxides in flames. The most useful spectral region of measurement is below *ca.* 300.0 nm where the plasma background is lowest. In comparison to high-temperature flames the plasma background radiation throughout the u.v./visible region of the spectrum is very low. Sheathing the plasma with argon reduces the background even further by removing the nitrogen and N–O bands appearing above *ca.* 300.0 nm. The system may also be used to monitor carbon emission at the 247.8-nm line and hence may have application in certain organic analyses.

In conclusion, the system described enables a highly sensitive analysis to be carried out on small volumes of liquid sample. Interferences in the case of cadmium were not serious, which is probably a result of the argon atmosphere surrounding the sample during all stages of the evaporation and excitation stages. The system is sufficiently versatile so that by modifying the method of sample introduction it should be possible to examine vaporised solids and gas mixtures. Future work is directed towards extending the field of application and to the use of photon counting as a read-out technique to improve the precision and detection limits.

We would like to thank the Science Research Council for supplying a research studentship to B.L.S., and I.C.I. Ltd., Agricultural Division (Billingham, England) for a research grant to K.M.A.

SUMMARY

A non-flame cell utilising a microwave-induced argon plasma at atmospheric pressure is described for emission spectroscopic purposes. The system operates at a microwave power of *ca.* 40 W (2450 MHz) and requires the use of only minute liquid samples. Optimal operating parameters are investigated and the method is tested on a range of elements. In addition, the use of a high-speed operational amplifier/integrator is described which is capable of following the weak and transient signals common to non-flame methods of atomisation.

RÉSUMÉ

On décrit un dispositif de cuve pour mesures spectroscopiques d'émission sans flamme. Ce système ne nécessite que de faibles quantités d'échantillon liquide. On examine divers paramètres. On propose l'utilisation d'un amplificateur permettant de suivre les signaux faibles et fugitifs communs aux méthodes d'atomisation sans flamme.

ZUSAMMENFASSUNG

Für emissionsspektroskopische Zwecke wird eine flammenlose Zelle mit einem mikrowellenerregten Argon-Plasma von Atmosphärendruck angewendet. Die Mikrowellenleistung beträgt *ca.* 40 W (2450 MHz); es sind nur sehr kleine flüssige Proben erforderlich. Die optimalen Bedingungen werden untersucht; die Methode wird mit einer Reihe von Elementen geprüft. Zusätzlich wird die Anwendung eines sehr schnellen Verstärker-Integrators beschrieben, der den schwachen und kurzzeitigen Signalen folgen kann, die bei flammenlosen Atomisierungsmethoden erhalten werden.

REFERENCES

1 B. V. L'vov, *Spectrochim. Acta*, 17 (1961) 761.
2 H. Massmann, *Spectrochim. Acta*, 23B (1968) 215.
3 T. S. West and X. K. Williams, *Anal. Chim. Acta*, 45 (1969) 27.
4 M. P. Bratzel Jr., R. M. Dagnall and J. D. Winefordner, *Anal. Chim. Acta*, 48 (1969) 197.
5 R. Mavrodineanu and R. C. Hughes, *Spectrochim. Acta*, 19 (1963) 1309.
6 C. D. West and D. N. Hume, *Anal. Chem.*, 36 (1964) 412.
7 S. Greenfield, I. L. Jones and C. T. Berry, *Analyst*, 89 (1964) 713.
8 R. H. Wendt and V. A. Fassel, *Anal. Chem.*, 37 (1965) 920; 38 (1966) 337.
9 R. J. Heemstra and N. G. Foster, *Anal. Chem.*, 38 (1966) 492.
10 A. J. McCormack, S. C. Tong and W. D. Cooke, *Anal. Chem.*, 37 (1965) 1470.
11 J. H. Runnels and J. H. Gibson, *Anal. Chem.*, 39 (1967) 1398.
12 G. McMilliam and H. C. Bolton, *Anal. Chem.*, 41 (1969) 1755, 1762.

Anal. Chim. Acta, 54 (1971) 233–243

Analytica Chimica Acta
Elsevier Publishing Company, Amsterdam
Printed in The Netherlands

THE DETERMINATION OF GOLD IN THE p.p.b. AND p.p.m. RANGES BY ATOMIC ABSORPTION SPECTROPHOTOMETRY

M. A. HILDON AND G. R. SULLY

Roan Consolidated Mines Limited, Chibuluma Division, RCM Research and Development Department, Kalulushi (Zambia)

(Received 10th November 1970)

The determination of gold in the p.p.b. (10^{-7} g-%) range in copper ores is of interest, as gold is concentrated into anode slimes during the copper refining process. Very low levels of gold (< 500 p.p.b.) can therefore be economically significant. The existing fire-assay and optical spectrographic technique in use in this laboratory was considered time-consuming and not sufficiently sensitive. Huffman *et al.*[1] have shown that atomic absorption spectrophotometry in combination with cyanide or fire-assay extraction and concentration into 4-methylpentan-2-one (MIBK) can be used with a detection limit of 15 p.p.b. Most atomic absorption methods however are useful only in the p.p.m. range[2-6].

This investigation describes the development of a method based on dissolution of the sample in acid followed by extraction into MIBK, which provides reasonable precision at the 100 p.p.b. level. The method finally adopted was applicable to a variety of solid matrices and had a detection limit of 2 p.p.b. when 25 g of sample were used.

DEVELOPMENT OF METHOD

Several authors have claimed that gold can be extracted from solutions containing large amounts of base metals with MIBK and that there are no interferences in the subsequent atomic absorption determination[7,8]. Tindall has recommended washing the organic layer with dilute hydrochloric acid[8]. The recovery of gold from solutions containing typical levels of cations that could result from the dissolution of 25 g of sample was investigated. These results are shown in Table 1. The MIBK extract was aspirated into a lean air–acetylene flame and the solutions were compared with a standard prepared in the same way containing only gold. Definite interferences resulted from a number of common cations, notably copper, iron and calcium. Boswell and Brooks[9] showed that in addition to gold, significant amounts of iron, molybdenum, gallium, indium, thallium, silver, tin and rhenium are extracted from 1 *M* (10% v/v) hydrochloric acid into MIBK and that several other elements are extracted to a lesser extent. Depression from high levels of copper was observed here when gold was determined in the air–acetylene flame. This effect would be expected to be more serious in the cooler flame produced when MIBK is aspirated. It would seem probable that the interferences observed were the result of chemical interference in the flame although it is possible that high levels of some elements may have reduced the efficiency of the extraction of gold into the organic phase.

The large amount of iron which was extracted could not be completely back-

TABLE I

INTERFERENCES IN DIRECT MIBK EXTRACTION

Interfering ion	*Equivalent to*[a] *this % in sample*	*Recovery*[b] *% Au*
Copper	20	30
Iron	40	74
Nickel	5	98
Cobalt	2	94
Calcium	20	57
Magnesium	20	78
Aluminium	20	66
Sodium	2	99
Potassium	10	95
Manganese	2	96
Arsenic	1	131
Bismuth	1	108

[a] 500 μg of Au was extracted into 25 ml of MIBK from 250 ml of a 10% hydrochloric acid solution containing the level of interfering ion (as chloride) equivalent to this % metal in 25 g of sample.

[b] Sprayed in a lean air–acetylene flame against a standard prepared in the same way.

extracted even by four or five washings with dilute hydrochloric acid, although two washings with 10 ml of a 20% (w/v) ascorbic acid solution, followed by a single hydrochloric acid wash, did quantitatively remove the iron. However, this process did not avoid the interferences produced by copper, calcium or aluminium.

It was considered that a better approach would be to coprecipitate the gold on a carrier and then extract it from a solution of the two with MIBK. This double extraction could provide a complete separation from possible interfering elements. Mercury[10] and tellurium[11-13] have both been used as precipitants. The use of tellurium was favoured as initial work showed that copper(I) chloride could be precipitated with mercury if the level of copper in the sample was high.

The efficiency of the recovery of gold with tellurium has been shown to be good[12,13] and this was confirmed in the present work. Gold (10 mg) was precipitated on 25 mg of tellurium carrier from 200 ml of a 10% (v/v) hydrochloric acid solution with hydrazine dihydrochloride. No gold was detected in the filtrate indicating that the collection at this level was at least 99.8% efficient. The precipitation was repeated with 25 μg of gold and the precipitate dissolved in aqua regia and made up to 25 ml. This solution was found to contain 1.00 p.p.m. gold, showing that the precipitation was quantitative within the precision of the determination (probably 100±1%). The tellurium separation is also selective[11,12] and only gold, palladium, selenium and tellurium were reduced under the conditions used. It was shown that ruthenium, rhodium, rhenium, osmium, iridium, platinum, gallium, indium, thallium, silver, cadmium, mercury, germanium, tin, lead, arsenic, antimony and bismuth were not reduced or co-precipitated with tellurium.

A single solvent extraction with MIBK was practically quantitative with 98.5% of the gold extracted into 5 ml of MIBK from 50 ml of a 10% (v/v) hydrochloric acid solution containing 100 μg of gold. As selenium, tellurium and palladium were precipitated with gold, their potential interferences were investigated. There was shown to be no effect on the recovery of gold from up to 100 mg of selenium and tellurium and up to 5 mg of palladium (0.4% and 0.02% respectively on a 25-g sample). The overall recovery and freedom from interferences of major constituents was similarly shown by extracting 2 mg of gold from a solution containing the concentrations of cations that would result from the complete dissolution of 25 g of sample of the following composition—iron 30%, copper 10%, nickel 2%, manganese 2%, calcium 10%, aluminium 5%, potassium 5%, sodium 2%. The recovery was 98–99%.

Chow and Beamish[13] have shown that an aqua regia attack is at least 99% efficient at removing gold from siliceous materials. Results were compared when identical samples were attacked with aqua regia (see Experimental) or with hydrofluoric acid and aqua regia which dissolved 99.9% by weight of the sample. No significant differences were found.

EXPERIMENTAL

Instrumental

A Techtron model AA5 Atomic Absorption Spectrophotometer fitted with a Jarrell-Ash model 82.025 0.5-metre Ebert monochromator and a Servoscribe potentiometric recorder was used. The monochromator had a variable curved slit assembly (10–400 μm aperture) and a grating with 1180 lines/mm blazed at 400 nm. The reciprocal dispersion was 1.6 nm per mm in the first order. Instrumental conditions are shown in Table II.

TABLE II

INSTRUMENTAL CONDITIONS

Hollow-cathode lamp	Varian Techtron 40 mm
Lamp current	10 mA
Wavelength	242.8 nm
Slit width	100 μm
Masks[a]	Two, 6 mm diameter
Gain	3
Burner	Techtron AB 52
Burner height	2–3 mm below light path
Oxidant	Air at 15–20 p.s.i.
Fuel	MIBK
Sensitivity	0.05 p.p.m./1% absorption

[a] See ref. 14.

Flame

High sensitivity was obtained by using the cool flame produced by burning MIBK in air. It was found that the flat-topped AB 42 burner head (slot width 2.0 mm) gave slightly higher sensitivity than the grooved AB 52 burner head, but the AB 52 was preferred as it gave a more stable flame and allowed the use of scale expansion. The air–MIBK flame will burn only if the ratio of fuel uptake rate to support flow falls in a certain range. It was found that only nebulizers which fulfilled the following specifications were satisfactory:

air flow	4.5–5.5 l min^{-1}
air pressure	15–25 p.s.i.
MIBK uptake rate	7–11 ml min^{-1}

As the glass bead used to break up the spray from the nebulizer caused excessive reduction in the volume of MIBK reaching the flame, it was turned so that it did not interrupt the MIBK aerosol. The flame was of course extinguished when aspiration of MIBK ceased but when the polythene capillary was moved rapidly from one tube to another, a batch of samples could be aspirated without trouble. The burner had to be pre-heated for at least 10 min to allow conditions to stabilise.

Reagents

Reagent-grade MIBK was used and all other chemicals were of analytical grade. Reagent blanks were regularly run but were usually insignificant.

PROCEDURE

The weight of sample used is determined by the level of gold. As a rough guide the following weights should be taken:

25 g	2–50 p.p.b. (with scale expansion) 50–1000 p.p.b. (normal mode)
5 g	0.5–5 p.p.m.
1 g	3–25 p.p.m.

Weigh the sample into a 600-ml beaker. Add 60 ml of hydrochloric acid and 20 ml of nitric acid (these volumes may be reduced if 1 g or 5 g are used), take to dryness and bake to remove nitric acid and to decompose nitrates. Baking should be prolonged if the sample contains high levels of copper or iron. Remove from the hotplate, add 50 ml of hydrochloric acid and 50 ml of water and boil to dissolve salts. Filter through a fluted paper into a 600-ml beaker, washing with deionised water. Add ammonia solution to precipitate hydroxides and just dissolve the precipitate in hydrochloric acid. The volume of solution at this stage should be 250–300 ml. Add sufficient hydrochloric acid to make the solution 10% (v/v), and then add 10 ml of tellurium solution (2.5 g l^{-1} in 10% hydrochloric acid) and 25 ml of 20% (w/v) hydrazine dihydrochloride solution. Place on a hotplate, cover the beaker, bring to the boil and boil gently to coagulate the precipitate. If the sample contains high levels of iron ($>30\%$) the precipitate may not form immediately, in which case further additions of hydrazine dihydrochloride solution should be made. Filter hot through a porosity 3 sintered glass crucible, washing with a minimum of cold 50% (v/v) hydrochloric acid to remove occluded copper, silver or lead. Place the crucible in the original beaker and add *ca.* 30 ml of hot aqua regia to dissolve the precipitate. Remove the crucible, washing with water and boil carefully just to dryness. Cool, add 5 ml of hydrochloric acid and 10 ml of water, and boil to dissolve the residue. Transfer the solution, with washing, to a calibrated 100-ml separating funnel and dilute to 50 ml. Add exactly 5 ml of MIBK and shake for 1 min. Allow the layers to separate and run off the aqueous layer. Run the organic layer into a test tube and stopper. This solution is stable for at least 24 h.

Standards

A 1000-p.p.m. primary standard was prepared by dissolving 1.000 g of pure gold foil in 10 ml of aqua regia and making the solution to 1 l with 10% (v/v) hydrochloric acid. Suitable MIBK standards were prepared with a batch of samples by extracting 50 ml of a solution containing the appropriate amounts of gold, tellurium and hydrochloric acid with 5 ml of MIBK.

Standards of 0, 2.5, 5.0 p.p.m. were used when scale expansion was not employed. When scale expansion was used, standards of 0, 0.5, 1.0 or 0, 0.25, 0.50 p.p.m. were aspirated. In these cases the chart recorder was used to improve precision (Fig. 1). Almost linear calibration curves were obtained.

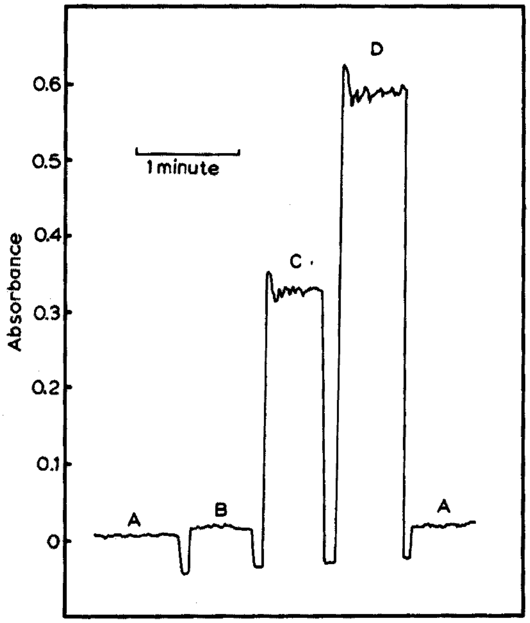

Fig. 1. Time scan of low gold standards. Approximately 10 × scale expansion. (A) MIBK; (B) 0.00 p.p.m. Au; (C) 0.25 p.p.m. Au; (D) 0.50 p.p.m. Au.

RESULTS

The method has been used on a routine basis in this laboratory for the last eighteen months in the analysis of a wide range of samples. Copper ores, copper concentrates, plant tailings, mineralogical specimens, are amongst the sample types analysed.

Detection limit

The detection limit (that concentration producing a signal equal to twice the background noise) was estimated from Fig. 1 at 50 ng. This is a concentration of 10 p.p.b. in the organic phase and is equivalent to a concentration of 2 p.p.b. in the original sample if 25 g of sample were taken.

Precision

The precision of the method was shown by analysing two samples five times. They were analysed: (*a*) on the same occasion and sprayed against the same standards, and (*b*) on separate occasions by preparing one sample and three standards each day for five days.

These results are shown in Table III. No significant variation was apparent between the long-term and short-term results, and the precision obtained, particularly at the 0.1-p.p.m. level was considered good.

TABLE III

PRECISION TESTS

(The samples were copper oxide ores. A was an Argillite and B a Dolomite Schist)

Sample	*Sample weight (g)*	*Mean*[c] *(p.p.m.)*	*Standard deviation (p.p.m.)*	*Relative standard deviation (%)*
A[a]	25	0.119	0.006	5.0
A[b]	25	0.115	0.006	5.2
B[a]	10	1.040	0.030	2.9
B[b]	10	1.060	0.026	2.5

[a] Analysed as 5 samples in one batch.
[b] Analysed singly on five occasions.
[c] Mean of five determinations.

Accuracy

As no pre-analysed samples were available at the p.p.b. level, two samples were analysed that contained *ca.* 10 p.p.m. and one that contained *ca.* 2 p.p.m. gold. These samples had been independently analysed in other laboratories. The results are shown in Table IV.

TABLE IV

ACCURACY TESTS

(Samples C and D were copper–bismuth residues from the copper refining process. Sample E was a copper concentrate. All results are quoted as p.p.m. gold)

Sample	*Sample weight (g)*	*Result*[a] *this method*	*Laboratory A (fire-assay)*	*Laboratory B (atomic absorption)*	*Laboratory C (fire-assay and spectrography)*
C	1	12.95	12.70	13.0	—
D	1	10.75	10.95	11.3	—
E	10	2.01	—	—	2.10

[a] Mean of 3 determinations.

The authors wish to thank Mr. D. M. L. Wordingham for helpful discussions, and the General Manager of Roan Consolidated Mines Limited, Chibuluma Division, for permission to publish this work.

SUMMARY

A method is described for the determination of gold in rocks, minerals, mining and metallurgical samples and similar materials in the range 2 p.p.b. to 25 p.p.m. ($2\cdot10^{-7}$–$2.5\cdot10^{-3}$%). The gold is separated by co-precipitation with tellurium followed by solvent extraction into 4-methylpentan-2-one (MIBK). This solution is nebulized with air and the MIBK is used as fuel. A relative standard deviation of 5% is obtained at the 100 p.p.b. level. The separation is specific for gold and the method is therefore interference-free.

RÉSUMÉ

Une méthode est décrite pour le dosage de l'or dans les roches, les minerais, les échantillons miniers et métallurgiques, de 2 p.p.b. à 25 p.p.m. ($2\cdot10^{-7}$–$2.5\cdot10^{-3}$%). L'or est séparé par coprécipitation avec le tellure, et extraction dans la méthyl-4-pentanone-2. Cette solution est vaporisée avec de l'air, le solvant servant de combustible. On obtient ainsi une déviation standard relative de 5% pour 100 p.p.b. Cette séparation est spécifique pour l'or. La méthode est par conséquent exempte d'interférence.

ZUSAMMENFASSUNG

Es wird eine Methode für die Bestimmung von Gold in Gesteinen, Mineralen, bergbaulichen und metallurgischen Proben und ähnlichen Stoffen im Bereich 2 p.p.b.–25 p.p.m. ($2\cdot10^{-7}$–$2.5\cdot10^{-3}$%) beschrieben. Das Gold wird durch Mitfällung mit Tellur und anschliessende Extraktion mit 4-Methylpentanon-(2) (MIBK) abgetrennt. Diese Lösung wird mit Luft zerstäubt, und das MIBK dient als Brenngas. Bei 100 p.p.b. wird eine relative Standardabweichung von 5% erhalten. Die Abtrennung ist für Gold spezifisch und die Methode daher störungsfrei.

REFERENCES

1 C. Huffman, Jr., J. D. Mensik and L. B. Riley, *U.S. Geol. Surv. Circ.*, No. 544, 1967.
2 T. Toyochuchi and H. Shimizu, *Japan Analyst*, 16 (1967) 565.
3 H. Spitzer and G. Tesik, *Z. Anal. Chem.*, 232 (1967) 40.
4 S. L. Law and T. E. Green, *Anal. Chem.*, 40 (1969) 1008.
5 E. N. Pollack and S. I. Andersen, *Anal. Chim. Acta*, 41 (1968) 441.
6 J. R. Beevers, *Econ. Geol.*, 62 (1967) 426.
7 F. W. E. Strelow, E. C. Feast, P. M. Mathews, C. J. C. Bothma and C. R. van Zyl, *Anal. Chem.*, 38 (1968) 115.
8 F. M. Tindall, *Atomic Absorption Newsletter*, 4 (1965) 339.
9 C. R. Boswell and R. R. Brooks, *Mikrochim. Acta*, (1965) 819.
10 E. Barnard and P. M. Seeman, *Tegnikon*, 11 (1958) 2.
11 H. Onishi, *Mikrochim. Acta*, 1 (1959) 9.
12 J. Marmenko and I. May, *Anal. Chem.*, 40 (1968) 1137.
13 A. Chow and F. E. Beamish, *Talanta*, 14 (1967) 219.
14 M. A. Hildon and G. R. Sully, *Anal. Chim. Acta*, to be published.

Analytica Chimica Acta
Elsevier Publishing Company, Amsterdam
Printed in The Netherlands

SIMULTANEOUS DETERMINATION OF COPPER AND BISMUTH IN HIGH-PURITY LEAD BY ANODIC-STRIPPING POLAROGRAPHY

IVAN ŠINKO AND SERGEJ GOMIŠČEK
Chemical Institute "Boris Kidrič", Department of Analytical Chemistry, Ljubljana (Yugoslavia)

(Received 21st November 1970)

The determination of low contents of copper and bismuth in pure lead is important because these two elements, especially bismuth, affect the properties and, in turn, the applicability of lead. The polarographic procedures for the determination of copper and bismuth in pure lead described in the literature[1-9], can be used only in cases in which the copper and bismuth contents are over $10^{-3}\%$ and $10^{-2}\%$, respectively. As the quality of pure lead is affected by the presence of as little as $10^{-3}\%$ of copper and bismuth, an attempt was made to devise a procedure for the determination of low contents of either element in pure lead by means of anodic-stripping polarography. The procedure described below permits the determination of as little as $10^{-5}\%$ of copper or bismuth in pure lead by means of the medium exchange method described previously[10,11]. With this procedure, the concentration of copper and bismuth ions can be directly determined without any preliminary separation of the lead ions as an insoluble salt, so that the possibility of the ions adsorbing on the precipitate is eliminated.

In recent years, attempts have been made to devise polarographic procedures by which bismuth and copper in lead can be directly determined[6-9]. In this laboratory, attempts to use these procedures in conjunction with anodic-stripping polarography have failed to yield satisfactory results. All the other polarographic procedures call for the preliminary removal of lead(II) from the solution as its insoluble sulphate[1-3] or chloride[4,5]. Bassett and Jones[6] state that these procedures can lead to the adsorption of ions on the precipitate, primarily bismuth ions on the lead sulphate, so that low results are obtained. The work described here showed that for low concentrations of bismuth and copper ions in solution, the effect of adsorption is considerable. Accordingly, an accurate determination of low bismuth and copper contents in pure lead ($10^{-4}\%$ and lower) by means of anodic-stripping polarography is possible only if the procedures used do not call for a preliminary removal of lead(II) as an insoluble salt.

EXPERIMENTAL

Apparatus

Anodic currents were recorded on a Radiometer PO4 polarograph. The hanging mercury drops were obtained with the Radiometer P-958 Kemula electrode. The reference electrode was a saturated calomel electrode (S.C.E.) connected to the electrolysis solution by a salt bridge filled with 1 *M* potassium chloride solution. The volume of the electrolysis cell was about 50 ml and the volume of the electrolysis solution 20 ml. The current–potential curves were recorded at a rate of change of applied e.m.f. of 0.2 V min^{-1}. Oxygen was removed by bubbling pure argon containing less than 0.01 % of oxygen through the solution for 10 min[12]. During electrolysis the solution was stirred with a glass stirrer at 400 rev min^{-1}.

Reagents

Analytical-grade chemicals (Riedel) were used to prepare the supporting electrolytes and other solutions. For the dissolution of lead, Merck suprapur nitric acid was used. Deionized water twice-distilled in a quartz apparatus was used throughout.

1 *M Hydrochloric acid*–1 *M ethylenediamine solution.* Transfer 30.0 ml of ethylenediamine p.a. (98 %) to a 500-ml volumetric flask, add 100 ml of distilled water, shake, add 42.0 ml of hydrochloric acid ($d = 1.19$ g cm^{-3}), and dilute to the mark with distilled water. Fresh solutions should be prepared daily; when old solutions are used, a decrease in the maximum anodic currents of bismuth and a shift of the half-peak potential towards positive values is observed.

Standard 10^{-2} *M bismuth solution.* Dissolve 0.5225 g of spectroscopically pure bismuth in 8 ml of nitric acid ($d = 1.40$ g cm^{-3}) by heating slightly, and then dilute to 250 ml with water.

Standard 10^{-2} *M copper solution.* Dissolve 0.6041 g of copper(II) nitrate trihydrate in water and dilute to 250 ml with water.

Lower concentrations of standard solutions were freshly prepared daily by diluting the 10^{-2} *M* solutions.

All experiments were carried out with Pb 6 N/1 (Caramant AG) containing 0.1 p.p.m. of bismuth and 0.3 p.p.m. of copper.

Choice of supporting electrolytes

Direct determination of bismuth and copper in pure lead by anodic-stripping polarography called for an adequate supporting electrolyte in which lead would not precipitate in the form of an insoluble salt and in which the half-peak potential for lead would be more negative than those for bismuth and copper. These two conditions are fulfilled by nitric acid (Fig. 1). When nitric acid was used as the supporting electrolyte, changes in the concentration of nitric acid from 0.5 *M* to 2.5 *M* did not affect the half-peak potential and the maximum anodic current for bismuth and copper. A change in the potential of electrolysis from −0.50 V to −0.15 V *vs.* S.C.E. in a nitric acid medium caused no change in the maximum anodic currents for bismuth and copper. On the basis of this observation, a potential of −0.25 V *vs.* S.C.E. was chosen for the electrolysis of bismuth and copper in a nitric acid medium; at more negative potentials, *e.g.*, −0.30 V *vs.* S.C.E., lead was electrolysed if present in large concentrations. In a nitric acid solution, however, the determination of bismuth and copper was impossible because their half-peak potentials are almost identical. In order to solve this problem the medium exchange technique[10,11] was used and the anodic currents for copper were recorded in 1 *M* hydrochloric acid as supporting electrolyte, and those for bismuth in 1 *M* hydrochloric acid–1 *M* ethylenediamine as supporting electrolyte.

In these supporting electrolytes the difference between the half-peak potentials for bismuth and copper is large enough to permit the measurement of the maximum anodic currents of one of the metals in the presence of the other[11,13]. The values of the half-peak potentials for each metal are shown in Fig. 1, which also shows the potential of electrolysis and the potential of stripping for bismuth and copper. Figure 1 further shows that in 1 *M* hydrochloric acid the maximum anodic currents for both copper and bismuth can be measured simultaneously but only when the concentration of the two ions is approximately equal. If the concentration of copper ions is higher than that of bismuth ions, the measurement of the maximum anodic currents for bismuth is not feasible. Experiments showed that the measurement of maximum anodic current for bismuth is made more accurate and precise by using 1 *M* hydrochloric acid–1 *M* ethylenediamine as supporting electrolyte; the concentration of copper(II) can then considerably exceed that of bismuth(III).

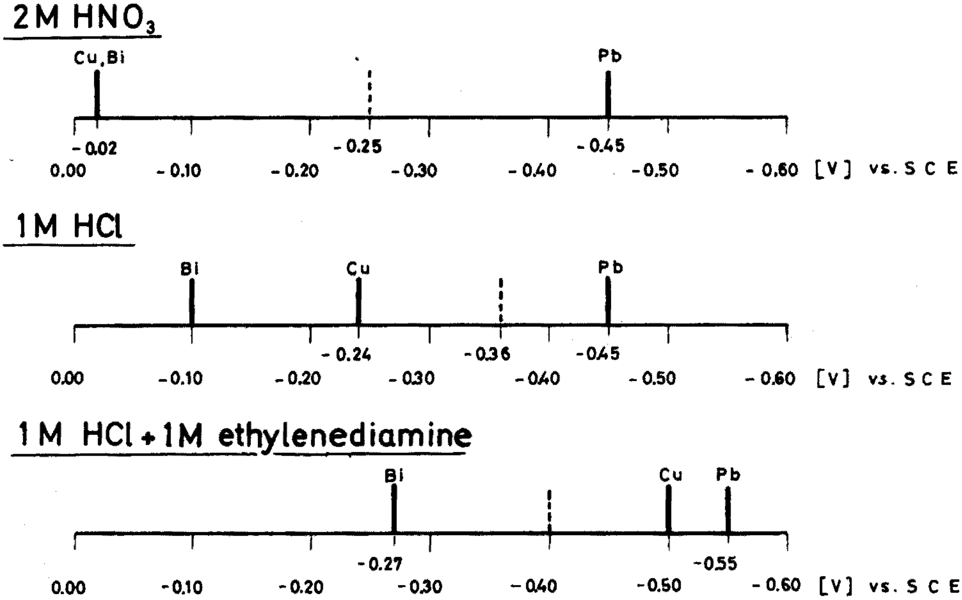

Fig. 1. Half-peak potentials for bismuth, copper and lead in different supporting electrolytes.

Procedure

Add 1 g of lead to 15 ml of 1+2 nitric acid (suprapur, $d = 1.40$ g cm^{-3}) and heat until completely dissolved. Slowly evaporate the solution until a white precipitate is formed, cool, quantitatively transfer to a 25-ml volumetric flask, and dilute to the mark with distilled water. After mixing, transfer 20 ml of the solution with a pipette to the electrolysis cell. In order to remove dissolved oxygen, pass argon through the solution for 10 min.

Prepare a hanging mercury drop with the micrometer screw (2 parts of the scale) and electrolyse at −0.25 V *vs.* S.C.E. During electrolysis stir the solution with a glass stirrer and pass argon over the surface of the solution. The electrolysis time is from 3 to 15 min and depends on the concentration of bismuth and copper ions. For the determination of copper at the end of electrolysis, quickly exchange the electrolysis cell for a cell which contains 20 ml of 1 *M* hydrochloric acid and from which oxygen has been removed by passing argon. Exchange of cells should not take more than 5 sec[10]; during the exchange the potential is changed to −0.36 V *vs.* S.C.E. Since during the exchange of the cells the solution absorbs a small amount of oxygen from the air, argon should be bubbled through it for 1 min. After another 1 min the anodic currents can be recorded.

The procedure for the determination of bismuth(III) differs from the above procedure for copper(II). After the initial electrolysis, exchange the electrolysis cell for a cell containing 20 ml of 1 *M* hydrochloric acid–1 *M* ethylenediamine and apply a potential of -0.40 V *vs.* S.C.E. during the exchange of cells.

Determine the concentration of bismuth and copper ions in solutions by the standard addition method or from calibration curves.

The above procedure permitted the determination of bismuth and copper in pure lead in concentrations of 10^{-5}–10^{-2}% depending on the weight of the sample and the electrolysis time. In the case of concentrations 10^{-5}–10^{-3}%, the dilution was 1 g of lead per 25 ml and the electrolysis time 3–15 min; in the case of concentrations of 10^{-3}–10^{-2}% the dilution was 0.1 g per 25 ml and the electrolysis time 3 min. It is considered that by the above method even smaller concentrations of bismuth and copper than cited above could be determined in pure lead. This claim, however, could not be tested because no lead of sufficient purity was available in this laboratory.

RESULTS AND DISCUSSION

Several samples of pure lead and several synthetic samples containing lesser amounts of impurities usually present in pure lead, were analysed. The accuracy of the method was tested by the simultaneous spectrographic analysis of two samples of pure lead (Table I) and by adding known amounts of bismuth and copper to the pure lead containing 0.3 p.p.m. copper and 0.1 p.p.m. bismuth (Table II).

TABLE I

THE DETERMINATION OF BISMUTH AND COPPER IN PURE LEAD BY ANODIC-STRIPPING POLAROGRAPHY (H.D.M.E.) AND SPECTROGRAPHY

Sample	*Cu (p.p.m.)*		*Bi (p.p.m.)*	
	H.D.M.E.	*Spectrography*	*H.D.M.E.*	*Spectrography*
1	0.7	0.5	2.5	1.8
2	14.0	17.0	2.4	1.0

TABLE II

THE DETERMINATION OF BISMUTH AND COPPER IN PURE LEAD BY ANODIC-STRIPPING POLAROGRAPHY

Sample	*Cu (p.p.m.)*		*Bi (p.p.m.)*	
	Added	*Found*	*Added*	*Found*
3	15.0	14.0	8.0	8.4
4	30.0	27.0	12.0	14.0

The precision of the method was determined by analyzing eleven times the same sample of pure lead. The mean concentrations found were 3.9 p.p.m. of copper and 1.9 p.p.m. of bismuth; the relative standard deviation was found to be 5.6% for copper and 6.2% for bismuth. The concentration of bismuth and copper ions was determined from the calibration curve; the determination by the standard addition method proved to be somewhat less precise.

Table III shows the effect of some metals usually contained in pure lead, on the determination of bismuth and copper in lead. These data indicate that the presence of arsenic, cadmium, zinc and tin has no effect on the maximum anodic currents for bismuth and copper. The presence of iron decreases the maximum anodic current for bismuth; but this effect can be eliminated by adding a small amount of ascorbic acid to the nitric acid solution before electrolysis. If the lead contains more than 10^{-2}% of silver, low concentrations of bismuth and copper ions in the solution will make for poorly shaped current–potential curves on which maximum anodic currents cannot be measured.

TABLE III

THE DETERMINATION OF BISMUTH AND COPPER IN LEAD IN THE PRESENCE OF OTHER ELEMENTS

(Lead contained 3.9 p.p.m. of copper and 1.9 p.p.m. of bismuth; mean value of eleven determinations)

Impurity added	*Copper found (p.p.m.)*	*Bismuth found (p.p.m.)*
0.10 % Arsenic	4.0	1.9
0.10 % Cadmium	4.1	1.8
0.10 % Tin	3.8	1.8
0.10 % Zinc	3.9	2.1
0.10 % Iron	3.5	1.1
0.10 % Iron[a]	3.7	2.0
0.0010 % Silver	4.0	1.9
0.010 % Silver	3.9	1.9
0.10 % Silver	—[b]	—[b]
0.0010 % Antimony	3.9	1.8
0.010 % Antimony		
0.10 % Antimony		

[a] Before electrolysis a few grains of ascorbic acid were added to the nitric acid solution.

[b] Could not be measured.

The determination of copper in lead is hampered by the presence of antimony because the difference between the half-peak potential of antimony and that of copper in 1 *M* hydrochloric acid is too small[11]. However, experiments showed that the concentration of copper ions in a solution can be determined precisely and accurately enough if the ratio between copper and antimony in lead is 1:25. The determination of bismuth is not hampered by the presence of antimony (Table III).

The influence of bismuth on the determination of copper in lead and *vice versa* was studied in detail. The current–potential curves (Fig. 2) show that bismuth can be determined even if the ratio between bismuth and copper in lead is 1:100; analyses for copper in lead likewise showed that a hundredfold amount of bismuth in lead does not affect the accuracy and precision of the determination of the concentration of copper ions in a solution. From the current–potential curves (Fig. 2a), it can be seen that, because of the dissolution of lead, the anodic maximum occurs at a potential of −0.35 V *vs.* S.C.E. This maximum appears only if during the exchange of supporting electrolytes, a substantial amount of lead ions is transferred to the 1 *M* hydrochloric acid solution. Figure 2b shows that with increasing concentration of copper(II), the anodic current increases at a potential of −0.4 V *vs.* S.C.E. (see galvanic zero!) because of the dissolution of copper. By analyzing a considerable number of samples of pure lead and of synthetic samples, it was found that the anodic current of copper does not affect the accuracy and precision of the determination of bismuth by the procedure described above.

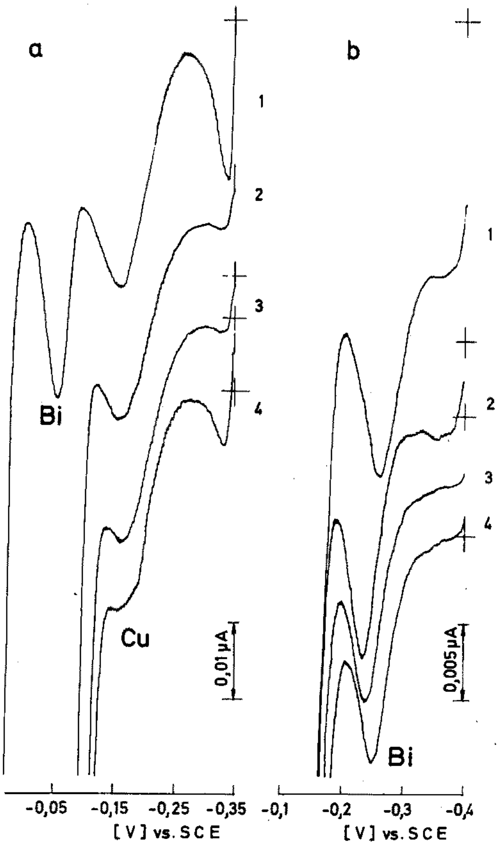

Fig. 2. Current–potential curves for copper and bismuth. The rate of change of e.m.f. was 0.2 V min^{-1}; the dilution was 1 g of lead per 25 ml; the supporting electrolyte for electrolysis was nitric acid solution; electrolysis time was 10 min at −0.25 V *vs.* S.C.E. Stripping was done: for copper in 1 *M* HCl at −0.35 V *vs.* S.C.E. and for bismuth in 1 *M* HCl + 1 *M* ethylenediamine at −0.40 V *vs.* S.C.E. The copper and bismuth content in lead was: (a) 1.3 p.p.m. of copper and (1) 0.1 p.p.m., (2) 10 p.p.m., (3) 50 p.p.m., (4) 100 p.p.m. of bismuth. (b) 1.0 p.p.m. bismuth and (1) 100 p.p.m., (2) 50 p.p.m., (3) 10 p.p.m., (4) 0.3 p.p.m. of copper.

Figure 3 shows that increased amounts of bismuth and copper in lead do not affect the calibration curves for bismuth and copper.

In view of the above findings it is considered that this method allows the determination of bismuth and copper in pure lead with sufficient accuracy and precision within a wide concentration range. The parallel determination of the two metals in pure lead takes about 2 h if the concentrations of bismuth and copper ions are read from the calibration curve and about 3 h if the standard addition method is used.

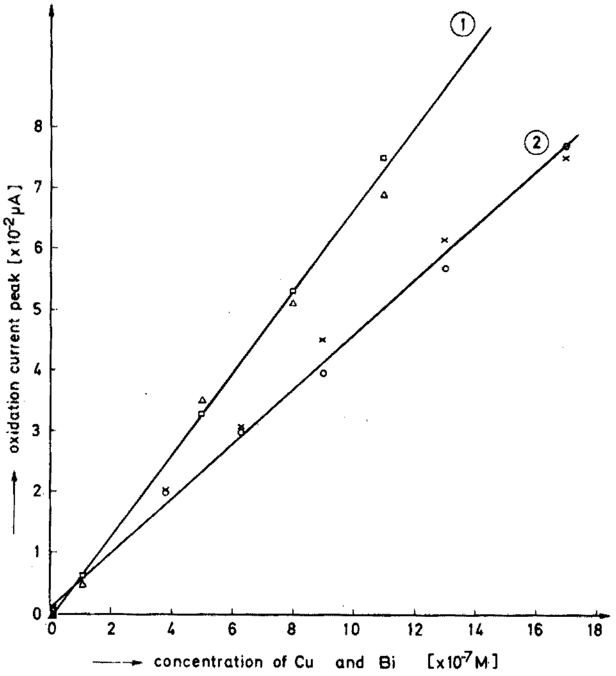

Fig. 3. Calibration curves for bismuth and copper in the presence of lead (1 g Pb/25 ml). Electrolysis time for copper was 10 min and for bismuth 3 min at −0.25 V *vs.* S.C.E. in a nitric acid medium. Stripping was done as described in the procedure. The calibration curve for bismuth (1) was obtained in the presence of 0.3 p.p.m. of copper (△) and 100 p.p.m. of copper (□); for copper (2) in the presence of 0.1 p.p.m. of bismuth (×) and 50 p.p.m. of bismuth (○).

SUMMARY

A procedure based on anodic-stripping polarography is described for the direct determination of 10^{-5}–10^{-2}% of bismuth and copper in lead. The electrolysis of bismuth and copper ions on the hanging mercury drop electrode is done at −0.25 V *vs.* S.C.E. in a nitric acid medium; after electrolysis, stripping for copper is done in 1 *M* hydrochloric acid at −0.36 V *vs.* S.C.E. and for bismuth in 1 *M* hydrochloric acid–1 *M* ethylenediamine at −0.40 V *vs.* S.C.E. In the case of pure lead containing 1.9 p.p.m. of bismuth and 3.9 p.m.m. of copper, the relative standard deviation for bismuth was 6.2% and for copper 5.6%. Analysis for the two metals takes about 2 h if the concentration of bismuth and copper ions is determined from calibration curves. Data are given on the effect of silver, arsenic, cadmium, iron, antimony, tin and zinc in pure lead on the determination.

RÉSUMÉ

On décrit une méthode polarographique par dissolutien anodique pour le dosage direct de 10^{-5} à 10^{-2}% de bismuth et de cuivre dans le plomb. L'électrolyse du bismuth et du cuivre sur l'électrode à goutte pendante de mercure est effectuée à −0.25 V *vs.* E.C.S. en milieu acide nitrique; après électrolyse, le "stripping" pour le cuivre est fait dans l'acide chlorhydrique 1 *M* à −0.36 V *vs.* E.C.S. et pour le bismuth, en milieu acide chlorhydrique 1 *M*–ethylenediamine 1 *M* à −0.40 V *vs.* E.C.S. L'analyse de ces deux métaux demande environ 2 h si la concentration du bismuth et du cuivre est déterminée à l'aide de courbes d'étalonnage. On examine l'influence de l'argent, de l'arsenic, du cadmium, du fer, de l'antimoine, de l'étain et du zinc dans du plomb pur.

ZUSAMMENFASSUNG

Es wird die direkte Bestimmung von 10^{-5}–10^{-2}% Wismut und Kupfer in Blei durch Polarographie nach dem anodischen "stripping"-Verfahren beschrieben. Die Elektrolyse von Wismut- und Kupferionen wird an einer Elektrode mit hängendem Quecksilbertropfen bei −0.25 V gegen ges. Kalomelelektrode in salpetersaurem Medium durchgeführt. Nach der Elektrolyse wird das Kupfer in 1 *M* Salzsäure bei −0.36 V und das Wismut in 1 *M* Salzsäure–1 *M* Äthylendiamin bei −0.40 V gegen ges. Kalomelelektrode wieder aufgelöst. Bei einem Gehalt von 1.9 p.p.m. Wismut und 3.9 p.p.m. Kupfer in reinem Blei beträgt die relative Standardabweichung für Wismut 6.2% und für Kupfer 5.6%. Die Analyse für die beiden Metalle dauert etwa 2 h, wenn die Konzentration der Wismut- und Kupferionen aus Eichkurven ermittelt wird. Es werden Zahlenwerte über den Einfluss von Silber, Arsen, Cadmium, Eisen, Antimon, Zinn und Zink in reinem Blei auf die Bestimmung vorgelegt.

REFERENCES

1 G. W. C. Milner, *The Principles and Applications of Polarography*, Longmans Green, London, 1962, p. 384.
2 M. Zotta, *Gazz. Chim. Ital.*, 78 (1948) 143.
3 D. Cozzi, *Anal. Chim. Acta*, 4 (1950) 204.
4 S. A. Pletenev, T. V. Arefeva, E. M. Tal and E. I. Dubovitskaya, *Zavodsk. Lab.*, 12 (1946) 38.
5 G. Conradi and M. Kopanica, *Chemist-Analyst*, 52 (1) (1963) 11.
6 J. Bassett and J. C. H. Jones, *Analyst*, 91 (1966) 591.
7 J. Musil and M. Kopanica, *Chemist-Analyst*, 55 (4) (1966) 106.
8 R. Ripan and G. Pop, *Rev. Chim. Bucharest*, 14 (8) (1963) 464; *Anal. Abstr.*, 11 (1964) 4212.
9 Takeshi Iga, Shohei Yamashita and Hiroyoshi Uehara, *Japan Analyst*, 10 (3) (1961) 227; *Anal. Abstr.*, 10 (1963) 2210.
10 M. Ariel, U. Eisner and S. Gottesfeld, *J. Electroanal. Chem.*, 7 (1964) 307.
11 R. Neeb, *Inverse Polarographie und Voltametrie*, Verlag Chemie GmbH, Weinheim/Bergstr., 1969.
12 I. Šinko and J. Doležal, *J. Electroanal. Chem.*, 25 (1970) 53.
13 E. N. Vinogradova and L. N. Vasileva, *Zh. Analit. Khim.*, 17 (5) (1962) 579.

Analytica Chimica Acta
Elsevier Publishing Company, Amsterdam
Printed in The Netherlands

THE POLAROGRAPHIC DETERMINATION OF ANTIMONY

EINAR JACOBSEN AND TROND ROJAHN
Department of Chemistry, University of Oslo, Blindern, Oslo 3 (Norway)

(Received 23rd November 1970)

The determination of antimony in biological samples and as a trace constituent in various commercial products is usually performed spectrophotometrically or by polarography. Accordingly, the polarographic behaviour of antimony has been studied in various supporting electrolytes[1-7]. In hydrochloric acid, antimony(III) produces well-defined d.c. and a.c. polarographic waves and this acid is usually preferred as supporting electrolyte for the determination of small amounts of antimony[8-12]. However, the a.c. current is not strictly proportional to the concentration[8] and at higher concentrations a maximum occurs on the d.c. wave which interferes in the a.c. polarographic determination[13]. In most other electrolytes (sulphuric acid, nitric acid, perchloric acid, citrate and tartrate buffers) antimony(III) is irreversibly reduced. Practically no a.c. wave is observed in these media and antimony can only be determined by the less sensitive d.c. polarographic method.

Recent experiments indicate that the presence of a surfactant may result in an increase in the height of an a.c. polarographic wave and this phenomenon has been applied for increasing the sensitivity of the a.c. polarographic method[14-17]. Preliminary experiments showed that the presence of cationic, anionic or non-ionic surfactants has no effect on the polarographic wave of antimony(III). However, upon addition of thiocyanate to an acidic solution of antimony a very well-defined a.c. polarographic wave is obtained.

The present work was carried out in order to investigate the polarographic behaviour of antimony(III) in the presence of thiocyanate and to ascertain the advantage of thiocyanate as supporting electrolyte in polarographic determination of antimony(III).

EXPERIMENTAL

Polarograms were recorded with a Metrohm E 261 R Polarecord connected to a Metrohm E 393 a.c. modulator. An Ag/AgCl/saturated KCl electrode served as reference electrode and a tungsten electrode was employed as auxiliary electrode. All a.c. polarograms were obtained with an a.c. amplitude of 10 mV r.m.s. The capillary characteristics of the dropping mercury electrode, measured in 0.1 M potassium nitrate (open circuit) at a mercury height of 49.2 cm, were $m = 3.659$ mg sec^{-1} and $t = 2.63$ sec. All experiments were performed at $25 \pm 0.1°$. Dissolved air was removed from the solutions by bubbling oxygen-free nitrogen through the cell for 10 min and passing it over the solution during the electrolysis.

Cyclic voltammograms were obtained with a Beckman Electroscan 30 with mercury indicator electrode and a saturated calomel reference electrode. The mercury electrode was made by abrading a platinum inlay electrode (Beckman No. 39273) with carborundum paper while the electrode surface was immersed in a pool of mercury[18]. When the electrode was not in use it was stored in pure mercury to ensure that it remained completely amalgamated. Before the stored electrode was used, the excess of mercury was removed by gentle tapping. Between each run, the mercury was wiped off and the electrode washed with pure mercury.

All chemicals were reagent-grade (E. Merck AG, Germany) and were used without further purification. A 0.025 *M* antimony(III) stock solution was prepared by dissolving the appropriate amount of antimony trioxide in 10 *M* sulphuric acid, and was standardized by titration with permanganate[19]. A 0.1 *M* potassium thiocyanate solution was prepared in distilled water.

RESULTS

In sulphuric acid media antimony(III) produces only ill-defined d.c. polarographic waves. Reproducible results are hard to obtain and often a splitting of the wave is observed. The half-wave potential of the single wave in 1 *M* sulphuric acid is -0.13 V *vs.* Ag/AgCl. Upon addition of thiocyanate to the electrolyte the electrode reaction becomes more reversible and the half-wave potential is shifted to a less negative potential. In the presence of 0.01–0.1 *M* thiocyanate, well-defined and reproducible waves are obtained and the half-wave potential is -0.09 V. The limiting current is not affected upon addition of thiocyanate to the electrolyte. In the presence of thiocyanate the d.c. wave is accompanied by a well-defined a.c. polarographic wave (Fig. 1) and the summit potential, E_s, coincides with the half-wave potential.

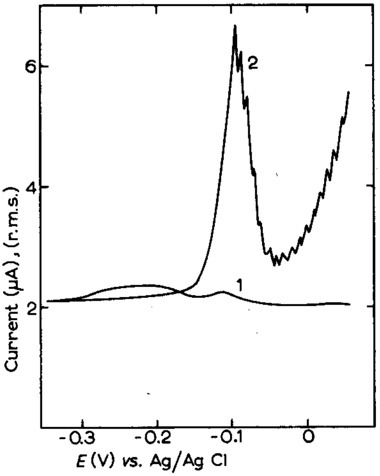

Fig. 1. A.c. polarograms of 10^{-4} *M* antimony(III) in 1 *M* sulphuric acid in the absence (curve 1) and in the presence of 0.01 *M* thiocyanate (curve 2).

Thiocyanate is strongly adsorbed at the dropping mercury electrode. Electrocapillary curves showed that the presence of 0.01 *M* thiocyanate in 1 *M* sulphuric acid causes a large decrease in the drop time at potentials more positive than -0.4 V.

Consequently, the presence of thiocyanate gives rise to a tensammetric wave. The peak potential of this wave in 1 *M* sulphuric acid, E_{T^+}, is +0.19 V *vs.* Ag/AgCl. When the concentration of thiocyanate is increased above 0.01 *M* the tensammetric wave produces a small a.c. current even at negative potentials and interferes with the a.c. polarographic wave of antimony(III). Consequently, in the following experiments the concentration of thiocyanate was not increased above 0.01 *M*.

TABLE I

POLAROGRAPHIC DATA OF 10^{-4} *M* ANTIMONY(III) IN SULPHURIC ACID AND 0.01 *M* POTASSIUM THIOCYANATE PRESENT AT VARIOUS pH VALUES

Supporting electrolyte	$-E_{1/2} = -E_s$ *(V)*	$E_{3/4} - E_{1/4}$ *(mV)*	*d.c. current (μA)*	*a.c. current (μA) (r.m.s.)*	$\Delta E_{s/2}$ *(mV)*
4 *M* H_2SO_4	0.09	−26	0.85		
2 *M* H_2SO_4	0.09	−24	1.24		
1 *M* H_2SO_4	0.09	−21	1.25	3.75	40
pH 1.1	0.13	−25	1.12	2.40	44
pH 1.5	0.15	−28	1.10		
pH 2.2	0.18	−29	1.10	1.85	46
pH 2.5	0.20	−32	1.10	1.40	48
pH 3.5	0.27	−44			
pH 4.5	0.34	−84		0.33	

The effect of pH on the reduction wave of antimony(III) in the presence of 0.01 *M* thiocyanate was studied by recording polarograms of 10^{-4} *M* antimony(III) in sulphuric acid at various pH values. The reversibility of the electrode reaction was tested by determining the value $E_{3/4} - E_{1/4}$ of the d.c. polarograms and the width of the a.c. wave at half-height, $\Delta E_{s/2}$. The lowest values, −21 mV and 40 mV, respectively, were obtained in 1–2 *M* sulphuric acid and indicate an almost reversible 3-electron reduction. Some data are given in Table I. The height of the d.c. as well as of the a.c. wave is constant in 1–2 *M* sulphuric acid but decreases with increasing pH values and above pH 5 no wave is observed. This decrease in the height of the waves and the decrease in reversibility is probably due to an increased hydrolysis of antimony(III) with increasing pH. As indicated in Fig. 2 the height of the a.c. waves, i_s, recorded

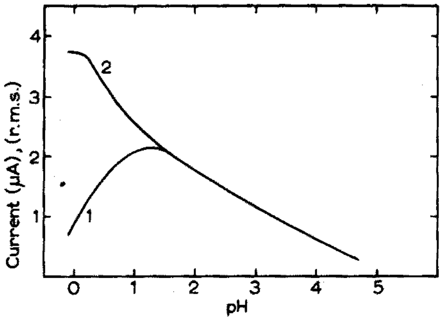

Fig. 2. Peak height of the a.c. polarographic wave of 10^{-4} *M* antimony(III) at various pH values in the presence of 10^{-4} *M* thiocyanate (curve 1) and 10^{-2} *M* thiocyanate (curve 2).

from strong acidic solutions is also very dependent on the thiocyanate concentration. However, in the presence of 0.01 *M* thiocyanate reproducible results are easily obtained even in 1–2 *M* sulphuric acid. When the pH is increased above 1.5, reproducible peak height is obtained also at lower thiocyanate concentration. The half-wave potential of the antimony(III) wave coincides with the summit potential at all pH values. In strong sulphuric acid (1–6 *M*) it is constant, but it is shifted about 45 mV per pH unit to more negative values in the pH range 0.05–4. Because the most reversible waves are obtained from 1 *M* sulphuric acid, the following experiments were performed in this electrolyte.

TABLE II

EFFECT OF PRESSURE OF MERCURY ON THE POLAROGRAPHIC WAVES OF 10^{-4} *M* ANTIMONY(III) IN 1 *M* SULPHURIC ACID WITH 0.01 *M* THIOCYANATE PRESENT

h_{corr} (*cm*)	i_s (*μA*) (*r.m.s.*)	i_d (*μA*)	$i_d/h^{\frac{1}{2}}_{corr}$	i_d/h_{corr}
37.6	3.80	1.10	0.179	0.0293
47.6	3.75	1.24	0.179	0.0261
52.6	3.75	1.33	0.183	0.0253
57.6	3.80	1.41	0.184	0.0245
62.6	3.75	1.46	0.184	0.0233

TABLE III

POLAROGRAPHIC DETERMINATION OF ANTIMONY(III) IN 1 *M* SULPHURIC ACID WITH 0.01 *M* THIOCYANATE PRESENT

Concn. of Sb^{3+} (*mM*)	i_d (*μA*)	i_d/C (*μA/mmole*)	i_s (*μA*) (*r.m.s.*)	i_s/C (*μA/mmole*)
1.00	12.00	12.0	23.00	23.0
0.50	6.10	12.2	17.50	35.0
0.10	1.24	12.4	3.75	37.5
0.08	0.98	12.3	3.05	38.0
0.06	0.73	12.3	2.25	37.5
0.04	0.50	12.5	1.50	37.5
0.02	0.25	12.5	0.75	37.5
0.01			0.38	38.0
0.005			0.18	36.0

The effect of droptime on the limiting current was determined by recording polarograms of 10^{-4} *M* antimony(III) in 1 *M* sulphuric acid containing 0.01 *M* thiocyanate at various heights of the mercury column. As indicated in Table II the a.c. peak current, i_s, is constant, whereas the d.c. limiting current increases with the height of the mercury column. The value $i/h^{\frac{1}{2}}$, where h is the height of the column after correction for the "back pressure", is constant and indicates that the current is diffusion-controlled. The temperature coefficients (determined in the range 25–50°) of the d.c. current, +1.2%/degree, and of the a.c. peak current, +0.68%/degree, also indicate that the current is controlled essentially by diffusion.

Polarograms recorded from solutions which contained 1 *M* sulphuric acid, 0.01 *M* thiocyanate and various amounts of antimony(III), showed that the current increases proportional to the bulk concentration of antimony. The results (Table III) show that antimony can be determined by d.c. polarography in the concentration range $2 \cdot 10^{-5}$–$5 \cdot 10^{-4}$ *M* and in the range $5 \cdot 10^{-6}$–10^{-4} *M* by the a.c. polarographic method. The diffusion current constant, $I = i_d/Cm^{2/3}t^{1/6}$, is 4.40.

The well-defined a.c. waves of antimony(III) and the fact that most other elements are reduced at considerably more negative potentials, indicate that 1 *M* sulphuric acid–0.01 *M* thiocyanate should be a suitable electrolyte for the determination of antimony. The presence of copper, lead, iron, bismuth and large amounts of arsenic usually interfere in the polarographic determination of antimony. Experiments showed that the presence of a 1000-fold excess of arsenic or a 10-fold excess of bismuth, lead or iron has no effect on the a.c. polarographic wave of antimony(III) in 1 *M* sulphuric acid–0.01 *M* thiocyanate. However, the presence of even small amounts of copper seriously interferes in the determination.

A second reduction wave of antimony(III) in sulphuric acid ($E_{\frac{1}{2}} = -1$ V *vs.* S.C.E.) has been reported. Lingane[2] suggests that this wave is a further reduction of antimony to stibine. According to Fujisawa[3], the second wave appears only on polarograms recorded from relatively high concentrations of antimony. On the basis of controlled potential electrolysis, he claims that this incompletely developed wave cannot be due to the formation of stibine. In agreement with Fujisawa, we observed the second wave only on polarograms recorded from solutions containing more than 10^{-3} *M* antimony and that the height of the wave is not related to the concentration of antimony(III). Moreover, the height of the wave is independent of the temperature and if the pH of the electrolyte is increased above 3, the whole wave disappears. Polarograms recorded at various heights of the mercury column showed that the height of the wave increases linearly with the height of the column, which implies that the current is not controlled by diffusion (Table IV). A possible electrode reaction is discussed below.

TABLE IV

EFFECT OF PRESSURE OF MERCURY ON THE SECOND POLAROGRAPHIC WAVE OF $1.25 \cdot 10^{-3}$ *M* ANTIMONY(III) IN 1 *M* SULPHURIC ACID

h_{corr}	*Current* (μA)	i/h_{corr}	$i/h^{\frac{1}{2}}_{corr}$
47.6	3.1	0.065	0.449
52.6	3.4	0.065	0.469
57.6	3.8	0.066	0.501
62.6	4.1	0.066	0.518

Cyclic voltammetry

In order to test the reversibility of the electroreduction of antimony(III), a few voltammetric experiments were performed. Reproducible results were obtained provided that the electrode was cleaned and washed carefully with pure mercury between each potential sweep. A typical cyclic voltammogram is given in Fig. 3. At low scan rates both a cathodic and an anodic peak are observed. The height of the anodic peak, resulting from the reoxidation of antimony, decreases rapidly with increasing scan rates. As indicated in Table V, the ratio of the anodic to the cathodic peak currents decreases with increasing scan rates, which indicates that the electron-transfer reaction is followed by an irreversible chemical reaction[20]. The current function, $(i_p)_c/v^{\frac{1}{2}} \cdot C$, decreases with increasing scan rate, which implies that the electron transfer is preceded by a slow chemical reaction[20]. It is obvious from the ratio of the anodic to the cathodic currents and from the separation of the two peak potentials, ΔE_p, that the overall electrode reaction becomes more reversible with decreasing scan rates. At the scan rate 0.002 V sec^{-1}—a time scale comparable to the polarographic data—the value $\Delta E_p = 22$ mV is observed, compared to 20 mV for a reversible 3-electron reduction.

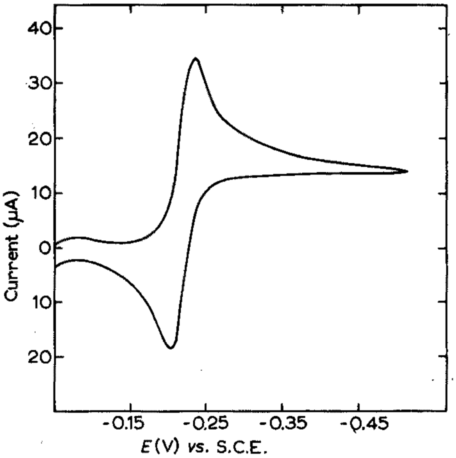

Fig. 3. Cyclic voltammogram of 10^{-3} M antimony(III) in 1 M sulphuric acid and 0.01 M thiocyanate. Scan rate, 0.002 V sec^{-1}.

TABLE V

VOLTAMMETRIC DATA FOR THE REDUCTION OF 10^{-3} M ANTIMONY(III) IN 1 M SULPHURIC ACID WITH 0.01 M THIOCYANATE PRESENT

Scan rate v (*V sec*$^{-1}$)	*Current*		$(i_p)_a/(i_p)_c$	$(i_p)_c/v^{\frac{1}{2}} \cdot C$	ΔE_p (*mV*)
	$(i_p)_c$ (μA)	$(i_p)_a$ (μA)			
0.10	190.0	85.0	0.45	600.4	70
0.05	152.5	83.5	0.55	680.8	53
0.02	98.0	75.0	0.76	695.0	40
0.01	70.0	65.0	0.93	700.0	36
0.002	32.5	31.5	0.97	726.7	22

DISCUSSION

The well-defined d.c. wave and the appearance of an a.c. wave in the presence of thiocyanate, imply that the rate of the electroreduction of antimony(III) is greatly increased by the presence of thiocyanate. The diffusion current constant is not affected and the half-wave potential is shifted to more *positive* values upon addition of thiocyanate to the supporting electrolyte. Hence, the increased reversibility is probably not the result of a complex formation between antimony(III) and thiocyanate in the bulk of the solution. However, thiocyanate is strongly adsorbed at the electrode and the increased rate of reduction may be the result of the formation of an activated bridge complex at the electrode surface[17,21].

Although the reduction rate of antimony(III) at a mercury electrode is slow, the electron transfer through an activated bridge complex between the positively charged mercury surface, the negatively charged thiocyanate and the positively charged depolarizer ($Hg^{+}\cdots SCN^{-}\cdots Sb^{3+}$) might take place more easily and thereby give rise to an almost reversible polarographic wave. This activated bridge can obviously only be established in the presence of thiocyanate ion and not by thiocyanic acid. Hence, in strongly acidic solutions the a.c. wave is completely developed only in the presence of a high concentration of thiocyanate (Fig. 2). In less acidic solution the reaction $HSCN \rightleftharpoons H^{+} + SCN^{-}$ is shifted to the right and the total concentration of thiocyanate present becomes less important.

It is evident from the experimental results that the polarographic wave is due to a diffusion-controlled 3-electron reduction of antimony(III). In strongly acidic solutions the half-wave potential is constant, which implies that hydrogen ions are not involved in the electrode reaction. Hence, the electron transfer reaction must be

$$Sb^{3+} + 3e^{-} \rightleftharpoons Sb$$

Cyclic voltammograms recorded at various scan rates indicate that the electron transfer is preceded by a chemical reaction. According to Jander and Hartmann[22] antimony exists mainly as SbO^{+} even in strongly acidic medium. Because the depolarizer is Sb^{3+}, the reaction that precedes the electron transfer is probably:

$$SbO^{+} + 2H^{+} \rightarrow Sb^{3+} + H_2O$$

The voltammetric data also imply that the electron transfer is followed by a chemical reaction which must be a slow formation of the amalgam:

$$Sb + Hg \rightarrow Sb(Hg)$$

Above pH 0.05 the half-wave potential of the antimony wave is shifted 0.045 V/pH unit to more negative values. The number of hydrogen ions, Z, taking part in the electrode reaction is given by

$$\Delta E_{\frac{1}{2}}/\Delta \mathrm{pH} = -0.045 = -0.059\, Z/\alpha n$$

where α is the transfer coefficient. The value of αn calculated from the voltammetric data is 2.7, which gives a Z value of 2.06. Because two hydrogen ions are consumed in the reduction of antimony(III) at pH values above 0.05, this electrode reaction is probably:

$$SbO^+ + 2\,H^+ + 3\,e^- \rightarrow Sb + H_2O$$

When the pH is increased above 5, SbO^+ is probably completely hydrolysed to polarographically inactive compounds and the wave disappears.

The second wave of antimony(III) ($E_{\frac{1}{2}} = -1$ V) appears only at low pH values and at relatively high concentrations of antimony. The current is not controlled by diffusion and it is not related to the concentration of antimony(III). Hence, this wave cannot be due to a further reduction of antimony to stibine as previously reported[2]. As stated above, the reduction product of the first wave is elemental antimony which reacts slowly with mercury to form the amalgam. At high concentrations of antimony, the mercury surface will be partly covered with metallic antimony. Because the hydrogen overpotential at an antimony electrode is less than that at mercury, the second wave is probably caused by reduction of hydrogen ions at that part of the electrode surface which is covered with antimony. Hence, the height of the wave becomes very dependent on pH and the wave disappears at pH values above 3.

SUMMARY

The electroreduction of antimony(III) in sulphuric acid–thiocyanate solutions has been investigated by polarography and cyclic voltammetry. In 1 *M* sulphuric acid–0.01 *M* thiocyanate media, antimony(III) produces almost reversible a.c. and d.c. polarographic waves. The current is proportional to the concentration over a large concentration range ($2 \cdot 10^{-5}$–$5 \cdot 10^{-4}$ *M* for the d.c. method and $5 \cdot 10^{-6}$–10^{-4} *M* for the a.c. method). No maximum is observed and the a.c. waves are not affected by the presence of a 1000-fold amount of arsenic or a 10-fold amount of iron, bismuth or lead. Only copper causes significant interference.

RÉSUMÉ

Une étude est effectuée sur l'électroréduction de l'antimoine(III), dans des solutions acide sulfurique–thiocyanate, par polarographie et voltammétrie cyclique. Le courant est proportionnel à la concentration: $2 \cdot 10^{-5}$ à $5 \cdot 10^{-4}$ *M* pour la méthode à courant continu, et $5 \cdot 10^{-6}$ à 10^{-4} *M* à courant alternatif. On n'observe pas de maximum; les vagues à courant alternatif ne sont pas affectées par la présence d'arsenic (en quantités 1000 fois supérieures) ou de fer, bismuth ou plomb (en quantitiés 10 fois supérieures). Seul le cuivre interfère sensiblement.

ZUSAMMENFASSUNG

Die Elektroreduktion von Antimon(III) in Schwefelsäure–Thiocyanat-Lösungen wurde mittels Polarographie und cyclischer Voltammetrie untersucht. In 1 *M* Schwefelsäure–0.01 *M* Thiocyanat ergibt Antimon(III) bei der Wechselstrom- und Gleichstrompolarographie fast reversible Stufen. Der Strom ist über einen grossen Konzentrationsbereich ($2 \cdot 10^{-5} - 5 \cdot 10^{-4}$ *M* bei der Gleichstrom- und $5 \cdot 10^{-6} - 10^{-4}$ *M* bei der Wechselstrommethode) der Konzentration proportional.

Es wird kein Maximum beobachtet, und die Wechselstrom-Stufen werden durch die Gegenwart einer 1000-fachen Menge Arsen oder einer 10-fachen Menge Eisen, Wismut oder Blei nicht beeinflusst. Nur Kupfer stört erheblich.

REFERENCES

1 J. E. Page and F. A. Robinson, *J. Soc. Chem. Ind. (London)*, 61 (1942) 93.
2 J. J. Lingane, *Ind. Eng. Chem., Anal. Ed.*, 15 (1943) 583.
3 T. Fujisawa, *Nippon Kagaku Zasshi*, 84 (1963) 629.
4 R. Geyer and M. Geissler, *Z. Anal. Chem.*, 187 (1962) 251; 201 (1964) 1.
5 G. Jander and H. J. Hartmann, *Z. Anorg. Allgem. Chem.*, 339 (1965) 256.
6 T. Takada, K. Nakano, A. Yamada and K. Morinaga, *J. Electrochem. Soc. Japan*, 31 (1963) 125.
7 G. P. Haight, Jr., *Anal. Chem.*, 26 (1954) 593.
8 T. Isshiki, Y. Mashiko and S. Tsukagoshi, *Pharm. Bull. (Tokyo)*, 2 (1954) 263.
9 E. Temmerman and F. Verbeek, *Anal. Chim. Acta*, 43 (1968) 263.
10 P. E. Toren, *Anal. Chem.*, 40 (1968) 1152.
11 Y. S. Lyalikov and L. S. Kopanokaya, *Ukr. Khim. Zh.*, 30 (1964) 90.
12 L. N. Vasil'eva, R. G. Pats and A. A. Pozdnyakova, *Zh. Analit. Khim.*, 22 (1967) 1459.
13 B. Breyer, F. Gutmann and S. Hacobian, *Australian J. Sci. Res.*, A-4 (1951) 595.
14 N. Gundersen and E. Jacobsen, *J. Electroanal. Chem.*, 20 (1969) 13.
15 G. C. Barker and J. A. Bolzan, *Z. Anal. Chem.*, 216 (1966) 215.
16 R. Kalvoda, W. Anstine and M. Heyrovský, *Anal. Chim. Acta*, 50 (1970) 93.
17 E. Jacobsen and G. Tandberg, *J. Electroanal. Chem.*, 1971, in press.
18 S. A. Moros, *Anal. Chem.*, 35 (1963) 1088.
19 W. Pugh, *J. Chem. Soc.*, (1933) 1.
20 R. S. Nicholson and I. Shain, *Anal. Chem.*, 36 (1964) 706.
21 R. W. Schmid and C. N. Reilley, *J. Amer. Chem. Soc.*, 80 (1958) 2101.
22 G. Jander and H. J. Hartmann, *Z. Anorg. Allgem. Chem.*, 339 (1965) 239.

Analytica Chimica Acta
Elsevier Publishing Company, Amsterdam
Printed in The Netherlands

THE POLAROGRAPHY OF AMINO ACIDS IN DIMETHYLSULFOXIDE*

THOMAS R. KOCH** AND WILLIAM C. PURDY
Department of Chemistry, University of Maryland, College Park, Md. 20742 (U.S.A.)

(Received 4th November 1970)

Numerous investigations have been concerned with the indirect polarographic determination of amino acids as metal complexes or other derivatives. Additionally, thorough polarographic studies have been made of the sulfur-containing amino acids, cysteine and cystine, and of the various iodine-containing amino acids. Dayan[1] investigated the direct reduction of six amino acids in aqueous 0.05 *M* tetraethylammonium bromide. Okazaki and Otsuki[2] reported half-wave potentials for eighteen amino acids in 80% dioxane. Simple amino acids gave single waves, attributed by the authors to the reduction of hydrogen.

In the present paper is reported the polarographic behavior of fourteen amino acids in 0.1 *M* tetraethylammonium perchlorate (TEAP) dissolved in dimethylsulfoxide (DMSO). Polarographic and other studies lead to several interesting conclusions concerning the mechanism of reduction.

EXPERIMENTAL

Apparatus

All polarographic measurements were made with a Leeds and Northrup Electrochemograph, Type E. When half-wave potential values were desired, the polarograph was undamped and a Lingane H-cell with a saturated calomel reference electrode (S.C.E.) was used. A fine sintered-glass disc and an agar plug separated the test compartment from the reference electrode. When half-wave potential values were not sought, the instrument was damped to a 6-sec response, and a cell with a mercury pool reference electrode was employed. In all cases, the cell was maintained at 25.0±0.1° by a water bath. Cell resistance was measured with an Industrial Instruments, Inc., conductance bridge. In circumstances where the S.C.E. was unsuitable for half-wave potential measurements, the saturated potassium chloride was replaced with saturated lithium chloride. The potential of this electrode was measured daily against a commercial S.C.E. The lithium chloride electrode maintained a stable potential within a given working period, but drifted by as much as 200 mV over a period of several days. This electrode was used for studying the first waves of glutamic acid, aspartic acid, and glutamine, and the third cathodic wave of cysteine, owing to the interference of potassium ion when the S.C.E. was used.

---

* Taken in part from the Ph.D. Dissertation of Thomas R. Koch, University of Maryland, 1970.
** Present address: Erie County Laboratories, E. J. Meyer Memorial Hospital Division, 462 Grider Street, Buffalo, N.Y. 14214.

Coulometric studies were carried out with an instrument described previously[3]. The cell used in these studies contained two side-arms to isolate anodic reduction products and water from the test solution. These side-arms were separated from the test compartment by sintered-glass discs. The side-arms held the commercial S.C.E. and platinum-foil auxiliary electrode and were filled with 0.1 *M* TEAP in DMSO. The surface of the mercury pool working electrode was stirred by a magnetic stirring bar.

Potentiometric titrations were made with a Leeds and Northrup Model 7405 pH meter. This meter was also used for the dual-polarized potentiometric end-point in Karl Fischer titrations; a current of about 1 μA was applied to the electrodes by the instrument.

Where necessary, accurate potential measurements were made with a Rubicon precision potentiometer.

Reagents

All amino acids were Calbiochem "A Grade".

"Baker Analyzed" reagent-grade DMSO required further purification. The DMSO was distilled over Fisher indicating, 8–14 mesh activated alumina, through a 36-inch column packed with porcelain saddles. The pot temperature was about 65–70°, the column temperature 50°, and the pressure less than 1 Torr. Of the 2-l total DMSO volume, the first 30–40 ml of distillate, and about the last 300 ml of residue were discarded. The distilled DMSO was collected in a sealed, evacuated flask, from which it was later dispensed directly for use by pressurizing the flask with ultra-pure nitrogen. This procedure minimized air contact and handling of the distilled solvent. The DMSO purified by this procedure gave no polarographic waves between -0.2 and -2.7 V *vs.* S.C.E. A very small anodic wave remained from -0.2 to $+0.5$ V, at which potential oxidation of the mercury electrode began. The water content of DMSO prepared in this fashion was determined by Karl Fischer titrations to be 3.15 p.p.m.

Tetraethylammonium perchlorate (TEAP) was used as the supporting electrolyte in all studies. The salt was obtained from the Eastman Company in an impure state. After double recrystallization from water, the TEAP was dried in a vacuum oven at about 60° for at least 24 h. The salt thus obtained was polarographically inert in DMSO in the potential range of $+0.4$ to -2.7 V *vs.* S.C.E.

Solutions were deaerated with Air Products Company Ultra-High purity nitrogen. The nitrogen was passed through a vanadium scrubber, prepared as described by Meites[4], then through two drying tubes containing Fisher activated alumina, and through a DMSO scrubber before reaching the test solution.

All other reagents were reagent grade or highest purity, and were used without further purification.

Procedure

Dissolution of amino acids in DMSO was, in most cases, difficult and was accomplished by heating the stirred mixture in an oil bath at 70–80° for 1–4 h. A number of amino acids, typically those of low molecular weight such as glycine, alanine, valine, and leucine, could not be dissolved at all.

Polarographic studies in the H-cell required fairly consistent technique to get good results; with either the potassium or lithium reference electrode, small amounts of the respective cations appeared in the test solutions, and increased somewhat in amount with time. Since saturated potassium chloride or lithium chloride solutions were kept in the test compartment of the cell to preserve the reference electrodes when the cell was not in use, some of the salts appeared to remain on the compartment walls even after thorough washing. Also some amount of each cation undoubtedly entered the test solution from the reference electrode at the cross arm.

This problem was dealt with by first cleaning the cell with water at the beginning of the day, and then bubbling nitrogen through the water-filled test compartment for about 2 h. The water was changed several times during this period. Before a sample was placed in the cell, the test compartment was rinsed thoroughly again with water, then with acetone. After the compartment had been dried by suction and nitrogen gas, the test solution was poured in and deaerated for about 15 min. A polarogram run after this procedure would exhibit a small potassium or lithium wave. When the potassium or lithium wave was large enough to require a less sensitive current scale on the polarograph than would be used for the amino acid wave in the absence of potassium or lithium, the polarogram was considered unacceptable.

Polarographic studies in the cell with a mercury pool reference electrode required none of the above precautions. However, this reference electrode is not suitable for accurate half-wave potential measurements, since it is not truly nonpolarizable[5,6].

The integrator of the constant-potential coulometer was calibrated each day of use by titrating 20 μmoles of either sodium(I) or lead(II) in a pretitrated solution of 0.1 M TEAP. The procedure for an amino acid solution was to titrate 10 ml of a $2 \cdot 10^{-3}$ M solution at the chosen potential. Nitrogen was maintained over the surface of the test solution during each run.

Karl Fischer titrations were performed as back-titrations; a potentiometric end-point was used with dual-polarized platinum indicating electrodes. Consumption of all Karl Fischer reagent in the solution was signaled by an increase in potential. In a typical titration, 50 ml of anhydrous methanol was placed in a 180-ml electrolyte beaker and a known excess of Karl Fischer reagent was added; the excess was titrated with a standard water–methanol solution. An excess of Karl Fischer reagent was again added, followed by a sample of the DMSO solution, after which the remaining excess of Karl Fischer reagent was titrated as above.

Potentiometric titrations of amino acids were carried out with a glass electrode and a commercial S.C.E. The glass electrode has been shown by Reddy[7] to give a nearly theoretical response to hydrogen ion in DMSO over a range of 0–25 "pH". Amino acid solutions made up directly in DMSO were titrated with hydrochloric acid and with sodium ethoxide, both made up in DMSO. The pH meter was standardized with a DMSO "pH" 10.0 buffer.

RESULTS AND DISCUSSION

Amino acids producing single cathodic waves

The electrocapillary curve for 0.1 M TEAP in DMSO exhibits a maximum at -0.2 V; the curve falls off sharply at higher voltages. The residual curve run on the same solution has a cathodic limit at -2.7 V and an anodic limit at $+0.5$ V.

TABLE I

ELECTROCHEMICAL DATA FOR THE NINE AMINO ACIDS EXHIBITING A SINGLE POLAROGRAPHIC WAVE IN DMSO

Amino acids	*Slope, i_l/concn. ($\mu A/mM$)*	*Std. devn. of slope, i_l/concn.*	*Intercept of plot i_l vs. concn. (μA)*	*Temperature coefficient (%)*	*n-Value*[a]
Asparagine	0.498	0.035	−0.050	1.95	0.635
Hydroxyproline	0.629	0.069	−0.005	1.40	0.899
Isoleucine	0.425	0.041	0.045	1.53	0.650
Methionine	0.615	0.071	0.000	1.35	1.088
Phenylalanine	0.555	0.060	0.005	1.84	0.926
Proline	0.881	0.036	−0.110	−0.07	1.027
Threonine	0.660	0.021	0.001	1.40	1.069
Tryptophan	0.618	0.076	−0.048	0.99	1.020
Tyrosine	0.499	0.042	−0.047	3.26	1.070

[a] Obtained by constant-potential coulometry.

Nine of the fourteen amino acids studied in DMSO gave a single cathodic wave. The wave was in every case well-formed and exhibited rounding on the plateau. This rounding was due to the rapid increase in drop time at these potentials. In each case the limiting current, i_l, was found to be linearly related to the total analytical amino acid concentration in the range $4 \cdot 10^{-4}$ to $2 \cdot 10^{-3}$ M.

Table I lists the values of slope (i_l/concn.) and intercept for each working curve. The slopes of these curves are considerably smaller than would be expected for a normal diffusion-controlled wave where all of the electroactive compound present is available for reduction. Also shown in Table I are standard deviations for the slope values; in most cases the standard deviations are prohibitively high. This is undoubtedly due to several factors. One problem is that, at best, the reduction waves are about 1 μA in height, at which height the error in the current measurement by the polarograph is larger than the usual 2–3 %. Also, difficulty in dissolution of the amino acids probably added uncertainty to the reducible amino acid concentration and thus error to the result. In any case, polarography is not a very good quantitative method for determination of amino acids in DMSO.

Several studies were undertaken to determine the transport mechanism involved in the reduction process. Temperature coefficients of the limiting currents are given in Table I; these values were measured between 25° and 38°. The possibility of kinetic control is eliminated on the basis of these values.

The effect on the limiting current of variations in the height, h, of the mercury column was extensively studied. All h values used in this study were corrected for back-pressure. Since h had a definite influence on i_l, the possibility of catalytic control was eliminated. However, no decision could be made as to whether diffusion or adsorption, or both, were involved, based on these data. In plots of i_l *vs.* $h^{\frac{1}{2}}$ and i_l *vs.* h, no distinction could be made as to which was curved and which was linear. The same was true of a Koutecký plot of i_l/h *vs.* $h^{\frac{1}{2}}$. This difficulty was undoubtedly due to the error involved in each point, caused by factors previously discussed. Thus the reduction waves are due either to diffusion or adsorption, or perhaps both.

Two other experimental observations, however, lead to the conclusion that at least some of the molecules undergoing reduction are adsorbed on the electrode surface. It was observed in amino acid solutions that the end reduction was shifted to more negative potentials than in electrolyte solutions. This type of behavior may be indicative of adsorption; the adsorbed amino acid molecules could help to dissipate the surface charge, partially depolarizing the electrode and permitting it to reach higher potentials before reducing the electrolyte or solvent. Also, it was sometimes observed that the electrode would abruptly and reproducibly begin to stream at a definite potential; when this effect was present, it was further observed that the streaming potential shifted to more anodic values as the concentration of amino acid decreased. This would be consistent with adsorption, where again the surface energy of the drop was partially dissipated by the adsorbed amino acid, whose surface concentration would decrease as the bulk concentration decreased. This conclusion is in agreement with that of Matthews[8], who found adsorption of amino acids on a mercury electrode in aqueous solution.

Plots of E *vs.* log $i/(i_l - i)$ were prepared for each of these nine amino acids. In no case was this plot linear, indicating that all these acids were irreversibly reduced. For several amino acids, cyclic oscillographic polarograms were run, with the oscillographic polarograph made by Chemtrix, Inc. The absence of an oxidation wave in the lower (return) cycle of the scan was proof of irreversible reduction.

The results of constant-potential coulometric studies for these nine amino acids are given in Table I. The n values for isoleucine and asparagine are lower than the others. This is inexplicable on any theoretical basis; apparently not all the molecules of these two amino acids are reducible under the conditions of the analysis. It is presumed, however, that all of the reduction waves due to amino acids in Table I are the result of one-electron processes.

TABLE II

EXPERIMENTAL HALF-WAVE POTENTIALS AND LITERATURE pK VALUES FOR AMINO ACIDS

Amino acid	$-E_{\frac{1}{2}}$ *(V)*	*pK(COOH)*	*pK(NH₂)*
Asparagine	2.382 ± 0.010	2.02	8.80
Hydroxyproline	2.317 ± 0.013	1.92	9.73
Isoleucine	2.465 ± 0.013	2.36	9.68
Methionine	2.435 ± 0.011	2.28	9.21
Phenylalanine	2.398 ± 0.007	1.83	9.13
Proline	2.307 ± 0.008	1.99	10.60
Threonine	2.368 ± 0.005	2.63	10.43
Tryptophan	2.388 ± 0.007	2.38	9.39
Tyrosine	2.379 ± 0.019	2.20	9.11
Glutamine (2)	2.428 ± 0.021	2.17	9.13

Table II lists half-wave potentials and literature values[9] for pK(COOH) and pK(NH_2), of the nine amino acids giving single waves and of glutamine (second wave only). The half-wave potentials were found to be very slightly dependent on concentration, a characteristic feature of irreversible waves.

Further data indicate that the reduction process is probably the catalytic reduction of a proton on the amino acid molecule. The one-electron reduction of a proton at either the carboxyl or amine site is the only likely possibility.

Evidence that hydrogen was reduced was found in a study of the effect of acidity on the limiting current. An amino acid solution was titrated with hydrochloric acid and with sodium ethoxide dissolved in DMSO. It was observed that the limiting current was linearly related to the acidity of the solution.

Further evidence for the postulation of hydrogen reduction was found when the "pH" of the amino acid solution was followed during a constant-potential electrolysis. The plot was identical in shape to a current–time curve for constant-potential coulometry plotted on the same time axis. This provided strong evidence that protons were being consumed in the reduction process.

Correlation of $E_{\frac{1}{2}}$ and pK values for amino acids

The question arises as to the location of the reducible proton on the amino acid molecule. No evidence exists in the literature to indicate which form amino acids assume in DMSO. The most likely possibilities would appear to be either the molecular form, or the zwitterion form found in water. In an attempt to determine the location of the reducible proton, the half-wave potentials obtained experimentally were related to literature pK values for the carboxyl and amine protons. The half-wave potentials and the pK values for the position of the reducible proton should be related linearly.

$$\begin{array}{ll}
\mathrm{AH}+e^- = \mathrm{A}^- + \tfrac{1}{2}\mathrm{H}_2 & \Delta G_1^0 = -nFE^0 \\
\mathrm{AH} = \mathrm{A}^- + \mathrm{H}^+ & \Delta G_2^0 = -RT\ln K = 2.303\,RT\,\mathrm{p}K \\
\hline
\mathrm{H}^+ + e^- = \tfrac{1}{2}\mathrm{H}_2 & \Delta G_1^0 - \Delta G_2^0 = \text{constant} = \\
 & \quad -nFE^0 - 2.303\,RT\mathrm{p}K
\end{array}$$

Plots of $E_{\frac{1}{2}}$ *vs.* pK(COOH) and $E_{\frac{1}{2}}$ *vs.* pK(NH_2) were made; the former plot was linear indicating that the reducible proton was probably located on the carboxyl group. No relationship was apparent in the plot of pK(NH_2) *vs.* $E_{\frac{1}{2}}$. However, these data can only be considered indicative of a relationship, since the pK values refer to aqueous solutions. Thus, implicit in any conclusion is the assumption that pK values in DMSO are in the same relative order as in water (although not necessarily of the same magnitude).

Other evidence which supports this conclusion is found by comparing the half-wave potentials obtained in DMSO for some amines and carboxylic acids (listed in Table III), with those of the amino acids. Under identical conditions, the carboxylic acids studied generally give half-wave potentials similar to those of the amino acids, whereas the amines undergo reduction at lower potentials. Thus, the evidence suggests that the reducible proton probably resides on the carboxyl group. Presumably, this indicates that the reducible amino acid species in DMSO solution is the molecular form.

Potentiometric titration of amino acids in DMSO

A question still remains of why the reduction wave is so much smaller than is expected. A possible explanation is that under the conditions of the analysis, an equilibrium exists between the reducible form and another form of the amino acid. Further information on this problem was obtained from potentiometric titrations.

TABLE III

HALF-WAVE POTENTIALS OF RELATED COMPOUNDS

Compound	$-E_{\frac{1}{2}}$ (*V*)
n-Butylamine	2.23
n-Propylamine	2.20
Aminophenylsulfone	2.24
Propionic acid	2.36
Butyric acid	2.36
Glutaric acid	2.39
Succinic acid	2.29
Methylglutaric acid	2.40
Methylsuccinic acid	2.41
Malic acid	2.25

Amino acid solutions in DMSO were titrated with hydrochloric acid and sodium ethoxide in DMSO. Titration of one of these reagents with the other gave a titration curve characteristic of a strong acid–strong base reaction.

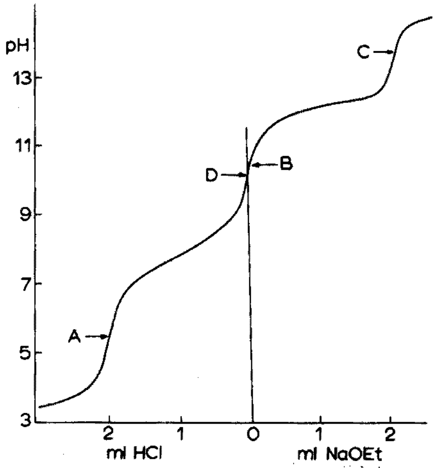

Fig. 1. A typical amino acid titration curve in DMSO.

A typical amino acid titration curve in DMSO is shown in Fig. 1. At position B on the titration curve, all of the amino acid molecules are in a "neutral" form, possessing no net charge. At A, all molecules are in an acidic cationic form, and at C, all are in a basic anionic form. A, B, and C are extrapolated equivalence points. In one titration the solution was acidified, then titrated through all three breaks; this titration confirmed the position of the equivalence point B found in the other titrations.

Position D on the titration curve indicates the "pH" of the initial titration solutions. These initial solutions were identical to those used in polarographic studies. The fact that D is almost identical to B indicates that virtually all of the amino acid molecules are in a neutral form in the initial solutions. Thus, no equilibrium between two acid–base forms existed in the solutions used for polarography.

It should be noted, however, that the above data say nothing about the possibility of an equilibrium between two neutral forms, *e.g.* the molecular and zwitterionic forms. However, the existence of a zwitterion in DMSO seems doubtful. In water, the solvent can form a hydrogen bridge to assist in transferring the proton to the amine group. DMSO, while a polar solvent which can participate in hydrogen bonding, cannot bridge like water since it has no ionic protons. Thus, a solvated amino acid molecule hinders rather than assists zwitterion formation.

Two distinct possibilities thus emerge to explain the low slope of the limiting current–concentration plot. The first is an equilibrium between a reducible molecular form and a strongly solvated, non-reducible molecular form. The reduction of the carboxyl proton occurs at very high potentials, and a small increase in the energy required for the reduction, which strong solvation may cause, could make the proton impossible to reduce in the usable potential range. Another possibility is that the amino acid is all in one solvated reducible form. If the molecule were highly solvated, it would have a small diffusion coefficient, which would give rise to a small slope on the i_l *vs.* concentration plot.

TABLE IV

ELECTROCHEMICAL DATA FOR THE FIVE AMINO ACIDS EXHIBITING MULTIPLE POLAROGRAPHIC WAVES IN DMSO

Amino acid (wave no.)	$-E_{\frac{1}{2}}$ *(V)*	*Slope, i_l/concn. ($\mu A/mM$)*	*Std. devn. of slope, i_l/concn.*	*Intercept of plot i_l vs. concn. (μA)*	*Temperature coefficient (%)*	*n-Val*
DOPA (1)	2.375±0.016	0.488	0.048	−0.019	2.55	1.227
DOPA (2)	2.625±0.026	0.578	0.069	0.087	−1.42	0.896
Glutamic acid (1)	2.123±0.019	0.545	0.064	0.009	2.11	0.913
Glutamic acid (2)	2.604±0.023	0.414	0.100	0.049	4.73	(1)
Aspartic acid (1)	2.141±0.020	0.612	0.039	−0.017	0.46	0.771
Aspartic acid (2)	2.618±0.007	0.866	0.049	0.141	2.30	0.724
Glutamine (1)	2.090±0.012	0.287	0.025	−0.059	2.68	0.881[a]
Glutamine (2)	2.428±0.021	0.272	0.071	0.180	1.35	
Cysteine·HCl (1)	0.168±0.007	1.878	0.457	0.289	0.89	1.62
Cysteine·HCl (2)	1.321±0.018	0.485	0.044	0.037	2.66	0.688
Cysteine·HCl (3)	1.788±0.008	0.343	0.082	−0.019	1.06	1.024
Cysteine·HCl (4)	2.014±0.011	0.994	0.074	0.016	1.06	1.123
Cysteine·HCl (5)	2.660±0.019	0.695	0.085	0.130	1.26	1.10

[a] The sum of the *n*-values for the two waves.

Polarographic behavior of other amino acids

In addition to the nine amino acids discussed above, several others were studied. Data for all are given in Table IV. Dihydroxyphenylalanine (DOPA) gave two one-electron, irreversible, cathodic waves. The first wave corresponds to the wave observed with the previously mentioned amino acids. The second wave is due to the reduction of a proton from one of the ring hydroxyl groups, a process which is favored by the formation of a hydrogen-bridge bond in a five-membered ring after reduction.

This postulation is supported by the fact that pyrocatechol was found to give a wave in DMSO of identical shape to the second DOPA wave, having a half-wave

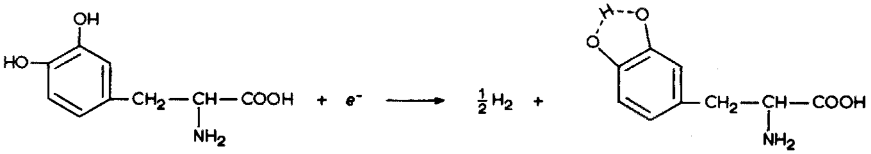

potential of −2.511 V *vs.* S.C.E. Tyrosine, which is similar to DOPA but lacks one hydroxyl group, does not exhibit a second reduction wave.

Two bifunctional amino acids, glutamic acid and aspartic acid, were each found to give two waves of equal height in DMSO. Neither wave has a half-wave potential near those for the first nine amino acids. Each wave is apparently due to reduction of a proton, but no data are available to indicate which protons are involved. The related compounds, glutaric and succinic acids and their mono-methyl esters, were studied in the hope that they could shed light on the problem. However, as shown in Table III, each of these compounds gave only one wave, and did not provide any clues as to the locations of the reducible protons in the amino acids.

Glutamine gives two waves in DMSO. Constant-potential coulometric reduction at the first wave indicated a one-electron process, and eliminated the second wave. Although both waves are linearly related in height to concentration, the coulometric data indicate that the first wave is probably an adsorption prewave. The second wave corresponds to the reduction of the carboxyl proton as in the first nine amino acids.

Cysteine hydrochloride was found to give one anodic and four cathodic waves in DMSO. Giang *et al.*[10] have previously studied this system; they attributed the anodic wave to a combined electrode reaction involving both chloride ion and the sulfhydryl group in the oxidation of mercury.

$$2\,Hg + RSH \cdot HCl \rightarrow \tfrac{1}{2}Hg_2Cl_2 + HgSR \cdot H^+ + H^+ + 2\,e^-$$

Present data support this suggestion.

None of the cathodic waves can be considered a prewave or a postwave, for each gave a reasonable *n*-value regardless of any pre-electrolysis at one or more of the preceding waves. The third cathodic wave exhibited a maximum at concentrations above $1.2 \cdot 10^{-3}$ *M* cysteine. While definite assignments cannot be made, it seems likely that one of these cathodic waves is due to reduction of the sulfhydryl proton, and that one is due to reduction of the hydrochloride proton, either as the $-NH_3^+$ group or as the solvated proton. The possibility of intramolecular hydrogen bonding between the sulfhydryl and amino groups may lead to reduction of another proton from the amino group, giving rise to the third wave. These seem to be logical postulates, but available data permit no definite conclusions.

Giang *et al.*[10] reported a wave at −2.14 V, which was not observed by the present authors. However, a wave was found at −2.66 V in the present work which was not reported in their paper. This wave is probably due to reduction of the carboxyl proton, which may be shifted to higher potentials by the presence of the chloride ion.

The authors are indebted to the U.S. Army Medical Research and Development Command for partial support of this work under Contract No. DADA17-67-C-7161.

SUMMARY

Polarographic reduction of nine amino acids in DMSO gave single waves, involving one-electron reduction of the proton of the carboxyl group. Possible reducible species are discussed. Five amino acids giving multiple waves were also investigated.

RÉSUMÉ

Les réductions polarographiques de neuf acides aminés, dans le diméthylsulfoxyde, ont donnés des vagues simples, comprenant une réduction à un électron du proton du groupe carboxylique. On a examiné également cinq acides aminés donnant des vagues multiples.

ZUSAMMENFASSUNG

Die polarographische Reduktion von neun Aminosäuren in DMSO ergab jeweils eine Stufe, die der Einelektronenreduktion des Protons der Carboxylgruppe zugeordnet wird. Mögliche reduzierbare Spezies werden diskutiert. Ausserdem wurden fünf Aminosäuren untersucht, die mehrere Stufen ergaben.

REFERENCES

1 V. H. DAYAN, *Diss. Abstr.*, 14 (1954) 1906.
2 Y. OKAZAKI AND T. OTSUKI, *Rev. Polarog. (Kyoto)*, 14 (1967) 307.
3 C. W. MANNING AND W. C. PURDY, *Anal. Chim. Acta*, 51 (1970) 483.
4 L. MEITES, *Polarographic Techniques*, 2nd Edn., Interscience, New York, 1965, p. 89.
5 L. MEITES, *Polarographic Techniques*, 2nd Edn., Interscience, New York, 1965, pp. 59–61.
6 J. J. LINGANE, *Electroanalytical Chemistry*, 2nd Edn., Interscience, New York, 1958, p. 242.
7 T. B. REDDY, *Ph.D. Dissertation*, University of Minnesota, 1960.
8 D. B. MATTHEWS, *J. Biomed. Materials Res.*, 3 (1969) 475.
9 H. R. MAHLER AND E. H. CORDES, *Biological Chemistry*, Harper and Row, New York, 1966, p. 10.
10 B. Y. GIANG, G. D. CHRISTIAN AND W. C. PURDY, *J. Polarog. Soc.*, 13 (1967) 17.

Analytica Chimica Acta
Elsevier Publishing Company, Amsterdam
Printed in The Netherlands

SPECTROPHOTOMETRIC DETERMINATION OF SILICON BY A STANDARD ADDITION PROCEDURE

P. PAKALNS
Australian Atomic Energy Commission Research Establishment, Lucas Heights, N.S.W. 2232 (Australia)

(Received 20th July 1970)

Standard procedures for the spectrophotometric determination of silicon by the blue molybdosilicate methods in steel[1,2], nickel[3], titanium[4,5], zirconium[5,6], aluminium[7] and uranium–silicon alloy[8] require the preparation of a standard silicon absorbance curve with solutions containing amounts of metal and acids similar to those present in the test solution. Standard curves correct for interferences caused by varying amounts of the base metal, acid concentrations, neutral salts, hydrofluoric and boric acids, and differences in the volume in which the colour development takes place. If the overall conditions are carefully controlled, reproducible results can be obtained. Recent work by the Standards Association of Australia[9] has shown that large amounts of alloying metals in steels can have an appreciable effect on the silicon absorbance, and to minimize this effect an aliquot containing not more than 10 mg of steel is recommended for spectrophotometry.

Preparation of standard curves which duplicate the sample solution is not possible in all cases, and for a precise determination of silicon a standard addition procedure must be used. A standard addition procedure has been used successfully in the spectrophotometric determination of silicon[10], phosphorus[11] and arsenic[12] by extraction methods. To make the standard addition procedure flexible, the exact pH ranges for the development of the yellow molybdosilicate in various acid media and the effect of various salts must be known.

Some information about the pH range for the development of the yellow molybdosilicate in sulphuric[10,13], hydrochloric[14] and nitric[15] acids was available. The first part of this paper describes the pH ranges for the development of the yellow molybdosilicate in sulphuric, hydrochloric, nitric and perchloric acids, and the effects of the sodium salts of these acids, fluoride–boric acid, zirconium–fluoride and titanium–fluoride mixtures on the pH in various acid media. This information enables silicon to be determined in any of these four acids and assists in the selection of the correct pH when salts are present and in cases where hydrofluoric acid has been used to convert silicon into a "reactive" form. The second part of this paper deals with the determination of silicon in various metals and alloys, and demonstrates the versatility of the standard addition procedure.

EXPERIMENTAL

Apparatus and reagents

A Unicam S.P. 600 spectrophotometer with 1-cm glass cuvettes was used.

An E.I.L. Model 23A direct reading pH meter and a GHS23 glass electrode were used. The electrode was standardized against 0.1 *M* hydrochloric acid (pH 1.08). A saturated (KCl) calomel reference electrode was used, except for perchloric acid systems where it was replaced by a saturated (NaCl) calomel electrode. For low pH work new glass electrodes were left in 1 *M* hydrochloric acid for 24 h before use. It is important that glass electrodes be immersed in 0.1 *M* hydrochloric acid between pH measurements, because this improves the reproducibility of pH readings at higher acidities. Glass electrodes in continuous operation lasted about 4 months before the response became erratic.

Glass electrodes were tested for reproducibility as follows. Pipette into a 250-ml polythene beaker 0.1 ml of 40% hydrofluoric acid, 2 ml of 9*N* sulphuric acid and 7.5 ml of 4% boric acid. Dilute to 60 ml and let stand for 15 min. Standardize the pH meter against 0.1 *M* hydrochloric acid (pH 1.08). Immerse the electrodes in the test solution for 5 min. Then wash with water and remove any adhering water. Immerse the electrodes in 0.1 *M* hydrochloric acid, when the pH should return to 1.08.

Standard silicon solutions, 1 *mg and* 10 *μg Si ml*$^{-1}$. Prepare a stock solution containing 1 mg Si ml^{-1} by fusing 0.535 g of pure calcined silica with 5 g of anhydrous sodium carbonate. Dissolve the cooled melt in water, dilute to 250 and store in a polythene bottle. Prepare a working solution (10 μg Si ml^{-1}) by dilution with water; store in a polythene bottle.

Reducing solution. Solution (a): Dissolve 90 g of sodium metabisulphite in 800 ml of water. Solution (b): Dissolve 14 g of sodium sulphite heptahydrate in 100 ml of water and then add 1.5 g of 1-amino-2-naphthol-4-sulphonic acid. Mix solutions (a) and (b) and dilute to one l with water.

Hydrofluoric acid (40%). "Suprapur" (Merck), containing less than 5 p.p.m. of silicon.

Preparation of absorbance–pH curves in various acids (with or without sodium salts)

Aliquots containing 100 μg of silicon were transferred to a number of 250-ml polythene beakers. Sodium salts were added when required. Various amounts of 9 *N* acid were added to the beakers and 0.1 ml of 10% hydroxylammonium chloride was added to nitric and perchloric acid solutions. (When excess of acid was added, the pH was adjusted with increasing amounts of ammonia.) Solutions were diluted to 60 ml, 10 ml of 5% ammonium molybdate was added, and the pH was determined. The pH readings were recorded after the electrodes had been in contact with the first solution for 5 min and each subsequent solution in a series for 1 min. The experiments were carried out in such a manner that solutions of a lower or a higher pH range were grouped together. Fifteen min after the addition of ammonium molybdate, 2 ml of 20% tartaric acid was added and the solutions were mixed. After 1 min, 5 ml of the reducing solution was added. The solution was transferred to a 100-ml volumetric flask and diluted to volume with water. After 30 min the absorbance was measured against a reagent blank at 725 nm in 1-cm cells.

Preparation of absorbance–pH curves for solutions containing fluoride (with or without sodium salts)

Solutions containing silicon, sodium salts, acid and, where necessary, hydroxylammonium chloride were prepared as above. An aliquot of 40% hydrofluoric acid was added and, after 10 min, 7.5 ml of 4% boric acid was added for each 0.1 ml of 40%

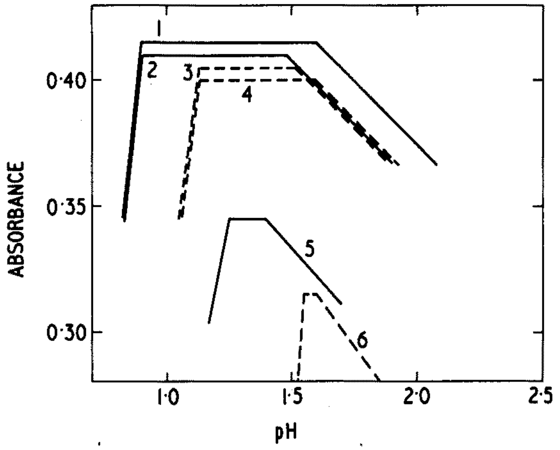

Fig. 1. The effect of pH and salts after ammonium molybdate addition on the absorbance in sulphuric acid solution (100 μg of Si, 70 ml volume). (1) Standard curve; (2) 7.5 ml of 4% H_3BO_3; (3) 0.1 ml of 40% HF and 7.5 ml of 4% H_3BO_3; (4) 0.5 ml of 40% HF and 37.5 ml of 4% H_3BO_3; (5) 5.25 g Na_2SO_4; (6) 5.25 g of Na_2SO_4, 0.1 ml of 40O HF and 7.5 ml of 4% H_3BO_3.

hydrofluoric acid. (Excess of acid was neutralized with increasing amounts of ammonia where necessary.) Solutions were then diluted to 60 ml, and after 15 min, molybdate was added, and the procedure completed as described above.

Preparation of absorbance–pH curves for solutions containing zirconium

A solution containing 50 mg Zr ml^{-1} was prepared by dissolving 5 g of zirconium metal in 10 ml of 40% hydrofluoric acid and diluting to 100 ml with water. Aliquots containing 50, 100 and 200 mg of zirconium were transferred to 250-ml polythene beakers containing 100 μg of silicon. Various amounts of 9 *N* acid were added (and 0.1 ml of 10% hydroxylammonium chloride for nitric acid only). After 10 min, 7.5 ml of 4% boric acid was added and the solutions were diluted to 60 ml. After another 15 min, 10 ml of 5% ammonium molybdate was added and the experiment was continued as for the preparation of absorbance–pH curves in various acids.

RESULTS AND DISCUSSION

The effect of pH on absorbance and dissolution of sample

Absorbance plateaux over reasonable pH ranges were obtained in all four acid media when no ammonia had been added to neutralize excess of acid. Figure 1 shows the results obtained for sulphuric acid media; similar graphs were observed for the other acids used. The pH ranges which gave the maximal development of the yellow molybdosilicate in various acids, even when small amounts of metals or salts were present, were *ca.* 0.7 pH units. Details of the permissible pH ranges with different acids and different additions are shown in Table I. Variations in the permissible pH range when titanium was present are shown in Fig. 2. Govett[13] reported that equal concentrations of hydrochloric or sulphuric acid were required to obtain the maximum absorbance plateau for the yellow molybdosilicate.

When solutions were strongly acidic, and *ca.* 0.7 ml of 15 *M* ammonia was used

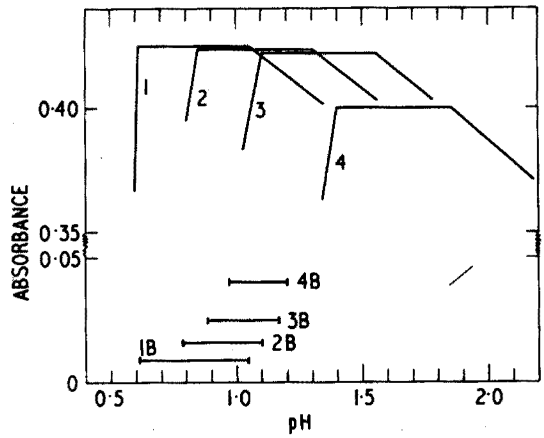

Fig. 2. The effect of pH, titanium and 1.5 g of sodium sulphate after 20 ml of 5% ammonium molybdate addition on the absorbance in nitric acid solution (100 μg Si, 80 ml volume). (1) No Ti, 7.5 ml of 4% H_3BO_3; (2) 0.025 g of Ti, 0.1 ml of 40% HF and 7.5 ml of 4% H_3BO_3; (3) 0.050 g of Ti, 0.2 ml of 40% HF and 15 ml of 4% H_3BO_3; (4) 0.100 g of Ti, 0.4 ml of 40% HF and 30 ml of 4% H_3BO_3. Curves 1B, 2B, 3B and 4B are blanks, containing no titanium, for curves 1, 2, 3 and 4 respectively.

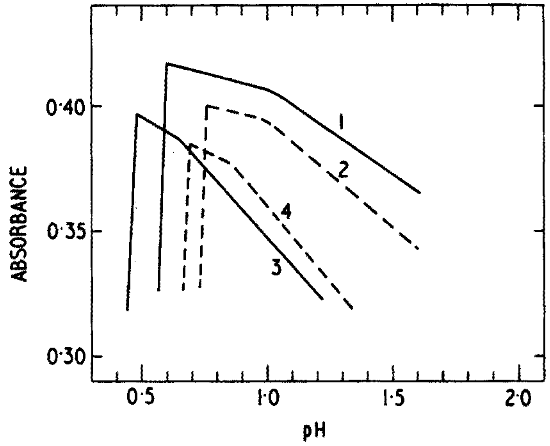

Fig. 3. The effect of pH and salts after ammonium molybdate addition on the absorbance containing 3.3 ml of 9 *N* hydrochloric acid (100 μg Si, 70 ml volume). (1) Excess acid only; (2) 0.1 ml of 40% HF and 7.5 ml of 4% H_3BO_3; (3) 4.3 g of NaCl; (4) 4.3 g of NaCl, 0.1 ml of 40% HF and 7.5 ml of 4% H_3BO_3.

to neutralize the acid, all the absorbance–pH curves reached a maximum absorbance and then sloped downwards with increasing pH, owing to increased ammonium salt concentrations. The absorbance–pH curves for hydrochloric acid are shown in Fig.3; rather similar curves were found for nitric acid, but with perchloric acid, and especially sulphuric acid, the absorbance decreased more steeply as the pH increased. The pH values for maximal absorbance under different conditions are shown in the last column of Table I. The decrease in absorbance with increased pH in the presence of ammonium ions indicates that an excess of acid must be avoided when possible in sample disso-

TABLE I

THE REQUIRED pH FOR THE COLOUR DEVELOPMENT AFTER THE ADDITION OF AMMONIUM MOLYBDATE (100 μg Si; volume 70 ml)

Acid medium	*Additions*			*pH for maximal colour development*		
	4% H_3BO_3 (ml)	*40% HF (ml)*	*NaX*[a] *(g)*	*Min.*	*Max.*	*in presence of NH_4^+*[g]
H_2SO_4	—	—	—	0.90	1.60	1.00
	7.5	—	—	0.90	1.48	—
	7.5	0.1	—	1.13	1.53	1.22
	37.5	0.5	—	1.13	1.57	—
	—	—	5.25	1.25	1.40	1.35
	7.5	0.1	5.25	1.55	1.60	1.70
HCl	—	—	—	0.64	1.38	0.60
	7.5	0.1	—	0.86	1.36	0.76
	37.5	0.5	—	1.03	1.52	—
	—	—	4.3	0.49	0.75	0.48
	7.5	0.1	4.3	0.74	0.92	0.69
HNO_3[b]	—	—	—	0.62	1.28	0.60
	7.5	—	—	0.62	1.15	—
	7.5	0.1	—	0.84	1.36	0.69
	37.5	0.5	—	1.00	1.43	—
	—	—	6.3	0.43	0.74	0.45
	7.5	—	6.3	0.43	0.74	—
	7.5	0.1	6.3	0.65	0.90	0.56
$HClO_4$[b,c]	—	—	—	0.49	1.16	0.48
	7.5	0.1	—	0.81	1.33	0.72
	37.5	0.5	—	0.87	1.30	—
	—	—	9.15	0.25	0.75	0.38
	7.5	0.1	9.15	0.38	0.85	0.62
HNO_3[b]	7.5	0.1	—[d]	0.76	1.36	—
	7.5	0.2	—[e]	0.74	1.34	—
	7.5	0.4	—[f]	0.71	1.30	—
H_2SO_4	7.5	0.1	—[d]	1.03	1.66	—
	7.5	0.2	—[e]	1.05	1.68	—
	7.5	0.4	—[f]	1.08	1.71	—

[a] Sodium salt of the acid used, the amount added being equivalent to 3 g NaOH.

[b] 0.1 ml of 10% $NH_2OH \cdot HCl$ added.

[c] Calomel (NaCl) electrode used in pH adjustment.

[d] 0.05 g Zr added.

[e] 0.1 g Zr added.

[f] 0.2 g Zr added

[g] 3.3 ml 9 *N* acid added and pH adjusted with ammonia solution.

lution procedures. When the existing practice of preparing standard curves for individual metals is used, the amount of acid must be carefully controlled, which prohibits the use of high concentrations of strong oxidizing acids, and temperatures below boiling point should be used in the dissolution to avoid changes in the acid concentration. The advantage of using the standard addition procedure is that samples can be dissolved in strong acids and fumed with sulphuric or perchloric acid, and silicon can be determined in very acid solutions if dilute ammonia (3 *M*) is added accurately to both test and standard addition solutions.

Salt effect

Addition of salts causes a shift in the minimal pH required for the development of the yellow silicomolybdate and narrows the optimal pH range. Sodium sulphate shifts the optimal pH towards higher values, and sodium chloride, nitrate and perchlorate shift this pH towards lower values. An amount of each salt equivalent to 3 g of sodium hydroxide was added to acid solutions. The minimal pH required for colour development in solutions containing smaller amounts of salt can be estimated from the difference between two curves in the presence and absence of salt. Sodium salts were studied because of the utility of alkaline dissolution or fusion processes.

Effect of fluoride

Addition of 7.5 ml of 4% boric acid when fluoride was not present did not change the minimal pH required for the colour development (Table I). When fluoride was present, an amount of 7.5 ml of 4% boric acid was added for each 0.1 ml of 40% hydrofluoric acid. The data indicate that when less than 0.1 ml of 40% hydrofluoric acid is present in solutions containing a small amount of salts, the total amount of boric acid must be increased to 7.5 ml. The correct pH is then selected from the curve drawn for solutions containing 0.1 ml of 40% hydrofluoric acid and 7.5 ml of boric acid. For solutions containing a large amount of salts, 0.1 ml of 40% hydrofluoric acid and 7.5 ml of boric acid should be added.The correct pH can then be read from the appropriate curve.

Zirconium forms a strong complex with fluoride, and 1 g of zirconium metal can be dissolved in 2 ml of 40% hydrofluoric acid. A constant amount of 7.5 ml of 4% boric acid was added to each aliquot of these zirconium–fluoride solutions to protect the glass electrodes. Carlson and Banks[16] reported absorbance curves which reached a maximum absorbance and then sloped at higher pH values; the procedure described here seems to permit reasonably wide pH ranges.

Standard addition and choice of wavelength

Standard addition gives a free choice in selecting various parameters which have an important effect on the absorbance of the blue molybdosilicate, *e.g.* acid concentration, solution volume, salts, fluoride, ammonium molybdate and tartaric acid concentrations, and standing times between additions of various reagents. It also provides an exact pH adjustment for the development of the yellow molybdosilicate, which is important when excess of acid must be neutralized with ammonia. The only error introduced by the standard addition procedure is in the preparation of the blank. When metal samples are dissolved, some acid is consumed in the dissolution, which, of course, does not occur in the blank. However, the absorbance of the blank, measured against its compensating solution was found to be so small (*ca.* 0.005 abs. units), that the difference in acid concentrations between blank and test solution has no practical effect on the absorbance measurements. Even when sodium hydroxide was used to dissolve aluminium metal, the blank measured against compensating solution was only 0.008 abs. units for 0.4 g of sodium hydroxide.

Beer's law was obeyed to 2.5 μg Si ml^{-1}; therefore it is recommended that a sample aliquot of about 100 μg of silicon is selected and a standard addition of 100 μg of silicon made. A wavelength of 725 nm was selected because 100 μg of silicon in 100 ml gave an absorbance of *ca.* 0.400 abs. units, and this wavelength could be used to determine silicon as low as 0.1% and 0.33% in aluminium and steels respectively (Table II). A wavelength of 800 nm should be selected when aliquots containing 50 μg of silicon are used; a standard addition of 50 μg of silicon is then recommended.

Adjustment of pH and measurement of absorbance

It is impractical to adjust the pH after ammonium molybdate addition because many metals may precipitate, and the washing of the electrodes will alter the final volume. It is recommended that a compensating solution be used which then can be used for pH adjustment before the addition of tartaric acid and ammonium molybdate. The same amount of acid or ammonia as added to the compensating solution must be added to the test and standard addition solutions before the addition of ammonium molybdate.

The alkalinity of the ammonium molybdate varies with different supplies. The alkalinity of the ammonium molybdate (May and Baker Ltd.) used in these experiments was such, that after the addition of 10 ml of 5% solution to 60 ml, the pH increased by *ca.* 0.10, 0.15 and 0.20, in the pH ranges of 0.4–0.7, 0.7–1.5 and above 1.5, respectively. In general, it is safer to adjust the pH to a higher than to a lower value. The technique used was to adjust the pH, before the ammonium molybdate addition, to the minimum pH required for maximal colour development.

Dissolution of samples in mixed acids

The above data refer only to single acid systems. Therefore an investigation was necessary to determine the pH–absorbance curves for nitric–sulphuric and nitric–hydrochloric–sulphuric acid systems. Mixtures of nitric and sulphuric acids were used to dissolve steels and irons, and nitric, hydrochloric and sulphuric acids to dissolve aluminium. For the hydrochloric–nitric acid system an average pH–absorbance curve may be selected from the data given in Table I.

A nitric–sulphuric acid solution was prepared by diluting 4.5 ml of 15 *M* nitric acid (67.5 meq) and 3.6 ml of 18 *M* sulphuric acid (130 meq) to 500 ml. When various aliquots of mixed acid were used, it was found that a minimal pH of 0.81 was required to obtain the maximal silicon absorbance.

A hydrochloric–nitric–sulphuric acid solution was prepared by diluting 10 ml of 4.5 *M* sulphuric acid (90 meq), 6 ml of 15 *M* nitric acid (90 meq) and 6 ml of 10 *M* hydrochloric acid (60 meq) to 250 ml. When various aliquots of mixed acid were used, a minimal pH of 0.73 was found to give the maximal silicon absorbance.

Calculations may be carried out to determine the minimal pH required for maximal colour development by the following equation:

$$\text{Minimal pH} = \frac{a_1 m_1 + a_2 m_2 + \ldots + a_n m_n}{m_1 + m_2 + \ldots m_n}$$

where $a_1 \ldots a_n$ is the minimal pH required for acid $1 \ldots n$, and $m_1 \ldots m_n$ is the amount of acid $1 \ldots n$ in milliequivalents.

TABLE II

DETERMINATION OF SILICON IN VARIOUS MATERIALS BY STANDARD ADDITION

Sample	*Certified Si (%)*	*Si found (%)*	*Absorbances on standard addition (100 μg Si)*
Steel 18Cr–8Ni	2.48	2.48, 2.50, 2.52	0.414, 0.416, 0.417
BCS 312 (13Ni–24Co+Ti, Nb)	1.13	1.09, 1.10, 1.11	0.410, 0.413, 0.415
	(Range 1.09–1.18)	1.09, 1.11, 1.12[a]	0.422, 0.423, 0.427
BCS 241/1(5Cr–V–18W–5Co–Mo)	0.33 (Range 0.31–0.35)	0.328, 0.329, 0.334[a]	0.406, 0.412, 0.413[b]
Al powder	—	0.118, 0.119, 0.119[c]	0.394, 0.395, 0.399
		0.112, 0.112, 0.113[d]	0.405, 0.410, 0.410
		0.118, 0.119, 0.120[e]	0.368, 0.370, 0.373
		0.119, 0.119, 0.119[f]	0.398, 0.398, 0.403
BCS 182/1(11Si–Al)	11.48 (Range 11.43–11.51)	11.4, 11.4, 11.5[g]	0.410, 0.412, 0.412
Ni–Si alloy	—	3.94, 3.96, 3.98	0.422, 0.423, 0.423
U_3Si alloy	—	3.76, 3.77, 3.79	0.411, 0.412, 0.416
KHF_2	—	0.196, 0.197, 0.200[h]	0.408, 0.410, 0.410
Ti sponge	—	0.0354, 0.0357, 0.0364	0.390, 0.393, 0.395

[a] Reduced with ascorbic acid.

[b] Absorbances on standard addition depend on dissolved W present.

[c] Dissolved in acid mixture with HF.

[d] Dissolved in acid mixture without HF.

[e] Dissolved in NaOH; H_2SO_4 and HNO_3 added, with HF.

[f] Dissolved in NaOH; H_2SO_4 and HNO_3 added, without HF.

[g] 0.25 g boiled for 30 min with 40 ml 10% NaOH; H_2SO_4 and HNO_3 added.

[h] As K_2SiF_6.

When the required pH for nitric–sulphuric acid and hydrochloric–nitric–sulphuric acid mixtures are determined by the given equation the pH values found were 0.80 and 0.73, respectively, which is in very good agreement with experimental results.

Reproducibility of the method

All determinations were carried out in triplicate and the results show that the reproducibility of the standard addition technique and measurement of the absorbance against the compensating solution is ±0.5% (Table II).

PRACTICAL APPLICATIONS

Steel samples containing standard amounts of silicon were selected first to determine the feasibility of the method. Various techniques were then used to determine silicon in aluminium–silicon, uranium–silicon and nickel–silicon alloys, and in potassium hydrogen difluoride and titanium sponges (Table II).

Steel

Dissolution of carbon and alloy steels in dilute acid before the spectrophotometric determination of silicon does not produce figures for total silicon but only for "soluble" silicon. The "soluble" silicon results are dependent largely on the time taken to dissolve steel samples. Total silicon can be determined by fusing the insoluble residue with sodium peroxide and adding it to the acid solution[9]. The present paper describes a procedure where samples are dissolved in oxidising acids, fumed with perchloric acid and transferred quantitatively to Teflon beakers, and the silicon dissolved with fluoride.

A reducing solution prepared from 1-amino-2-naphthol-4-sulphonic acid can be used only when the iron content does not exceed 5 mg per determination. When more than 5 mg of iron is present, 5 ml of 4% ascorbic acid must be used, 6 ml of 8% oxalic acid being added to destroy molybdophosphoric and molybdoarsenic acids.

Recommended procedure. Weigh 0.5 g of steel into a 250-ml glass beaker, add 7 ml of water, 7 ml of 15 M nitric acid and 7 ml of 10 M hydrochloric acid. When reaction ceases, add 20 ml of 70% perchloric acid and evaporate to fumes. Fume so that the perchloric acid refluxes on the sides of the beaker for 5 min. Add 50 ml of water, dissolve the salts and quantitatively transfer the contents of the beaker to a 250-ml Teflon beaker. Add 2 ml of 40% hydrofluoric acid and heat at 85° for 20 min. Add 80 ml of 4% boric acid and cool. Transfer to a volumetric flask containing 70 ml of 4% boric acid and dilute to volume so as to obtain about 10 μg Si ml^{-1}. Mix and store in a polythene bottle.

Transfer 3 aliquots containing *ca.* 100 μg of Si and not more than 25 mg of iron to separate 250-ml polythene beakers (when solutions are turbid as in the case of tungsten steels, filter 50 ml of solution through a medium filter paper). The first solution is the compensating solution, the second the test solution. To the third solution, add a standard addition of 100 μg of silicon. To all solutions add 0.1 ml of 10% hydroxylammonium chloride and sufficient boric acid to increase the total amount of boric acid to a minimum of 7.5 ml. Dilute to 60 ml and let stand for 15 min.

Adjust the pH (use calomel–NaCl reference electrode for perchlorate solutions) of the compensating solution to 0.81 (Table I) with 9 N perchloric acid. Add an equal amount of perchloric acid to test and standard addition solutions.

Iron consumes ammonium molybdate, and even when no visible precipitates can be seen, iron in amounts above 25 mg gives lower absorbances. The ammonium molybdate must be increased to 20 ml, but then the maximum absorbance for 50 mg of iron plus 0.2 ml of 40% hydrofluoric acid and 15 ml of 4% boric acid will be obtained in the pH range between 0.72 and 1.05. Therefore the pH before ammonium molybdate addition must be adjusted to 0.62 so as to obtain a final pH of 0.83.

Colour development (less than 5 mg of iron). Add to the test and standard addition solutions 10 ml of 5% ammonium molybdate. After 15 min add 5 ml of 20% tartaric solution. After 1 min, add 5 ml of reducing solution, transfer to a 100-ml volumetric flask and dilute to volume. Measure the absorbance at 725 nm after 30 min in 1-cm cells against the compensating solution. Subtract the blank.

Add to the compensating solution 5 ml of 20% tartaric acid. After 1 min add 10 ml of 5% ammonium molybdate and 5 ml of reducing solution, transfer to a 100-ml volumetric flask and dilute to volume.

Blank. Prepare a compensating and a test solution as described above for the blank solution. The correction for the blank is equal to the difference in absorbance between the compensating and the test solution.

Colour development (5–25 mg of iron present). Add to the test and standard addition solutions 10 ml of 5% ammonium molybdate. After 15 min add 10 ml of 9 N sulphuric acid, 6 ml of 8% oxalic acid, and 5 ml of 4% ascorbic acid, mixing between additions. Transfer to a 100-ml volumetric flask and dilute to volume. Continue as in the case of less than 5 mg of iron, except for the compensating solution.

Add to the compensating solution 10 ml of 9 *N* sulphuric acid, 6 ml of 8% oxalic acid, 10 ml of 5% ammonium molybdate and 5 ml of 4% ascorbic acid mixing after each addition. Transfer to a 100-ml volumetric flask and dilute to volume.

Aluminium

Carlson and Banks[16] showed that when aluminium metal is dissolved in a sulphuric–hydrofluoric acid mixture, the results are low. They recommended that aluminium metal be dissolved in sodium hydroxide solution, neutralized with nitric acid, and a small amount of fluoride added to convert all silicon to a "reactive" form. In this work it was found that dissolution by mixed acids prepared from sulphuric, hydrochloric and nitric acids with subsequent activation of insoluble silicon with fluoride gave as good results as dissolution with sodium hydroxide (Table II).

Method A (dissolution in mixed acids). Transfer 0.5 g of aluminium metal to a tall 400-ml beaker, add 18 ml of water, 10 ml of 9 *N* sulphuric acid, 6 ml of 15 *M* nitric acid and 6 ml of 10 *M* hydrochloric acid. Dissolve with gentle heating. After reaction ceases, transfer to a 250-ml Teflon beaker, add 0.5 ml of 40% hydrofluoric acid and heat at 85° for 20 min. Add 37.5 ml of 4% boric acid. Cool. Transfer to a 100-ml volumetric flask and dilute to volume. Store in a polythene bottle. Pipette 3 aliquots containing *ca.* 100 μg of silicon into 250-ml polythene beakers. Continue as in the case of steel except for adjusting the pH to 0.96 before the ammonium molybdate addition with a dilute solution of mixed acids or dilute ammonia.

Method B (dissolution in sodium hydroxide for high silicon alloys). Transfer a 0.25-g sample to a 400-ml tall stainless steel beaker and add 40 ml of 10% sodium hydroxide. Cover with a steel cover and boil gently to dissolve. Pour the solution into a beaker containing 40 ml of 9 *N* sulphuric acid. Bring the solution to the boil and add 1 ml of 15 *M* nitric acid to oxidize any insoluble residue. Cool. Dilute to volume in a volumetric flask to obtain *ca.* 10 μg Si ml^{-1}. Transfer 3 aliquots from each assay containing *ca.* 100 μg of silicon to 250-ml polythene beakers. Continue as for steel, except for adjusting the pH with 9 *N* sulphuric acid; the optimal pH depends on the amount of sodium sulphate present and can be derived from the difference between curves 1 and 5, Fig. 1. Omit the addition of boric acid. For an aliquot containing 0.5 g of sodium hydroxide the pH would be 0.95.

Nickel–silicon alloy

Nickel–silicon electrode material could be dissolved in 50% nitric acid only. On prolonged heating, some colloidal silica precipitated from the strong acid solution, but the addition of fluoride converted all silicon to a "reactive" form.

Recommended procedure. Transfer 0.25 g of electrode material to a 250-ml Teflon beaker, add 10 ml of water and 10 ml of 15 *M* nitric acid. Warm gently to dissolve. After dissolution add 50 ml of water and 0.5 ml of 40% hydrofluoric acid, and heat at 85° for 20 min. Add 37.5 ml of 4% boric acid and cool. Transfer to a 500-ml volumetric flask and dilute to volume. Store in a polythene bottle. Pipette 3 aliquots containing *ca.* 100 μg of silicon into 250-ml polythene beakers. Continue as in the case of steel, except for adjusting the pH to 0.84 with nitric acid (Table I) before ammonium molybdate addition.

Uranium–silicon alloy

Silicon has been determined in uranium–silicon alloy after heating the alloy in a muffle furnace at 800° to convert uranium to uranium oxide and silicon to silica[8]. The silica was converted by treatment with nitric and hydrofluoric acids to "reactive" silicon and determined by the blue silicomolybdate method using a previously prepared standard curve.

In this work the uranium–silicon alloy was crushed to pass through a B.S. 100-mesh sieve and a 10-fold amount of sodium peroxide was used for sintering the sample[17].

Recommended procedure. Mix 0.2 g of crushed alloy ($<$ 100 mesh) with 2 g of sodium peroxide in a platinum crucible and sinter at 480° for 30 min. Cool. Dissolve in a Teflon beaker containing 70 ml of water and 10 ml of 15 *M* nitric acid. Heat the solution to boiling and add 2% potassium permanganate solution until a permanent pink colour persists. Add 10% hydroxylammonium chloride to discharge the pink colour. Add 1 ml of 40% hydrofluoric acid and heat at 80° for 20 min. Then add 75 ml of 4% boric acid and cool. Transfer to a 250-ml volumetric flask and dilute to volume. Store in a polythene bottle. Pipette 3 aliquots containing *ca.* 100 μg of silicon into 250-ml polythene beakers. Continue as in the case of steel, except for adjusting the pH to 0.84 (Table I) with dilute nitric acid before the addition of ammonium molybdate.

Potassium hydrogen difluoride

Jewsbury[18] has reported that 0.36 g of fluoride may be complexed with 100 ml of 4% boric acid. Results presented in this paper show that 0.2 g of fluoride can be complexed satisfactorily with 37.5 ml of 4% boric acid in 60 ml. Therefore a maximal amount of 0.4 g sample may be taken to determine silicon in potassium hydrogen difluoride.

Recommended procedure. Dissolve 1 g of potassium hydrogen difluoride in water add 2 ml of 9 *N* sulphuric acid and dilute to 100 ml in a polythene cylinder. Transfer 3 aliquots containing *ca.* 100 μg of silicon but not more than 400 mg of the salt to 250-ml Teflon beakers. Dilute to 50 ml with water. Add 100 μg of silicon to the standard addition solution. After 10 min add 4% boric acid, 7.5 ml for each 80 mg of salt, and heat at 85° for 15 min. Cool. Dilute all solutions to 60 ml and let stand for 15 min. Continue as in the case of steel except for adjusting the pH to 1.12 (Fig. 1, curves 3 and 4) with 9 *N* sulphuric acid.

Zirconium metal

The pH ranges for the formation of the yellow silicomolybdate in nitric or sulphuric acid containing zirconium fluoride and 7.5 ml of 4% boric acid are different from solutions containing various amounts of fluoride and boric acid (Table I). For blank solutions containing no zirconium, an amount of 7.5 ml of 4% boric acid must be added to each 0.1 ml of 40% hydrofluoric acid. Therefore, either the pH before the addition of ammonium molybdate must be adjusted for the blanks and zirconium solutions from separate figures, or a compromise pH may be selected; pH 1.00 and 1.15 for nitric and sulphuric acid solutions, respectively. Two minor errors become apparent; one is the larger amount of boric acid needed to complex fluoride in the blank, and the second the higher silicon absorbance obtained in zirconium solutions than in blank solutions containing no zirconium. Fluoride introduced as hydrofluoric acid contributes most of the silicon impurity in blank and zirconium solutions. The use of electronic-grade hydrofluoric acid reduces the absorbance due to the silicon impurity appreciably, and blanks containing 0.4 ml of 40% hydrofluoric acid gave an absorbance of 0.019. Silicon in zirconium solutions has a 10% higher absorbance than in blank solutions, but even then the error in the absorbance of the blank will be only 0.002.

Recommended procedure. Transfer a 1-g sample to a 250-ml Teflon beaker and add 30 ml of water, 3 ml of 15 *M* nitric acid and 2 ml of 40% hydrofluoric acid. Dissolve the sample at 85°. Add 37.5 ml of 4% boric acid and cool. Transfer to a 100-ml volumetric flask and dilute to volume. Store in a polythene bottle. Pipette 3 aliquots containing *ca.* 100 μg of silicon and not more than 0.2 g of zirconium into 250-ml polythene beakers. Add 0.1 ml of 10% hydroxylammonium chloride and boric acid to increase the total amount of boric acid to 7.5 ml. Continue as in the case of steel, except for adjusting the pH to 1.00 before ammonium molybdate addition. To blanks add 7.5 ml of 4% boric acid for each 0.1 ml of 40% hydrofluoric acid, and adjust the pH as for the sample.

Titanium metal

Titanium precipitates with molybdate and depletes the amount available for the formation of molybdosilicate. Therefore large amounts of titanium must be hydrolyzed before the addition of ammonium molybdate[4], or the amount of titanium in a sample aliquot should be limited to 20 mg[5]. Even then the absorbance of the molybdosilicate decreases when the sample aliquot contains more than 5 mg of titanium.

Sodium sulphate was used previously to complex thorium[11] and prevent the precipitation of thorium molybdate. It was found that 1.5 g of sodium sulphate also delayed the precipitation of titanium molybdate, thus allowing molybdate to react with silicon. The volume of 5% ammonium molybdate had to be increased to 20 ml, but even then more than 50 mg of titanium gave lower absorbances, and titanium must be limited to 100 mg per sample aliquot (Fig. 2). One gram of titanium requires 4 ml of 40% hydrofluoric acid for dissolution. Titanium does not form a sufficiently strong complex with fluoride to prevent fluoride interference, and hence for 0.1 ml (or less) of 40% hydrofluoric acid, 7.5 ml of 40% boric aid must be added.

The blanks, containing all reagents except titanium, formed maximal absorbance plateaux at pH ranges different from those for solutions containing titanium. Therefore the pH adjustments for maximum absorbance vary for blanks and test solutions. The addition of 20 ml of 5% ammonium molybdate increases the pH approximately 0.3 pH units, and to obtain the correct acidity it is recommended that the pH be adjusted before ammonium molybdate addition to 0.15 pH units less than the minimum pH required for maximal colour development. Titanium steel contains up to 5% vanadium, which interferes slightly by giving a constant error (5 mg V ≡ 0.035 abs. units). The interference can be compensated by adding the same amount of vanadium to the blank as to the sample aliquot. The amount of hydroxylammonium chloride was increased to 0.5 ml to assist with the reduction of the yellow molybdosilicate.

Recommended procedure. Transfer a 0.5-g sample to a 250-ml Teflon beaker, add 30 ml of water, 3 ml of 15 *M* nitric acid, and 2 ml of 40% hydrofluoric acid. Dissolve the sample at 85°. Add 150 ml of 4% boric acid and cool. Transfer to a 250-ml volumetric flask and dilute to volume. Store in a polythene bottle. Pipette 3 aliquots containing *ca.* 100 μg of silicon and not more than 0.1 g of titanium into 250-ml polythene beakers. Add 0.5 ml of 10% hydroxylammonium chloride and 5 ml of 30% sodium sulphate. Continue as for steel (5–25 mg), but adjust the pH (Fig. 2, curves 1 to 4) and add 20 ml of 5% ammonium molybdate. To blanks add 7.5 ml of 4% boric acid for each 0.1 ml of 40% hydrofluoric acid and adjust the pH according to Fig. 2.

SUMMARY

The pH ranges suitable for the development of yellow molybdosilicate in sulphuric, hydrochloric, nitric, and perchloric acids have been established, and the effect of sodium salts of these acids, fluoride–boric acid mixtures, zirconium–fluoride and titanium–fluoride system on the pH various acid media has been studied. A method is given for calculating the required minimum pH in mixed acid systems. Procedures are described for determining silicon in steels, aluminium, nickel–silicon, uranium–silicon, potassium hydrogen difluoride and titanium sponge by a standard addition procedure.

RÉSUMÉ

Une étude est effectuée, examinant l'influence du pH sur la formation de molybdosilicate jaune, en milieu acides sulfurique, chlorhydrique, et perchlorique, ainsi que l'influence de sels de sodium de ces acides, des mélanges fluorure–acide borique, et des systèmes zirconium–fluorure, titane–fluorure. On propose des méthodes avec étalon interne pour le dosage du silicium dans les aciers, l'aluminium, le nickel–silicium, l'uranium–silicium, l'hydrogènofluorure de potassium et le titane spongieux.

ZUSAMMENFASSUNG

Es wurde der pH-Bereich festgelegt, der sich für die Bildung des gelben Molybdatosilicats in Schwefel-, Salz-, Salpeter- und Perchlorsäure eignet. Der Einfluss von Natriumsalzen dieser Säuren, Fluorid–Borsäure-Gemischen, Zirkon–Fluorid- und Titan–Fluorid-Systemen auf den pH-Wert in verschiedenen Säuren wurde untersucht. Es wird eine Methode für die Berechnung des erforderlichen Mindest-pH-Wertes in gemischten Säuresystemen angegeben. Es werden Verfahren beschrieben für die Bestimmung von Silicium in Stählen, Aluminium, Nickel–Silicium, Uran–Silicium, Kaliumhydrogenfluorid und Titanschwamm nach einer Standardadditionsmethode.

REFERENCES

1 *I.S.O. Document*, ISO/TC/17SC1 Doc. 115, 1965.
2 *British Standard 1121:19:1951.*
3 ASTM, *Part 32, E 107, para 42*, 1965.
4 ASTM, *Part 32, E 120-63, para 110*, 1965.
5 W. T. ELWELL AND D. F. WOOD, *Analysis of the New Metals*, Pergamon Press, Oxford, 1966, pp. 94 and 172.

6 ASTM, *Part 32, E146-64T, para 18*, 1965.
7 ASTM, *Part 32, E34-58, para 88*, 1965.
8 E. B. READ, P. R. HICKS, H. M. LAWLER, E. POLLOCK, H. M. READ AND L. ZOPATTI, *USAEC Report NMI-1178*, 1957.
9 STANDARD ASSOCIATION OF AUSTRALIA, COMMITTEE CH/4, *Draft for the Determination of Silicon in Iron and Steel*, Document CH/4/70-2, 1970.
10 P. PAKALNS, *Anal. Chim. Acta*, 38 (1967) 403.
11 P. PAKALNS, *Anal. Chim. Acta*, 40 (1968) 1.
12 P. PAKALNS, *Anal. Chim. Acta*, 47 (1969) 225.
13 G. J. S. GOVETT, *Anal. Chim. Acta*, 25 (1961) 69.
14 P. G. JEFFERY AND A. D. WILSON, *Analyst*, 85 (1960) 478.
15 T. R. ANDREW, *Analyst*, 82 (1957) 423.
16 A. G. CARLSON AND C. V. BANKS, *Anal. Chem.*, 24 (1952) 472.
17 G. W. C. MILNER, D. H. ROWE AND G. PHILLIPS, *UKAEC Report AERE-R5129*, 1966.
18 A. JEWSBURY, *Analyst*, 75 (1950) 256.

Analytica Chimica Acta
Elsevier Publishing Company, Amsterdam
Printed in The Netherlands

SPECTROPHOTOMETRIC DETERMINATION OF RUTHENIUM(III) WITH TROPOLONE BY SOLVENT EXTRACTION

G. H. RIZVI, B. P. GUPTA* AND R. P. SINGH
Department of Chemistry, University of Delhi, Delhi-7 (India)

(Received 10th September 1970)

Beamish[1] has reviewed the many reagents available for the spectrophotometric determination of ruthenium. Few of these reagents are selective and there is no suitable method for the determination of ruthenium in presence of other platinum metals, without a preliminary separation, usually by distillation of ruthenium tetroxide[2]. In the present study, it was found that tropolone (2-hydroxy-2,4,6-cycloheptatrienone) reacts with ruthenium (III) on heating on a boiling water bath to give a yellow solution. The coloured species can be extracted with chloroform, and has an absorbance maximum at 415 nm. The reaction can be used directly for the spectrophotometric determination of ruthenium in presence of moderate amounts of most other platinum metals, and simple modifications make the reagent extremely selective for ruthenium.

EXPERIMENTAL

Apparatus

Absorbance measurements were made with a Unicam SP 600 spectrophotometer, in matched 10-mm glass cells. A Metrohm E 350 pH-meter, with saturated calomel and glass electrodes was used for pH measurements.

Reagents

Tropolone (Aldrich Chemical Company) was used as received after checking the melting point. The reagent solution was freshly prepared in double-distilled water just before use.

Ruthenium (III) chloride (Johnson and Matthey, London) was used. A stock solution (0.002 *M*) was prepared in 1 *M* hydrochloric acid, and standardized gravimetrically by precipitating ruthenium as the hydrated oxide followed by careful ignition in air and then reduction to the metal in the presence of hydrogen.

Sodium acetate–acetic acid buffers, prepared by mixing 0.5 *M* solutions of the components, were used for pH adjustment. All other chemicals used were of analytical-reagent quality. Twice-distilled water was used throughout.

General procedure

Transfer a suitable aliquot of solution containing 10–40 μg of ruthenium to a 50-ml Corning glass-stoppered bottle and add 2.5 ml of 0.01 *M* tropolone solution, 1.0 ml of 1 *M* sodium acetate and 5.0 ml sodium acetate–acetic acid buffer pH 5.5. Dilute it to 15.0 ml and heat the solution on a water bath for about 10 min to ensure complete reaction. Cool the solution to room temperature and extract with 10.0 ml

---

* Present address: Chemistry Department, Hindu College, Delhi-7, India.

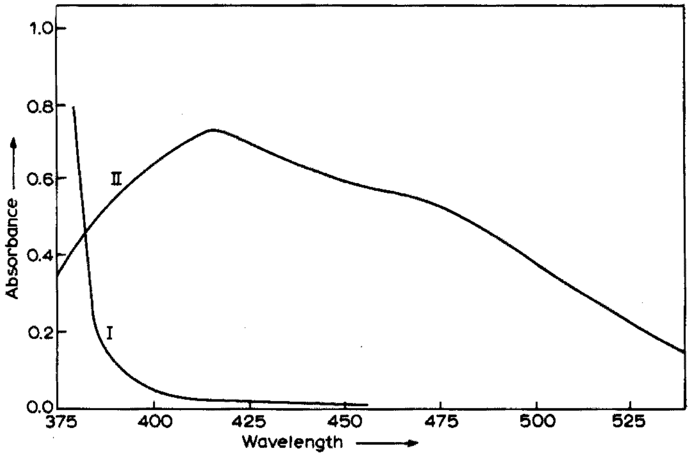

Fig. 1. Absorption spectra of ruthenium–tropolone complex: (I) reagent blank containing $1.0 \cdot 10^{-3}$ *M* tropolone, (II) complex *vs.* reagent blank containing Ru(III), $4.0 \cdot 10^{-5}$ *M*.

of chloroform. Measure the absorbance at 415 nm against a reagent blank similarly prepared. Determine the concentration of the ruthenium from a previously prepared calibration curve.

RESULTS AND DISCUSSION

Absorption spectra

The absorption curve of the extracted complex (*vs.* reagent blank) along with that of the ligand is given in Fig. 1. Maximal absorbance occurs at 415 nm, at which the absorbance of the ligand is very small. Subsequent studies were therefore made at 415 nm.

Effect of pH, temperature and time

The absorbance of the solution increased as the pH was raised, and decreased after a certain limit. Maximal absorbance was exhibited between pH 4.5–6.0. A pH value of 5.5 was used in all further work.

At room temperature, the ruthenium–tropolone solution was practically colourless. The absorbance of the solution increased rapidly on heating and became constant after heating for about 6 min on a boiling water bath. Further heating for about 2 h had no effect on the absorbance of the extracted complex. The extracted complex showed constant absorbance for several days.

Effect of reagent concentration

Samples containing a fixed amount of ruthenium (2.02 p.p.m.) and varying amounts of reagent were prepared. The complex was extracted into chloroform and the absorbance measured. The study showed that full colour development required about a 25-fold molar excess of the reagent.

Calibration curve, range and sensitivity

The ruthenium–tropolone system obeyed Beer's law over the range 0.0–5.7 p.p.m. The optimum range for determination of ruthenium, as deduced from a

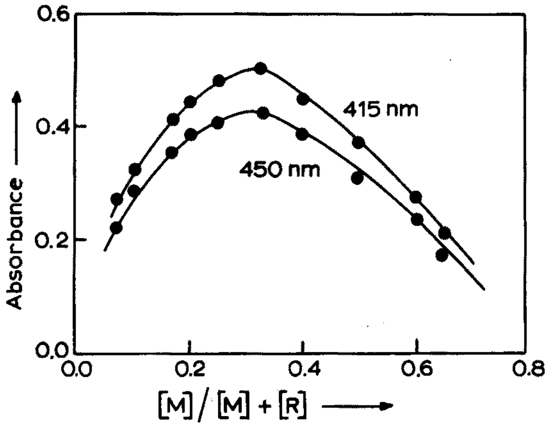

Fig. 2. Job's method of continuous variations. Total molarity $3.0 \cdot 10^{-4}$ *M*.

Ringbom plot, was 1.0–4.0 p.p.m. of ruthenium. The molar absorptivity was $1.87 \cdot 10^4$ l·mol^{-1}cm^{-1} and the sensitivity was 0.0054 μg Ru cm^{-2} for log $I_0/I = 0.001$.

The precision of the method was tested by measuring the absorbance of 10 samples, each containing a final ruthenium concentration of 2.02 p.p.m., a value in the middle of the optimum range. The mean absorbance was 0.388 with a standard deviation of 0.001.

Composition of the complex

Job's method of continuous variations[3]. Equimolar solutions of metal ion and reagent were mixed in varying amounts, keeping the total molarity constant. The absorbance was measured at 415 and 450 nm. The results are shown in Fig. 2, which indicates a 1:2 metal:reagent ratio in the complex.

Bent and French method[4]. A graph between log R and log $A/A_0 - A$ was plotted from the results obtained in the study of the effect of excess of reagent. The slope of the curve was found to be 2, which confirmed that the complex had a 1:2 metal: reagent ratio.

Interferences

Interferences caused by foreign ions in the system were studied by taking solutions containing 2.02 p.p.m. of ruthenium and the desired amounts of foreign ion. The complex was extracted into chloroform as described above. The results are summarised in Table I.

It is clear that ruthenium can be determined with a fair degree of accuracy in the presence of a large number of foreign ions. However, vanadium(V), uranium(VI), rhodium(III), iron(III) and palladium(II) interfered seriously. Interferences from these ions could be removed by using the modified procedure described below. Of the anions tested, only citrate, iodide and sulphite have been found to interfere.

RUTHENIUM IN THE PRESENCE OF INTERFERING IONS

Determination of ruthenium in presence of iron(III)

Ammonium fluoride (1.0 ml of 0.5 *M* solution) was added to an aqueous

TABLE I

EFFECT OF FOREIGN IONS
(Ruthenium taken 2.02 p.p.m.)

Foreign ion	*Amount taken (p.p.m.)*	*Absorbance*	*% Error*
Tartrate	5000	0.380	−2.06
Citrate	1000	0.280	−27.80
EDTA	200	0.381	−1.80
Oxalate	1000	0.387	−0.25
F^-	1500	0.388	0.00
Cl^-	8875	0.388	0.00
Br^-	1500	0.388	0.00
I^-	600	0.150	−61.34
BO_3^{3-}	5000	0.384	−1.03
PO_4^{3-}	4000	0.388	0.00
$P_2O_7^{2-}$	100	0.379	−2.32
NO_3^-	6200	0.388	0.00
SO_4^{2-}	4000	0.388	0.00
SO_3^{2-}	1000	0.061	−83.27
ClO_4^-	9000	0.388	0.00
SCN^-	100	0.370	−4.64
Ni(II)	117	0.388	0.00
Cd(II)	140	0.388	0.00
Zn(II)[a]	100	0.388	0.00
Mn(II)	220	0.388	0.00
Pb(II)	410	0.388	0.00
Co(II)	250	0.386	0.51
Be(II)	50	0.388	0.00
Ca(II)	200	0.388	0.00
Sr(II)	200	0.388	0.00
Ba(II)	200	0.388	0.00
Mg(II)	200	0.388	0.00
Cu(II)[b]	13	0.388	0.00
Pd(II)	20	1.500	+286.59
Tl(I)	410	0.388	0.00
Ga(III)	12	0.390	+0.51
In(III)	23	0.382	−1.54
Al(III)[c]	27	0.388	0.00
Fe(III)	5	0.688	+77.32
Sb(III)	20	0.390	+0.51
Bi(III)	10	0.388	0.00
La(III) (and other lanthanons)	60	0.388	0.00
Sc(III)	9	0.388	0.00
Ir(III)	20	0.392	+1.03
Rh(III)	11	0.590	+52.06
Zr(IV)	10	0.393	+1.28
Th(IV)	20	0.394	+1.54
Sn(IV)	24	0.388	0.00
Ge(IV)	140	0.388	0.00
Pt(IV)	25	0.388	0.00
Ti(IV)[c]	15	0.388	0.00
V(V)	30	0.690	+77.83

(*continued*)

TABLE I (*continued*)

Foreign ion	*Amount taken* (*p.p.m.*)	*Absorbance*	*% Error*
As(V)	50	0.388	0.00
Mo(VI)	200	0.388	0.00
W(VI)	27	0.390	+0.51
Cr(VI)	20	0.390	+0.51
U(VI)	50	0.640	+64.94
Os(VIII)	8	0.388	0.00

[a] Masked by potassium dihydrogen phosphate. [b] Masked by potassium sodium tartrate. [c] Masked by ammonium fluoride.

solution containing 1.0 ml of a 40.4-p.p.m. ruthenium solution and 1.0 ml of a 200-p.p.m. iron(III) solution in a 100-ml separating funnel. To this solution, 2.0 ml of 0.01 *M* tropolone, 1.0 ml of 1 *M* sodium acetate and 4.0 ml of sodium acetate–acetic acid buffer pH 5.5 were added. The solution was diluted to exactly 20.0 ml with water and the aqueous solution was immediately extracted with 20.0 ml of chloroform at room temperature. Under these conditions, only the iron–tropolone complex was extracted and ruthenium remained in the aqueous phase. The chloroform layer was separated and the aqueous phase was again shaken with 10 ml of chloroform to ensure complete removal of iron from the aqueous phase. A portion (10.0 ml) of the aqueous phase was then taken in a 50-ml reagent bottle and 1.0 ml of 0.01 *M* tropolone was added. The solution was diluted to 15.0 ml and heated on the water bath for about 10 min. The determination was then completed as in the *General procedure.* With this modified procedure, 2.02 p.p.m. of ruthenium could be determined in the presence of 10 p.p.m. of iron.

Determination of ruthenium in presence of vanadium(V)

To a solution containing 1.0 ml of a 40.4-p.p.m. ruthenium solution and 1.0 ml of a 400-p.p.m. vanadium(V) solution in a 100-ml separating funnel, 1.5 ml of 1 *M* hydrochloric acid and 5.0 ml of 0.01 *M* tropolone were added. The solution was diluted to exactly 20 ml with water. The aqueous phase was then immediately extracted with two 10-ml portions of chloroform, which removed vanadium quantitatively from the aqueous phase. A portion (10.0 ml) of the aqueous phase was then mixed with 1.0 ml of 1 *M* sodium acetate, 2.0 ml of sodium acetate–acetic acid buffer pH 5.5 and 1.0 ml of 0.01 *M* tropolone solution and diluted to 15.0 ml. The determination was then completed as in the *General procedure.* With this modification, 2.02 p.p.m. of ruthenium can be determined in presence of 20 p.p.m. of vanadium.

Determination of ruthenium in presence of uranium(VI)

To a solution containing 1.0 ml of a 40.4-p.p.m. ruthenium solution and 1.0 ml of a 400-p.p.m. uranium(VI) solution were added 1.0 ml of 1 *M* sodium acetate, 5.0 ml of sodium acetate–acetic acid buffer pH 5.5, and 5.0 ml of 0.01 *M* tropolone. The solution was diluted to exactly 20 ml with water and immediately extracted with two 10-ml portions of chloroform. The determination was then completed as for ruthenium in the presence of iron(III); 2.02 p.p.m. of ruthenium could be determined in presence of 20 p.p.m. of uranium.

Determination of ruthenium in presence of palladium(II) and rhodium(III)

To an aqueous solution containing 1.0 ml of a 20.2-p.p.m. ruthenium solution, 1.0 ml of a 50-p.p.m. rhodium solution and 1.0 ml of a 50-p.p.m. palladium solution, 5.0 ml of 0.01 M tropolone, 1.0 ml of 2 M sodium acetate and 2.0 ml of sodium acetate–acetic acid buffer pH 5.5, were added. The solution was diluted to exactly 15 ml with water and heated on a water bath for about 10 min. The solution was cooled to room temperature and extracted into 10.0 ml of chloroform. The absorbance was measured at 480 nm against a reagent blank and the ruthenium content was determined from an appropriate calibration curve. With this procedure, 2.02 p.p.m. of ruthenium could be satisfactorily determined in presence of 5 p.p.m. each of rhodium and palladium.

COMPARISON WITH OTHER REAGENTS

None of the many earlier spectrophotometric reagents for ruthenium[1,2] is without disadvantages; lack of sensitivity or selectivity frequently occurs, and with many of these reagents the reaction conditions are critical. Recently, oximidobenzotetronic acid[5], thiosalicylamide[6], 8-quinolinol[7], 2,3-diaminopyridine[8] and 2,4,6-tri-(2′-pyridyl)-s-triazine[9] have been used for the purpose. Oximidobenzotetronic acid is selective but the sensitivity is very poor. Palladium and some of the base metals interfere in case of thiosalicylamide. In the 8-quinolinol method, cobalt, chromium, molybdenum, palladium and rhodium interfere, and the sensitivity is poor. 2,3-Diaminopyridine requires a prior distillation of ruthenium.

In the proposed method, the reaction conditions are not critical, and the method can be made very selective by extracting the interfering ions as complexes at room temperature. Most of the platinum metals do not interfere in this case; only

TABLE II

COMPARISON OF THE SENSITIVITY OF REAGENTS FOR RUTHENIUM

Reagent	*Sandell sensitivity* ($\mu g\ cm^{-2}$)	*Wavelength* (*nm*)
Dithiooxamide	0.020	630
1,3,5,7-Naphthylaminetrisulphonic acid	0.010	530
1,10-Phenanthroline	0.0054	448
p-Nitrosodimethylaniline	0.0028	610
Anthranilic acid	0.024	620
2-Nitroso-1-naphthol	0.015	600
Thiocyanate/CCl_4	0.007	590
1,4-Diphenylthiosemicarbazide	0.010	565
1-Nitroso-2-naphthol-3,6-disulphonic acid	0.0047	586
2,4,6-Tri(2′-pyridyl)-s-triazine	0.0055	510
2,3-Diaminopyridine	0.0084	572
Acetylacetone	2.5	505
Oximidobenzotetronic acid	0.35	520
Tropolone (present method)	0.0054	415

palladium and rhodium interfere seriously, and these interferences can be eliminated by measuring the absorbance at 480 nm.

A comparison of some of the commonly used sensitive reagents with tropolone is given in Table II, which shows that tropolone ranks amongst the most sensitive reagents for the spectrophotometric determination of ruthenium.

One of the authors (G.H.R.) is grateful to the Council of Scientific and Industrial Research (India), for financial assistance.

SUMMARY

Ruthenium(III) reacts with tropolone in aqueous medium at pH 4.5–6.0 to yield a yellow 1:2 complex which can be extracted with chloroform, and has an absorbance maximum at 415 nm. Full colour development requires heating for 10 min on a water bath; the colour is then stable for days. Beer's law is obeyed in the range 0–5.7 p.p.m. of ruthenium. The molar absorptivity is $1.87 \cdot 10^4$ l $\mathrm{mol}^{-1}\,\mathrm{cm}^{-1}$. Common anions do not interfere. Of 37 cations examined, only Fe(III), V(V), U(VI), Rh(III) and Pd(II) interfere; these interferences can be avoided by a preliminary extraction of the tropolone complex of the interfering metal, or by measuring the absorbance at 480 nm.

RÉSUMÉ

Le ruthénium(III) réagit avec la tropolone en milieu aqueux, pH 4.5 à 6.0, pour former un complexe jaune (1:2). Ce complexe peut s'extraire dans le chloroforme et présente une absorption maximum à 415 nm. La coloration obtenue après chauffage de 10 min au bain marie est stable plusieurs jours. La loi de Beer s'applique de 0 à 5.7 p.p.m. de ruthénium. Le coefficient d'extinction molaire est de $1.87 \cdot 10^4$ l mol^{-1} cm^{-1}. Des 37 cations examinés, seuls Fe(III), V(V), U(VI), Rh(III) et Pd(II) gènent. Ces interférences peuvent être évitées par extraction préliminaires du complexe tropolone du métal gênant ou par mesure de l'absorption à 480 nm.

ZUSAMMENFASSUNG

Ruthenium(III) reagiert mit Tropolon in wässrigem Medium bei pH 4.5–6.0 unter Bildung eines gelben 1:2-Komplexes, der mit Chloroform extrahiert werden kann und ein Extinktionsmaximum bei 415 nm hat. Für die vollständige Entwicklung der Färbung muss die Lösung 10 min auf dem Wasserbad erhitzt werden; die Färbung ist dann tagelang beständig. Das Beersche Gesetz ist im Bereich 0–5.7 p.p.m. Ruthenium erfüllt. Der molare Extinktionskoeffizient ist $1.87 \cdot 10^4$ l mol^{-1} cm^{-1}. Die üblichen Anionen stören nicht. Von 37 untersuchten Kationen stören nur Fe(III), V(V), U(VI), Rh(III) und Pd(II); diese Störungen können durch vorhergehende Extraktion des Tropolonkomplexes des störenden Metalls oder durch Messung der Extinktion bei 480 nm vermieden werden.

REFERENCES

1 F. E. Beamish, *Talanta*, 12 (1965) 789.
2 F. E. Beamish, *The Analytical Chemistry of the Noble Metals*, Pergamon Press, New York, 1966.
3 P. Job, *Ann. Chim. (Paris)*, (10) 9 (1928) 113.
4 H. E. Bent and C. L. French, *J. Amer. Chem. Soc.*, 63 (1941) 568.
5 G. S. Manku, A. N. Bhat and B. D. Jain, *Talanta*, 14 (1967) 1229.
6 K. Sur and S. C. Shome, *Anal. Chim. Acta*, 48 (1969) 145.
7 H. Hashitani, K. Katsuyama and K. Motojima, *Talanta*, 16 (1969) 1553.
8 G. H. Ayres and D. T. Eastes, *Anal. Chim. Acta*, 44 (1969) 67.
9 W. A. Embry and G. H. Ayres, *Anal. Chem.*, 40 (1968) 1499.

Analytica Chimica Acta
Elsevier Publishing Company, Amsterdam
Printed in The Netherlands

FLUORESCENCE AND METALLIC VALENCY STATES

PART V. DETERMINATION OF IRON WITH PHTHALIC ACID

K. J. KOH AND D. E. RYAN*
Department of Chemistry, Dalhousie University, Halifax, Nova Scotia (Canada)

(Received 21st October 1970)

Few papers have reported the fluorimetric analysis of transition metals based on fluorescence production; most methods presently available involve determination by fluorescence quenching. Previous papers in this series[1-3] have shown, however, that advantage can be taken of variable metallic valency states to produce analytically useful fluorescence; aromatic carboxylic acids have been used to produce characteristic fluorescent species with vanadium, iron and copper[3].

Most methods for determining small amounts of iron are subject to extraction, preconcentration or severe interference by diverse ions. Fluorescence quenching with 2,2′,2″-terpyridine[4] permits the determination of 50–500 p.p.b. of iron. Atomic absorption detection limits by direct aspiration of aqueous samples are 0.05–1 p.p.m.[5] but 0.4–200 p.p.b. have been determined through extraction of the oxine–iron chelate with methyl isobutyl ketone[6]. Iron at p.p.b. levels has been determined in various waters and reagent-grade chemicals by anodic stripping voltammetry with a relative error of $\pm 7\%$ for 59 p.p.b.[7]. This paper describes a simple, sensitive and selective fluorimetric method for determining p.p.b. of iron with potassium hydrogen phthalate.

EXPERIMENTAL

Apparatus, reagents and solutions

An Aminco-Bowman spectrophotofluorimeter was used for recording excitation and emission spectra.

A Vortex mixer (Scientific Industries, Inc.) coupled with 1-min timer and constant voltage transformer was used for mixing solutions with zinc amalgam.

The stock reagent solutions ($1 \cdot 10^{-3}$ *M* and $2 \cdot 10^{-4}$ *M*) were prepared by dissolving potassium hydrogen phthalate (99.99%) NBS sample in twice-distilled water.

The stock iron solution (100 p.p.m.) was prepared by dissolving 0.1000 g of iron wire (99.99%) in 50 ml of 1 + 3 nitric acid, boiling to expel oxides of nitrogen, and diluting to 1 l with twice-distilled water. Solutions of 0.1, 1.0 and 10 p.p.m. iron were prepared by dilution; final solutions were adjusted to pH of *ca.* 4.

The 1 *M* acetate buffer solution (pH 5.2) was made in the usual manner[8].

The 7.0% (w/v) solution of sodium sulfite was prepared by dissolving analytical reagent in twice-distilled water.

The zinc amalgam was prepared as previously described[3].

---

* To whom all correspondence should be addressed.

Procedure

To 1 ml of solution (pH 4–5) containing 0.01–4 μg of iron in a 10-ml volumetric flask, add 1 ml of $2 \cdot 10^{-4}$ M reagent solution and 0.5 ml of 1 M acetate buffer respectively. After mixing the solutions in the flask, add 0.5 ml of zinc amalgam from a 10-ml burette. Mix immediately for 2 min with a Vortex mixer coupled with a timer and constant voltage transformer. Dilute the solutions to the mark with freshly prepared 7.0% sodium sulfite solution. Measure the fluorescence intensity at 415 nm with an excitation wavelength of 300 nm. A reagent blank should be run concurrently.

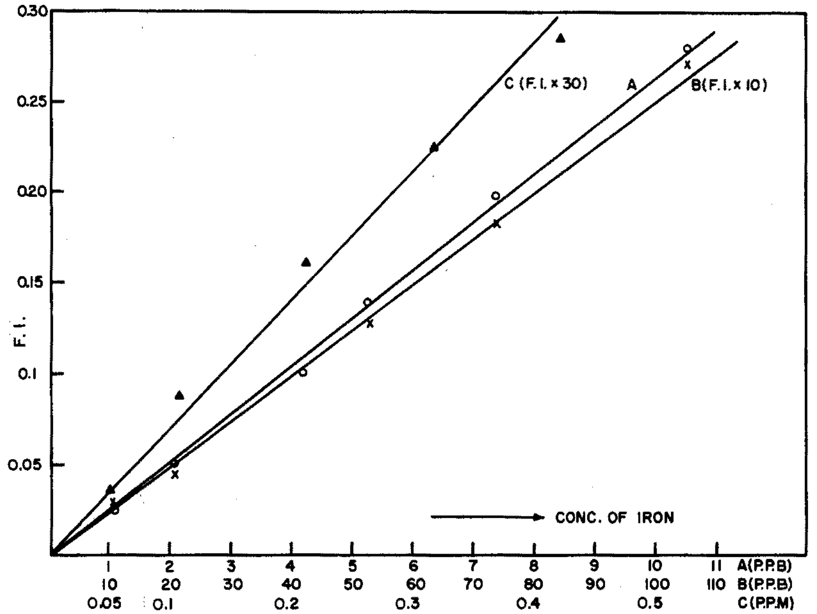

Fig. 1. Calibration curves. F.I. is the meter multiplier setting × % fluorescence intensity.

Typical calibration curves are shown in Fig. 1. Excitation and emission spectra are shown in Fig. 2.

RESULTS AND DISCUSSION

Factors affecting fluorescence intensity

Optimum results were obtained by close adherence to the procedure. A change in the order of addition of reagents, for example, resulted in poor reproducibility of fluorescence intensity and non-linearity with concentration.

Good results were obtained at pH 5.2 and there was no appreciable change in intensity up to pH 6.0. Above pH 6.0 precipitation took place during mixing with the amalgam, and below pH 5.2 the intensity was decreased; for 10 p.p.b. of iron the fluorescence intensity was 29 at pH 5.2, 14 at pH 4.7, and 8 at pH 4.3 (MM = 0.01 and S = 0). Close control of buffer concentration was necessary. If less than 0.3 ml of buffer solution was added in the procedure, precipitation frequently occurred during the mixing with the amalgam; the intensity decreased as the buffer concentration was increased. For 10 p.p.b. of iron the intensity was 45 with 0.3 ml, 29 with 0.5 ml, 14

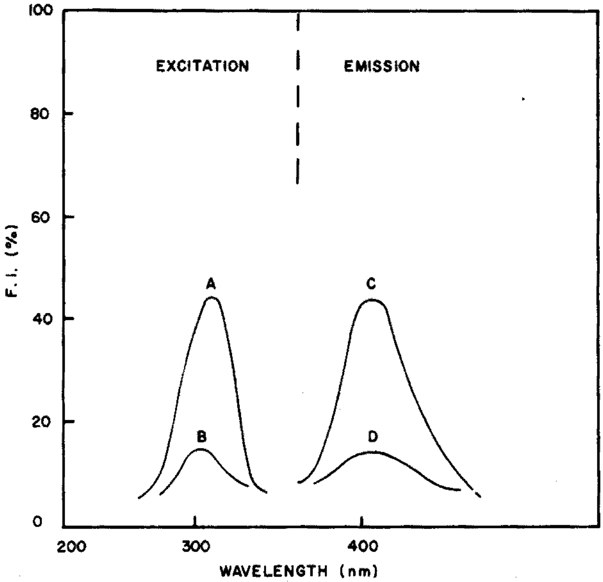

Fig. 2. Fluorescence spectra. A and B are excitation spectra of product (10 p.p.b. Fe) and reagent respectively (emission wavelength, 415 nm); C and D are corresponding emission spectra (excitation wavelength, 300 nm).

with 0.8 ml and 9 with 1 ml of 1 *M* acetate buffer added. Good results were obtained with 0.5 ml of 1 *M* buffer solution for 1–400 p.p.b. of iron.

The fluorescence intensity varied with the mixing time with the amalgam; the longer the mixing time, the higher the intensity. For 10 p.p.b. of iron the net intensity was 9 after 1-min mixing with amalgam, 29 after 2 min, 39 after 3 min and 52 after 4 min (after 3-min mixing there was occasional precipitation). Good intensity and a linear relationship for 1–400 p.p.b. of iron were obtained with 2-min mixing.

The manner of mixing with the amalgam was also important for reproducible results; the vortical motion of the amalgam along the flask wall (by placing the flask directly into neoprene cup of the mixer) ensured reproducibility during the mixing process; mixing by hand or mechanical shaker gave poor reproducibility.

Although the fluorescence intensity of the blank increased with increasing reagent concentrations, the difference in intensity between blank and iron sample remained constant; for example, for 100 p.p.b. of iron and 1 ml of $2 \cdot 10^{-4}$, $1 \cdot 10^{-3}$ and $1 \cdot 10^{-2}$ *M* reagent, the difference between iron and reagent (corrected to the same meter multiplier and sensitivity settings) was 73, 74 and 67, respectively.

Figure 3 shows the effect of the amalgam on the fluorescence intensity; 0.5 ml of the amalgam is recommended for satisfactory results.

In order to stabilize the fluorescence intensity, sodium sulfite (7%), which is known as an inhibitor of autoxidation reactions, was added after mixing the system with the amalgam; the intensity remained constant at 28–29 for 40 min in the presence of 10 p.p.b. of iron. When the system was diluted with twice-distilled water, the intensity, although sometimes stable for 1 h, often increased from 29 to 35 (for 10 p.p.b. of iron) within a few minutes; the reason for this erratic behavior is not clear.

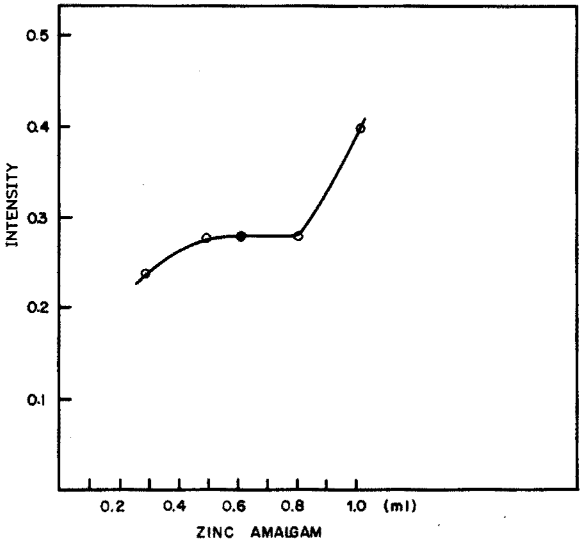

Fig. 3. Effect of amount of amalgam on the fluorescence intensity of 10 p.p.b. of iron.

The stability of fluorescence was dependent upon the concentration of sodium sulfite used; in more concentrated sodium sulfite solutions, the fluorescence was stabilized but the fluorescence sensitivity decreased; dilution with 2, 4, 7, and 9% of sodium sulfite solution gave the intensities of 36, 32, 29, and 26, respectively, at the same instrument setting. However, when the solution was diluted to the mark with 7% of sodium sulfite, good stability (for 40 min) was obtained without an excessive decrease in the fluorescence over the concentration range 1–400 p.p.b. of iron.

Pyrogallol and methanol may also be used to stabilize the fluorescence.

Range and precision

The fluorescence intensity was linear for 1–400 p.p.b. of iron. Samples containing 5.0 and 10.0 p.p.b. of iron in distilled water were analyzed by the above procedure, and 5.0 ± 0.5 (6 determ.) and 10.0 ± 0.5 (12 determ.) p.p.b., respectively, were found. Analysis of synthetic tap water[9] by addition of 2.0 and 10.0 p.p.b. of iron showed 2.0 ± 0.3 and 9.8 ± 0.3 p.p.b. (for 4 determ.), respectively.

The method may prove applicable to the determination of iron in sea water; for example, fluorescence intensities of 38, 62 and 77 were found for synthetic sea water[10] blank and sea water to which 2.0 and 5.0 p.p.b. of iron were added.

Interferences

Iron (p.p.b.) was successfully determined in the presence of large amounts (at least 10 p.p.m.) of Na^+, K^+, Ca^{2+}, Mg^{2+}, Sr^{2+}, Zn^{2+}, Al^{3+}, Cl^-, NO_3^- and SO_4^{2-}. Similarly, 100-fold amounts of Cd^{2+}, Co^{2+}, Cu^{2+}, Ni^{2+}, Pb^{2+}, CN^-, F^- and 30-fold amounts of Mn^{2+}, Cr^{3+} and Mo^{3+} did not interfere. Even p.p.b. of vanadium(V) and titanium(IV) increased the fluorescence and these elements must be absent.

Nature of reaction

The fluorescent reaction product obtained on reacting iron(III) with potassium hydrogen phthalate in the presence of zinc amalgam is not formed in the absence of oxygen. The fluorescence intensity of solutions containing reagent and 10 p.p.b. of iron(II), iron(III), or iron(II)+iron(III) was the same as that of the reagent blank. The fluorescent product was rapidly formed only in solutions of reagent and iron(II) or iron(III) to which zinc amalgam was added. Hydrogen peroxide has been stated[11] to be formed in the reduction of iron(III) by zinc amalgam in oxygen-containing solutions but addition of hydrogen peroxide to solutions of either iron(III) or iron(II) and reagent gave only a slight increase in the fluorescent intensity. These experiments suggest that the fluorescence is the result of an electron-transfer process involving iron(II), oxygen, and phthalate at the surface of the zinc amalgam.

Addition of hydrogen peroxide to phthalaldehyde gave a blue fluorescence similar to that obtained with iron, phthalic acid and zinc amalgam; with terephthalaldehyde a yellow fluorescence, similar to that observed with iron, terephthalic acid and amalgam, was obtained on addition of hydrogen peroxide. It is possible, therefore, that the product responsible for fluorescence is either an intermediate or the peracid[12] formed as a result of an electron-transfer reaction to the phthalic acid which then reacts with oxygen. Studies are continuing.

This work was supported by grants from the National Research Council and the Defence Research Board. It is a pleasure for K. J. K. to thank Dalhousie University for the award of a Killam graduate scholarship.

SUMMARY

Iron (1–400 p.p.b.) in solution is selectively and simply determined by measuring the fluorescence intensity produced on reaction with potassium hydrogen phthalate in the presence of zinc amalgam. Excitation and emission wavelengths are 300 nm and 415 nm, respectively. Very few common ions interfere.

RÉSUMÉ

Le fer (1 à 400 p.p.b.), en solution, peut être dosé d'une façon simple et sélective, en mesurant l'intensité de fluorescence produite sur la réaction avec l'hydrogénophtalate de potassium, en présence d'amalgame de zinc. Les longueurs d'onde d'excitation et d'émission sont 300 et 415 nm, respectivement. Très peu d'ions communs gênent.

ZUSAMMENFASSUNG

Eisen (1–400 p.p.b.) in Lösung wird selektiv und einfach durch Messung der Fluoreszenzintensität bestimmt, die bei der Reaktion mit Kaliumhydrogenphthalat in Gegenwart von Zinkamalgam entsteht. Die Wellenlänge für die Anregung ist 300 nm, die der Emission 415 nm. Nur sehr wenige der üblichen Ionen stören.

REFERENCES

1 D. E. Ryan and B. K. Pal, *Anal. Chim. Acta*, 44 (1969) 385.
2 B. K. Pal and D. E. Ryan, *Anal. Chim. Acta*, 47 (1969) 35; 48 (1969) 227.
3 K. J. Koh and D. E. Ryan, *Anal. Chim. Acta*, 52 (1970) 503.
4 D. W. Fink, J. V. Pivnichny and W. E. Ohnesorge, *Anal. Chem.*, 41 (1969) 833.
5 W. Slavin, S. Sprague and D. C. Manning, *At. Absorption Newsletter*, No. 18 (1964) 1.
6 J. L. Jones and R. D. Eddy, *Anal. Chim. Acta*, 43 (1968) 165.
7 T. M. Florence, *J. Electroanal. Chem.*, 26 (1970) 293.
8 A. I. Vogel, *A Textbook of Quantitative Inorganic Analysis*, Longmans, New York, 1951, p. 869.
9 E. F. McFarren and R. J. Lishka, *Trace Inorganics in Water*, Advan. in Chem. Series 73, A.C.S., Washington, D.C., 1968, p. 254.
10 J. Lyman and R. A. Fleming, *J. Marine Res.*, 3 (1940).
11 R. A. Chalmers, D. A. Edmond and W. Moser, *Anal. Chim. Acta*, 35 (1966) 404.
12 S. Patai, *The Chemistry of Carboxylic Acids and Esters*, Interscience, New York, 1969, p. 672.

Anal. Chim. Acta, 54 (1971) 303–308

Analytica Chimica Acta
Elsevier Publishing Company, Amsterdam
Printed in The Netherlands

SEPARATION AND DETERMINATION OF CESIUM-137 IN URINE

R. J. EVERETT AND H. A. MOTTOLA
Department of Chemistry, Oklahoma State University, Stillwater, Okla. 74074 (U.S.A.)

(Received 29th October 1970)

Analytical procedures for the determination of ^{137}Cs in biological and environmental samples have often employed the ammonium salt of molybdophosphoric acid (AMP) for the isolation of ^{137}Cs from bulk matter[1–3]. AMP has been investigated mainly by Smit *et al.*[4,5] and Krtil[6] and has shown a high selectivity for cesium over the other alkali ions and other monovalent cations. However, this selectivity is not satisfactory in many cases and tedious precipitations, such as the chloroplatinates, cobaltinitrites and tri-iodides have been added to eliminate interfering elements. This paper reports an analytical method for the determination of ^{137}Cs in urine in which the AMP ion-exchange properties and solvent extraction with 4-sec-butyl-2-(α-methylbenzyl)phenol (BAMBP) are utilized to obtain samples suitable for low-level β-counting.

EXPERIMENTAL

Apparatus

The pH of the samples was measured with the aid of a Beckman Zeromatic pH meter and a glass-calomel electrode pair. Radioactive counting and γ-energy distributions were measured with a multichannel γ-spectrometer (Nuclear Data Inc., series 1100) and a 3 × 3 in. well-type NaI crystal detector. All measurements were made at room temperature (28–29°).

Preparation of AMP

A saturated solution of phosphomolybdic acid ($10\ MoO_3 \cdot H_3PO_4 \cdot 24H_2O$) was prepared in about 2 l of distilled water. The acid was only slightly soluble and the addition of about 5 ml of concentrated phosphoric acid and heating improved the solubility. An excess of saturated solution of ammonium nitrate was added to the phosphomolybdic acid. The AMP precipitate was filtered (Whatman #42) under suction. The precipitate was washed repeatedly with 0.1 *M* ammonium nitrate until the supernatant liquid showed a pH greater than 3. The AMP was then dried at 100° for 8 h. The fine yellow powder was passed through a 200-mesh screen, insuring a particle size less than 74 μm.

Reagents and solutions

4-Sec-butyl-2-(α-methylbenzyl)phenol (K & K laboratories) was used as received. All other reagents were A.R. grade.

---

* Address inquiries to this author.

Rubidium-86 and cesium-137 (New England Nuclear Corp., Boston, Mass.) were obtained as their chloride solution in hydrochloric acid.

Sample preparation

Sample type I. To 200 ml of fresh urine, 5 ml of concentrated nitric acid was added and the sample was evaporated to dryness on a hot plate. The sample was oxidized to a white ash by several additions of nitric acid and the application of heat. The residue was then dissolved with 200 ml of 0.1 *M* ammonium nitrate and the pH adjusted to 1.

Sample type II. Fresh urine (200 ml) was ashed as described above. The residue was then dissolved in 100 ml of 0.1 *M* ammonium nitrate and the pH adjusted to 1.

Sample type III. Fresh urine (200 ml) was ashed similarly to sample type I. The residue was dissolved in 100 ml of distilled water and the pH adjusted to 1.

Sample type IV. Fresh urine was made 0.1 *M* in ammonium nitrate and the pH adjusted to 1.

Sample type V. Fresh urine was adjusted to a pH of 1.

Sample type VI. A 0.1 *M* ammonium nitrate solution at pH 1.

Experimental procedure for the determination of D values

Distribution ratios, D, defined as D = (counts per g of AMP)/(counts per ml of solution) were determined by equilibration (1 min was found enough to attain equilibrium) of 10 ml of the given sample type and 0.50 g of AMP. After phase separation the activity of the aqueous phase was measured. The activity in the exchanger was calculated by difference.

Analytical procedure

To a measured volume of urine, add 20 ml of concentrated nitric acid and evaporate the sample to dryness on a hot plate. Ash repeatedly with small portions of nitric acid and the application of heat. Dissolve the white residue in one half the original volume of distilled water and adjust the pH to 1 with nitric acid.

Prepare the ion-exchange column ($6.25\ \text{cm}^2 \times 40$ cm) by making a slurry of 10 g of AMP, 5 g of asbestos and about 50 ml of 0.1 *M* ammonium nitrate. Pour the mixture into the column. Rinse with 0.1 *M* ammonium nitrate solution. A wad of glass wool at the bottom and at the top of the column was found to be beneficial in preventing loss of AMP or entrainment of the AMP in the sample solution to be added. Allow the column to drain and settle for several hours. Add the sample to the column in portions maintaining a flow rate of about 3 ml min^{-1}. Allow the column to drain, and then elute interfering elements with two 100-ml portions of 4 *M* ammonium nitrate. Allow the column to drain thoroughly. Add 6 *M* sodium hydroxide to the column in 10-ml portions until the AMP is completely dissolved. Collect each portion in a 125-ml separatory funnel. Adjust the pH to 12.5 with sodium hydroxide or nitric acid as required. Extract the sample five times with 10-ml portions of 0.5 *M* BAMBP in kerosene. Evaporate the combined extracts and assay by γ-counting. Alternatively, back-extract the BAMBP–kerosene with a strongly acid solution, evaporate this solution to a small volume and transfer quantitatively to a counting planchet for a low-level β-count.

RESULTS AND DISCUSSION

Although AMP has been utilized as a primary collecting medium for cesium in many applications, its usefulness as both a collecting and purification medium has not been adequately investigated. The most troublesome natural activity to be removed from biological samples is ^{40}K, which has some affinity for AMP under conditions suitable for ^{137}Cs collection. The usual approach is to resort to selective precipitations to insure adequate purity of cesium. Often these precipitations are tedious and time-consuming, and result in loss of cesium.

In this study the urine–AMP system was investigated in order to design an AMP ion-exchange column that would provide the necessary purity of ^{137}Cs. As part of this design the distribution ratios between AMP and various samples were determined in batch equilibrations of 1-min duration. These are summarized in Table I.

TABLE I

DISTRIBUTION RATIOS
(See text for sample description)

Sample type	*D(Cs)*	*D(Rb)*
II	2100	98
III	4200; 4030	358; 417
IV	1840; 1890	82; 97
V	2966	388
VI	6770	277

The rubidium distribution was also determined, since a good separation from ^{86}Rb would insure freedom from other alkali ions.

It is interesting to note the rather large *D* values for ^{137}Cs in these types of samples. Sample type III is the most advantageous since the sample can be concentrated 2:1 after ashing, no ammonium nitrate is required, and a large *D* value is obtained.

A computation as discussed by Helfferich[7] and Glueckauf[8] was performed such that only 0.01% rubidium would contaminate the cesium eluate. This high degree of purity was thought necessary to compensate for several unknown ion-exchange parameters. These calculated values were utilized in a trial elution of ^{137}Cs and ^{86}Rb activities. In Table II the important calculated and measured ion-exchange parameters are compared.

Considering the numerous assumptions made in the initial calculation, the correlation is satisfactory and indicates the usefulness of prior elution calculations. The final elution procedure was determined by the addition of ^{137}Cs and ^{86}Rb activities to sample type III and monitoring of these activities in the eluate by γ-spectrometry.

The large volume of saturated ammonium nitrate required for elution of ^{137}Cs presented a problem. Methylamine, which is expected to have a size larger than ammonium ion, but slightly smaller than cesium, was studied as eluting agent, but failed to give any displacement of cesium from the column. Probably the larger

TABLE II

ELUTION PARAMETERS

(See refs. 7 and 8 for calculations)

Calculated	*Measured*
$V(\mathrm{Max})_{\mathrm{Rb}}$: 20.7 ml	70 ml
$V(\mathrm{Max})_{\mathrm{Cs}}$: 96.8 ml	145 ml
$\#D(\mathrm{Cs})^{a}$: 44	33
$\#D(\mathrm{Rb})^{a}$: 8.6	15
β^{b}: 0.5[c]	0.105

[a] $\#D$ = Volume distribution ratios.

[b] β = Fraction of total column volume occupied by AMP.

[c] Estimated from ref. 7.

size of the solvated cation is responsible for this behavior. Sizewise hydroxylammonium ion would also qualify as a potential eluting agent but its strong reducing action prevents its use in presence of AMP. Other cations such as $\mathrm{Ba(OH)^+}$ or francium cannot be used owing to thermodynamic and radioactivity considerations, respectively. As such the ammonium ion appears as a very selective eluting agent for the separations reported here.

The procedure described yielded a $^{137}\mathrm{Cs}$ recovery of 93% with no detectable $^{40}\mathrm{K}$ or $^{86}\mathrm{Rb}$ contamination. The small $^{137}\mathrm{Cs}$ loss is attributed to solution transfers and adsorption on glass or asbestos surfaces. The BAMBP extraction could be readily improved by increasing the BAMBP concentration in the organic phase or use of other diluents instead of kerosene[9,10].

The method reported here is equally applicable to other biological and environmental samples. Simple column modifications may be needed depending upon batch equilibration data with the sample in question.

SUMMARY

A method is described for the analysis of $^{137}\mathrm{Cs}$ in either raw or ashed urine. The method relies upon an ammonium molybdophosphate ion exchange and solvent extraction with 4-sec-butyl-2-(α-methylbenzyl)phenol in order to collect and separate $^{137}\mathrm{Cs}$ from interfering activity. The analysis time on 1 l of urine is *ca.* 4.5 h, with only 1 h of working time. The procedure can be used on raw urine if necessary, and requires no addition of cesium carrier or yield corrections. The final residue is suitable for low-level β-counting. A 93% recovery of $^{137}\mathrm{Cs}$ is obtained.

RÉSUMÉ

Une méthode est décrite pour l'analyse de $^{137}\mathrm{Cs}$ dans l'urine. Elle consiste en un échange ionique au molybdophosphate d'ammonium et en une extraction dans un solvant, avec le 4-sec-butyl-2-(α-méthylbenzyl)phénol, afin de recueillir et séparer $^{137}\mathrm{Cs}$ d'avec des activités gênantes. La durée d'analyse pour 1 l d'urine est d'environ 4 à 5 h, avec une heure de travail seulement. Si nécessaire, le procédé peut s'appliquer à l'urine brute et ne nécessite aucune addition de césium marqué ou de corrections de rendement.

ZUSAMMENFASSUNG

Es wird eine Methode für die Analyse von ^{137}Cs in sowohl nicht vorbehandeltem als auch veraschtem Urin beschrieben. ^{137}Cs wird durch Ionenaustausch mit Ammoniummolybdatophosphat und durch Extraktion mit 4-sek-Butyl-2-(α-methylbenzyl)-phenol gesammelt und von störender Aktivität abgetrennt. Die Analyse von 1 l Urin dauert *ca.* 4.5 h bei einem Arbeitsaufwand von 1 h. Das Verfahren kann, falls erforderlich, auf nicht vorbehandelten Urin angewendet werden und bedarf keiner Zugabe eines Cäsiumträgers und keiner Korrektion der Ausbeute. Der erhaltene Rückstand eignet sich für "low level"-β-Messungen. 93% des ^{137}Cs werden erfasst.

REFERENCES

1 W. W. FLYNN, *Anal. Chim. Acta,* 50 (1970) 365.
2 A. J. R. DAFONSECA, M. H. D. DEMATOS AND M. M. DACRUZ, *Rev. Port. Quim.*, 6 (1964) 17.
3 A. MORGAN AND G. M. ARKELL, *Health Phys.*, 9 (1963) 857; *Nature,* 191 (1961) 1100; *AERE-R-3675*, 1961.
4 J. VAN R. SMIT, *Nature,* 181 (1958) 1530.
5 J. VAN R. SMIT, W. ROBB AND J. J. JACOBS, *J. Inorg. Nucl. Chem.*, 12 (1959) 95, 104; 26 (1964) 509; *Nucleonics*, 17 (1959).
6 J. KRTIL, *J. Inorg. Nucl. Chem.*, 24 (1962) 1139.
7 F. HELFFERICH, *Ion Exchange*, McGraw-Hill, New York, 1962.
8 E. GLUECKAUF, *Trans. Faraday Soc.*, 51 (1955) 34.
9 B. Z. EGAN, R. A. ZINGARO AND B. M. BENJAMIN, *J. Inorg. Nucl. Chem.*, 4 (1965) 1055.
10 *Chemical Technology Division Annual Report for period ending May 31, 1963*, Oak Ridge National Laboratory, ORNL3452, 1963.

Analytica Chimica Acta
Elsevier Publishing Company, Amsterdam
Printed in The Netherlands

SELECTIVE EXTRACTION OF THORIUM WITH N-BENZYLANILINE IN CHLOROFORM FROM SULPHURIC ACID MEDIA

M. M. L. KHOSLA
Defence Laboratory, Jodhpur (India)
AND S. P. RAO
University of Jodhpur, Jodhpur (India)

(Received 4th November 1970)

Many solvent extraction methods for thorium have been reported in the literature. 2-Thenoyltrifluoroacetone (TTA)[1-7] is a well known chelating agent for the extraction of thorium from hydrochloric and nitric acid media; the isolation of thorium with TTA is usually done after thorium has been freed from major constituents by some other separation method, such as ion exchange[1], nitrate extraction [8,9] or fluoride separation[2]. Any complexing of thorium in the aqueous phase is quantitatively reflected in a decrease of the extraction of thorium into the organic phase. Since the solubility of the thorium–TTA complex in the various solvents used is rather small, the analytical applications of the reagent have been limited to the isolation of less than 10 mg of thorium and to the evaluation of equilibrium constants of various thorium complexes. Iron cannot easily be separated from thorium by extraction with TTA in benzene. Other chelating agents used for the extraction of thorium include 8-hydroxyquinoline[10], cupferron[11] and 1,1-diantipyrinylethane[12].

The extractability of thorium(IV) from aqueous solutions into organic solvents has been studied for dozens of representative solvents. Most of these studies have been concerned with hydrochloric acid systems, nitric acid systems, sulphuric acid systems or mixed nitric acid–neutral salt systems. The most important of these solvents are tri-*n*-butylphosphate[13-17], mesityl oxide[18,19], cyclohexanone[20], and long-chain aliphatic amines[21-26]. In the extraction of thorium from nitric acid media with tri-*n*-butylphosphate, the elements that are highly extracted under most conditions are scandium, uranium(VI), plutonium(IV or VI), neptunium(IV or VI), zirconium, hafnium and cerium(IV). Fluoride, phosphate or sulphate in the aqueous phase decreases the value of the distribution ratio of thorium in the order given. Extraction with mesityl oxide separates thorium from most elements, except uranium, vanadium, zirconium, scandium and bismuth. The mesityl oxide extraction is successful in the presence of moderate amounts of phosphate, arsenate and sulphate and these ions are complexed when aluminium nitrate is used as a salting-out agent. However, in methods which involve the use of lithium nitrate as a salting-out agent, phosphate and other ions which form stable complexes or insoluble complexes with thorium interfere. Uranium(VI), cerium(III), iron(III), zirconium(IV) and titanium interfere in the extraction of thorium with cyclohexanone; fluoride, phosphate, sulphate, and oxalate also interfere. Various long-chain aliphatic amines have been used for the extraction of thorium from nitric acid and sulphuric acid media, but the reported methods are not selective for the extraction of thorium. Further, no detailed analytical investigation on the extraction of thorium from sulphuric acid media has been made especially in the presence of various diverse ions, both cations and anions.

In this paper, N-benzylaniline in chloroform is reported as a new analytical extraction reagent for thorium from sulphuric acid media. Thorium(IV) is quantitatively extracted from 1.5–2 *M* sulphuric acid media. The separation of the organic and aqueous phases is very rapid. Thorium(IV) is easily stripped from the organic phase with water and titrated with EDTA in the presence of xylenol orange indicator[27]. Salting-out agents, which are generally required in most extraction methods for thorium, are unnecessary in this method. Very few cations interfere when ascorbic acid and EDTA are present. Common anions such as phosphate, citrate, oxalate, borate, nitrate, arsenate, chloride and tartrate do not interfere. Barium and lead(II) which form insoluble sulphates must be removed. Palladium(II) and platinum(II or IV) remain in the organic phase. Uranium(VI) is co-extracted with thorium(IV), but does not interfere in the titration of thorium with EDTA in presence of xylenol orange indicator. Fluoride, which interferes in the extraction of thorium, can be easily masked with boric acid in dilute sulphuric acid. The proposed method is simple and rapid, and effects a clean-cut separation.

EXPERIMENTAL

Apparatus and reagents

A Cambridge pH meter was used to check the pH of the solutions, but for general purposes, narrow-range indicator papers sufficed.

All solutions were prepared from analytical-grade reagents, and double-distilled water was used.

Thorium(IV) solution. A 0.05 *M* solution was prepared by dissolving the required amount of thorium nitrate tetrahydrate in 0.001 *M* nitric acid. The solution was standardized against standard 0.01 *M* EDTA with xylenol orange indicator. The EDTA solution was standardized against a standard zinc solution at pH 5.0 with xylenol orange indicator.

N-Benzylaniline (B.D.H. Ltd.). Dissolve 7.0 g of purified[28] reagent (m.p. 36° ; b.p. 180°/12 mm) in 100 ml of distilled chloroform. The solution on standing for some time assumes a yellow colour, but this does not affect the extraction of thorium(IV).

General procedure

To an aliquot of solution containing up to 45 mg of thorium(IV), add enough sulphuric acid and water to give 1.5–2 *M* acid in a volume of 10 ml. Shake the solution for 2 min with 15 ml of N-benzylaniline solution. Swirl the separating funnel slightly and separate the chloroform layer. Re-extract the aqueous layer with 10 ml of N-benzylaniline solution. Combine the organic layers and strip thorium(IV) from the organic phase by shaking for 2 min with 30 ml of water. Transfer the aqueous layer to a 250-ml conical flask and dilute to about 100 ml. Adjust the pH to 2.5±0.5 with 2 *M* ammonia solution, using a narrow-range pH paper as indicator or a pH meter. Add 8 drops of aqueous 0.1% (w/v) xylenol orange indicator and titrate with 0.01 *M* EDTA solution until the colour changes from red-violet to yellow.

RESULTS AND DISCUSSION

Interference of diverse ions

Thorium(IV) could be selectively and quantitatively extracted from most of the cations tested when sufficient 0.1 *M* EDTA was added to obviate their interferences (Table I). Vanadium(V), iron(III), chromium(VI), osmium(VIII), ruthenium(VIII), titanium(IV) and cerium(IV) hindered the extraction of thorium(IV) but did not interfere after reduction with ascorbic acid; excess of ascorbic acid did not interfere. Uranium(VI) was extracted along with thorium(IV), but no interference was found during the recommended titration of thorium(IV) with EDTA. Palladium(II) and platinum(II, IV) remained in the organic layer. Nitrate, chloride, borate, arsenate, citrate and tartrate did not interfere; phosphate and oxalate which interfere in most methods for the extraction of thorium(IV) caused no interference in the proposed method, even when present in relatively large amounts. Fluoride, which interfered seriously, could be easily complexed with boric acid in dilute sulphuric acid; 0.4 g of boric acid was sufficient to mask 20 mg of fluoride as sodium fluoride. Thorium fluoride dissolved easily in the presence of boric acid and dilute sulphuric acid. EDTA in amounts up to 5.0 ml of 0.1 *M* did not interfere in the extraction.

TABLE I

PERMISSIBLE AMOUNTS OF VARIOUS IONS IN THE EXTRACTION OF THORIUM(IV)
(Thorium(IV) = 17.346 mg, 2 *M* H_2SO_4, 0.1 *M* EDTA, 7% N-benzylaniline in chloroform)

Foreign ion	*Amount (mg)*	*Foreign ion*	*Amount (mg)*
Hg(II)	100	Ni(II)	30
Ag(I)	100	Ca(II)	30
Pd(II)	20	Sr(II)	30
Au(III)	20	Mg(II)	30
Ru(III)	30	Mo(VI)	30
Ru(VIII)[a]	30	W(VI)	30
Os(VIII)[a]	30	V(III)	30
Cu(II)	30	V(V)[a]	30
Cd(II)	30	Ti(IV)[a]	30
Sb(III)	24	Sc(III)	25
Bi(III)	60	Tl(III)	40
Sn(II)	24	In(III)	30
Fe(II)	30	Y(III)	30
Fe(III)[a]	30	Cr(VI)[a]	30
Al(III)	30	Cr(III)	30
Be(II)	30	Fluoride[b]	20
Zr(IV)	27	Chloride	100
Ce(IV)[a]	30	Nitrate	100
Ce(III)	30	Phosphate	100
U(VI)	30	Citrate	100
Zn(II)	30	Tartrate	100
Mn(II)	30	Oxalate	100
Co(II)	30	EDTA	186

[a] Reduced with ascorbic acid.
[b] Masked with boric acid.

The determination of thorium in the presence of uranium is of considerable interest and was therefore studied further. Excellent recoveries of 17.34 mg of thorium(IV) were obtained in the presence of 2.4–31 mg of uranium(IV); with larger amounts of uranium, results tended to be low, probably because insufficient reagent was present to form complexes with both ions.

Effect of acidity and reagent concentration

The concentration of sulphuric acid was varied from 1 *M* to 2.5 *M* while the concentrations of thorium(IV) and the extractant were kept constant. The ratio of the organic to the aqueous phase was 1.5. Thorium(IV) was quantitatively extracted from 1.5–2 *M* sulphuric acid (Table II). The percentage extraction of different amounts of thorium(IV) with a fixed quantity of the extractant are given in Table III. The results indicate that, as expected, the percentage extraction of thorium(IV) in the first extraction decreased as the amount of thorium(IV) increased. However, 25 ml of 7% N-benzylaniline solution was sufficient to extract 57.0 mg of thorium(IV), and larger amounts could be dealt with by further extractions.

TABLE II

PERCENTAGE EXTRACTION OF THORIUM(IV) WITH N-BENZYLANILINE IN CHLOROFORM
(Thorium(IV) added, 17.346 mg. Conditions as in *General procedure* except for acidity)

M H_2SO_4	*1st Extraction* (%)	*2nd Extraction* (%)
1.0	79.2	20.8
1.25	90.0	10.0
1.5	98.0	2.0
2.0	98.0	2.0
2.5	96.7	3.3

TABLE III

PERCENTAGE EXTRACTION OF DIFFERENT AMOUNTS OF THORIUM(IV)
(Conditions as in *General procedure* at 2 *M* H_2SO_4)

Amount of thorium(IV) (mg)	*1st Extraction* (%)	*2nd Extraction* (%)	*3rd Extraction*[a] (%)
5.78	100	–	–
11.56	99	1	–
17.34	98	2	–
34.69	87.7	12.3	–
46.26	82.9	17.1	–
57.82	77.0	23.0	–
69.38	63.3	32.5	4.2

[a] With 10 ml of N-benzylaniline solution.

CONCLUSIONS

The proposed method is very simple and is remarkably free from interferences. Moreover, the reagent used is very cheap and readily available. None of the experimental conditions are highly critical. Few of the available procedures for the extraction of thorium(IV) seem to be applicable in the presence of large concentrations of sulphuric acid, and the suggested extraction seems worthy of consideration, particularly for the extraction of relatively large amounts of thorium(IV).

SUMMARY

N-Benzylaniline in chloroform is shown to be a selective extraction reagent for thorium(IV) in 1.5–2 *M* sulphuric acid media. Few cations interfere when ascorbic acid and EDTA are present. Phosphate, oxalate, citrate, tartrate, nitrate, chloride, borate and arsenate do not interfere, nor do dichromate, chromate and vanadate after reduction with ascorbic acid. Fluoride can be easily masked with boric acid in dilute sulphuric acid. Uranium(VI) is co-extracted but does not interfere with the EDTA titration of thorium(IV) to a xylenol orange end-point. The method is simple and rapid, and effects clean-cut separation.

RÉSUMÉ

La N-benzylaniline dans le chloroforme constitue un réactif d'extraction sélectif pour le thorium(IV) en milieu sulfurique 1.5–2 *M*. La plupart des ions ne gêne pas en présence d'acide ascorbique et d'EDTA. Phosphate, oxalate, citrate, tartrate, nitrate, chlorure, borate et arséniate ne gênent pas, de même que dichromate, chromate et vanadate après réduction à l'acide ascorbique. Les fluorures peuvent être facilement masqués par l'acide borique, dans l'acide sulfurique dilué. L'uranium(VI) est co-extrait, mais il ne gêne pas lors du titrage du thorium(IV) par l'EDTA, en présence de xylénol orange comme indicateur. Cette méthode est simple et rapide.

ZUSAMMENFASSUNG

N-Benzylanilin in Chloroform ist ein selektives Extraktionsreagenz für Thorium(IV) in 1.5–2 *M* schwefelsaurem Medium. In Gegenwart von Ascorbinsäure und EDTA stören nur wenige Kationen. Phosphat, Oxalat, Citrat, Tartrat, Nitrat, Chlorid, Borat und Arsenat stören nicht, ebensowenig Dichromat, Chromat und Vanadat nach Reduktion mit Ascorbinsäure. Fluorid kann leicht mit Borsäure in verdünnter Schwefelsäure maskiert werden. Uran(VI) wird mitextrahiert, stört aber bei der EDTA-Titration von Thorium(IV) mit Xylenolorange als Indikator nicht. Die Methode ist einfach und schnell und bewirkt einwandfreie Abtrennung.

REFERENCES

1 O. Menis, D. L. Manning and G. Goldstein, *Anal. Chem.*, 29 (1957) 1426.
2 R. W. Perkins and R. D. Kalkwarf, *Anal. Chem.*, 28 (1956) 1989.
3 R. A. Day, Jr. and R. W. Stroughton, *J. Amer. Chem. Soc.*, 72 (1950) 5562.
4 F. L. Moore, *Anal. Chem.*, 30 (1958) 1020.
5 E. K. Hyde and J. Tolmach, *Nucl. Sci. Abstr.*, 10 (1956) 4163.
6 W. W. Meinke and R. E. Anderson, *Anal. Chem.*, 24 (1952) 708.
7 F. Hageman, *J. Amer. Chem. Soc.*, 72 (1950) 768.
8 D. Ledent, E. Picciotto and G. Poulaert, *Bull. Soc. Belge Geol. Paleontol. Hydrol.*, 65 (1956) 233.

9 G. R. Tilton, L. T. Aldrich and M. S. Inghram, *Anal. Chem.*, 26 (1954) 894.
10 D. Dyrssen and V. Dahlberg, *Acta Chem. Scand.*, 7 (1953) 1186.
11 J. S. Fritz, M. J. Richards and A. S. Bystroff, *Anal. Chem.*, 29 (1957) 557.
12 V. P. Zhivopistsev and L. P. Pyatosin, *Zh. Analit. Khim.*, 22 (1967) 70.
13 D. F. Peppard, G. W. Mason and J. L. Maier, *J. Inorg. Nucl. Chem.*, 3 (1956) 215.
14 D. F. Peppard, G. Asanovich, R. W. Atteberry, O. DuTemple, M. V. Gergel, A. V. Ganaedinger, G. W. Mason, V. H. Meschke, E. S. Nachtman and I. O. Winsch, *J. Amer. Chem. Soc.*, 75 (1953) 4576.
15 D. F. Peppard, G. W. Mason and M. V. Gergel, *J. Inorg. Nucl. Chem.*, 3 (1957) 370.
16 T. H. Siddall, *Ind. Eng. Chem.*, 51 (1959) 41.
17 E. Hensford, H. A. C. McKay and D. Scargill, *J. Inorg. Nucl. Chem.*, 4 (1957) 321.
18 C. V. Banks and C. H. Byrd, *Anal. Chem.*, 25 (1953) 416.
19 J. S. Fritz and J. J. Ford, *Anal. Chem.*, 25 (1953) 1640.
20 M. Ishibashi and S. Higashi, *Japan Analyst*, 4 (1955) 14.
21 C. F. Coleman, K. B. Brown, J. G. Moore and K. A. Allen, *Proc. Intern. Conf. Peaceful Uses At. Energy, 2nd, Geneva*, 28 (1958) 278.
22 K. W. Allen and W. J. McDowell, *J. Phys. Chem.*, 67 (1963) 1138.
23 T. Sato, *J. Appl. Chem. (London)*, 13 (1963) 254.
24 I. Yagi, *Kogyo Kagaku Zasshi*, 65 (1962) 27.
25 K. S. Venkateswarlu, V. Subramanyan, M. R. Dhaneswar, R. Shanker, Manohar Lal and J. Shanker, *Indian J. Chem.*, 3 (1965) 448.
26 T. Sato, *Anal. Chim. Acta*, 43 (1968) 303.
27 J. Korbl and R. Pribil, *Chemist-Analyst*, 45 (1956) 102.
28 H. Gilman and A. H. Blatt, *Organic Syntheses*, Coll. Vol. I, 2nd Edn., Wiley, New York, 1958, p. 103.

Anal. Chim. Acta, 54 (1971) 315–320

Analytica Chimica Acta
Elsevier Publishing Company, Amsterdam
Printed in The Netherlands

CHARACTERIZATION OF PHENOLS AS THEIR 2,4-DINITROPHENYL ETHERS

AN IMPROVED PROCEDURE AND LIST OF KNOWN DERIVATIVES*

PEDRO A. LEHMANN F.

Department of Chemistry, Center for Research and Advanced Studies, National Polytechnic Institute, A.P. 14-740, Mexico 14, D. F. (Mexico)

(Received 2nd November 1970)

A large number of 2,4-dinitrophenyl (DNP) ethers of phenols** have been made and reported during the last hundred years[2-64]. A few were prepared expressly as derivatives of phenols[9,16,48], but the great majority were synthesized or isolated incidentally in work directed toward other objectives. In the early part of the present work on the properties and conformations of highly hindered aryl ethers, it was necessary to prepare an extensive series of DNP ethers of a variety of phenols[35]. Although it was possible to obtain most of these by previously described methods[9,48], in many cases the results were unsatisfactory. Since many further examples were still required for a p.m.r. study[65], it was of interest to explore other possible syntheses.

By combining elements of a number of the available syntheses[38,45,46,64], a simplified procedure was worked out, which turned out to be eminently practical as a means of characterizing phenols:

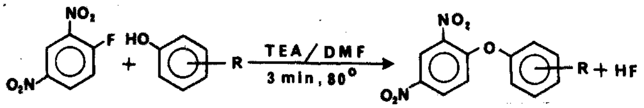

CHARACTERIZATION OF PHENOLS

In the last thirty years, during which the systematic characterization of organic compounds has become consolidated as a branch of organic chemistry, many derivatives have been proposed for the identification of individual phenols[16,66,67]. The most common are listed in Table I. Many others have also been advanced (see Ref. 66, pp. 68–9) but have not received such wide acceptance. However, all of these derivatives suffer from one or more of the following drawbacks:

1. preparation is long or inconvenient;
2. crystallization is difficult or frequently impossible;
3. impurities difficult to separate are formed;

---

* This constitutes Part VII of the series on "Conformations of highly hindered aryl ethers"; for the previous Part, see Ref. 1.

** Abbreviations used in this paper are DNP = 2,4-dinitrophenyl, FDNB = fluoro-2,4-dinitrobenzene, CDNB = chloro-2,4-dinitrobenzene, DMF = dimethylformamide, and TEA = triethylamine.

4. reagents are poisonous, expensive or unstable;
5. formation is sometimes difficult or impossible;
6. a limited number of derivatives is known;
7. formation of more than one product is possible;
8. composition is uncertain.

TABLE I

COMMONLY EMPLOYED DERIVATIVES FOR THE CHARACTERIZATION OF PHENOLS[a]

Name	*Structure*	*Number*[b]
Acetates	$ArO—COCH_3$	250
Benzoates	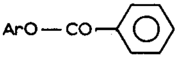	200
Aryloxyacetic acids	$ArO—CH_2COOH$	68
p-Toluenesulfonates	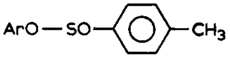	65
N-Phenylurethanes	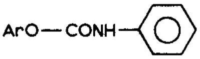	59[c]
p-Nitrobenzoates	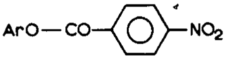	52
2,4-Dinitrophenyl ethers	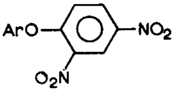	46
Brominated derivatives	$Ar(Br)_n\ OH$	43
3,5-Dinitrobenzoates	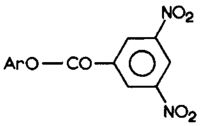	36[c]
α-Naphthylurethanes	$ArO—CONHC_{10}H_7$	32[c]
N,N-Diphenylurethanes	$ArO—CON(Ph)_2$	19
p-Xenylurethanes	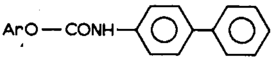	15

[a] For the appropriate references, see Refs. 66 and 67. [b] Number of derivatives whose m.p. is reported by Cheronis *et al.*[16] out of a total of 468 phenols listed. [c] Derivatives recommended by Cheronis *et al.*[16].

2,4-Dinitrophenyl ethers have been proposed twice before as suitable derivatives for phenols: in 1935 Bost and Nicholson[9] prepared 28 derivatives by a procedure in which the phenol is dissolved in sodium hydroxide, mixed with an equimolar quantity of chloro-2,4-dinitrobenzene, and refluxed, usually for 30 min. In 1957 Reinheimer *et al.*[48] called attention to the fact that this apparently simple procedure very often resulted in oily products, difficult to crystallize. This is due to the fact that in the reaction medium there are present in addition to the phenoxide anion, two other nucleophilic anions, namely hydroxide and ethoxide, which can also react with the reagent to give 2,4-dinitrophenol and 2,4-dinitrophenetole. On working up the reaction mixture, the first remains in solution, but the second precipitates and contaminates the product. In order to avoid this, they improved the procedure by: (*a*) using the fluoro compound (FDNB) which is more reactive than the chloro compound (CDNB); (*b*) using acetone instead of ethanol; and (*c*) catalyzing the reaction with TEA instead of sodium hydroxide. In this way they were successful in preparing 38 derivatives out of 41 attempts, and reported 14 new ones[48].

This total of 42 derivatives accounts for most of the 46 listed in Cheronis *et al.*[16]. Nevertheless, DNP ethers did not find favor as phenol derivatives[68].

The existing literature on the subject includes some reports[38,45,46,64] in which DMF successfully replaced acetone in this type of reaction. This solvent, with its large dielectric constant (36.7), high dissolving power and water miscibility, has great advantages in reactions involving displacements of organic halogens[69]. All of this suggested that it might prove to be an ideal solvent for this procedure, and a systematic investigation was undertaken.

EXPERIMENTAL

Preparation of phenol DNP ethers (Tables II and III)

The phenol (1.0 mmole, 150–300 mg), in a 20-ml Erlenmeyer flask or in a 15-ml centrifuge tube, was dissolved in 5 ml of DMF. The FDNB (1.0 mmole, 186 mg; *Caution: Skin Irritant*) was added, followed by TEA (1.1 mmole, 111 mg). The mixture was kept between 80° and 100° for 5 min, and while still warm, water (1–2 ml) was added dropwise to incipient turbidity. It was allowed to cool slowly, during which time the derivative usually crystallized. It was filtered off, and after washing with water, could be recrystallized from aqueous ethanol or aqueous DMF, although the m.p. was rarely improved. In the case of polyphenols 2 or 3 equivalents of FDNB and TEA had to be used. The identity of the product as a DNP ether was easily established by observing the blue-violet color produced on adding two drops of aqueous 10% sodium hydroxide to 3 mg of the derivative dissolved in acetone as described previously[1].

Determination of optimum conditions

Salicylaldehyde (1.22 g, 0.01 mole) in DMF (40 ml) was treated with TEA (1.01 g, 0.01 mole), and the mixture was warmed to 90°. At $t=0$ there was added FDNB (1.86 g, 0.01 mole) dissolved in 10 ml of DMF. While the reaction mixture was kept between 90° and 95°, at times $t=1, 3, 5, 10, 15, 30$ and 60 min, aliquots of 5.0 ml were removed and added to 2.5 ml of water. The oil which formed initially, solidified slowly on icing, and after 30 min was filtered off, washed with a minimum amount of water and air-dried. The first six aliquots each yielded 230 mg of salicylaldehyde–DNP ether with m.p. 108–111° (lit.[27] 111–2°), showing that in this case the reaction is very fast. However, those removed at $t=15$, 30 and 60 min precipitated as orange oils and gave material of increasingly pink color, showing that other reactions, detrimental to the purity of the derivative, also take place and that prolonged reaction times should be avoided. Thus reaction times of 5–15 min are preferred. A total of 2.32 g (80% yield) was obtained.

TABLE II

NEW ARYL 2,4-DINITROPHENYL ETHERS[a]

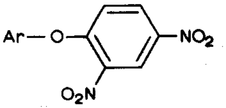

Designation[b]	Ar	Method of preparation[c]	Yield (%)[d]	M.p. (°)	Empirical formula	% C[e] Fd. Calc.	% H Fd. Calc.	% N Fd. Calc.	% Other Fd. Calc.
VII-1	2-Pyridyl	A	38	70–3	$C_{11}H_7N_3O_5$	—	—	15.9 16.1	—
VII-2	2,3,5,6-Tetrafluorophenyl	F	62	100–3	$C_{12}H_4F_4N_2O_5$	43.4 43.4	1.2 1.2	8.3 8.4	F, 23.1 F, 22.9
VII-3	2,6-Dibromo-4-nitrophenyl	A	31	193–6	$C_{12}H_5Br_2N_3O_7$	— 31.1	— 1.1	6.5[h] 9.1	Br, 37.4 Br, 34.5
VII-4	Pentafluorophenyl	F	35	84–6	$C_{12}H_5F_5N_2O_5$	40.9 41.2	0.7 0.8	8.0 8.0	F, 27.0 F, 27.1
VII-5	2,4,6-Triiodophenyl	B	86	244–9	$C_{12}H_5I_3N_2O_5$	22.5 22.6	1.0 0.8	4.2 4.4	F, 59.3 F, 59.7
VII-6	2,6-Dibromophenyl	B	81	149–52	$C_{12}H_6Br_2N_2O_5$	34.4 34.5	1.4 1.4	6.6 6.7	Br, 38.1 Br, 38.2
VII-7	2-Fluoro-6-nitrophenyl	A	62	126–30	$C_{12}H_6FN_3O_7$	—	—	—[h] 13.0	F, 5.8 F, 5.9
VII-8	4,6-Dimethyl-2-pyrimidyl	A	72	127–9	$C_{12}H_{10}N_4O_5$	49.5 49.7	3.5 3.5	19.2 19.3	—
VII-9	4-Cyanophenyl	A	72	108–10	$C_{13}H_7N_3O_5$	—	—	14.7 14.7	—
VII-10	3,5-Di(trifluoromethyl)phenyl	C	65	141–3	$C_{14}H_6F_6N_2O_6$	42.5 42.4	1.4 1.5	7.1 7.1	F, 28.9 F, 28.8
VII-11	2-Bromo-4-carboxymethylphenyl	D	20	102–3	$C_{14}H_9BrN_2O_7$	42.4 42.3	2.4 2.3	7.1 7.1	Br, 20.0 Br, 20.1
VII-12	2-Acetylphenyl	A	42	84–6	$C_{14}H_{10}N_2O_6$	—	—	9.2 9.3	—
VII-13	3-Acetylphenyl	A	66	93–5	$C_{14}H_{10}N_2O_6$	—	—	8.9 9.3	—
VII-14	3-Acetoxyphenyl	A	56, 65	184–8	$C_{14}H_{10}N_2O_7$	—	—	11.7, 12.4[h] 8.8	—
VII-15	2-Hydroxyacetanilide	A	—	146–8[f]	$C_{14}H_{11}N_3O_6$	52.7 53.0	3.3 3.5	13.2 13.2	—
VII-16	5-Chloro-8-quinolyl	A	41	189–90	$C_{15}H_8ClN_3O_5$	52.2 52.1	2.0 2.3	11.9 12.2	Cl, 10.5 Cl, 10.3
VII-17	5-Indanyl	A	83	124–5	$C_{15}H_{12}N_2O_5$	—	—	9.4 9.3	—
VII-18	2-Isopropylphenyl	E	36, 48	101–3	$C_{15}H_{14}N_2O_5$	59.4 59.6	4.6 4.7	9.1 9.3	—
VII-19	1-Bromo-2-naphthyl	C	21	147–9	$C_{16}H_9BrN_2O_5$	49.5 49.4	2.3 2.3	7.1 7.2	Br, 20.5 Br, 20.5
VII-20	1-Nitroso-2-naphthyl	A	—	196–8	$C_{16}H_9N_3O_6$	55.8 56.6	2.5 2.7	12.3 12.4	—
VII-21	2-tert-Butylphenyl	C	19	94–7	$C_{16}H_{16}N_2O_5$	60.7 60.7	5.1 5.1	8.8 8.9	—
VII-22	N-(2′,4′-Dinitrophenyl)-3-aminophenyl[g]	A	—	169–71	$C_{18}H_{11}N_5O_9$	—	—	15.6 15.9	—
VII-23	9-Anthranyl	A	25	270 d	$C_{20}H_{12}N_2O_5$	—	—	—[h] 7.8	—

(continued)

TABLE II *(continued)*

esig-ation[b]	Ar	*Method of preparation*[c]	*Yield (%)*[d]	*M.p. (°)*	*Empirical formula*	*% C*[e] *Fd. Calc.*	*% H Fd. Calc.*	*% N Fd. Calc.*	*% Other Fd. Calc.*
II-24	4-Acetamido-2-(carboxyphenyl)-phenyl	A	47	140–3	$C_{21}H_{15}N_3O_8$	—	—	9.7 9.6	—
II-25	1,3-Dihydroxynaphthalene bis-DNP ether	A	42	184–5	$C_{22}H_{12}N_4O_{10}$	—	—	11.4 11.4	—
II-26	2,7-Dihydroxynaphthalene bis-DNP ether	A	13	153–4	$C_{22}H_{12}N_4O_{10}$	—	—	11.2 11.4	—
II-27	Estrone DNP ether	A	100	164–7	$C_{24}H_{22}N_2O_6$	—	—	6.3 6.5	—
II-28	4-*n*-Hexylresorcinyl bis-DNP ether	A	51	56–8	$C_{24}H_{22}N_4O_{10}$	—	—	10.9 10.6	—
II-29	Diethylstilbestrol bis-DNP ether	A	45	230–3	$C_{30}H_{24}N_4O_{10}$	—	—	9.1 9.3	—

The DNP ethers of 2-ethyl-, 2-*n*-propylphenol and *n*-propyl 4-hydroxybenzoate were obtained as oils. They were not nalyzed, but their structure was confirmed by p.m.r.[65].

The ethers have been arranged by increasing complexity of their empirical formula according to *Chemical Abstracts*, nd are designated by the number of the current paper followed by its number in the sequence.

Method of preparation: (A) present method (TEA, DMF, 3 min at 80°); (B) FDNB, NaOH, 30 min reflux; (C) FDNB, laOH, 60 min at 25°; (D) 2,4-dinitrophenol, methanesulfonyl chloride–pyridine, 6 min reflux; (E) FDNB, pyridine, 0 min at 100°; (F) FDNB, acetone, TEA, 30 min reflux.

Yield of purified material.

Analyses by Galbraith Laboratories, Knoxville, Tenn., U.S.A.

A m.p. of 116–7° has been reported for this compound[27].

3-Aminophenol N,O-bis-DNP derivative; the O-DNP derivative has been described[26].

No satisfactory analysis could be obtained.

TABLE III

2,4-DINITROPHENYL ETHERS OF PHENOLS

	Phenol[a]	*Phenol*[b,c] *m.p. or (b.p.) (°)*	*2,4-DNP derivative m.p. (°) and Ref.*[c–l]
1	2,6-Diisopropylphenol	(124–6)	82–4[35] f[29]
2	2,3,5,6-Tetrafluorophenol	(142)	100–3[e]
3	Pentafluorophenol	(143)	84–6[e]
4	2-Fluorophenol	(171–2)	82–3[35]
5	2-Fluoro-4-methylphenol	(175)	99[32]
6	2-Chlorophenol	(176)	99[9] 99–100[27] 99–100[34] 99[43] 99–100[48]
7	2-Bromophenol	(195)	89[9] 87–8[48]
8	Salicylaldehyde (2-hydroxybenzaldehyde)	(197)	g[10] 112[11] 111–2[27] 112[64] 111[h,l]
9	3-Methylphenol (*m*-cresol)	(202)	74[9] 71–2[27] 72–4[41] 74[43] 73–4[48]
10	2-Ethylphenol	(207)	oil[e]
11	2,4-Dimethylphenol	(211)	106[23] 101–2[48] f[57]

(continued)

TABLE III *(continued)*

	Phenol[a]	*Phenol*[b,c] *m.p. or (b.p.)* (°)	*2,4-DNP derivative m.p.* (°) *and Ref.*[c–l]
12	2-Isopropylphenol	(212)	101–3[e] f[14]
13	2-Hydroxyacetophenone	(215)	84–6[e,h]
14	2-tert-Butylphenol	(224)	94–7[e] f[14]
15	Methyl salicylate (methyl 2-hydroxybenzoate)	(232)	89–90[27] 88[53] 89[55]
16	2,3-Dimethoxyphenol (pyrogallol 1,2-dimethyl ether)	(233–4)	69–70[79]
17	2-Methyl-5-isopropylphenol (carvacrol)	(240)	oil[9,45,48]
18	3-Methoxyphenol (resorcinyl monomethyl ether)	(243)	87–8[27] 87–9[45] 87–8[48]
19	3-Ethoxyphenol (resorcinyl monoethyl ether)	(246–7)	113–5[48]
20	4-Allyl-2-methoxyphenol (eugenol)	(255)	114–5[21] 114–6[48]
21	2-Methoxy-4-propenylphenol (isoeugenol)	(268)	130[9] 129–30[21] 127–8[48]
22	3-Acetoxyphenol (resorcinol monoacetate)	(283d)	184–8[e,h]
23	2,4,6-Triallylphenol	(134–6, 8 Torr)	60–1[36]
24	2-Methylphenol (*o*-cresol)	31	90[9] 90–1[27,30] 91–2[35] 89–90[41] 90[43] 88–9[48]
25	2-Methoxyphenol (guaiacol)	32	97[9] 95–6[27] 92–4[45,48] 93–4[l]
26	3-Chlorophenol	33	75[9] 73–4[27] 72–4[34] 74–6[48]
27	4-Methyl-2-nitrophenol[j]	35	175–6[23]
28	2,6-Di-tert-butylphenol	35–8	g[18,45,e]
29	2,4-Dibromophenol	36	135[9] 129–31[35] 135–6[48]
30	4-Methylphenol (*p*-cresol)	36	93[9,11,17] 97–8[23] 92–3[27] 91–3[41] 93[43] 93–4[48,l]
31	1,2-Dihydroxy-3-methoxybenzene (pyrogallol 1-methyl ether)	38–41	158–60[79]
32	3-Iodophenol	40–2	89–90[27] 90–1[l]
33	Phenylsalicylate (phenyl 2-hydroxybenzoate, Salol)	41–3	113–4[11]
34	Phenol	42	69[9] 70[17] 66[18] f[31] 71–2[35] 69[38] 70–1[41] 76–7[43] 70[47] 70–1[48] 70[58] 72[62]
35	4-Chlorophenol	43	126[9] 123–4[26] 125–7[34] 122–4[41] 123[47] 125–6[48]
36	2,4-Dichlorophenol	43	119[9] 117[18] 118–9[48] 116–8[l]
37	2-Iodophenol	43	95[9] 94[27] 92–3[35] 93–4[48]
38	2-Nitrophenol	45	142[9] 136[11] 137[26] 139[38] 118[43] 139–41[48] 119[59] 118–21[l] 137[47]
39	4-Bromo-2-chlorophenol[j]	45	122–3[23]
40	4-Fluorophenol	47–9	103–4[25] 103–5[h,l]
41	5-Methyl-2-isopropylphenol (thymol)	49	67[9] 64–5[11] 67[43] 64–6[45,48]
42	2,6-Dimethylphenol	49	110–2[35] f[57]
43	4-Chloro-2-methylphenol	49	103–4[34]
44	2,4-Di-tert-butylphenol	52–7	f[14]
45	2,6-Dimethoxyphenol (pyrogallol 1,3-dimethyl ether)	53–6	167–8[45] 161[l] 162[79]

(continued)

TABLE III (*continued*)

Phenol[a]		*Phenol*[b,c] *m.p. or* (*b.p.*) (°)	*2,4-DNP derivative m.p.* (°) *and Ref.*[c–l]
46	2,6-Dibromophenol	54–6	149–52[e]
47	5-Indanol	54–6	124–5[e,h]
48	4-Methoxyphenol (hydroquinone monomethyl ether)	56	110[7,12] 111[26] 112[45] 111–2[48] 109–10[l] 110[83]
49	2-Cyclohexylphenol	56–7	76–7[48]
50	2-Phenylphenol	57	114–5[45] 113–4[48] 113[55] 110–2[e]
51	3,4-Dimethylphenol	62	105–6[48] f[57]
52	2,6-Diiodo-4-methylphenol	62	200–2[4] 196–8[l]
53	4-Chloro-5-methyl-2-isopropylphenol (chlorothymol)	62–4	68–70[46]
54	4-Bromophenol	64	141[9] 138[25] 141[43] 138[47] 140–1[48] 137–8[l]
55	3,5-Dimethylphenol	64	94–7[15] 110–1[48] f[57]
56	2-Methoxy-4-methylphenol	65	124–5[30]
57	4-Chloro-3-methylphenol	66	112[9]
58	2,6-Dichlorophenol	67	135[19]
59	4-*n*-Hexylresorcinol	67–9	56–8[e,h] oil[9]
60	2,4,6-Trichlorophenol	68	136[9] 130[19] 121[23] 134–5[48] 130–2[l]
61	2,4,5-Trichlorophenol	68	150–2[34]
62	3,4-Dichlorophenol	68	126–8[34]
63	2-Bromo-4-chlorophenol[j]	68–9	140–1[23]
64	2-Bromo-4,6-dichlorophenol[j]	68–9	133–4 (impure)[18]
65	2,3,4,6-Tetrachlorophenol	69	g[e]
66	Salicylaldehyde N-methyl N-phenylhydrazone	69	117[10]
67	5,6,7,8-Tetrahydro-1-naphthol	69–71	116–7[45]
68	Methyl 3-hydroxybenzoate	70	126–7[27]
69	2,4,6-Trichloro-3-nitrophenol[j]	71–2	144–5[23]
70	3,4-Dimethyl-2-nitrophenol	71–2	157–8[37]
71	3-Ethoxysalicylaldehyde N-methyl N-phenylhydrazone	72	164[10]
72	2,3-Dimethylphenol	73–5	f[57]
73	8-Hydroxyquinoline	75–6	167–8[46] 165 d[48] 171–3 d[h,l]
74	2-Chloro-4-phenylphenol	76–7	109–11[16]
75	4-Hydroxy-3-methoxybenzaldehyde (vanillin)	81	131[21] 128–30[l]
76	2,6-Dibromo-4-chloro-3-nitrophenol[j]	81–2	158–9[23]
77	2-Hydroxy-1-naphthaldehyde	82–5	g[10]
78	4-Bromo-2-chloro-5-nitrophenol[j]	83	132–3[23]
79	4-Benzylphenol	84	74–6[45] 75–6[48]
80	4-Methyl-2,6-dinitrophenol (3,5-dinitro-*p*-cresol)[i]	84	oil (b.p. at 10^{-4} Torr = 40–60°)[7]
81	1-Bromo-2-naphthol	85	147–9[e]
82	2-(β-Phenylethyl)phenol	85	69[50]
83	2-Hydroxybenzyl alcohol (Saligenin)	85–6	oil[64]
84	4-Chloro-2-nitrophenol	86–7	154[47]

(*continued*)

TABLE III *(continued)*

	Phenol[a]	Phenol[b,c] m.p. or (b.p.) (°)	2,4-DNP derivative m.p. (°) and Ref.[c–l]
85	Ethyl β-(4-hydroxy-3,5-diiodophenyl)propionate	86–8	128–30[4]
86	4-Bromo-2-nitrophenol	89	148[47]
87	2,6-Dibromo-4-chlorophenol[j]	89	145–6[23]
88	2,4,6-Tribromo-3-nitrophenol[j]	89–90	177–8[23]
89	2-Fluoro-6-nitrophenol	91–2	126–30[e,h]
90	4-Iodophenol	93–4	157[26] 156[60]
91	1-Naphthol	94	128[9,43] 127–8[41,45,48] 127[51] 122–4[l]
92	3-Hydroxyacetophenone	94–7	93–5[e,h]
93	2,4,6-Tribromophenol	95	135[9] 131–2[23] 114–6[35] 130[47] 137–8[48]
94	2,4-Dimethyl-6-nitrophenol[j]	95	129–30[23]
95	*n*-Propyl 4-hydroxybenzoate (Propyl paraben)	96–7	oil[e]
96	3-Nitrophenol	97	138[9] 136[11,24,38] 135–6[26,48] 134–5[43] 135[47]
97	4-tert-Butylphenol	100	108–10[48]
98	2,5-Di-tert-butylphenol	102–4	g[e]
99	3-Methoxy-4-hydroxy-Δ^5-dihydro-N-methylmorphinan	103–6	167–8[44]
100	3-Hydroxybenzaldehyde	104	125[10] 123–4[27]
101	Catechol (1,2-dihydroxybenzene)	105	131–2[43] 136–8[48] 142[64] 139–42[h,l]
102	2-Hydroxypyridine	105–7	70–3[e,h]
103	5-Bromo-2-hydroxybenzaldehyde	105–8	g[10]
104	3,4,5-Trimethylphenol		
105	Methyl 3-bromo-4-hydroxybenzoate	107	102–3[e]
106	3,5-Dihydroxytoluene (orcinol)	108	153–4[48] 148–51[h,l]
107	4,4′-Dihydroxy-3,3′-dimethoxydiphenylmethane	108–9	175–6[79]
108	1-Nitroso-2-naphthol	109	196–8[e,h]
109	4-Hydroxyacetophenone	109	134–5[25]
110	Resorcinol (1,3-dihydroxybenzene)	110	194[9] 191–2[11,48] 184[32] 192[43] 191–3[h,l]
111	4-Cyanophenol	110–3	108–10[e,h]
112	N-Acetyl-3,5-diiodo-L-tyrosine[i]	112–8	210–2[4]
113	4-Nitrophenol	114	120[9] 116–7[11,26] 121[38] 115–6[41] 120[43] 116[47] 118–9[48] 114[59] 116–8[l] 115–6[83]
114	2,4-Dinitrophenol[i]	114	210[20] 195–7[35] 197[38] g[48] 195[51] 194–5[54] 197–9[83]
115	4-Hydroxy-3-methoxyacetophenone (acetovanillone)	115	156–7[80]
116	2-Methylresorcinol (2,6-dihydroxytoluene)	115–8	f[57]
117	3,4-Dihydroxyacetophenone	116	75[80]
118	4-Hydroxybenzaldehyde	116–7	105[10] 103–4[25] 95–125[52] f[57]
119	9-Hydroxyanthracene (9-anthranol)	120	270 d[e,h]
120	2,4,6-Trinitrophenol (picric acid)[i]	122	210[39] 208–10[42] 210[51]

(*continued*)

TABLE III *(continued)*

Phenol[a]	*Phenol*[b,c] *m.p. or (b.p.)* (°)	*2,4-DNP derivative m.p.* (°) *and Ref.*[c–l]
121 3-Aminophenol	122	O-DNP = 123–4[27]; O,N-bis-DNP = 169–71[e,h]
122 4-Benzyloxyphenol (Benoquin)	122	129–30[48]
123 2-Naphthol	123	95[9,22,43] 93[38] 93–5[41] 94–5[45,48] 94[55]
124 l-3-Methoxy-4-hydroxy-N-methylmorphinan	123–4	202–3[44]
125 1,3-Dihydroxynaphthalene	124	184–5[e]
126 5-Chloro-8-hydroxyquinoline	125	189–90[e,h]
127 3-Hydroxypyridine	125–8	127–9[2]
128 2-Hydroxy-5-nitrobenzaldehyde	126	g[10]
129 Methylhydroquinone	127–9	f[57]
130 Methyl 4-hydroxybenzoate (Methyl paraben)	131	151–2[25] 150–1[l] 151[182]
131 4-Cyclohexylphenol	132	100–1[48]
132 Pyrogallol (1,2,3-trihydroxybenzene)	133	oil[48] 203[64] 165–72[h,l]
133 4-Hydroxybenzophenone	135	142–3[25]
134 4-Hydroxy-2-methoxyacetophenone (isopeonol)	138	128–9[80]
135 2-Hydroxybenzamide (salicylamide)	140	121[53]
136 4-Hydroxy-3-nitrobenzaldehyde	144	169[52]
137 2,6-Dibromo-4-nitrophenol	144	193–6[e,h]
138 N-(*p*-Toluenesulfonyl) 4-aminophenol	145	202[5]
139 N-Acetyl 3,5-diiodo-D,L-tyrosine ethyl ester[i]	145–6	204–6[4]
140 3,4-Dihydroxypropiophenone	146	75[80]
141 3-Hydroxyacetanilide	148–50	88–9[27]
142 4,4′-Dihydroxyphenylsulfide	151	109[3]
143 3,4-Dihydroxybenzaldehyde (protocatechualdehyde)	153–4	120–3[80]
144 N-Acetyl 3,5-diiodo-L-tyrosine ethyl ester	154–5	102–4[3]
145 4-Phenylazophenol	155–6	137–8[61]
146 4-Methyl-2,3-dinitrophenol[i,j]	156–7	184[23]
147 2-Hydroxybenzoic acid (salicylic acid)[i]	157–9	164[53]
148 2,4,6-Triiodophenol	159	244–9[e]
149 7-Hydroxymetameconine	159–60	183–4[82]
150 2,4-Dimethyl-3,5-dinitrophenol[i,j]	162–3	198[23]
151 3,3′,5,5′,6,6′-Hexachloro-2,2′-dihydroxydiphenylmethane (Hexachlorophene)	164–5	237–8[46] 229–32[h,l]
152 4-Phenylphenol	165	118[9] 116[55] 110–2[l]
153 Methyl 4-hydroxy-3,5-diiodobenzoate	167	181–2[4]
154 4-Hydroxyacetanilide (4-acetamidophenol)	168	196[5] 195[25,49]
155 Diethylstilbestrol	169–72	230–3[e,h]
156 Hydroquinone (1,4-dihydroxybenzene)	172	O-DNP = 133[25]; O,O′-bis-DNP = 240[6] 243–6[48] 245–50[h,l]
157 5-Chloro-8-hydroxy-7-iodoquinoline	172 d	186–9[46] 182–6[h,l]
158 2-Aminophenol	174	O-DNP = 120–1[27]
159 4-Hydroxy-3-methoxycinnamic acid (ferulic acid)[i]	174	f[57] 266[78]

(*continued*)

TABLE III *(continued)*

	Phenol[a]	*Phenol*[b,c] *m.p. or (b.p.)* (°)	*2,4-DNP derivative m.p.* (°) *and Ref.*[c–l]
160	3-Bromo-4-hydroxybenzoic acid[i]	177–8	214[18]
161	4-Hydroxy-1-naphthaldehyde	181	158[10]
162	4-Aminophenol	184 d	146[5] 143–4[26] 144[49]
163	4-Hydroxy-3-nitrobenzoic acid[i]	186–7	205–7[52]
164	2,7-Dihydroxynaphthalene	190	153–4[e]
165	4-Acetamidophenyl salicylate (Salophen)	190	140–3[e,h]
166	Pentachlorophenol	191	f[56]
167	2-Hydroxy-4,6-dimethylpyrimidine	201–3	127–9[e,h]
168	5,7-Dibromo-8-hydroxyquinoline	202–3	183–4[46]
169	2-Hydroxyacetanilide (2-acetamidophenol)	203–4	116–7[27] 146–8[e,h]
170	4-Hydroxy-2-methoxyacetophenone 2,4-dinitrophenyl hydrazone	209, 216–7	137–8[81]
171	4-Hydroxy-3-methoxybenzoic acid (vanillic acid)[i]	210	212[78]
172	4-Hydroxybenzoic acid[i]	215 d	>200[17] 254[55]
173	Phloroglucinol (1,3,5-trihydroxybenzene dihydrate)	218 d	183[64] 60–80[h,l]
174	2,4,6-Trihydroxyacetophenone (phloracetophenone)	222	102–3[80]
175	2-Hydroxy-4-methoxyacetophenone (peonol) 2,4-dinitrophenylhydrazone	234–5	192–3[81]
176	3,4-Dihydroxypropiophenone 2,4-dinitrophenylhydrazone	238	206–7[81]
177	2,4,6-Trihydroxyacetophenone 2,4-dinitrophenylhydrazone	242	132 d[81]
178	4-Hydroxy-N-methylacetanilide	243–5	142[5]
179	4-Methylaminophenol (sulfate)	245 d	104[5]
180	3,4,5-Trihydroxybenzoic acid (gallic acid)[i]	253 d	292 d[64]
181	Morphine	254	260 d[33]
182	4-Hydroxy-3-methoxyacetophenone 2,4-dinitrophenylhydrazone	255	242[81]
183	7,8-Dihydroxycoumarin (daphnetin)	257–8	215–7[80]
184	Estrone	258–62	164–7[e,h]
185	4-Hydroxybenzaldehyde 2,4-dinitrophenylhydrazone	270–1	241–2 d[81]
186	4-Hydroxy-3-methoxybenzaldehyde 2,4-dinitrophenylhydrazone	271 d	278–9 d[81]
187	2,2′-Dihydroxy-3,3′-dimethoxybiphenyl-5,5′-dicarboxaldehyde bis-2,4-dinitrophenylhydrazone	280	220 d[81]
188	4-Triphenylmethylphenol (4-tritylphenol)	280–3	242–5[46]
189	D,L-Tyrosine[i]	316 d	195 d[63]
190	5,5′-Diacetyl-2,2′-dihydroxy-3,3′-dimethoxybiphenyl bis-2,4-dinitrophenylhydrazone	330–5	175–80 d[81]
191	3,5-Di(trifluoromethyl)phenol	(97, 50 Torr)	141–3[e,h]
192	2-Allyl-4-methylphenol	—[k]	64–5[e,h]
193	Salicylaldehyde oxime O-methyl ether	—[k]	106[10]
194	2,4-Dibromo-6-phenylphenol	—[k]	148[19]
195	2-Bromo-4-hydroxy-6-iodobenzoic acid[i]	—[k]	227–8[18]

(*continued*)

TABLE III *(continued)*

	Phenol[a]	*Phenol*[b,c] *m.p. or (b.p.)* (°)	*2,4-DNP derivative m.p.* (°) *and Ref.*[c-1]
196	4-Hydroxy-3,5-diiodobenzaldehyde	—[k]	258–9 d[4]
197	L-3,5-Diiodotyrosine[i]	dec[k]	212–6[4]
198	N-*p*-Toluenesulfonyl N-methyl 4-aminophenol	—[k]	175[5]
199	Dinitrophloroglucinol[i]	—[k]	279[8]
200	4-Hydroxyphenyl methyl sulfone	—[k]	172–3[25]
201	4-Hydroxybenzenesulfonic acid[i]	—[k]	98–105[28]
202	Trinitrothymol[i]	—[k]	85[43]
203	4-Isooctylphenol	—[k]	94[55]
204	N-Phenyl 3-hydroxy-1,2,3,4-tetrahydroquinoline	—[k]	126[55]
205	4-Iodosophenol	—[k]	131 d[60]
206	4-Iodoxyphenol	—[k]	193 expl.[60]

[a] Substituents are listed alphabetically except for the prefixes iso-, sec-, tert-, di-, tri-, etc.

[b] Phenols are listed in order of increasing b.p. if normally liquids, and increasing m.p. if normally solids.

[c] All b.p. and m.p. have been rounded off to the next lowest degree.

[d] All m.p. reported are listed in alphabetical order of their authors' names.

[e] DNP derivative described here for the first time; see Table II.

[f] No m.p. reported.

[g] No DNP ether was isolated after attempted preparation.

[h] Prepared by the method described in this paper.

[i] DNP ether cannot be prepared by the method described in this paper.

[j] DNP ether was not prepared directly from the phenol.

[k] Phenols whose b.p. or m.p. is not known or could not be determined.

[l] Known DNP derivatives prepared again in this laboratory.

Materials

The phenols employed were commercially available and were used without further purification. The reagents used were DMF and acetone (Merck-Uvasol), TEA (Eastman Kodak), while the FDNB (Eastman Kodak, Aldrich Chemical Co., Pierce Chemical Co.) was used as received. Pure FDNB has m.p. 24–5° (supercools readily), b.p. 122–4° at 1 Torr, and $n_D^{20°} = 1.5699$ [70]. The estrone was kindly provided by Dr. J. Medina of Syntex S.A. Melting point standards were A. H. Thomas and Fisher Thermetric Standards. Analytical samples were prepared by recrystallization (aqueous EtOH or aqueous DMF) to constant m.p., and dried somewhat below their m.p. *in vacuo* (less than 1 Torr) over P_2O_5 for at least 8 h.

Instruments

Melting points were obtained on a Kofler hot-stage and are given uncorrected. Although the melting points reported in Tables II and III were obtained over a five-year span, calibration of the hot-stage with a series of m.p. standards at the beginning and end of this period, showed that no correction was necessary.

RESULTS

New derivatives

Table II shows 29 derivatives of phenols which have not been described previously. Most of them were prepared by the simplified procedure given above. Initially, carbon, hydrogen, nitrogen and halogens were determined, but when several examples had shown that no unusual changes were to be expected, only nitrogen was determined. The preparations were made on a semi-micro scale, but since the yields are excellent (70–90%), and the molecular weight is usually doubled, it is feasible to carry out the reaction with only 15–30 mg without major adaptation, or on a micro-scale with the appropriate equipment[71].

Complete list of derivatives

In Table III have been collected over 200 aryl DNP ethers whose preparation has been described or attempted. It includes a large number that *were not prepared* by the method described here. The boiling and melting points of the phenols were mostly taken from standard references[16,68]; all the data which were found reported are given since in many cases different values have been given by different authors (*e.g.* 2-nitro-2,4,6-trichloro-, 2,4,6-tribromophenol and 2-hydroxyacetanilide) and may represent different crystal modifications. Phenols and/or their DNP derivatives of uncertain structure have not been included. Table III does not include DNP derivatives of alcohols, aliphatic and aromatic thiols, amines and related compounds, nor of amino acids[72]. Derivatives of di- and tri-hydroxy compounds are understood to be the bis- and tris-DNP ethers unless stated otherwise.

DISCUSSION

Advantages of the proposed procedure

The procedure proposed here has several features that recommend it over other methods.

The replacement of acetone[48] by DMF results in a much faster reaction, because the latter solvent probably also exerts a catalytic role through its proton-accepting properties. In addition, the reaction is cleaner since the formation of Janovsky-type compounds (acetone-anion addition to *m*-dinitrobenzenes[1]) is avoided. Although DMF can be substituted by dimethylsulfoxide, malodorous sulfur-containing compounds are often formed as by-products[38], and reaction rates are comparable[46]. Dimethylacetamide was examined in the present work, but has no advantage over DMF. Further, the excellent solubility of phenols in DMF (no insoluble ones were encountered) as well as that of 2,4-dinitrophenol (which is formed from FDNB by any water present), together with the low solubility of the derivative, make it an ideal reaction medium. The present procedure also incorporates a simpler work-up than does the method of Vorozhtsov[54,55] which also requires anhydrous potassium fluoride.

The use of TEA as the catalyst avoids the problems of hydroxylic bases, although its volatility (b.p. = 89–90° at 760 Torr) does not allow the temperature of the reaction medium to be raised, and reaction times must be lengthened in recalcitrant cases. It is very soluble in aqueous DMF so that it does not contaminate the product.

The advantages of using FDNB have been confirmed: in addition to reacting much faster than the chloro analog[73], it is cheap and readily available and can be synthesized conveniently[70,74]. Its steric requirements are less than those of fluoro-2,6-dinitrobenzene which has also been proposed[75], and the difficulties of complex formation and detonation sensitivity of picryl chloride derivatives are absent.

As can be seen from the results of Tables II and III, the derivatives of a great variety of phenols have been successfully derived: alkyl- and aryl-phenols, halo- and nitrophenols, bis- and tris-phenols, heterocyclic phenols, naphthols, etc. Even 9-anthranol, which exists mainly in the keto form yielded a derivative, although a longer reaction time had to be used. Primary (but not secondary or tertiary) alcohols, as well as amines and thiols also react under these conditions, so that bis-DNP derivatives should be expected in polyfunctional compounds. Thus indirect methods must be employed to obtain the O-DNP product[26].

Even relatively hindered phenols such as 2-tert butylphenol and 2,6-diisopropylphenol react with ease, which is probably a reflection of the great facility with which the fluorine atom can be approached and displaced by nucleophiles:

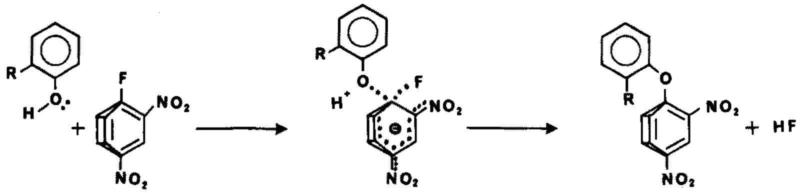

It should be pointed out that the DNP ethers listed melt over a wide range (60–230°), and that in most cases their melting points differ considerably (often by 50–100°) from those of the starting phenol, both useful features of a derivative.

Although the quantitative aspects of this reaction have not been emphasized in this study, the modified procedure proposed should be applicable in quantitative gravimetric[64,71], spectrophotometric[71] or colorimetric[1] analyses.

Limitations of the proposed procedure

Two types of phenols do not yield DNP ethers under the conditions employed:

1. "*Acidic phenols*". Although mono-nitrophenols do give derivatives, polynitrophenols (such as 2,4-dinitrophenol and picric acid) do not, nor do phenols bearing another acidic function (*e.g.* carboxyl). The latter type can be prepared by Vorozhtsov's procedure[54,55].

2. *Cryptophenols.* A few very highly hindered phenols such as 2,6- and 2,5-di-tert-butylphenol, do not react. The latter was somewhat unexpected since it had been possible to prepare the 2,5-di-tert-butylphenyl 2′,4′-dinitro-1-naphthyl ether (unpublished observation). For such phenols derivatization by reaction with *p*-nitrochlorobenzene as described by Wright and Jorgensen might be substituted[76].

Out of a total of nearly 150 phenol derivatives, only six (2-ethyl-, 2-*n*-propyl-, 4-methyl-2,6-dinitro-, carvacrol, *n*-propyl-4-hydroxybenzoate and 2-hydroxybenzyl alcohol) were obtained as oils which could not be crystallized. This is a lower number by far than that for many procedures, *e.g.* the recently proposed N-methyl- and N-phenylpiperazine salts which have as a further disadvantage their uncertain composition[77].

CONCLUSIONS

From these results it can be seen that DNP ethers are nearly ideal derivatives for phenols since most of the usual drawbacks are absent. The listing of nearly 200 examples shows that they are good contenders for becoming the most popular phenol derivative. The varied uses of DNP ethers[72], other than as derivatives of phenols, should make the simplified synthetic procedure described, as well as the complete list of known examples helpful in various areas.

Note added in proof.

Dr. W. Wildenhain kindly provided the m.p.'s of a number of phenols and their DNP derivatives, as yet unpublished[78], which have been of great help in extending Table III. 4-Acetyl-2-nitrophenyl ethers (formed by phenols upon reaction with 4-fluoro-3-nitroacetophenone) are also useful derivatives[78], especially in t.-l.c.[84], although their m.p.'s have not yet been reported.

It is a pleasure to acknowledge here the technical assistance of M. P. González, J. Guerrero E., M. Flores and C. Hernández in the realization of this work.

SUMMARY

The reaction of phenols with fluoro-2,4-dinitrobenzene, clean and quick when catalyzed by triethylamine in dimethylformamide, is shown to be ideal for the characterization of phenols. The resulting 2,4-dinitrophenyl ethers crystallize well and can be used in spectrophotometric and colorimetric quantitative analyses as well as for other purposes. Thirty new derivatives are described, and a list has been compiled of nearly 200 aryl 2,4-dinitrophenyl ethers scattered in the literature.

RÉSUMÉ

La réaction des phénols avec le fluorodinitro-2,4-benzène, nette et rapide quand elle est catalysée par la triéthylamine dans la diméthylformamide, se révèle idéale pour la caractérisation des phénols. Les dinitro-2,4-phényléthers que l'on obtient, cristallisent bien et peuvent être utilisés tant pour l'analyse quantitative (spectrophotométrique ou colorimétrique), que pour d'autres fins. Trente nouveaux dérivés sont décrits; on donne une liste d'environ 200 aryl dinitro-2,4-phényléthers trouvés dans la littérature.

ZUSAMMENFASSUNG

Es wird gezeigt dass die Reaktion von Phenolen mit Fluor-2,4-dinitrobenzol, die eindeutig und schnell verläuft, wenn sie in Dimethylformamid durch Triäthylamin katalysiert wird, für die Charakterisierung von Phenolen ideal ist. Die entstehenden 2,4-Dinitrophenyl-äther kristallisieren gut und können für quantitative spektrophotometrische und kolorimetrische Analysen sowie für andere Zwecke verwendet werden. Die Herstellung von dreissig neuen Derivaten wird beschrieben, und nahezu 200 in der Literatur beschriebene Aryl 2,4-dinitrophenyl-äther werden in einer Liste zusammengestellt.

REFERENCES

1 P. A. LEHMANN F., *Part VI, Rev. Latinoamer. Quim.*, 1 (1970) 112.
2 ALDRICH CHEMICAL CO., *Catalog #14*, Milwaukee, Wisc., 1969, p. 193.
3 A. ARCORIA AND R. PASSERINI, *Atti Accad. Gioenia Sci. Nat. Catania*, 11 (1957) 184; *Chem. Abstr.*, 54 (1960) 353.
4 J. H. BARNES, E. T. BORROWS, J. ELKS, B. A. HEMS AND A. G. LONG, *J. Chem. Soc.*, (1950) 2824.
5 A. L. BECKWITH AND J. MILLER, *J. Org. Chem.*, 19 (1954) 1708.
6 F. K. BEILSTEIN, *Handbuch der Organischen Chemie, Vol. 6*, 4th Edn., Springer, Berlin, 1923, p. 845.
7 E. T. BORROWS, J. C. CLAYTON, B. A. HEMS AND A. G. LONG, *J. Chem. Soc., Suppl. Issue*, 1 (1949) 198.
8 W. BORSCHE AND E. FESKE, *Chem. Ber.*, 59B (1926) 683.
9 R. W. BOST AND F. NICHOLSON, *J. Amer. Chem. Soc.*, 57 (1935) 2368.
10 O. L. BRADY AND W. H. BODGER, *J. Chem. Soc.*, (1932) 952.
11 H. BRÄUNIGER AND K. SPANGENBERG, *Pharmazie*, 12 (1957) 335.
12 R. Q. BREWSTER AND H. S. CHOGUILL, *J. Amer. Chem. Soc.*, 61 (1939) 2702.
13 R. Q. BREWSTER AND R. SLOCOMBE, *J. Amer. Chem. Soc.*, 67 (1945) 562.
14 T. L. CANTRELL AND J. O. TURNER, *U.S. Patent 2,134,434* (1938); *Chem. Abstr.*, 33 (1939) 1487.
15 L. C. CASE, *J. Appl. Polymer Sci.*, 8 (1964) 533.
16 N. D. CHERONIS, J. B. ENTRIKIN AND E. M. HODNETT, *Semimicro Qualitative Organic Analysis*, 3rd Edn., Interscience, New York, 1965, pp. 485, 490, 924 ff.
17 A. N. COOK, *J. Amer. Chem. Soc.*, 32 (1910) 1285.
18 M. DAHLGARD, *Thesis*, University of Kansas, 1956.
19 M. DAHLGARD AND R. Q. BREWSTER, *J. Amer. Chem. Soc.*, 80 (1958) 5861.
20 L. DESVERGNES, *Mon. Sci.*, 16 (1926) 201; *Chem. Abstr.*, 21 (1927) 740.
21 A. EINHORN AND G. FRYE, *Chem. Ber.*, 27 (1894) 2457.
22 M. ERNST, *Chem. Ber.*, 23 (1890) 3429.
23 D. L. FOX AND E. E. TURNER, *J. Chem. Soc.*, (1930) 1853.
24 *German Patent #281,053; Chem. Zentr.*, 86 I (1915) 74.
25 S. S. GITIS AND A. V. IVANOV, *J. Gen. Chem. USSR*, 34 (1964) 3431.
26 S. S. GITIS AND A. V. IVANOV, *J. Org. Chem. USSR*, 1 (1965) 906.
27 S. S. GITIS AND A. V. IVANOV, *J. Org. Chem. USSR*, 2 (1966) 107.
28 V. HAHN, Z. KOCHANSKY AND V. TEŽAK-JENIĆ, *Arkh. Kem.*, 26 (1954) 257; *Chem. Abstr.*, 50 (1956) 858.
29 H. KESSLER, A. RIEKER AND W. RUNDEL, *Chem. Commun.*, (1968) 475.
30 R. KUHN, H. J. HAAS AND A. SEELIGER, *Chem. Ber.*, 94 (1961) 1259.
31 G. MAIKOPAR, *Chem. Ber.*, 6 (1873) 564.
32 V. P. MAMAEV AND L. S. SANDAKHCHIEV, *Izv. Otd. Akad. Nauk SSSR*, 1 (1962) 68; *Chem. Abstr.*, 58 (1963) 3501.
33 C. MANNICH, *Arch. Pharm. Ber. Deut. Pharm. Ges.*, 273 (1935) 97.
34 G. W. MASON AND E. G. BROOKER, *Proc. N. Z. Weed Pest Contr. Conf.*, (1968) 163; *Chem. Abstr.*, 70 (1969) 77494.
35 D. M. MCEACHERN AND P. A. LEHMANN F., *J. Mol. Structure*, in press.
36 B. M. MIKHAILOV, F. S. TER-SARKISYAN AND N. A. NIKOLAEVA, *Izv. Akad. Nauk SSSR, Ser. Khim.*, (1968) 541; *Chem. Abstr.*, 69 (1968) 67448.
37 G. P. MUELLER AND W. S. PELTON, *J. Amer. Chem. Soc.*, 71 (1949) 1504.
38 J. MURTO, *Suomen Kemistilehti*, B38 (1965) 49.
39 J. MURTO, *Acta Chem. Scand.*, 20 (1966) 310.
40 R. NIETZKI AND B. SCHÜNDELEN, *Chem. Ber.*, 24 (1891) 3586.
41 Y. OGATA AND M. OKANO, *J. Amer. Chem. Soc.*, 71 (1949) 3212.
42 K. OKÓN, *Bull. Acad. Polon. Sci.*, 6 (1958) 319; *Chem. Abstr.*, 52 (1958) 20152.
43 D. P. PARIHAR, S. P. SHARMA AND K. C. TEWARI, *J. Chromatog.*, 21 (1966) 261.
44 W. H. PIRKLE AND M. GATES, *J. Org. Chem.*, 30 (1965) 1769.
45 W. H. PIRKLE AND J. L. ZABRISKIE, *J. Org. Chem.*, 29 (1964) 3124.
46 W. POETHKE AND H. KÖHNE, *Pharm. Zentralhalle*, 104 (1965) 630; 107 (1968) 339.
47 L. C. RAIFORD AND J. C. COLBERT, *J. Amer. Chem. Soc.*, 4 (1926) 2652.
48 J. D. REINHEIMER, J. P. DOUGLASS, H. LEISTER AND M. P. VOELKEL, *J. Org. Chem.*, 22 (1957) 1743.
49 F. REVERDIN AND O. DRESSEL, *Chem. Ber.*, 37 (1904) 1516.
50 P. RUGGLI AND A. STAUB, *Helv. Chim. Acta*, 20 (1937) 37.

51 H. Ryan and P. J. Drumm, *J. Sci. Proc. Roy. Dublin Soc.*, 17 (1924) 313; *Chem. Abstr.*, 18 (1924) 1655.
52 K. H. Slotta and K. H. Soremba, *Chem. Ber.*, 68B (1935) 2059.
53 B. Tozer and S. Smiles, *J. Chem. Soc.*, (1938) 2052.
54 N. N. Vorozhtsov and G. G. Yakobson, *J. Gen. Chem. USSR*, 27 (1957) 1741.
55 N. N. Vorozhtsov and G. G. Yakobson, *J. Gen. Chem. USSR*, 28 (1958) 40.
56 C. J. Weinman and G. C. Decker, *J. Econ. Entomol.*, 40 (1947) 74.
57 W. Wildenhain and G. Henseke, *J. Chromatog.*, 19 (1965) 438.
58 C. W. Willgerodt, *Chem. Ber.*, 12 (1879) 762.
59 C. W. Willgerodt and E. Huetlin, *Chem. Ber.*, 17 (1884) 1765.
60 C. W. Willgerodt and G. Wiegand, *Chem. Ber.*, 42 (1909) 3763.
61 E. O. Woolfolk, E. Donaldson and M. Payne, *J. Org. Chem.*, 27 (1962) 2653.
62 G. G. Yakobson, *Zh. Vses. Khim. Obshchestva im. D. I. Mendeleeva*, 5 (1960) 708; *Chem. Abstr.*, 55 (1961) 11344.
63 H. Zahn and R. Kockläuner, *Biochem. Z.*, 325 (1954) 339.
64 H. Zahn and A. Würz, *Z. Anal. Chem.*, 134 (1951) 183.
65 P. A. Lehmann F., in preparation.
66 R. L. Shriner, R. C. Fuson and D. Y. Curtin, *The Systematic Identification of Organic Compounds*, 5th Edn., John Wiley, New York, 1964.
67 F. Wild, *Characterization of Organic Compounds*, 2nd Edn., University Press, Cambridge, 1962.
68 C. D. Hodgman (Editor-in-Chief), *Tables for Identification of Organic Compounds*, Chemical Rubber Publishing Co., Cleveland, Ohio, 1960.
69 R. S. Kittila, *Dimethylformamide. Chemical Uses*, Du Pont & Co., Wilmington, Del., 1967.
70 G. C. Finger and C. W. Kruse, *J. Amer. Chem. Soc.*, 78 (1956) 6034.
71 N. D. Cheronis and T. S. Ma, *Organic Functional Group Analysis by Micro and Semimicro Methods*, Interscience, New York, 1964.
72 These as well as other uses of DNP compounds will be discussed in a separate communication.
73 J. F. Bunnett, E. W. Garbisch, Jr. and K. M. Pruitt, *J. Amer. Chem. Soc.*, 79 (1957) 385.
74 G. C. Finger and J. L. Finnerty, *Biochem. Prep.*, 3 (1953) 120.
75 N. N. Vorozhtsov, Jr., V. A. Sokolenko and G. G. Yakobson, *Izv. Sibirsk. Otd. Akad. Nauk SSSR*, (1962) 87; *Chem. Abstr.*, 59 (1963) 1507.
76 J. Wright and E. C. Jorgensen, *J. Org. Chem.*, 33 (1968) 1245.
77 D. Yung, L. Whitehouse and E. Lo, *J. Chem. Educ.*, 47 (1970) 474.
78 W. Wildenhain, personal communication.
79 W. Wildenhain and G. Henseke, *Monatsh. Chem.*, 100 (1969) 479.
80 W. Wildenhain and G. Henseke, *J. Prakt. Chem.*, in press.
81 W. Wildenhain and G. Henseke, *Chimia (Aarau)*, 20 (1966) 357.
82 J. A. McRae, R. Y. Moir, J. J. Ursprung and H. H. Gibbs, *J. Org. Chem.*, 19 (1954) 1500.
83 J. F. Bunnett and C. F. Bernasconi, *J. Org. Chem.*, 35 (1970) 70.
84 W. Wildenhain, G. Henseke and G. Bienert, *J. Chromatog.*, 45 (1969) 158.

Analytica Chimica Acta
Elsevier Publishing Company, Amsterdam
Printed in The Netherlands

COMPARAISON DES HYPOTHESES EXTRATHERMODYNAMIQUES DANS LES MELANGES EAU–ETHANOL

J. BESSIÈRE

Laboratoire de Chimie Analytique, Faculté des Sciences associé au C.N.R.S., Ecole de Physique et Chimie, 10 rue Vauquelin, Paris Ve (France)

(Reçu le 21 novembre 1970)

Il est nécessaire de faire appel à des hypothèses extrathermodynamiques pour comparer les niveaux d'acidité atteints dans des solvants différents, la mesure du potentiel chimique d'un ion pris isolément étant par principe impossible[1-4].

Gaboriaud[5,6] définit une fonction f(*H*) pour caractériser les niveaux d'acidité dans les mélanges eau–solvant. Cette fonction implique en réalité un certain nombre d'hypothèses concernant la valeur du potentiel de jonction existant entre deux phases liquides de composition différente.

La mesure du niveau d'acidité dans les mélanges eau–alcool diffère sensiblement selon la nature des hypothèses envisagées[5]. Neanmoins, dans les mélanges eau–éthanol, les variations des fonctions H_0[7] et R_0[8] présentent une certaine similitude: elles passent toutes deux par un maximum qui correspond à une composition en volume éthanol 80%–eau 20%[9,10].

Deux interprétations ont été proposées pour justifier de telles variations. La première fait intervenir l'évolution des propriétés basiques du solvant[10], alors que la seconde attribue ces variations à une modification du comportement de l'indicateur[5].

Dans le premier cas, on suppose que dans les mélanges eau–éthanol, les molécules d'eau sont moins associées que dans l'eau pure. Elles présenteraient alors une affinité plus grande pour le proton, le milieu deviendrait plus basique. Quand la proportion d'éthanol devient suffisante, les ions H_3O^+ sont alors remplacés par les ions $EtOH_2^+$ et la basicité du milieu décroît.

Dans le second cas, on admet que ces variations sont essentiellement dues au fait que la solubilité des indicateurs de Hammett et du ferrocène sous leur forme moléculaire augmente sensiblement avec la teneur en solvant organique, la solvatation des cations correspondants étant en principe peu modifiée. La réaction de protonation de l'indicateur I est donc moins quantitative. Dans les mélanges riches en éthanol, cet effet est contrebalancé par l'augmentation de l'acidité du couple H_3O^+/H_2O due à l'appauvrissement en eau. On peut représenter graphiquement ces deux interprétations (Fig. 1).

Sur la Fig. 1a, on suppose que la différence de solvatation entre I et IH^+ est la même dans tous les mélanges, par conséquent la différence de p*K* de l'indicateur I, mesurée dans l'eau et dans le mélange M représente la différence de basicité entre ces deux milieux. Sur la Fig. 1b, la basicité des mélanges est voisine de celle de l'eau; la différence de p*K* de l'indicateur I dans l'eau puis dans le mélange S n'est pas caractéristique de la différence de basicité entre ces deux milieux.

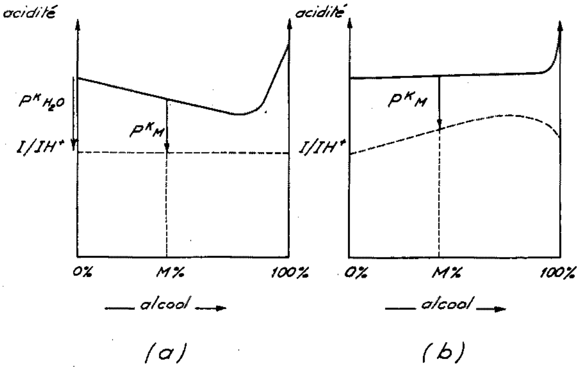

Fig. 1. Variation du pK d'un indicateur I dans les mélanges eau–alcool. (a) La variation est due à l'évolution des propriétés basiques du solvant. (b) La variation est dûe à l'évolution du comportement de l'indicateur I.

Dans le but de trancher entre ces deux interprétations, il nous a paru intéressant de faire appel à une hypothèse extrathermodynamique ne reposant plus sur la solvatation des constituants d'un couple M/M^+ comme dans le cas des indicateurs de Hammett I/I^+ ou de Strehlow Fc^+/Fc pour étudier les niveaux d'acidité dans les mélanges eau–éthanol. Nous avons fait appel à un couple du type M^+X^- pour lequel on suppose une solvatation identique de M^+ et de X^- dans tous les milieux. C'est l'hypothèse de Popovych[4] reprise par Parker et Alexander[3]. Elle ne fait pas intervenir la solvatation d'espèces non chargées. Si la fonction d'acidité déduite de cette hypothèse présente le même type de variation que H_0 et $R_0(H)$ dans les mélanges eau–éthanol (Fig. 1a), il est logique d'admettre qu'elles rendent compte toutes les trois de l'évolution des propriétés basiques des différents mélanges puisqu'il n'est pas possible d'avancer, dans le dernier cas, les mêmes arguments que ceux développés pour H_0 et $R_0(H)$, le système de référence n'étant pas du même type. La fonction $P_0(H)$ s'établit aisément à partir de la mesure du coefficient de solvatation du proton Γ_{H^+}, le tétraphénylborate de tétraphénylarsonium étant le couple M^+X^- choisi ($P_0(H) = -\log \Gamma_{H^+}[H^+]$).

Pour évaluer Γ_{H^+}, il suffit en principe de mesurer la solubilité des composés $As\phi_4B\phi_4$ et $HB\phi_4$ dans le mélange considéré puis dans l'eau. En réalité, la préparation de $HB\phi_4$ est délicate et le composé est peu stable. Aussi est-il nécessaire d'appliquer une méthode de détermination indirecte.

On peut mettre à profit la remarque suivante: le rapport $(\Gamma_{M^+})_1/(\Gamma_{M^+})_2$ des coefficients de solvatation d'une particule M^+, évalués à partir de deux hypothèses extrathermodynamiques différentes, 1 et 2, est le même quelle que soit la nature du cation M^+. De la même manière, le rapport $(\Gamma_{X^-})_1/(\Gamma_{X^-})_2$ est indépendant de la nature de l'anion X^-. On a de plus entre ces deux rapports, la relation $(\Gamma_{M^+})_1/(\Gamma_{M^+})_2 = (\Gamma_{X^-})_2/(\Gamma_{X^-})_1$. Il suffit de connaître la valeur de $(\Gamma_{X^-})_1/(\Gamma_{X^-})_2$ et celle de $(\Gamma_{M^+})_2$ pour en déduire celle de $(\Gamma_{M^+})_1$.

L'anion iodure[11] a été choisi préférentiellement à l'anion tétraphénylborate[12] pour évaluer le rapport des coefficients de solvatation du proton $(\Gamma_{H^+})_S/(\Gamma_{H^+})_P$ à partir des hypothèses de Strehlow[8] et de Popovych[4]. La connaissance de la fonction $R_0(H)$ permet de déduire facilement $(\Gamma_{H^+})_S$. On peut ainsi mesurer $(\Gamma_{H^+})_P$ sans qu'il soit nécessaire de mesurer la solubilité de $HB\phi_4$.

PARTIE EXPÉRIMENTALE

Les déterminations expérimentales ont été réalisées dans les mélanges à 80% et à 99% en éthanol, en présence de perchlorate de lithium à la concentration 0.2 *M*. L'ensemble des résultats expérimentaux sont rassemblés dans le Tableau I.

Les mesures spectrophotométriques montrent que le logarithme du taux de protonation des indicateurs varie linéairement avec le pH dans chacun des milieux. Les pentes des droites obtenues sont égales à l'unité.

TABLEAU I

COEFFICIENTS DE SOLVATATION

	H_2O	*H_2O–EtOH* 80%	*H_2O–EtOH* 99%
p*K* Amino-4-azobenzène	2.8[15]	1.7	—
p*K* 4-Nitroaniline	1.1[15]	—	0.7
$E_{0,\mathrm{Fc^+/Fc}} - E_{0,\mathrm{H_2/H^+}} = E_{\mathrm{H^+}}^{\mathrm{Fc^+}}$	−0.400 V[9]	−0.580 V	−0.540 V
$E_{0,\mathrm{Fc^+/Fc}} - E_{0,\mathrm{Ag(s)/AgI(s)}} = E_{\mathrm{AgI}}^{\mathrm{Fc^+}}$	−0.565 V	−0.775 V	−0.820 V
$\mathrm{p}s_{\mathrm{As\phi_4B\phi_4}}$	16.7[16]	7.8	7.8
$\mathrm{p}s_{\mathrm{As\phi_4I}}$	5.1[16]	6.3	7.7

Les systèmes électrochimiques ferrocène/ferricinium, H_2/H^+ et Ag(s)/AgI(s) obéissent à la loi de Nernst dans les deux solvants. La quantité $E_{0,\mathrm{Fc^+/Fc}} - E_{0,\mathrm{Ag(s)/AgI(s)}}$ dans l'eau a été calculée à partir des données de la littérature[13,14].

L'iodure de tétraphénylarsonium a été préparé selon la méthode proposée par Lyon et Mann[11]. Pour déterminer la solubilité de $\mathrm{As\phi_4B\phi_4}$ et $\mathrm{As\phi_4I}$, le solvant est agité en présence d'un grand excès de sel plusieurs heures à 40°, puis une semaine à la température ordinaire. La solution saturée est ensuite titrée par l'argent, le titrage étant suivi par potentiométrie à une électrode d'argent.

A partir des résultats du Tableau I, il est possible de calculer les coefficients de solvatation du proton et des ions tétraphénylborate et iodure relatifs à chacune des hypothèses extrathermodynamiques examinées. Les résultats sont portés dans le Tableau II. Les quantités $\log \Gamma_{\mathrm{H^+}}$ sont données par les relations:

$$\log(\Gamma_{\mathrm{H^+}})_{\mathrm{Hammett}} = \mathrm{p}K_{\mathrm{M}}^{\mathrm{I}} - \mathrm{p}K_{\mathrm{H_2O}}^{\mathrm{I}} = -H_0 \quad (1\ M\ \text{acide fort})$$

$$\log(\Gamma_{\mathrm{H^+}})_{\mathrm{Strehlow}} = \tfrac{1}{0.058}(\Delta E_{\mathrm{H^+}}^{\mathrm{Fc^+}})_{\mathrm{H_2O}} - (\Delta E_{\mathrm{H^+}}^{\mathrm{Fc^+}})_{\mathrm{M}}$$

$$\log(\Gamma_{\mathrm{I^-}})_{\mathrm{Strehlow}} = \tfrac{1}{0.058}(\Delta E_{\mathrm{AgI}}^{\mathrm{Fc^+}})_{\mathrm{H_2O}} - (\Delta E_{\mathrm{AgI}}^{\mathrm{Fc^+}})_{\mathrm{M}}$$

$$\log(\Gamma_{\mathrm{I^-}})_{\mathrm{Popovych}} = [\mathrm{p}s_{\mathrm{M}} - \mathrm{p}s_{\mathrm{H_2O}}]^{\mathrm{As\phi_4I}} + \tfrac{1}{2}[\mathrm{p}s_{\mathrm{H_2O}} - \mathrm{p}s_{\mathrm{M}}]^{\mathrm{As\phi_4B\phi_4}}$$

$$\log(\Gamma_{\mathrm{H^+}})_{\mathrm{Popovych}} = \log(\Gamma_{\mathrm{H^+}})_{\mathrm{Strehlow}} + \log(\Gamma_{\mathrm{I^-}})_{\mathrm{Strehlow}} - \log(\Gamma_{\mathrm{I^-}})_{\mathrm{Popovych}}$$

L'incertitude sur les valeurs des coefficients de solvatation dépend de la nature de l'hypothèse considéré. Ainsi la quantité $\log(\Gamma_{\mathrm{H^+}})_{\mathrm{Popovych}}$ résulte de la détermination de huit valeurs de produits de solubilité, ce qui entraîne une incertitude importante (0.8 unité logarithmique).

Sur la Figure 2 sont portées les valeurs des fonctions d'acidité H_0, $R_0(H)$ et $P_0(H)$ dans les mélanges à 80% et à 99% pour une concentration molaire en acide fort.

TABLEAU II

RÉSULTATS EXPÉRIMENTAUX

		H_2O-$EtOH$ 80%	H_2O-$EtOH$ 99%
log $(\Gamma_{H^+})_{Hammett}$	±0.1	−1.1	−0.3
log $(\Gamma_{H^+})_{Strehlow}$	±0.2	−3.0	−2.4
log $(\Gamma_{B\phi_4^-})_{Popovych}$	±0.2	−4.4	−4.4
log $(\Gamma_{I^-})_{Strehlow}$	±0.2	+3.6	+5.4
log $(\Gamma_{I^-})_{Popovych}$	±0.4	+5.6	+7.0
log $(\Gamma_{H^+})_{Popovych}$	±0.8	−5.0	−4.0

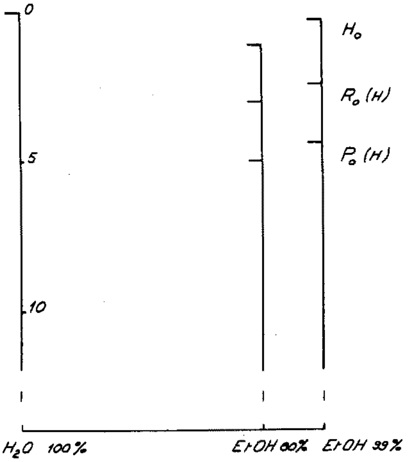

Fig. 2. Fonctions H_0, $R_0(H)$ et $P_0(H)$ dans les mélanges eau–éthanol 80% et eau–éthanol 99%.

DISCUSSION

Les valeurs de log Γ_{H^+} diffèrent sensiblement avec le choix de l'hypothèse extrathermodynamique. De telles constatations ont déjà été soulignées[5,9]. Contrairement au cas des milieux aprotoniques où l'on observe généralement une bonne concordance entre les hypothèses de Strehlow et de Popovych, on note ici un écart de près de 2 unités dans le solvant à 80% en éthanol, celui-ci restant sensiblement de même ordre de grandeur dans le mélange à 99% en éthanol. De tels écarts ont déjà été observés par Parker et Alexander dans le méthanol[3]. A cet égard, il n'est pas inutile de rappeler que les déterminations de la solubilité des sels de tétraphénylarsonium rencontrent dans les milieux protoniques certaines difficultés liées à la cinétique de dissolution ou à l'existence hypothétique de réactions secondaires; d'autre part, les valeurs du produit de solubilité de certains composés tels que le tétraphénylborate d'argent dans l'eau sont en désaccord avec celles obtenues dans les milieux aprotoniques[12]. C'est une des raisons pour laquelle les valeurs des coefficients de solvatation déterminés à partir des mesures de solubilité ne peuvent être connues que de façon approchée.

Ces réserves étant faites, si l'on admet la validité de l'hypothèse de Popovych en première approximation, l'expérience montre que H_0, $R_0(H)$ et $P_0(H)$ varient de la même façon de l'eau pure au mélange à 80% puis à 99% en éthanol : le mélange à 80% apparaît comme plus basique que l'eau et que le mélange à 99% en éthanol.

On peut évidemment se demander si la quantité $\log(\Gamma_{H^+})_{\text{Popovych}}$ mesurée est bien caractéristique de la solvatation du seul proton ou s'il ne caractérise pas en réalité la modification de solvatation des constituants du couple de référence utilisé pour la déterminer. Cela revient à mettre en question la validité de l'hypothèse extrathermodynamique, autrement dit, le choix des couples de référence.

Un calcul simple indique que si l'on admet la basicité du mélange à 80% en éthanol très voisine de celle de l'eau pure, cela reviendrait à supposer que $\log \Gamma_{As\phi_4^+}$ est voisin de 0.6 et $\log \Gamma_{B\phi_4^-}$ voisin de -9.7. Cela signifierait qu'il n'y aurait pas de solvatation identique de $As\phi_4^+$ et de $B\phi_4^-$ comme le laissent supposer des considérations d'ordre structural, et que les anions $B\phi_4^-$ seraient considérablement plus solvatés dans le mélange à 80% que dans l'eau pure, ce qui paraît à priori improbable.

Bien que les hypothèses extrathermodynamiques soient peu concordantes entre elles, les variations de $\log \Gamma_{H^+}$ enregistrées dans les mélanges eau–éthanol sont parallèles. Du fait que les systèmes de référence sont de types différents, il semble logique d'admettre que les fonctions H_0, $R_0(H)$ et $P_0(H)$ rendent compte d'une variation du pouvoir basique du milieu lorsque la fraction de solvant organique augmente. Elles caractérisent donc bien en première approximation une modification des propriétés du solvant.

Enfin, on doit rappeler que les variations de conductivité électrique, des propriétés catalytiques et des chaleurs de transfert de HCl dans les mélanges eau–éthanol sont parallèles à celles des fonctions d'acidité H_0, $R_0(H)$ et $P_0(H)$, ce qui est un argument supplémentaire en faveur d'une modification des propriétés solvatantes du milieu vis-à-vis des ions[16].

Nous tenons à remercier Madame Badoz-Lambling, Directeur de Recherches au C.N.R.S. pour l'intérêt qu'elle a bien voulu porter à cette étude.

RÉSUMÉ

La basicité des mélanges eau–éthanol à 80% puis 99% d'éthanol a été déterminée à partir de l'hypothèse extrathermodynamique basée sur la solvatation du tétraphénylborate de tétraphénylarsonium. Les variations de basicité entre l'eau et ces différents mélanges sont parallèles à celles déduites des fonctions d'acidité H_0 et $R_0(H)$.

SUMMARY

The basicity of water–ethanol mixtures containing 80% or 99% ethanol has been determined by means of extrathermodynamic hypotheses based on solvation of tetraphenylarsonium tetraphenylborate. The differences in the basicities of water and these mixtures are paralleled by those deduced from the acidity functions H_0 and $R_0(H)$.

ZUSAMMENFASSUNG

Die Basizität von Wasser–Äthanol-Gemischen mit 80% und 99% Äthanol wurde auf Grund ausserthermodynamischer Hypothesen ermittelt, die auf der

Solvatation von Tetraphenylarsoniumtetraphenylborat beruhen. Die Unterschiede in den Basizitäten von Wasser und diesen Gemischen werden mit jenen verglichen, die aus den Aciditätsfunktionen H_0 und $R_0(H)$ abgeleitet werden.

BIBLIOGRAPHIE

1 W. A. PLESSKOW, *Usp. Khim.*, 7 (1947) 254.
2 H. M. KOEPP, H. WENDT ET H. STREHLOW, *Z. Elektrochem.*, 64 (1960) 483.
3 A. J. PARKER ET R. ALEXANDER, *Chem. Rev.*, 69 (1969) 1.
4 O. POPOVYCH, *Anal. Chem.*, 38 (1966) 558.
5 R. GABORIAUD, *Thèse*, Paris, 1967, A.O. 1408.
6 R. GABORIAUD, *J. Chim. Phys.*, 67 (1970) 349.
7 P. A. PAUL ET I. A. LONG, *Chem. Rev.*, 57 (1957) 1.
8 H. STREHLOW, in J. J. LAGOWSKI, *The Chemistry of Non-aqueous Solvents*, Vol. 1, Academic Press, New York, 1966.
9 J. VEDEL, *Ann. Chim. (Paris)*, (1967) 335.
10 E. A. BRAUDE ET S. STERN, *J. Chem. Soc.*, (1948) 1976.
11 D. R. LYON ET F. G. MANN, *J. Chem. Soc.*, (1942) 666.
12 A. J. PARKER, *J. Amer. Chem. Soc.*, 89 (1967) 5549.
13 W. M. LATIMER, *Oxydation Potentials*, Prentice Hall, New York, 1951.
14 G. CHARLOT, *L'Analyse Qualitative et les Réactions en Solution*, Masson, Paris, 1963.
15 G. CHARLOT ET B. TRÉMILLON, *Les Réactions Chimiques dans les Solvants et les Sels Fondus*, Gauthier-Villars, Paris, 1963, p. 85.
16 A. J. PARKER ET R. ALEXANDER, *J. Amer. Chem. Soc.*, 90 (1968) 3313.

Anal. Chim. Acta, 54 (1971) 337–342

Analytica Chimica Acta
Elsevier Publishing Company, Amsterdam
Printed in The Netherlands

NEUTRALISATION DE LA TRI-ISO-OCTYLAMINE EN SOLUTION CHLOROFORMIQUE PAR L'ACIDE MALONIQUE

CHARLES KABWE
Laboratoire de Chimie Analytique, Faculté des Sciences, Université Lovanium, Kinshasa (Congo)

(Reçu le 2 octobre 1970)

Depuis que Smith et Page[1] ont découvert les qualités extractives des amines aliphatiques à longue chaîne, de nombreux travaux ont été publiés sur l'extraction des acides minéraux[2-20]. Cependant, en ce qui concerne l'extraction des acides organiques, les informations sont très peu nombreuses et incomplètes[21-29]. Il est généralement admis que l'extraction des acides par les amines s'explique par une réaction acide–base entre les amines et les acides[29-33].

La réaction de neutralisation d'une amine par un monoacide fort conduit à l'obtention d'un sel d'amine neutre[5-10,12,19]. Dans le cas de la neutralisation des amines tertiaires aliphatiques à longue chaîne, comme la tri-iso-octylamine, par un diacide fort comme l'acide sulfurique, il y a formation de sel neutre d'abord, puis celle de sel acide[2,4,8,13,16,20,30]. Il s'en suit que les deux protons de l'acide participent à la réaction de neutralisation selon le mécanisme suivant:

$$2\,R_3N_{org} + 2\,H^+_{aq} + X^{2-}_{aq} \rightleftharpoons (R_3NH)_2X_{org} \tag{1}$$

$$(R_3NH)_2X_{org} + 2\,H^+_{aq} + X^{2-}_{aq} \rightleftharpoons 2\,R_3NHX_{org} \tag{2}$$

R_3N désigne une amine tertiaire, ici la tri-iso-octylamine (TIOA), X^{2-} l'anion d'un acide dibasique, les indices "org" et "aq" signifient respectivement phase organique et phase aqueuse.

L'extraction des monoacides carboxyliques par les amines est pareille à celle des monoacides minéraux[21,25,27,28].

Pour les diacides organiques le problème est controversé. On sait en effet que le deuxième proton de ces acides est faiblement ionisable. Aussi certains auteurs[26] soutiennent-ils qu'avec les acides dicarboxyliques tel que l'acide oxalique, seul le sel acide peut se former. D'autres[24], au contraire, estiment qu'il y a formation de sel neutre d'abord, puis de sel acide comme dans le cas des diacides forts.

Dans le but d'étudier ultérieurement l'équilibre d'extraction de l'acide malonique par la TIOA, il nous a semblé nécessaire d'examiner ce problème dans le cadre précis de la neutralisation de la TIOA par cet acide organique. Nous avons à cette fin employé la méthode spectrophotométrique.

PARTIE EXPÉRIMENTALE

Réactifs

Tri-iso-octylamine (Serlabo, France), insoluble dans l'eau, soluble dans le chloroforme. La nature isomérique de sa molécule rend malaisée la définition de la structure exacte de cette amine[34]. Elle est purifiée par distillation sous vide, à pression réduite (10 mm de Hg) et à la température de 215°. Son poids moléculaire est de 353.7. La teneur en tri-iso-octylamine du produit commercial est de 98%, résultat obtenu par dosage. Les nombreux travaux[18,28,34-38] sur l'extraction avec la tri-iso-octylamine prouvent les qualités extractives excellentes de cette amine.

Chloroforme et alcool éthylique (Merck p.a.), distillés à 61 et 78°, respectivement. C'est le chloroforme qui a été choisi comme diluant en raison de sa grande transparence dans presque toutes les régions où absorbent l'amine et l'acide malonique. Dans l'infrarouge en effet, le spectre du chloroforme ne présente que deux pics d'absorption situés à 1225 et 755 cm^{-1}.

Acide malonique (Merck) purifié[39], environ 100% en poids.

Dosage

On prépare une solution de l'amine à 5% en volume, dans le chloroforme. A une aliquote de 5 à 10 ml on ajoute 50 ml d'alcool et 10 ml d'eau[4]. Le titrage s'effectue par l'acide perchlorique, en utilisant un pH-mètre (Radiomètre, Copenhague). Toutes les solutions d'amine sont préparées au moment de l'emploi. Les solutions aqueuses d'acide malonique à différentes concentrations sont préparées par pesée. Leurs titres sont contrôlés par dosage alcalimétrique.

Extraction

Nous avons utilisé des volumes égaux (20 ml) de solution aqueuse d'acide malonique à différentes concentrations et de solution chloroformique de tri-iso-octylamine, dans un erlenmeyer à bouchon rodé. Des essais préliminaires ayant démontré que l'équilibre était atteint rapidement, nous proposons une agitation magnétique de 20 min, à la température de 25°. Il n'y a pas de troisième phase, ni de variation de volume des deux phases qui sont décantées et filtrées sur verre fritté. La

TABLEAU I

ANALYSE DES PHASES ORGANIQUES SOUMISES À L'EXAMEN SPECTROPHOTOMÉTRIQUE

TIOA (M) initiale	*$CH_2(COOH)_2$ (M)*			
	Initiale	*Soluble dans $CHCl_3$, à l'équilibre*	*Org. éq. corr.*[a]	*Org. éq. corr. / TIO A (M) initiale*
0.110	0.010	—	0.009	0.08
0.110	0.058	0.001	0.055	0.50
0.110	0.100	0.005	0.092	0.83
0.110	0.400	0.013	0.110	1.00
0.200	0.730	0.013	0.200	1.00

[a] A l'équilibre, corrigé.

phase organique est limpide; des parties aliquotes sont prélevées pour les différentes mesures. La teneur en acide malonique de la phase aqueuse, à l'équilibre, est déterminée par titrage au pH-mètre, au moyen d'hydroxyde de sodium, dans un mélange ternaire chloroforme–alcool éthylique–eau, en tenant compte de la solubilité de l'acide dans le chloroforme pur (Tableau I). Nos résultats expérimentaux varient de ±1%; les valeurs données dans le Tableau correspondent à la moyenne de deux essais au moins.

Spectroscopie infrarouge

Pour enregistrer le spectre de l'acide malonique solide, des pastilles sont préparées par dilution de l'acide dans une matrice de bromure de potassium (2 mg d'acide dans 200 mg de KBr). Le spectre de l'amine pure est obtenu avec des films liquides, entre deux disques de chlorure de sodium. Les spectres de la tri-iso-octylamine diluée et des sels d'amine sont enregistrés dans des cellules à fenêtre en chlorure de sodium de 25 µm d'épaisseur. Pour ces derniers spectres, la technique du double faisceau a été utilisée.

Ces essais ont été effectués avec des solutions fraîchement préparées, à la température de 25°, et avec un spectrophotomètre Perkin-Elmer 221, dans la gamme spectrale s'étendant de 4000 à 200 cm^{-1}.

Les résultats sont donnés dans les Tableaux II et III.

DISCUSSION

Une interprétation qualitative satisfaisante des bandes spectrales nous

TABLEAU II

ATTRIBUTION DES BANDES D'ABSORPTION ET FRÉQUENCES

Fréquence observée (cm^{-1})	*Assignation*
1. *Amine pure*	
1090	Vibration de la liaison C–N
1363	Vibration symétrique de déformation du groupement CH_3
1373	Vibration symétrique de déformation du groupement CH_3
1460	Soit vibration de déformation du groupement CH_2, soit vibration de déformation asymétrique du groupement CH_3, ou les deux
2795	Vibration du groupement C–H couplé avec l'azote de la TIOA
2863	Vibration de valence symétrique du groupement CH_3
2920	Vibration de valence en phase du groupement CH_2
2950	Vibration de valence asymétrique du groupement CH_3
2. *Amine dissoute dans le chloroforme*	
Toutes les bandes de la TIOA pure se retrouvent à la même fréquence dans la solution de l'amine 0.110 *M* dans le chloroforme, celle à 2795 cm^{-1} cependant, n'est plus qu'un faible épaulement situé à 2800 cm^{-1}.	
3. *Acide malonique solide*	
917	Vibration de déformation OH du carboxyle
1173, 1215, 1310, 1395, 1435	Vibration de valence du groupement C–O couplé avec la vibration de déformation OH du carboxyle
1740	Vibration de valence du groupement carbonyle C=O

TABLEAU III

BANDES D'ABSORPTION EN INFRAROUGE ET FRÉQUENCES (cm^{-1}) DES SOLUTIONS DE TIOA DANS $CHCl_3$, CONTENANT DIFFÉRENTES CONCENTRATIONS D'ACIDE MALONIQUE

$C = 0.110$[a] $R = 0.08$	$C = 0.110$ $R = 0.50$	$C = 0.110$ $R = 0.83$	$C = 0.110$ $R = 1.00$	$C = 0.200$ $R = 1.00$
1090	—	—	—	—
1375	1375	1375	1375	1375
—	—	1400	1400	1400
1465	1465	1465	1465	1465
1600	1600	1600	1600	1600
1625	1625	1625	1625	1625
1725	1725	1725	1725	1725

[a] C = concentration molaire initiale de la tri-iso-octylamine dans le chloroforme.
R = rapport $CH_2(COOH)_2\,(M)_{org.\,eq.\,corr.}/C$.

renseignera sur les divers composés chimiques contenus dans la phase organique après extraction, l'attribution des autres bandes étant clairement indiquée dans le Tableau II.

La bande située à 1090 cm^{-1}, attribuée à la liaison C–N[15,26] indique la présence de l'amine libre pure, ou dans le chloroforme. Sa disparition (Tableau III) est une preuve que la tri-iso-octylamine n'est plus libre et qu'elle s'est combinée à l'acide malonique (rapport acide : amine 1 : 2; ou R = 0.5) selon la réaction

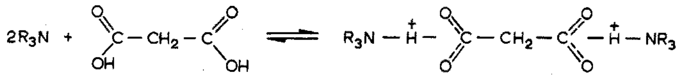

Bulloc *et al.*[24], dans leur étude sur l'extraction de l'acide oxalique par la méthyldioctylamine en solution chloroformique, prouvent aussi par spectroscopie infrarouge que l'oxalate d'amine pur se forme dans un rapport stoéchiométrique acide oxalique et méthyldioctylamine de 0.5.

Par contre, Lipovskii et Kuzina[26] qui ont étudié la structure des composés formés dans l'extraction de l'acide oxalique par la trioctylamine dissoute dans le benzène et le tétrachlorure de carbone démontrent, à l'aide des spectres infrarouges, qu'il n'y a jamais formation d'oxalate de trioctylamine neutre. Ils se basent sur le fait que la bande spectrale située à 1090 cm^{-1} ne disparait pas quand le rapport molaire de 0.5 entre l'acide oxalique et la trioctylamine est atteint dans la phase organique.

Comme on le voit, en ce qui concerne les formules des composés formés après extraction de l'acide oxalique par les amines aliphatiques à longue chaîne les avis sont divergents. Cette diversité d'opinion peut être due à la différence de propriétés des solvants organiques utilisés et du pouvoir accepteur de proton des amines employées. Il est intéressant de noter que la méthyldioctylamine a un pK_B de 3.9, la tri-iso-octylamine 4.2 et la trioctylamine 4.3[40].

L'apparition d'une bande d'absorption à 1400 cm^{-1} (Tableau III), indice de la vibration de valence du groupement C–O couplée avec la vibration de déformation

-OH du carboxyle[24,26,41] permet de constater qu'il y a production du groupement carboxylique en phase organique. Comme cette bande apparait dans les solutions dès que le rapport devient plus grand que 0.5, le bimalonate de la tri-iso-octylamine se forme après le malonate neutre et à partir de celui-ci selon l'équilibre suivant:

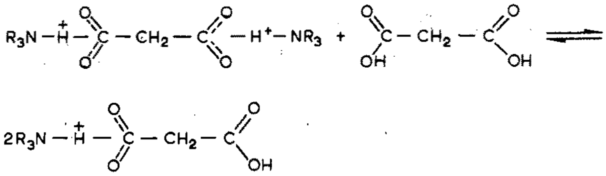

Quand, dans la phase organique, le rapport est de 1 : 1 (Tableau III), il n'y a plus en solution que le bimalonate de la tri-iso-octylamine seul. La littérature concernant l'extraction des acides dicarboxyliques par les amines aliphatiques à longue chaîne est concordante à ce point de vue[24,26].

Le mécanisme de l'extraction de l'acide malonique par les amines aliphatiques à longue chaîne est donc pareil à celui de l'acide sulfurique[4].

Les bandes de 1625 et 1600 cm^{-1} sont attribuées à des vibrations de valence asymétrique du carboxylate[41]. L'interaction du groupement -OH avec le second atome d'oxygène du groupement carboxylate provoquerait une nouvelle bande d'absorption située aux environs de 1772 cm^{-1} [24,26]. Cette dernière bande, caractéristique du groupement carboxylique, n'est pas présente sur nos spectres.

Située à 1740 cm^{-1} dans le spectre de l'acide malonique solide (Tableau II), la bande de vibration de valence du groupement carbonyle de l'acide malonique subit, dans le solvant, un léger déplacement vers une fréquence légèrement plus faible et se situe à 1725 cm^{-1} (Tableau III).

Hibbert et Satchell[27] ont utilisé l'intensité relative de cette bande pour calculer la constante d'équilibre de la réaction d'extraction de quelques acides monocarboxyliques, dont l'acide acétique par la *n*-butylamine dans l'éther diéthylique. D'après ces auteurs, la position du pic à cette longueur d'onde indique que les espèces étudiées sont sous forme monomérique en phase organique, la vibration du dimère se serait située à des longeurs d'onde plus grandes.

La bande de l'amine pure, située à 2795 cm^{-1} (Tableau II) est attribuée à un mode de vibration C–H de la tri-iso-octylamine. Le doublet libre de l'azote de l'amine est couplé avec l'oscillateur correspondant aux vibrations C–H de la chaîne carbonée de l'amine. En présence de chloroforme, l'hydrogène actif de ce dernier entre en liaison avec l'azote de l'amine. Il y a alors affaiblissement du couplage entre le doublet et les vibrations C–H, la bande de 2795 cm^{-1} devient un faible épaulement et subit une légère élévation vers 2800 cm^{-1}. En présence d'une très faible quantité d'acide malonique dans le solvant, le couplage N–C–H est encore davantage perturbé et sa bande d'absorption disparaît complètement.

CONCLUSIONS

L'étude spectrophotométrique de la tri-iso-octylamine pure et de sa solution dans le chloroforme permet de constater que l'hydrogène actif de ce diluant réagit avec l'amine par le doublet libre de l'azote de cette dernière. Son caractère quelque peu acide et sa forte concentration (95%) en solution organique expliquent ce comportement du chloroforme.

La réaction de l'acide malonique avec la tri-iso-octylamine conduit d'abord à l'obtention du malonate neutre de l'amine. Le bimalonate se forme ensuite lorsqu'on augmente la concentration en acide malonique.

Les sels formés dans la phase organique jusqu'à la concentration 0.2 *M* en amine semblent essentiellement monomériques dans le chloroforme.

Nous tenons à exprimer nos très vifs remerciements au Professeur Aliette S. Vieux pour ses conseils critiques qui nous ont été précieux pour cette étude. Nous remercions aussi le Professeur Jean Charette qui a bien voulu mettre son spectrophotomètre à notre disposition.

RÉSUMÉ

L'extraction de l'acide malonique par la tri-iso-octylamine est examinée à 25°. Les spectres infrarouges de la phase organique montrent qu'il y a d'abord formation de malonate d'amine; le bimalonate se forme ensuite, à partir de ce dernier.

SUMMARY

The extraction of malonic acid by tri-iso-octylamine has been studied at 25°. Infrared spectroscopy of the organic phase shows that the neutral amine malonate is formed first; the hydrogenomalonate salt is formed afterwards from the neutral salt on further additon of malonic acid. The compounds formed in the organic phase up to concentrations of 0.2 *M* appear to be monomeric.

ZUSAMMENFASSUNG

Die Extraktion von Malonsäure mit Tri-iso-octylamin wurde bei 25° untersucht. Die Infrarotspektren der organischen Phase zeigen, dass zunächst das neutrale Aminmalonat gebildet wird; nach weiterer Zugabe von Malonsäure bildet sich aus dem neutralen Salz Hydrogenmalonat. Die in der organischen Phase gebildeten Verbindungen scheinen bei Konzentrationen bis 0.2 *M* monomer zu sein.

BIBLIOGRAPHIE

1 L. S. Smith et J. E. Page, *J. Soc. Chem. Ind.*, 67 (1948) 49.
2 K. A. Allen, *J. Phys. Chem.*, 60 (1956) 239.
3 K. A. Allen, *J. Phys. Chem.*, 62 (1958) 1119.
4 C. Boirie, *Bull. Soc. Chim. France*, (1958) 980.
5 L. Newman et P. Klotz, *J. Phys. Chem.*, 65 (1961) 796.
6 A. A. Mazurova et L. Gindin, *Russ. J. Inorg. Chem. English Transl.*, 10 (1965) 1389.
7 J. M. P. J. Verstegen, *Trans. Faraday. Soc.*, 58 (1962) 1878.
8 J. M. P. J. Verstegen et J. A. A. Ketelaar, *J. Phys. Chem.*, 66 (1962) 216.
9 G. Duyckaerts, J. Fuger et W. Muller, *Eur. 426 f*, 1963.
10 G. Scibona, F. Orlandini et P. R. Danesi, *J. Inorg. & Nucl. Chem.*, 28 (1966) 1701.
11 W. Muller et R. M. Diamond, *J. Phys. Chem.*, 70 (1966) 3469.

12 M. A. LODHI, *Arkiv Kemi*, 27 (1967) 309.
13 R. FOPPEMA, *Rec. Trav. Chim.*, 87 (1968) 443.
14 I. A. FEDOROV, J. F. ZHDANOV ET U. M. SUTYAGIN, *Russ. J. Inorg. Chem. English Transl.*, 13 (1968) 897.
15 H. BRUSSET, C. DUBOC ET F. HAFFNER , *Bull. Soc. Chim. France*, (1968) 354.
16 A. S. VIEUX, *Bull. Soc. Chim. France*, (1968) 4281.
17 H. BRUSSET ET F. HAFFNER, *Bull. Soc. Chim. France*, (1969) 1829.
18 R. KOLLAR, V. PLICHON ET J. SAULNIER, *Bull. Soc. Chim. France*, (1969) 2193.
19 T. KOJIMA, H. FUKUTOMI ET H. KAHIHAMA, *Bull. Soc. Chim. Japan*, 42 (1969) 875.
20 T. K. KIM ET V. CHIOLA, *Separation Science*, 3 (1968) 455.
21 G. M. BARROW ET E. A. YERGER, *J. Amer. Chem. Soc.*, 76 (1954) 5211.
22 E. A. YERGER ET G. M. BARROW, *J. Amer. Chem. Soc.*, 77 (1955) 6206.
23 L. MOORE, *Anal. Chem.*, 29 (1957) 1660.
24 J. I. BULLOC, S. S. CHOI, D. A. GOODRICK, D. G. TURJ ET E. J. WOODHOUSE, *J. Phys. Chem.*, 68 (1964) 2687.
25 L. KUCA ET E. HOGFELDT, *Acta Chem. Scand.*, 21 (1967) 1017.
26 A. A. LIPOVSKII ET M. G. KUZINA, *Radiokhimiya*, 10 (1968) 175.
27 H. F. HIBBERT ET D. M. P. SATCHELL, *J. Chem. Soc. (B)*, (1968) 573.
28 A. S. VIEUX, *Bull. Soc. Chim. France*, (1969) 3364.
29 M. A. LODOHI ET E. HOGFELDT, *Solvent Extraction Chemistry*, North-Holland, Amsterdam, 1967, p. 421.
30 W. E. KEDER ET A. S. WILSON, *Nucl. Sci. Eng.*, 17 (1963) 287.
31 V. S. SCHMIDT ET MEZHOV, *Russ. Chem. Rev.*, 34 (1965) 585.
32 W. MULLER, G. DUYCKAERTS ET J. FUGER, *Solvent Extraction Chemistry of Metals*, Mac Millan, London, 1965, p. 233.
33 R. M. DIAMOND, *Solvent Extraction Chemistry*, Amsterdam, 1967, p. 350.
34 F. L. MOORE, *Anal. Chem.*, 30 (1958) 908.
35 W. L. OTT, H. R. MACMILLAN ET W. R. HATCH, *Anal. Chem.*, 36 (1964) 363.
36 B. E. MCCLELLAN ET V. M. BENSON, *Anal. Chem.*, 36 (1964) 1965.
37 A. R. SELMER-OLSEN, *Anal. Chim. Acta*, 31 (1964) 33.
38 F. L. MOORE, *Anal. Chem.*, 32 (1960) 1075.
39 G. A. HALL, *J. Amer. Chem. Soc.*, 71 (1949) 2691.
40 A. RIEUX, M. RUMEAU ET B. TRÉMILLON, *Bull. Soc. Chim. France*, (1964) 1053.
41 L. J. BELLAMY, *The Infrared Spectra of Complex Molecules*, 2e Edn., Methuen, London, 1956, p. 140.

Analytica Chimica Acta
Elsevier Publishing Company, Amsterdam
Printed in The Netherlands

SHORT COMMUNICATIONS

Mixed secondary complexes of siiver(I) and phenylmercury(II) cations with dithizone

In a previous paper evidence was produced for the formation of a mixed (secondary) complex $Hg(AgDz)_2$ when solutions of primary mercury dithizonate $Hg(HDz)_2$ in chloroform were shaken with a very large excess of aqueous silver nitrate[1]. Since it has already been shown that the remaining imino-hydrogen in PhHg(HDz), the primary dithizonate derived from the phenylmercury(II) cation, can be ionised at a sufficiently high pH ($pK=11.46\pm0.01$) in 52.75% (v/v) ethanol–water mixtures[2], it seemed likely that a mixed complex such as PhHg(AgDz) should be capable of formation too. However, experiments were not conclusive when chloroform was used as the solvent since precipitation of violet materials (possibly secondary dithizonates) removed part of the solutes from the organic phase. It was then decided to study the system with a medium in which all reaction products might remain in homogeneous solution.

A monophase containing chloroform, ethanol and water in the proportions 1:8:1 by volume was adopted. Figure 1, curve 1, shows the spectrum of $2.0\cdot10^{-5}$ *M* phenylmercury(II) dithizonate alone (λ_{max} 478 nm, ε_{max} 31,500); the values previously reported for pure chloroform were λ_{max} 476 nm and ε_{max} 32,300[2]. On the addition of a few drops of 0.1 *M* sodium hydroxide, the corresponding anion was obtained (curve 2; λ_{max} 528 nm, ε_{max} 40,000). The addition of an approximately 10-fold excess of phenylmercury(II) chloride to phenylmercury(II) dithizonate produced no significant change (curve 3). However, the addition of excess silver nitrate produced a lowered absorbance and a hypsochromic shift. This increased as the relative concentration of silver nitrate was increased up to a 4-fold ratio; there was little further change if the ratio was increased progressively to 10-fold. Figure 1, curve 4, shows the spectrum for a 5-fold excess of silver (λ_{max} 500 nm, ε_{max} 20,000). If, however, alkali is present in addition to the 5-fold excess of silver nitrate and phenylmercury(II) dithizonate there is a small increase in absorbance and a bathochromic shift as shown in curve 5 (λ_{max} 516 nm, ε_{max} 25,000).

Without speculating at this stage on the nature of the species responsible for curve 5, it can be seen that it is not identical with that of primary or secondary phenylmercury dithizonate, nor does it in any way resemble that of primary or secondary silver dithizonate (q.v.).

In Fig. 2 are shown spectra obtained starting from a $2.06\cdot10^{-5}$ *M* solution of primary silver dithizonate (curve 1; λ_{max} 462 nm, ε_{max} 17,000) by adding a few drops of alkali (curve 2; λ_{max} 500 nm, ε_{max} 17,500). However, on adding a five-fold excess of phenylmercury(II) chloride there is a marked increase in absorbance but only a small shift in λ_{max} to 475 nm. While the spectrum is similar in some respects to that of phenylmercury(II) dithizonate (Fig. 1, curve 1; λ_{max} 478 nm, ε_{max} 31,500) there cannot have been a simple and incomplete exchange of cations for the following reason. Had phenylmercury dithizonate and silver chloride been formed by methathesis, the reaction between the former and the excess of phenylmercury chloride would, in presence of alkali, have produced violet secondary phenylmercury(II) dithizonate (*cf.* Fig. 1,

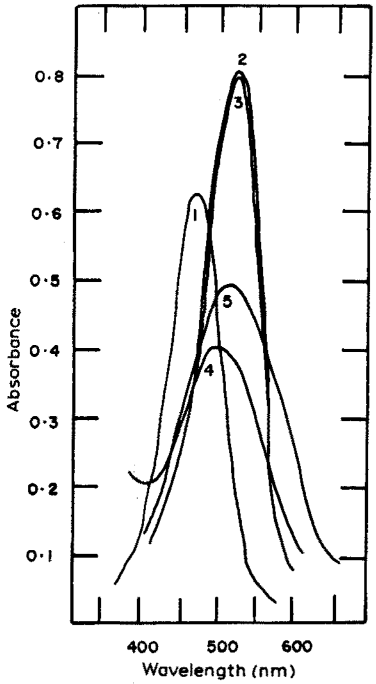

Fig. 1. Reaction between PhHg(HDz) ($2.0 \cdot 10^{-5}$ M) and silver nitrate in a monophase composed of chloroform, ethanol and water in a volume ratio of 1:8:1, respectively. (1) PhHg(HDz) alone (λ_{max} 478 nm, ε_{max} 31,500); (2) PhHg(HDz) + a few drops of 0.1 M NaOH (λ_{max} 528 nm, ε_{max} 40,000); (3) PhHg(HDz) + 5-fold excess PhHgCl + alkali (λ_{max} 528, ε_{max} 40,000); (4) PhHg(HDz) + 5-fold excess of $AgNO_3$ (λ_{max} 500 nm, ε_{max} 20,000); (5) PhHg(HDz) + 5-fold excess $AgNO_3$ + alkali (λ_{max} 516 nm, ε_{max} 25,000).

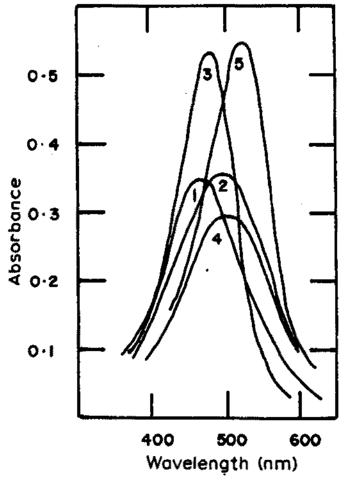

Fig. 2. Reaction between Ag(HDz) ($2.06 \cdot 10^{-5}$ M) and PhHgCl in a monophase composed of chloroform, ethanol and water in a volume ratio of 1:8:1, respectively. (1) Ag(HDz) alone (λ_{max} 462 nm, ε_{max} 17,000); (2) Ag(HDz) + a few drops of 0.1 M NaOH (λ_{max} 500 nm, ε_{max} 17,500); (3) Ag(HDz) + 5-fold excess of PhHgCl (λ_{max} 475 nm, ε_{max} 26,200); (4) Ag(HDz) + 5-fold excess of PhHgCl + alkali (λ_{max} 500 nm, ε_{max} 15,000); (5) Ag(HDz) + excess $AgNO_3$ + alkali (λ_{max} 520 nm, ε_{max} 26,700).

curve 3; λ_{max} 528 nm, ε_{max} 40,000). As shown in Fig. 2, curve 4, this combination gave a species absorbing at 500 nm and with a much lower extinction coefficient (ε_{max} 15,000) It could readily be distinguished from secondary silver dithizonate (curve 5; λ_{max} 520 nm, ε_{max} 26,700).

It is difficult not to conclude that mixed secondary complexes are being formed, different of course in the two cases. These may be formulated as PhHg(AgDz) and Ag(PhHgDz), but precise stoicheiometry must await more detailed studies.

Department of Inorganic and
Structural Chemistry,
The University,
Leeds 2 (England)

A. M. Kiwan
H. M. N. H. Irving

1 H. M. N. H. Irving and T. Nowicka-Jankowska, *Anal. Chim. Acta*, in press.
2 H. M. N. H. Irving and A. M. Kiwan, *Anal. Chim. Acta*, 45 (1969) 271.

(Received 28th November 1970)

Analytica Chimica Acta
Elsevier Publishing Company, Amsterdam
Printed in The Netherlands

A Dewar tube sample cell assembly for low-temperature fluorimetry

During an extensive study of the application of fluorescence measurements at liquid nitrogen temperatures to inorganic trace analysis, difficulties were encountered with the use of commercially available low-temperature phosphorimetry attachments. In the most widely used arrangement, the silica sample tube is immersed in liquid nitrogen in a Dewar flask which has a fused silica transparent base. The sample is illuminated and viewed through the liquid nitrogen in the base of the flask. A collar with two spring clips, about 10 and 15 cm away from the viewing section, is attached to the upper end of the sample tube. The collar and clips position the sample tube in the flask. Quantitative observations of low-temperature fluorescence or phosphorescence are complicated by the reproducibility with which the tube may be positioned in the Dewar flask, by noise on the analytical signal caused by gaseous nitrogen bubbles in the light path, and by condensation of water vapour in the liquid nitrogen and on the outside of the Dewar. Hollifield and Winefordner[1] have developed a rotating sample cell assembly to minimise this error and to average out optical inhomogeneities in the sample tubes.

This communication describes the construction and performance of a sample compartment and cell assembly based on a Dewar tube; the assembly is designed to reduce problems from noise, liquid nitrogen contamination and irreproducible sample cell positioning. It also permits the measurement of a standard before measurement of the fluorescence of the sample; this reduces errors otherwise incurred when the instrumental sensitivity varies.

Experimental

Construction. Figure 1 shows the assembly. A fused silica Dewar tube (200 mm long, 22 mm o.d., 10 mm i.d., 2 mm wall thickness) (A) was supported in the low-temperature phosphorescence attachment of an Aminco spectrophotofluorimeter (American Instrument Co. Inc., Silver Spring, Md.) (B) after removal of the phosphoroscope can and motor. The base of the tube was fitted via a rubber sleeve into the Dewar flask (C) (284 ml capacity). A single turn of Nichrome wire (D) (15.6 ohm m^{-1}) was employed as a heating element on the outside of the tube in the position shown; this prevented condensation of water vapour on the walls of the viewing area. A second Nichrome heating element (15.6 ohm m^{-1}, 450 mm in length) (E) was introduced into the Dewar flask via the rubber sleeve; this was used to boil off nitrogen from the flask. Both heating filaments were operated at 24 V a.c. from a mains transformer. The demister filament was used in series with an 80 ohm rheostat adjusted to provide a current of 1 A.

The sample cell (F) was constructed from fused silica tubing (380 mm in length, 5 mm o.d., 2.5 mm i.d.) and contained three sections: (*a*) an open-ended 15-mm length at the base which allowed the passage of cold nitrogen gas; (*b*) a middle compartment 25 mm in length which contained the sample solution (*ca.* 0.1 ml) and was located between 15 and 40 mm from the end of the tube; and (*c*) a compartment above the sample cell which may be used for a fluorescence standard. The lower and middle sections of the tube had holes of 2 mm diameter blown in the wall of the tube. In the lower section this permitted the passage of gas, and in the middle section was used for introduction and removal of the sample solution. The standard solution in the upper section was introduced at the top of the tube. The sample tube was supported in a Terry clip on an aluminium plate (G) cut to fit into the cylindrical metal housing used as a light shield with the Aminco phosphoroscope attachment. Rings cut from P.V.C. tubing (H) were used as positioning markers at the top of the sample tube. The rubber support (I) fitted round the lower section of the sample tube assisted its reproducible positioning in the Dewar tube. This support, shown in cross-section and plan in Fig. 1, permitted nitrogen gas to pass and was cut from a rubber bung after the bung had been cooled in liquid nitrogen. It was cut so that it could be inserted into the Dewar tube while flexible at room temperature; after immersion in liquid nitrogen the hardened rubber was an exact fit in the tube and prevented vibration of the sample tube.

A heavy gauge black cardboard tube was constructed to fit over the top of the sample tube where it stood above the cell housing; this prevented stray light entering the viewing area by reflection down the length of the sample tube.

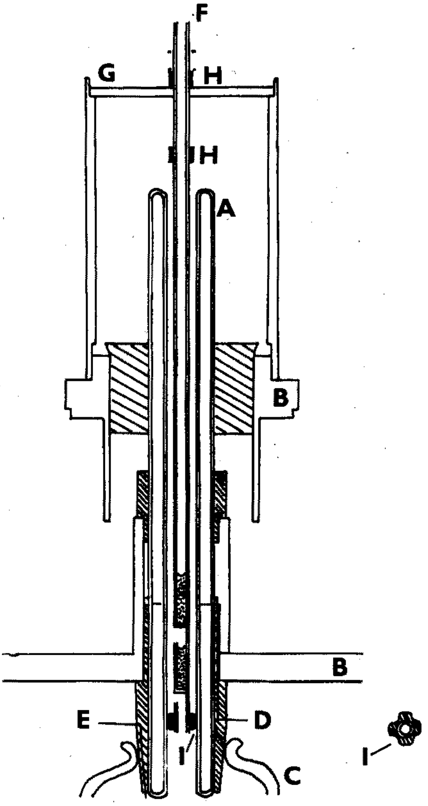

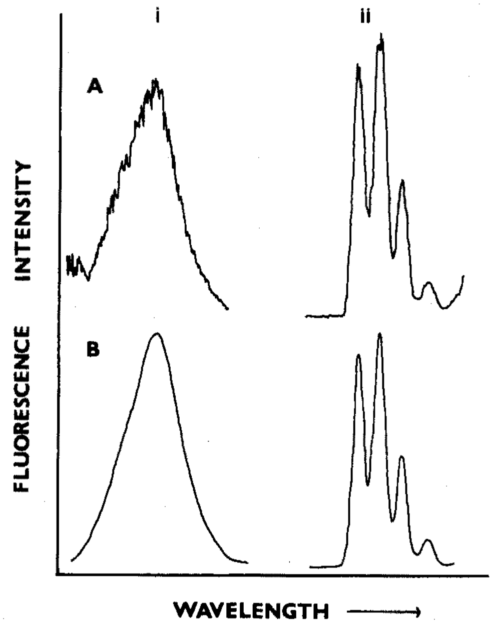

Fig. 1. Dewar tube cell assembly. For lettering, see text.

Fig. 2. Fluorescence excitation (i) and emission (ii) spectra (uncorrected) for $4 \cdot 10^{-4}$ *M* uranium(VI) solution in 6 *M* hydrochloric acid at low temperature. (A) Conventional Dewar flask assembly; (B) Dewar tube assembly.

Operation. Switch on the demister heater with the instrument. Fill the centre section of the tube with sample solution using a small dropping pipette. Place the required standard solution in the upper section of the tube by the same method. Then insert the sample tube as far as possible into the cell assembly so that both sample and standard compartments are immersed in liquid nitrogen in the Dewar flask. When boiling subsides, switch on the liquid nitrogen heater and lift the sample tube into position in the Dewar tube. In this position, with the "standard" positioning marker level with the cell top-plate (G) measure the fluorescence intensity of the standard solution. Then lift the sample tube so that the "sample" positioning marker is level with the cell top-plate and measure the fluorescence intensity of the sample solution. If necessary, obtain a second reading for the standard solution by lowering the tube to the "standard" position again. However, as the standard becomes warmer in the upper part of the Dewar tube, it must be left in position for about 1 min to return to the equilibrium temperature. Then switch off the heating element, and remove the sample tube from the cell for emptying, washing and refilling.

Results

Figure 2 shows the fluorescence excitation and emission spectra for $4 \cdot 10^{-4}$ *M* uranium(VI) solution in 6 *M* hydrochloric acid at −196°, with a conventional Aminco phosphoroscope attachment (with rotating can and motor removed) and with the Dewar tube assembly. The slit arrangement and detector gain settings were identical in each case. The variation of fluorescence intensity *vs.* time with both types

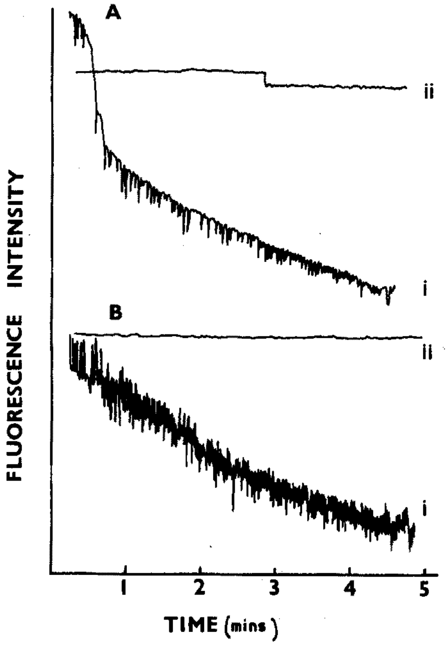

Fig. 3. Variation of fluorescence intensity with time with Dewar flask (i) and Dewar tube (ii) assemblies at similar instrumental sensitivities. (A) $4 \cdot 10^{-4}$ *M* uranium(VI) in 6 *M* hydrochloric acid; (B) 10^{-5} *M* quinine sulphate in 6 *M* sulphuric acid.

of cell assembly is shown in Fig. 3 for measurements of quinine sulphate and uranium(VI). The random signal noise level was decreased by a factor of ten. The signal drift caused by misting of the Dewar flask in the conventional arrangement was also eliminated. The discontinuity which occurred after 3 min for the Dewar tube assembly in Fig. 3A is commonly encountered because of variation in the xenon arc or detector sensitivity. The ability to measure the sample and a standard under identical conditions with the Dewar tube assembly facilitated correction for this type of instrumental instability. The standard deviations shown in Table I were obtained by making ten fluorescence measurements for each sample under the same conditions with the Dewar flask and Dewar tube arrangements. The lower standard deviations (up to 7-fold) with the Dewar tube assembly reflect the greater precision of positioning.

TABLE I

REPRODUCIBILITY DATA OBTAINED

Sample soln.	*Phosphor concn. (M)*	*Wavelength of measurement*		*Standard deviation*[a]	
		Excitation (nm)	*Emission (nm)*	*Conventional assembly (%)*	*Dewar tube (%)*
UO$_2^{2+}$/6 *M* HCl	$4 \cdot 10^{-4}$	270	510	6.5	1.6
					1.4
	$4 \cdot 10^{-5}$	—	—	5.0	1.9
					2.0
Tl^{+}/6 *M* HCl	$4 \cdot 10^{-4}$	230	395	8.2	1.7
	$4 \cdot 10^{-6}$	—	—	14.0[b]	2.4
Pb^{2+}/6 *M* HCl	$1 \cdot 10^{-6}$	250	385	3.0	1.9
					1.9
Pyrene/EPA	$5 \cdot 10^{-5}$	315	385	4.6	1.6
Quinine SO$_4$/6 *M* HCl	$1 \cdot 10^{-4}$	335	410	4.9	0.7
	$1 \cdot 10^{-5}$	—	—	—	0.6[c]

[a] Calculated from ten determinations.
[b] Systematic decrease in fluorescence intensity observed.
[c] Calculated from only eight readings.

Although we have principally been interested in the use of this sample assembly for low-temperature fluorescence studies with inorganic glasses, it may be used satisfactorily with organic solvents. As shown in Table I improved precision was obtained in low-temperature fluorescence measurements for pyrene in EPA. However, in order to prevent loss of organic solvent to the liquid nitrogen in the Dewar flask on immersion, it was necessary to seal the sample compartment after filling. This was done by fitting a thin-walled rubber sleeve round the tube near the centre sample compartment; after this section had been filled, the sleeve was pushed along the tube to seal off the compartment. With an organic solvent in the standard section of the tube a stable reading was only obtained after about 1 min. An inorganic standard did not suffer from this disadvantage.

Discussion

The Dewar tube sample cell assembly permits more reproducible sample cell positioning and gives lower signal noise levels in low-temperature fluorimetry than the more conventional arrangement. Less trouble has also been experienced with condensation of water vapour on the walls of the Dewar; long-term signal noise is thus improved. The assembly enables measurements to be made as rapidly as the conventional method, and it is also possible to measure the fluorescence intensity of a standard calibration solution immediately before that of the sample solution. This is valuable when frequent calibration of the instrument is required because of its lack of stability. It appears that the sample tube temperature is not significantly higher in the cold nitrogen gas stream than in liquid nitrogen. Figures 2 and 3 indicate that there is no appreciable loss in fluorescence intensity with the Dewar tube assembly. When a heater is used to boil the liquid nitrogen, the rate of consumption of nitrogen is approximately double that used with the Dewar flask method.

We are grateful to the Science Research Council for a grant for the purchase of the spectrophotofluorimeter used in this work.

Chemistry Department,
Imperial College,
London, S.W.7 (England)

G. F. Kirkbright
P. J. Mayne
T. S. West

1 H. C. Hollifield and J. D. Winefordner, *Anal. Chem.*, 40 (1968) 1759.

(Received 17th December 1970)

Extraction separation of carrier-free bismuth from lead and zinc

For the production of radioactive ^{206}Bi and ^{207}Bi, a lead target is irradiated with deuterons or protons. A thorough separation of the bismuth from the lead target is necessary, since the ^{206}Bi may be used, as the citrate, for brain-scanning techniques. Furthermore, ^{65}Zn is formed from the copper backing of the target and hence, as there may be ^{65}Zn contamination, provision for the removal of this isotope must also be made.

A procedure for the purification of ^{207}Bi from the lead target has been described by Gile *et al.*[1]. It is based on scavenging of bismuth with iron(III) hydroxide. Scavenging of bismuth sulphide on copper(II) sulphide[2] and cadmium sulphide[3] has also been reported. These techniques[1-3] require an additional separation of bismuth from the iron, copper or cadmium, however. Separation from lead by hydroxide precipitation of bismuth can be performed in EDTA medium[4], but this does not apply to carrier-free amounts of bismuth. An internal electrolysis procedure for the lead–bismuth separation[5] is equally ineffective for carrier-free amounts of bismuth. A good cation-exchange separation is based on elution of bismuth(III) with 0.3 *M* hydrobromic acid, lead(II) being adsorbed on the Dowex 50 W-X8 resin[6]; but the adsorption of several hundred milligrams of lead requires a quite voluminous column. An anion-exchange procedure devised by Kraus and Nelson[7] may be applied to small columns, as the lead is eluted first with 8 *M* hydrochloric acid from the Dowex 1-X8 resin. Zinc can also be easily removed by elution with 0.5 *M* hydrochloric acid. However, the desorption of bismuth(III) from the resin is time-consuming if done with 0.25 *M* nitric acid. It can also be done by elution with 1 *M* sulphuric acid, but removal of this solute is tedious.

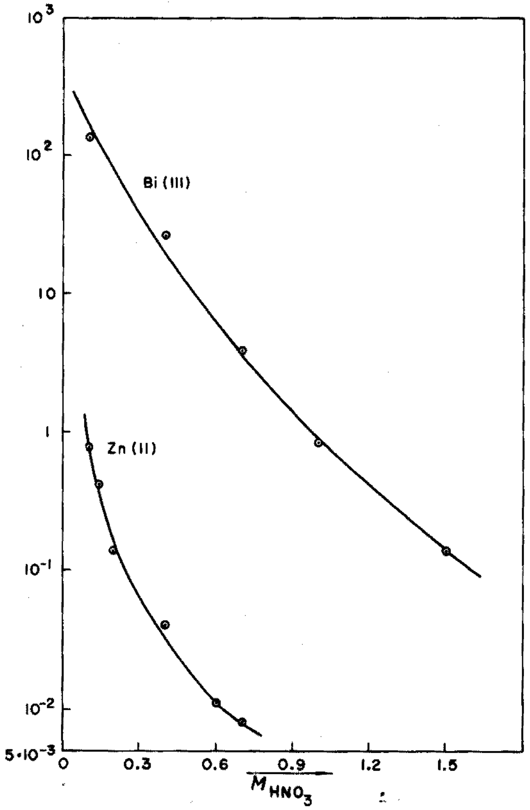

Fig. 1. Distribution constants of bismuth(III) and zinc(II) between nitric acid and 0.3 *M* HDEHP in *n*-heptane, as a function of the nitric acid concentration.

Bismuth(III) may be extracted as the iodide complex from nitric acid[8] or with di(2-ethylhexyl)phosphoric acid from perchloric acid[9]. The behaviour of lead in these procedures has not been reported.

In this communication, a procedure based on extraction with di(2-ethylhexyl)-phosphoric acid from nitric acid is described.

Experimental

Reagents and tracers. Di(2-ethylhexyl)phosphoric acid (HDEHP; B.D.H. Laboratory Chemical) and 65% nitric acid (analytical grade) were used.

^{203}Pb was produced in the Pretoria variable-energy cyclotron by deuteron bombardment of thallium[10], ^{207}Bi by deuteron bombardment of a lead target, and ^{65}Zn by deuteron bombardment of a copper target.

For irradiation of the lead target, spectrographically pure lead was bombarded for 1 week in the variable-energy cyclotron with a 100-μA beam of 16-MeV deuterons.

Apparatus. The final measurements were made by means of γ-spectrometry, performed with a 40-cm^3 Ge(Li) detector[11], connected to a 4096-channel pulse-height analyser.

Extraction experiments. Because of the different ionization states of the bismuth(III), lead(II) and zinc(II), a separation based on extraction of the bismuth(III) with di(2-ethylhexyl)phosphoric acid seemed possible.

The distribution constants for bismuth(III), lead(II) and zinc(II) between varying concentrations of nitric acid and 0.3 *M* HDEHP in *n*-heptane, were determined by using the radioactive tracers ^{207}Bi, ^{203}Pb and ^{65}Zn; 100 mg of lead carrier was added for each experiment. Figure 1 shows the variation of the distribution constant (K_D) of bismuth(III) and zinc(II) between nitric acid and 0.3 *M* HDEHP in *n*-heptane, as functions of the nitric acid concentration. The distribution constant for lead(II) was always less than 0.005 in 0.1–9 *M* nitric acid.

Results and discussion

The distribution constants of bismuth(III) and zinc(II) between 0.3 *M* HDEHP (in *n*-heptane) and nitric acid, showed a steady decrease as the nitric acid concentration increased from 0.1 to 1.5 *M*, whereas the distribution constant for lead(II) remained very low over the acid range tested. As the K_D values for bismuth(III) and zinc(II) differed by a factor of roughly 100, a separation could readily be obtained. As it was preferred to extract almost all the bismuth(III) from the original solution, a low concentration of nitric acid was chosen for the extraction. One extraction from 0.2 *M* nitric acid with an equal volume of 0.3 *M* HDEHP in *n*-heptane, collected 98.7% of the bismuth(III), less than 0.5% of the lead(II) and 15% of zinc(II). Two subsequent washings of the organic fraction with equal volumes of 0.20 *M* nitric acid left 96% of the bismuth(III), less than 10^{-5}% of the lead(II) and 0.3% of the zinc(II) in the organic fraction. This was generally sufficient for a pure bismuth(III) fraction. If the impurity level was too high, one more washing was carried out. If the yield for bismuth(III) was too low, the aqueous layers were collected, extracted once more with an equal volume of 0.3 *M* HDEHP, and dissolved in *n*-heptane, and this organic layer was washed three times with equal volumes of 0.20 *M* nitric acid.

The bismuth(III) was then back-extracted with 9 *M* nitric acid. In this medium the K_D value for bismuth(III) was less than 10^{-3}.

The separated bismuth fraction was radiochemically pure, judged by a comparison of its Ge(Li) spectrum with that of a ^{207}Bi standard (Amersham). After a 5-month cooling period, no ^{206}Bi could be detected in the separated fraction, although immediately after bombardment, the ^{206}Bi activity was roughly 1000 times that of the ^{207}Bi.

National Physical Research Laboratory,
South African Council for Scientific and
Industrial Research,
Pretoria (South Africa)

R. D. Neirinckx

1 J. D. Gile, W. M. Garrison and J. G. Hamilton, *J. Chem. Phys.*, 19 (1951) 256.
2 V. J. Moore, *Analyst*, 81 (1956) 553.

3 M. Ziegler and Mya Tha Maung, *Z. Anal. Chem.*, 196 (1963) 81.
4 F. W. Lima and A. Abrao, *Anal. Chem.*, 32 (1960) 492.
5 P. Deschamps and Y. Bonnaire, *Mikrochim. Acta*, 3 (1962) 463.
6 J. S. Fritz and B. B. Gerralda, *Anal. Chem.*, 34 (1962) 102.
7 K. A. Kraus and F. Nelson, *J. Amer. Chem. Soc.*, 76 (1954) 5916.
8 E. Jackwerth and H. Specker, *Z. Anal. Chem.*, 177 (1960) 327.
9 I. S. Levin, Yu. M. Yukhin and I. A. Vorsina, *Zh. Analit. Khim.*, 25 (1970) 752.
10 R. D. Neirinckx, *Radiochem. Radioanal. Letters*, to be published.
11 A. S. M. de Jesus, *C.S.I.R. Res. Rept.*, 283 (1969) 1.

(Received 12th November 1970)

Comparaison des fonctions d'acidité dans le solvant peu dissociant: acide trifluoroacétique–perchlorate de tétraéthylammonium 0.5 *M*

Par analogie avec les solvants dissociants, la fonction d'acidité (H_0) apparent a été définie en milieu de faible constante diélectrique pour caractériser le niveau d'acidité des mélanges solvant–acide fort[1]. Il est possible d'introduire de la même façon la fonction R_0 (H) apparent pour rendre compte de ces niveaux d'acidité[2].

Ce n'est qu'en présence de sel ionisé en forte concentration que ces fonctions d'acidité apparentes sont caractéristiques du niveau d'acidité, non seulement des mélanges solvant–acide fort, mais plus généralement de toute solution, que cette solution soit acide, basique ou neutre[3].

Les fonctions $(H_0)_{\text{app}}$ et $R_0(\text{H})_{\text{app}}$ font appel à des indicateurs de types différents dont la solvatation est supposée obéir à des critères précis[4,5].

Il est intéressant d'examiner la concordance des résultats obtenus à partir de chacune de ces deux fonctions dans un milieu très acide comme l'acide trifluoro-

TABLEAU I

VARIATION DE $(H_0)_{\text{app}}$ AVEC L'ADDITION DE *n*-BUTYLAMINE DANS LE SOLVANT CF_3COOH–NEt_4ClO_4 0.5 *M*

log C	$\log \frac{[I]}{[IHClO_4]}$	$(H_0)_{app}$
−2.70	0.00	−4.53
−2.53	0.16	−4.37
−2.40	0.28	−4.25
−2.30	0.37	−4.16
−2.22	0.44	−4.09
−2.16	0.53	−4.00
−2.10	0.58	−3.95
−2.05	0.62	−3.91
−2.00	0.65	−3.88
−1.80	0.82	−3.71

acétique, puis de comparer ces résultats avec ceux obtenus dans un autre milieu de faible constante diélectrique, l'acide acétique.

Partie expérimentale

Les réactifs et les dispositifs expérimentaux sont décrits dans les mémoires précédents[6,7].

Par spectrophotométrie, nous avons mesuré le rapport des concentrations des formes basique et acide d'un indicateur de Hammett, la 2,4-dinitroaniline ($pK_{H_2O} = -4.53$)[4] en fonction de l'addition de *n*-butylamine, dans le solvant CF_3COOH–NEt_4ClO_4 0.5 *M*. Les résultats expérimentaux sont présentés dans le Tableau I. Nous avons suivi le potentiel pris par une électrode à hydrogène en fonction de l'addition de *n*-butylamine dans CF_3COOH–NEt_4ClO_4 0.5 *M*, le potentiel normal apparent du système ferrocène/perchlorate de ferricinium étant pris comme origine. Les résultats expérimentaux sont présentés dans le Tableau II.

TABLEAU II

VARIATIONS DE $R_0(H)_{app}$ EN FONCTION DE L'ADDITION DE *n*-BUTYLAMINE DANS CF_3COOH–NEt_4ClO_4 0.5 *M*

$\log C_B$	$(E_0^{fc})_{app}-E$ (mV)	$R_0(H)_{app}$
−2.33	−199	−10.37
−2.03	−181	−10.06
−1.72	−165	− 9.79
−1.63	−160	− 9.70
−1.33	−141	− 9.37
−1.03	−123	− 9.06
−0.86	−113	− 8.89
−0.73	−105	− 8.75
−0.64	− 98	− 8.63

Analyse des résultats et discussion

La *n*-butylamine—symbolisée par B—en présence de perchlorate de tétraéthylammonium en excès, est transformée en perchlorate de *n*-butylaminium suivant la réaction[8]:

$$B + CF_3COOH + NEt_4ClO_4 \rightarrow CF_3COONEt_4 + BHClO_4$$

Le niveau d'acidité de la solution sera fixée par la concentration de base forte $CF_3COONEt_4$.

La 2,4-dinitroaniline est partiellement protonée dans la solution considérée suivant l'équilibre:

$$I + \underbrace{CF_3COOH + NEt_4ClO_4}_{\text{solvant}} \rightleftharpoons IHClO_4 + CF_3COONEt_4$$

avec

$$[I]/[IHClO_4][NEt_4CF_3COO^-] = K_s$$

L'addition de base forte modifie le rapport $[I]/[IHClO_4]$. La fonction $(H_0)_{app}$

est alors définie par la relation

$$(H_0)_{\mathrm{app}} = \mathrm{p}K^{\mathrm{I}}_{\mathrm{H_2O}} + \log\,[\mathrm{I}]/[\mathrm{IHClO_4}]$$

où $\mathrm{p}K^{\mathrm{I}}_{\mathrm{H_2O}}$ représente le pK de la 2,4-dinitroaniline rapporté à l'eau. On montre facilement que la courbe $(H_0)_{\mathrm{app}} = \mathrm{f}(\log C_{\mathrm{B}})$ est une droite de pente théorique +1. La pente de la courbe expérimentale déduite des valeurs du Tableau I est égale à 0.97, C_{B} variant de $2 \cdot 10^{-3}$ à $1.6 \cdot 10^{-2}$ *M*.

La fonction d'acidité $R_0(\mathrm{H})_{\mathrm{app}}$ est définie dans le solvant $\mathrm{CF_3COOH}$–$\mathrm{NEt_4ClO_4}$ par la relation

$$R_0(\mathrm{H})_{\mathrm{app}} = \frac{1}{0.058}\,[(E^{\mathrm{Fc}}_0)_{\mathrm{app}} - E]_{\mathrm{CF_3COOH}} - [E^{\mathrm{Fc}}_0 - E^{\mathrm{H_2}}_0]_{\mathrm{H_2O}}$$

où $[E^{\mathrm{Fc}}_0 - E^{\mathrm{H_2}}_0]_{\mathrm{H_2O}}$ représente la différence des potentiels normaux des systèmes $\mathrm{H_2/H^+}$ et ferrocène/ferricinium ($\mathrm{Fc/Fc^+}$) dans l'eau. $(E^{\mathrm{Fc}}_0)_{\mathrm{app}}$ est le potentiel normal apparent du système ferrocène/perchlorate de ferricinium dans le milieu $\mathrm{CF_3COOH}$–$\mathrm{NEt_4ClO_4}$ 0.5 *M*, *E* le potentiel pris par l'électrode à hydrogène plongeant dans une solution de *n*-butylamine dans le même solvant.

La concentration des ions $\mathrm{NR_4^+}$ apportée par la faible dissociation de $\mathrm{NEt_4ClO_4}$, en forte concentration, étant pratiquement constante, le potentiel *E* varie linéairement avec le logarithme de la concentration en base forte selon l'expression $E = \mathrm{const.} - 0.058 \log[\mathrm{CF_3COONEt_4}]$. La réaction électrochimique est en effet la suivante:

$$\mathrm{CF_3COOH} + \mathrm{Et_4N^+} + e \rightarrow \tfrac{1}{2}\mathrm{H_2} + \mathrm{CF_3COONEt_4}\,.$$

Il résulte de ces considérations que la courbe $R_0(\mathrm{H})_{\mathrm{app}} = \mathrm{f}(\log C_{\mathrm{B}})$ est une droite de pente théorique égale à +1. La pente expérimentale déduite des valeurs du Tableau II est égale à cette valeur, C_{B} variant de $4.6 \cdot 10^{-3}$ à $2.2 \cdot 10^{-1}$ *M*.

Il est important de noter que pour un même état d'acidité de la solution, les deux fonctions $(H_0)_{\mathrm{app}}$ et $R_0(\mathrm{H})_{\mathrm{app}}$ prennent des valeurs qui diffèrent de près de 6 unités logarithmiques, ce qui est considérable. Il est possible, à partir de ces valeurs, de remonter aux valeurs de H_0 et de $R_0(\mathrm{H})$ en faisant intervenir les constantes de dissociation ionique des paires d'ions mises en jeu[2]. Moyennant certaines approximations légitimes[2], on constate que l'écart entre H_0 et R_0 est aussi voisin de 6 unités logarithmiques. Il en résulte donc que les hypothèses extrathermodynamiques à partir desquelles sont déduites ces fonctions d'acidité, ne sont pas concordantes lorsque l'on compare l'eau à l'acide trifluoroacétique.

Il est intéressant de comparer ces résultats avec ceux obtenus dans l'acide acétique où les fonctions $R_0(\mathrm{H})_{\mathrm{app}}$ et $(H_0)_{\mathrm{app}}$ peuvent être déterminées pour des solutions d'acide perchlorique[9].

Ainsi, le pK de la 4-chloro-2-nitroaniline est égal à 3.25 sur l'échelle $\mathrm{pHClO_4}$[10], son $\mathrm{p}K_{\mathrm{H_2O}}$ étant égal à −1.0. Le calcul montre que la fonction $(H_0)_{\mathrm{app}} = \mathrm{p}K^{\mathrm{I}}_{\mathrm{H_2O}} + \log[\mathrm{I}]/[\mathrm{IHClO_4}]$ est égale à −2.6 lorsque la concentration d'acide est égale à $2.4 \cdot 10^{-2}$ *M*.

Une électrode à hydrogène plongeant dans cette même solution prend un potentiel de −200 mV par rapport au potentiel normal apparent du système ferrocène/perchlorate de ferricinium. La fonction $R_0(\mathrm{H})_{\mathrm{app}}$ est donc égale à −3.4.

L'écart mesuré entre $R_0(\mathrm{H})_{\mathrm{app}}$ et $(H_0)_{\mathrm{app}}$ est seulement de 0.8 unité logarithmique. On note donc une concordance des résultats lorsque l'on compare l'acide acétique à l'eau.

Il découle de ces considérations que l'acide trifluoroacétique a un comportement très différent de celui de l'acide acétique quant à la solvatation des espèces chimiques[11,12], ce qui est prévisible étant donné le caractère fortement électrophile du groupement CF_3.

Si l'on admet la validité de l'hypothèse de Strehlow, cela revient à conclure que la différence de solvatation entre I et IH^+ dans l'eau est voisine de celle existant dans l'acide acétique, alors qu'elle est très différente dans l'acide trifluoroacétique, le cation IH^+ subissant une variation de solvatation très inférieure à celle de la molécule I.

Par voie de conséquence, le solvant apparaîtra moins basique et plus acide de 6 unités de pK par rapport aux limites de l'échelle acide–base déduites à partir de la fonction $(H_0)_{\mathrm{app}}$[6].

Nous tenons à exprimer nos remerciements à Madame Badoz-Lambling, Directeur de Recherches au C.N.R.S., pour l'intérêt qu'elle a bien voulu porter à cette étude, ainsi que le Commissariat à l'Energie Atomique qui a subventionné ces recherches.

Laboratoire de Chimie Analytique,
associé au C.N.R.S.,
E.S.P.C.I. 10 rue Vauquelin,
Paris Ve (France)

J. Bessière
G. Petit

1 S. Bruckenstein, *J. Amer. Chem. Soc.*, 82 (1960) 307.
2 J. Bessière et G. Petit, *Anal. Chim. Acta*, 1971, à paraître.
3 J. Bessière, *Thèse*, Paris, 1969.
4 M. A. Paul et F. A. Long, *Chem. Rev.*, 57 (1957) 1n.
5 H. Strehlow, in J. J. Lagowski, *The Chemistry of Non-Aqueous Solvents, Vol. 1*, Academic Revs., New York, 1966, p. 129.
6 J. Bessière, *Bull. Soc. Chim. France*, (1970) 3356.
7 G. Petit et J. Bessière, *J. Electroanal. Chem.*, 1971, à paraître.
8 J. Bessière, *Compt. Rend.*, 269 (1969) 1636.
9 G. Duraud, *Bull. Soc. Chim. France*, (1970) 1220.
10 G. Charlot et B. Trémillon, *Les Réactions Chimiques dans les Solvants et Sels Fondus*, Gauthier-Villars, Paris, 1963, p. 221.
11 R. E. Buckles et K. F. Mills, *J. Amer. Chem. Soc.*, 76 (1954) 6021.
12 G. Petit et J. Bessière, *J. Electroanal. Chem.*, 25 (1970) 317.

(Reçu le 21 novembre 1970)

Analytica Chimica Acta
Elsevier Publishing Company, Amsterdam
Printed in The Netherlands

Determination of trace amounts of gold in natural sweet waters by non-destructive activation analysis after preconcentration

Many investigations have already been made on the determination of trace amounts of gold in water. Most have dealt with the determination of gold content in sea waters[1-10], but several are concerned with the gold content of other natural waters. Grimanis *et al.*[11] determined the gold contents of some Greek lakes, and Abdullaev *et al.*[12] studied underground waters from the Kyzylkum deposit and Uzbekistan regions. Neutron activation analysis has been applied to measure the gold in several studies[9-12], samples of about 5–10 ml being directly irradiated followed by chemical separation. Abdullaev *et al.*[13] used a 100-ml sample of natural water which was made 1 *M* in perchloric acid and passed through an anion-exchange column; the resin was dried, irradiated, and burned, and the ash was dissolved in 6 *M* hydrochloric acid before the chemical separation of gold from interfering elements, with a final reduction of gold to the metal and measurement of the 410-keV γ-ray of gold-198.

However, in the interests of speed, it is desirable to avoid chemical seaprations as far as possible and to use non-destructive neutron activation analysis. But in natural waters, the amount of gold is so small that its direct measurement in some milliliters of sample after irradiation is not possible. Accordingly, the method described here is based on a simple preconcentration of gold before irradiation followed by non-destructive activation analysis of the carrier containing adsorbed gold. It was obviously necessary to find a carrier which had optimal adsorption efficiency for gold and which introduced no interferences in the direct γ-spectrometric determination of the gold. In the present work, the coprecipitation of gold with iron(III) hydroxide, lead sulphide and aluminium hydroxide, and the separation of gold from water with Dowex 1-X8 resin (100–200 mesh) and flexible polyurethane foam were investigated. Bowen[14] reported the latter material for extracting various substances from dilute aqueous solution. For gold he recommended[15] Dunlopillo foam and a foam/solution ratio of 1 : 50 or 1 : 100 (w/w). The sorption is most efficient from 6 *M* hydrochloric acid but good efficiency is also obtained from 0.2 *M* hydrochloric acid.

Experimental

Apparatus and reagents. For measuring samples labelled with gold-198, a 3 × 3 in NaI(Tl) detector in conjunction with a 400-channel pulse-height analyser was used. For measurement of irradiated samples, a 18-cm^3 or 40-cm^3 coaxial Ge(Li) detector (Nuclear Diodes) was connected to a Tennelec TC 202 BRL linear amplifier followed by a Northern NS-610 1024-channel analyser. The integral counting rate of every sample was determined in a separate time-pickoff channel. Irradiations were carried out for 8 h at a flux of $1.75 \cdot 10^{12}$ n cm^{-2} sec^{-1} in a Triga reactor.

All reagents were analytical grade. For the standard, metallic gold was dissolved in aqua regia and diluted to a suitable concentration with 6 *M* hydrochloric acid.

Sample preparation. Tap water (90 ml) was acidified with 10 ml of concentrated hydrochloric acid. Chao *et al.*[16] have shown that gold is not adsorbed on to the vessel surface from 1 *M* hydrochloric acid. An aliquot (1 ml) of solution containing gold-198 (activity 146,000 counts min^{-1}) was added to the water. The gold-198 solution used was prepared as a mixture of ionised, colloidal and very fine precipitated gold; all these forms are believed to occur in natural waters.

Measurement of the coprecipitation of gold. The gold-198 content of the sample was first measured (with a suitable aliquot). The appropriate reagent was added (sufficient to yield about 1 g of precipitate) and then precipitated with ammonia in the case of iron or aluminium, and ammonium sulphide for lead. No precipitant was, of course, necessary for the polyurethane foam (specification 649/33, Dunlopillo Factory, Aberdare, Wales) which was cut into small pieces about 3 mm diameter, or for the Dowex 1-X8 resin (100–200 mesh, chloride form). The precipitate or additive was shaken for 30 or 90 min with the solution, and then separated by centrifugation. An aliquot of the solution was removed and measured for its gold-198 content to determine the efficiency of sorption.

Results and discussion

The results of the experiments carried out with gold tracer are shown in Table I. The sorption efficiency of each carrier is the ratio of the activity of the gold-198 coprecipitated with the absorbent divided by the total amount of gold-198 present.

TABLE I

EFFICIENCY OF DIFFERENT CARRIERS FOR SORPTION OF GOLD

Carrier[a]	*Sorption efficiency*	
	30 *min*	90 *min*
PbS [$Pb(CH_3COO)_2 + (NH_4)_2S$]	1.000	1.000
$Fe(OH)_3$ [$FeCl_3 + 3\ NH_4OH$]	0.660	0.700
$Al(OH)_3$ [$AlCl_3 + 3\ NH_4OH$]	0.994	0.996
Dowex 1-X8	0.970	0.983
Polyurethane foam	0.984	0.994

[a] 1 g per 100 ml of solution.

Lead sulphide was the best carrier, as it sorbed the gold from water samples completely after shaking for 30 min. Aluminium hydroxide also had good sorption efficiency, but its large volume made it less suitable. Polyurethane foam had good properties for gold separation, but the 90-min shaking time necessary for the best results is a slight disadvantage. The relatively low efficiency of Dowex resin is probably due to the presence of non-ionised gold in the samples. The poor efficiency of iron(III) hydroxide is somewhat surprising, as it is a well known radiochemical scavenger but the results agree with Haber[2,3] who considered iron hydroxide as unsuitable, not only because it does not occlude all the gold, but also because of its awkward filtering properties. On the other hand, Lal *et al.*[17] described iron(III) hydroxide as a suitable adsorbent for many elements present in trace quantities in sea water.

Of the various materials tested, lead sulphide and polyurethane foam can be considered the most efficient for the separation of traces of gold from natural waters. Further experiments were carried out in order to investigate any possible inter-

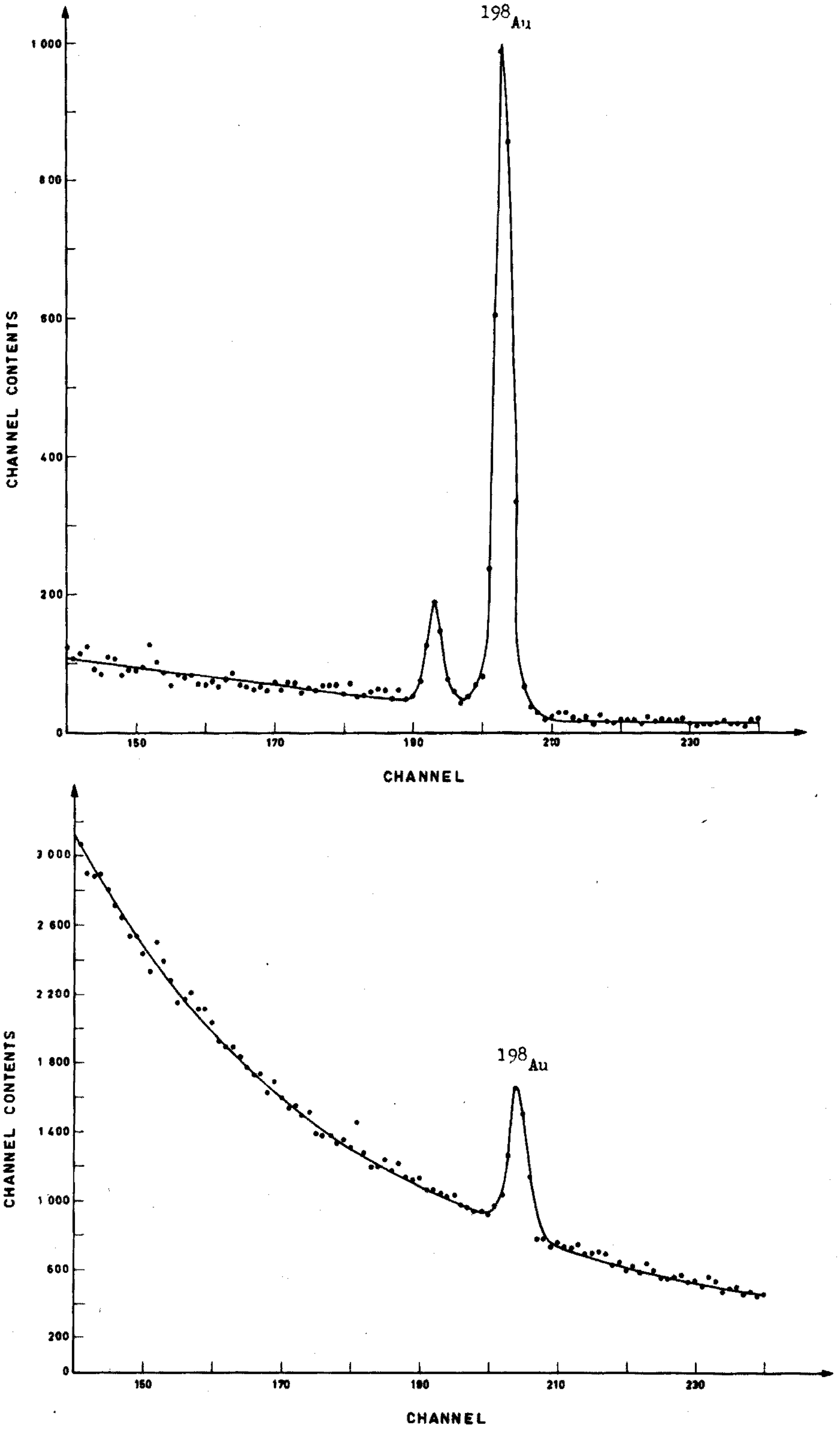

Fig. 1. Peak area of 0.2 p.p.b. gold sorbed on: (a) polyurethane carrier; (b) lead sulphide carrier.

TABLE II

THE SENSITIVITY OF THE DETERMINATION OF GOLD

Carrier used for separation	*Au (p.p.b.)*	*Peak area (counts)*	σ (%)	*Peak-to-back-ground ratio*	*Cooling time (days)*
PbS	0.11	186	26.9	1.100	4
PbS	0.22	291	13.4	1.180	
P.U. foam	0.11	169	22.1	1.090	
P.U. foam	0.22	270	19.6	1.170	
PbS	0.11	171	2.6	1.400	12
PbS	0.22	210	8.2	1.700	
P.U. foam	0.11	55	16.5	1.770	
P.U. foam	0.22	101	7.1	2.450	

ferences from trace elements originally present in the carriers, on the determination of gold by neutron activation. Lead sulphide and polyurethane foam were irradiated under the conditions given in the *Experimental* part, and their γ-spectra were measured. The same procedure was used with both the carriers plus 0.2 p.p.b. of gold. Figure 1 shows that under these conditions no interfering γ-lines were present in the carriers, hence the non-destructive determination of gold is possible.

The sensitivity of the determination of gold by the methods described is illustrated in Table II. The samples were prepared from 450 ml of redistilled water and 50 ml of concentrated hydrochloric acid, to which 0.05 μg or 0.1 μg of gold was added as a solution taken from the gold standard. The irradiation conditions and measuring time were as described above. All data for peak areas and peak-to-background ratios are averages of five samples run in parallel. The standard deviation of the results shows an improvement when the cooling time is longer, owing to the better peak-to-background ratio. Because of differences in the activity level at 4 and 12 days, it was necessary in the former case to measure samples 5 cm distance from the detector, whereas at 12 days, the source containers could be placed in contact. It can be seen that the results for gold on lead sulphide after cooling for 12 days are rather far from the correct 1:2 ratio for the amounts of gold taken. The reason is not clear but may lie in some experimental error plus the fact that the amounts taken are close to the limits of detection.

The assistance of Mrs. E. Wölfl in carrying out extensive experimental work is gratefully acknowledged.

IAEA Laboratory,
Seibersdorf near Wien (Austria)

P. Schiller
G. B. Cook

1 E. Sonstadt, *Chem. News*, 26 (1872) 159.
2 F. Haber, *Z. Angew. Chem.*, 40 (1927) 303.
3 F. Haber, *Z. Ges. Erdk. (Berlin)*, 1928, Suppl. 3, 3.
4 J. Jaenicke, *Naturwissenschaften*, 23 (1935) 57.
5 W. E. Caldwell, *J. Chem. Educ.*, 15 (1938) 507.
6 E. Bauer, *Helv. Chim. Acta*, 25 (1942) 1202.

7 W. Stark, *Helv. Chim. Acta*, 26 (1943) 424.
8 G. L. Putnam, *J. Chem. Educ.*, 30 (1953) 576.
9 R. W. Hummel, *Analyst*, 82 (1957) 483.
10 Y. Oka, T. Kato and M. Sasaki, *Nippon Kagaku Zasshi*, 85 (1967) 643.
11 A. P. Grimanis, G. Pantazis, C. Papadopulos and N. Tsamos, *Proc. III. Intern. Conf. Peaceful Uses At. Energy, Geneva, 1964*, Vol. 15, p. 412–417 (P/854).
12 A. A. Abdullaev, A. S. Zaklidov and V. A. Grakhov, *Izv. Akad. Nauk Uz. SSR, Ser. Fiz.-Mat. Nauk*, 11 (1967) 66.
13 A. A. Abdullaev, E. S. Gureev, V. A. Grakhov, L. I. Zhuk and A. S. Zakhidov, *Izv. Akad. Nauk Uz. SSR, Ser. Fiz.-Mat. Nauk*, 12 (1968) 59.
14 H. J. M. Bowen, *J. Chem. Soc.*, (A 1970) 1082.
15 H. J. M. Bowen, private communication, 1969.
16 T. T. Chao, E. A. Jenne and L. M. Heppting, *Prevention of Adsorption of Trace Amounts of Gold by Containers*, Report of U.S. Geological Survey, Water Resources Division, Denver, Colo., 1968.
17 D. Lal, J. R. Arnold and B. L. K. Somayajulu, *Geochim. Cosmochim. Acta*, 28 (1964) 1111.

(Received 20th November 1970)

Polarographic reduction of perrhenate in the presence of ascorbic acid

The cathodic waves of perrhenate in hydrochloric and perchloric acid have frequently been studied[1-9]. Although the waves obtained in the two acids are very similar, there is no simple interpretation of the nature of the wave. It has been observed that in less than 2 *M* hydrochloric acid a rounded maximum appears on the wave. Even traces of maximum suppressors such as gelatin affect the wave seriously. Below 2 *M* acid concentrations the waveheight increases with increasing acid concentration, but above 2 *M* acid concentrations there is no further increase in the height of the wave. Lingane[1] attributes this wave to the reduction of rhenium(VII) to rhenium(IV), *i.e.* to the hexachlororhenate ion which has been found to be stable. However, according to Rulfs and Elving[2], such a simple interpretation is invalid, for controlled potential coulometry fails to show that perrhenate undergoes any reduction corresponding to more than 0.2 electron, even after several hours of electrolysis. Rulfs and Elving also indicated the possible adsorption nature of the wave, which has found further support from recent investigators[8,9].

The present work provides further evidence that the reduction of perrhenate at the dropping mercury electrode is associated with adsorption of the rhenium(VII) species at the mercury drops. In an investigation of the effect of L(+)ascorbic acid (Vitamin C) on polarograms of perrhenate in acidic solutions, it has been found that the presence of ascorbic acid influences the polarographic waves of rhenium(VII). While very small concentrations of ascorbic acid do not interfere with the reduction wave, increasing concentrations reduce the waveheight. This effect is attributed to adsorption of the ascorbic acid on the mercury drops, which thus prevents the adsorption of perrhenate.

Materials and methods

Perrhenate solution was prepared by dissolving rhenium metal powder (purity >99.9%; Schuchardt) in hydrogen peroxide and isolating as sodium perrhenate. The rhenium content of the stock solution was determined by the tetraphenylarsonium chloride method[10]. L(+)Ascorbic acid (crystalline extra pure; Merck) was used without further purification. All the other reagents used were of analytical grade.

A Radiometer PO4 polarograph was used to record the waves, with an external calomel electrode containing saturated potassium chloride solution. The capillary used had the following characteristics: mean drop time at -0.5 V in 1 *M* hydrochloric acid, 4.35 sec; $m=2.37$ mg sec^{-1}, and corrected mercury pressure, 47.5 cm.

All the measurements were carried out at $25\pm0.2°$.

Pure nitrogen was bubbled for 15 min through the solution before measurements. The gas was first passed through a trap which usually contained distilled water to minimise evaporation of the test solution. In experiments with camphor, the trap was filled with the experimental solution so as to avoid any loss of camphor by volatilisation.

Results and discussion

The earlier work of Lingane on rhenium showed that in very dilute hydrochloric acid perrhenate gives only a slight indication of a polarographic wave but on increasing the acid concentration the wave is better defined. At acid concentrations less than about 2 *M* a rounded maximum appears on the wave. As little as 0.013% gelatin completely obliterates the wave. The pronounced effect of gelatin was attributed by Rulfs and Elving and later workers to the adsorption nature of the wave.

Figure 1 shows the effect of varying amounts of ascorbic acid on the polarographic waves of perrhenate in 2 *M* hydrochloric acid. In the absence of ascorbic acid, the half-wave potential of perrhenate appears at -0.45 V; as can be seen (Fig. 1, curve a), a smoothly curved maximum fades into the hydrogen evolution wave at -0.9 V. Curve f of Fig. 1 shows the polarogram of 0.02 *M* ascorbic acid alone in 2 *M* hydrochloric acid; under the conditions used, ascorbic acid produces no cathodic wave. Whereas very low concentrations of ascorbic acid have no appreciable effect on the waveheight of perrhenate, the higher concentrations of ascorbic acid tested decrease the waveheight considerably; *e.g.* in the presence of 0.06 *M* ascorbic acid the waveheight is almost halved (compare curves a and c of Fig. 1). Moreover, with increasing ascorbic acid concentration the maximum on the perrhenate wave disappears.

Figure 2 shows a plot of varying molar concentrations of ascorbic acid against the percentage ratio of the perrhenate diffusion current in the presence of ascorbic acid to the perrhenate diffusion current alone, at three different hydrochloric acid concentrations. It is clear that the effect of ascorbic acid is more pronounced at lower hydrochloric acid concentrations. A plot of the concentration of ascorbic acid against the decrease in limiting current (Fig. 3) shows that there is a definite relationship between the two. At constant hydrochloric acid concentration, the decrease in diffusion current of perrhenate almost reaches a limiting value as the amount of ascorbic acid increases. This relationship offers a method for the determination of ascorbic acid, provided that the total acidity is kept constant.

The possibility that a reduction of perrhenate by ascorbic acid causes the decrease in the waveheight can be eliminated, because ascorbic acid does not reduce perrhenate[11]. Under the conditions of the present study, there was no indication of

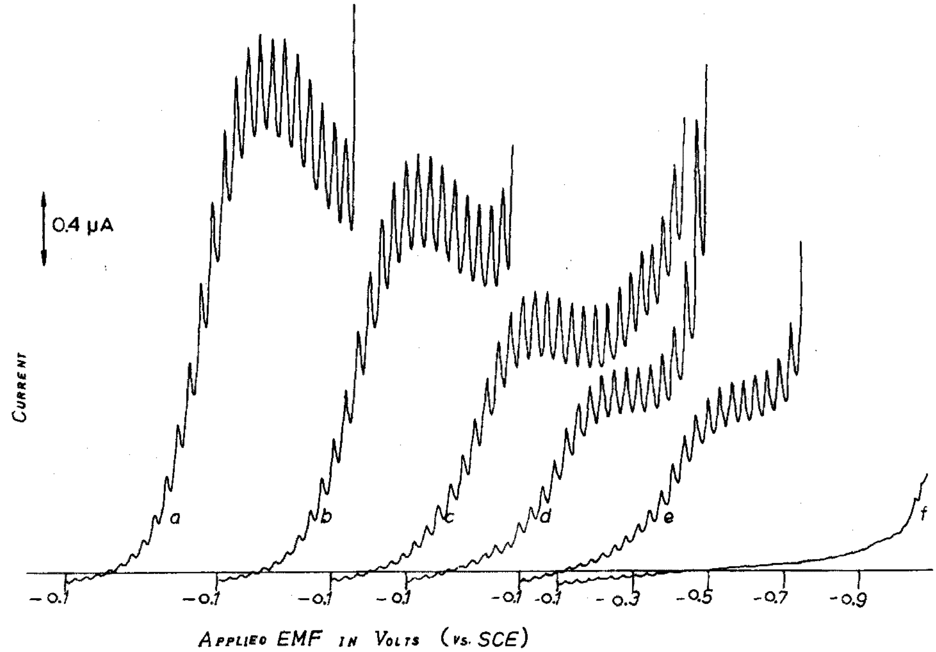

Fig. 1. The effect of ascorbic acid on the polarographic waves of perrhenate. $4 \cdot 10^{-4}$ *M* perrhenate in 2 *M* hydrochloric acid in the presence of (a) 0, (b) 0.012, (c) 0.06, (d) 0.2 and (e) 0.3 *M* ascorbic acid; (f) 0.02 *M* ascorbic acid alone in 2 *M* hydrochloric acid.

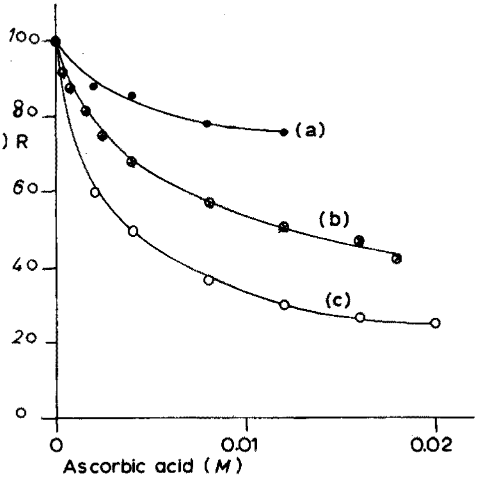

Fig. 2. The effect of hydrochloric acid concentration on the decrease in the perrhenate limiting current in the presence of ascorbic acid. %R = (limiting current in presence of ascorbic acid : limiting current in absence of ascorbic acid) × 100. Concentration of hydrochloric acid : (a) 3 *M*, (b) 2 *M*, and (c) 1 *M*.

chemical reduction, nor was there evidence of complex formation between ascorbic acid and perrhenate or any of its reduction products; for the half-wave potential remained constant with varying amounts of ascorbic acid.

If the reduction of perrhenate at the dropping mercury electrode (D.M.E.) is associated with adsorption of the rhenium species on the mercury, any substance which is also adsorbed should partly or completely prevent reduction of the rhenium species. Substances with strong adsorption tendencies, such as gelatin or Triton X-100, completely obliterate the rhenium wave even in very low concentrations. Ascorbic acid at *ca.* 0.3 *M* concentrations greatly decreases the rhenium waveheight (Fig. 1e), but the effect is not strong enough to obliterate the wave. The less pronounc-

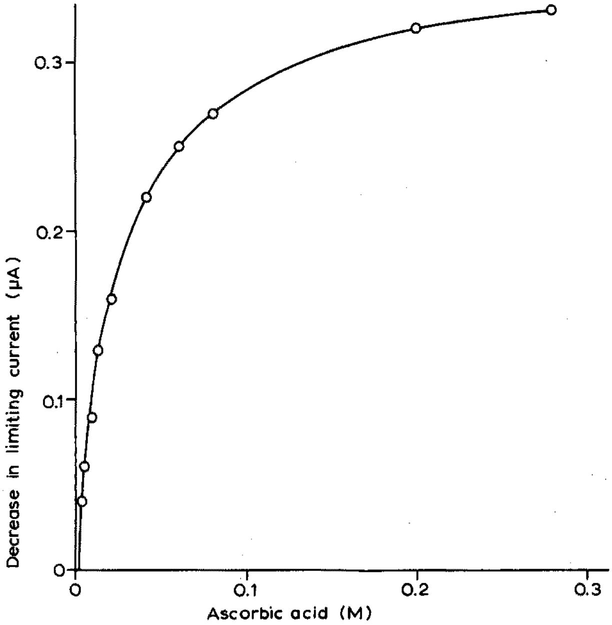

Fig. 3. Effect of ascorbic acid concentration on the perrhenate limiting current.

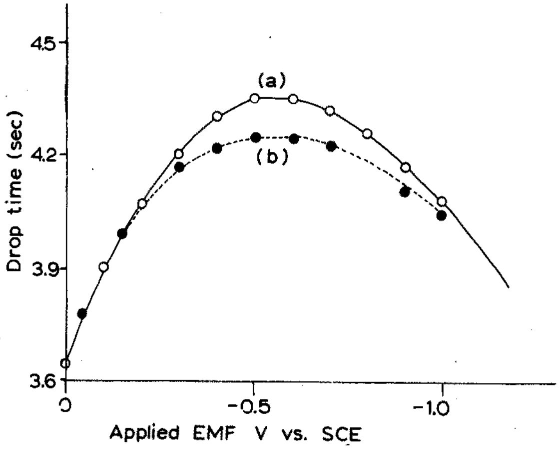

Fig. 4. The effect of ascorbic acid on the electrocapillary curve. (a) 1 *M* HCl and (b) 1 *M* HCl+0.1 *M* ascorbic acid.

ed effect of ascorbic acid at higher acidities can be attributed to its reduced adsorption under these conditions.

Figure 4 shows the electrocapillary curves of 1 *M* hydrochloric acid alone and in the presence of 0.1 *M* ascorbic acid. There is no shift in the maximum in the presence of ascorbic acid, but the flatter maximum can be attributed to the adsorption of ascorbic acid.

The effect of camphor, which has been found to adsorb at the D.M.E.[12,13], further supports the adsorption nature of the rhenium wave. While 0.002 % camphor had no effect on the polarographic wave of perrhenate, saturating the solution with camphor completely obliterated the wave.

The polarographic characteristics of rhenium do not appreciably differ in perchloric acid from those found in hydrochloric acid; the effect of ascorbic acid is similar in both acids.

One of the authors (A.N.) gratefully acknowledges the Alexander von Humboldt Stiftung for the award of a fellowship.

Anorganisch-Chemisches Institut der Universität Münster,
44 Münster, Westfalen (Federal Republic of Germany)
A. Narayanan*
F. Umland

1 J. J. Lingane, *J. Amer. Chem. Soc.*, 64 (1942) 1001.
2 C. L. Rulfs and P. J. Elving, *J. Amer. Chem. Soc.*, 73 (1951) 3284.
3 R. Colton, J. Dalziel and G. Wilkinson, *J. Chem. Soc.*, (1960) 71.
4 R. Geyer, *Z. Anorg. Chem.*, 263 (1950) 47.
5 J. A. Shropshire, *J. Electroanal. Chem.*, 16 (1968) 265.
6 A. M. Demkin and S. I. Sinyakova, *Electrokhimiya*, 3 (1967) 1175.
7 R. J. Magee, I. A. P. Scott and C. L. Wilson, *Talanta*, 2 (1959) 376.
8 R. Munze, *Z. Physik. Chem. (Leipzig)*, 226 (1964) 415.
9 D. W. Letcher, T. J. Cardwell and R. J. Magee, *J. Electroanal. Chem.*, 25 (1970) 473.
10 H. H. Willard and G. H. Smith, *Ind. Eng. Chem., Anal. Ed.*, 15 (1939) 305.
11 H. Spitzy, R. J. Magee and C. L. Wilson, *Mikrochim. Acta*, (1957) 354.
12 I. M. Kolthoff and C. Barnum, *J. Amer. Chem. Soc.*, 63 (1941) 520.
13 H. A. Laitinen and E. Ionstott, *J. Amer. Chem. Soc.*, 72 (1950) 4565.

(Received 16th November 1970)

---

* Alexander von Humboldt Fellow.

Analytica Chimica Acta
Elsevier Publishing Company, Amsterdam
Printed in The Netherlands

Spectrophotometric determination of chloride at the parts-per-billion level by the mercury(II) thiocyanate method

Chloride, even at the parts per billion (10^9) level in feed water, may be concentrated by boiling and cause serious corrosion of stainless steel and other metal components of steam-generating systems. Rapid methods must be available in power plants for the determination of chloride at concentrations of 50 p.p.b. or less[1]. Because potentiometric and other electroanalytical techniques generally lack the required sensitivity, several indirect spectrophotometric methods have been devised for determining chloride at these levels. The two most promising methods involve diphenylcarbazone[2-4] and the mercury(II) thiocyanate–iron(III) system[5-11].

The diphenylcarbazone method relies on the depression by chloride of the colour of a suspension of the mercury(II)–diphenylcarbazone complex. The effective molar absorptivity for chloride is 4,000. The disadvantages of the method arise from the difficulty in reproducing the colour-forming reaction; the colloidal suspension of mercury(II) diphenylcarbazonate must be stabilised by a reagent such as gum arabic, and its colour is critically dependent on factors such as temperature, pH, reaction time, and order of mixing. It does not appear to be reliable enough for routine use.

The mercury(II) thiocyanate method involves the reaction of chloride with mercury(II) thiocyanate to form a chloromercurate(II) complex ion, with the liberation of thiocyanate ions which then react with iron(III) to give the familiar red colour. Although this method is slightly less sensitive than the diphenylcarbazone method, it is far more reliable, can tolerate reasonable changes in the experimental conditions, and is remarkably reproducible even in the low p.p.b. chloride range. The method has been in widespread use for many years, but no systematic investigation of the solution variables seems to have been published. This communication outlines such an investigation, and shows that with correct conditions and with a precision spectrophotometer, the limit of detection is 15 p.p.b. chloride at the 95% confidence level.

Experimental

Apparatus. Cary 16 and Hilger "Uvispek" manual spectrophotometers were used for absorbance measurements. Absorption spectra were recorded on a Hitachi EPS-3T recording spectrophotometer.

Reagents. Iron(III) nitrate. Dissolve 15.1 g of $Fe(NO_3)_3 \cdot 9H_2O$ in 45 ml of 72% perchloric acid and dilute to 100 ml with water. This solution is 0.375 *M* in iron(III), and 5.25 *M* in perchloric acid.

Mercury(II) thiocyanate. Saturated solution in ethanol.

Recommended procedure. Pipette a 20-ml aliquot of the sample, containing less than 50 μg of chloride, into a 25-ml volumetric flask. Add 2.00 ml of iron(III) nitrate reagent, 2.00 ml of mercury(II) thiocyanate reagent, then dilute to volume with distilled demineralised water and mix. Measure the absorbance against a reagent blank at 460 nm after 5 min, in 5-cm or 4-cm cells.

Prepare a calibration curve by pipetting 0, 1, 2, 5, 10 and 20 ml of a 1 μg chloride per ml standard solution into 25-ml flasks. Develop the colour as described above. An absorbance of 0.073 is obtained for 5 μg of chloride in 5-cm cells.

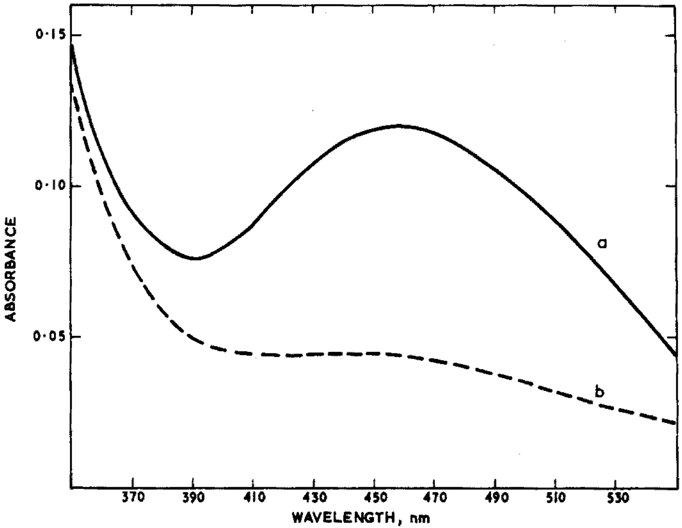

Fig. 1. Absorbance spectra. 2 ml of mercury(II) thiocyanate reagent plus 2 ml of iron(III) nitrate reagent per 25 ml. (a) Sample (25 μg Cl^-) *vs.* water, 1-cm cell; (b) blank *vs.* water, 1-cm cell.

Results

Absorption spectra. Absorption spectra are shown in Fig. 1. The colour developed within 5 min and was unchanged after 8 h.

Beer's law was obeyed to at least 2 μg of chloride per ml in the final solution, and the effective molar absorptivity for chloride was calculated as $2.60 \cdot 10^3$.

Type and concentration of acid. The effect of varying concentrations of nitric, perchloric, and sulphuric acids on the absorbance is shown in Fig. 2. Nitric and perchloric acids give similar sensitivities, while the use of sulphuric acid leads to a much lower sensitivity. Perchloric acid was chosen in preference to nitric acid for the lower blank absorbance, and because low and erratic readings were often obtained with nitric acid. The low results were traced to the presence of nitrogen peroxide in acid

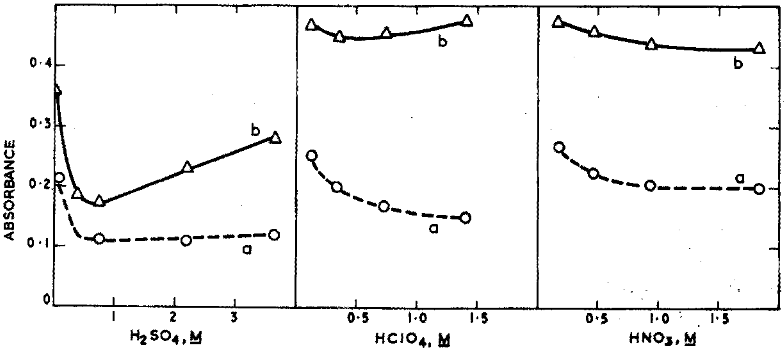

Fig. 2. Effect of acid concentration. 2 ml of mercury(II) thiocyanate reagent plus 2 ml of 0.375 *M* iron(III) nitrate per 25 ml. (a) Blank *vs.* water, 4-cm cell; (b) sample (40 μg Cl^-) *vs.* blank, 4-cm cell.

which had been exposed to strong light. Acid which had been stored in the dark and was colourless gave excellent results, but when the same acid was exposed to sunlight for a few hours and developed a yellow colour, the absorbance of the blank increased, and the chloride absorbance decreased markedly. Nitric acid is therefore suitable for use in the chloride method only if it is stored in a dark bottle, or away from light. For routine use it is safer to use perchloric acid.

Iron(III) nitrate was used in preference to the perchlorate because of the high chloride content of A.R. iron(III) perchlorate.

Effect of iron(III) nitrate and mercury(II) thiocyanate concentrations. The effect of iron(III) nitrate concentration on the sample and blank absorbances is shown in Fig. 3. At high iron concentrations the absorbance changes only slightly as the concentration of iron(III) nitrate increases.

Figure 4 shows that a constant absorbance is obtained when 1 ml or more of saturated mercury(II) thiocyanate solution is used.

Effect of ethanol concentration. Both the blank and sample absorbances increased slightly with increasing ethanol concentration. However, the net increase in absorbance was insufficient to justify adding more than the 2 ml of ethanol contained in the mercury(II) thiocyanate reagent. Acetone increased the blank and markedly decreased the sample absorbance.

Precision and limit of detection. The limit of detection for chloride by the recommended procedure was determined by preparing 11 blank solutions and measuring ten of these on the Cary 16 spectrophotometer against the remaining one. The minimum detectable difference between a mean sample and blank reading, $(i_s - i_b)$, was calculated from $(i_s - i_b) = 2\, S_b\sqrt{2}$ (95% confidence level) where S_b is the standard deviation of the blank. A value of 5 p.p.b. chloride was found for S_b, which gives a limit of detection of 15 p.p.b. chloride in the final solution. With the Hilger "Uvispek" spectrophotometer the limit of detection was 55 p.p.b.

At the 50 and 2,500 p.p.b. chloride levels, the relative standard deviations (7 measurements) were 12% and 0.14%, respectively, with the Cary 16 instrument.

Study of interferences. Bromide and iodide are known to interfere seriously with the determination of chloride by the mercury(II) thiocyanate method, but most

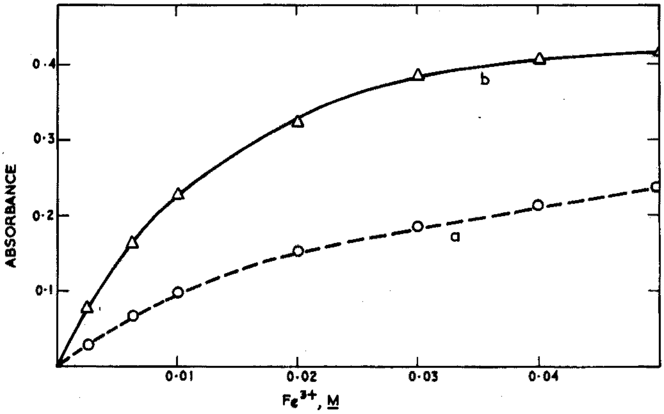

Fig. 3. Effect of iron concentration. 2 ml of mercury(II) thiocyanate reagent plus 2 ml of 5.25 M perchloric acid per 25 ml. (a) Blank *vs.* water, 4-cm cell; (b) sample (35 μg Cl^-) *vs.* blank, 4-cm cell.

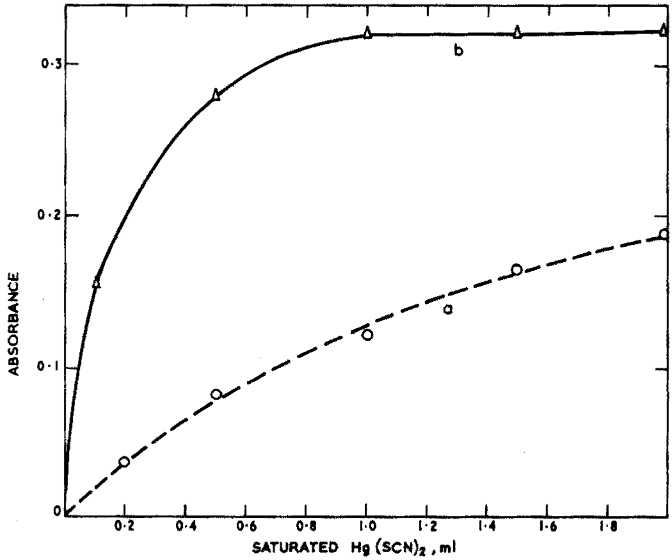

Fig. 4. Effect of mercury(II) thiocyanate concentration. 2 ml of iron(III) nitrate reagent per 25 ml. (a) Blank *vs.* water, 4-cm cell; (b) sample (30 μg Cl^-) *vs.* blank, 4-cm cell.

common metals have no effect[5,8]. The laboratory atmosphere should be free of halogen-containing gases and hydrogen sulphide.

Ammonia was tested up to a concentration of 85 p.p.m., and had no effect on the determination of 100 p.p.b. chloride. Hydrazine at the 1 p.p.m. level did not interfere, but 5 p.p.m. caused an error of +13%, and 20 p.p.m. an error of +45% in the determination of 100 p.p.b. chloride. Hydrogen peroxide gave no interference at 60 p.p.m., which was the highest peroxide concentration tested.

Discussion

The mercury(II) thiocyanate method for chloride was found to be simple, reliable, and able to tolerate reasonable changes in the reagent concentrations. With a modern precision spectrophotometer a limit of detection of 15 p.p.b. chloride can be attained.

Yamamoto *et al.*[12] recently published a modification of the mercury(II) thiocyanate method. In their procedure the liberated thiocyanate ions are extracted into nitrobenzene as an ion-association complex with tris(1,10-phenanthroline)-iron(II). The red colour of the organic phase is measured at 516 nm. The extracted iron(II)–1,10-phenanthroline–thiocyanate complex in nitrobenzene has a molar absorptivity similar to that of the aqueous iron(III) thiocyanate complex, but the blank in the extraction procedure is very much higher. The net absorbance (sample minus blank) is almost identical for both methods, so the more complicated and time-consuming extraction procedure leads to little practical gain in sensitivity.

Several other ion-association complex systems involving thiocyanate (*e.g.* methylene blue and rhodamine B) were investigated in an attempt to improve the sensitivity of the chloride method. However, any reagent which extracted thiocyanate well, also tended to dissociate the mercury(II) thiocyanate complex, producing high blanks. Aqueous reactions of chloride involving mercury(II) and thallium(III) complexes other than thiocyanate were also tested, but none led to a satisfactory analytical method. Consideration of the stability constants[13] of the various complexes involved in the aqueous mercury(II)–thiocyanate–iron(III) method shows that this remarkably useful reaction is only just thermodynamically possible. The search for a similar, but superior, spectrophotometric method for chloride is likely to be difficult.

Chemistry Division,
Australian Atomic Energy Commission Research Establishment,
Lucas Heights, N.S.W. 2232 (Australia)
T. M. Florence
Yvonne J. Farrar

1 A. L. Wilson, *Effl. Water Treat. J.*, 6 (1966) 125.
2 F. E. Clarke, *Anal. Chem.*, 22 (1950) 553.
3 J. L. Gerlach and R. C. Frazier, *Anal. Chem.*, 30 (1958) 1142.
4 W. Kemula, A. Hulanicki and A. Janowski, *Talanta*, 7 (1960) 65.
5 I. Iwasaki, S. Utsumi and T. Ozawa, *Bull. Chem. Soc. Japan*, 25 (1952) 226.
6 I. Iwasaki, S. Utsumi, K. Hageno and T. Ozawa, *Bull. Chem. Soc. Japan*, 29 (1956) 860.
7 I. Iwasaki, T. Tashiro and T. Ozawa, *Bunseki Kagaku*, 5 (1956) 275.
8 D. M. Zall, D. Fisher and M. Q. Garner, *Anal. Chem.*, 28 (1956) 1665.
9 R. D. Britt, *Anal. Chem.*, 34 (1962) 1728.
10 T. F. Demmitt, *U.S.A.E.C. rept. HW-74333*, 1962.
11 H. N. Elsheimer and R. L. Kochen, *Anal. Chem.*, 38 (1966) 145.
12 Y. Yamamoto, T. Kumamaru, A. Tatehata and N. Yamada, *Anal. Chim. Acta*, 50 (1970) 433.
13 L. G. Sillén and A. E. Martell (Eds.), *Stability Constants*, The Chemical Society, London, 1964.

(Received 1st December 1970)

ANNOUNCEMENTS

EUCHEM CONFERENCE "ORGANIC CHEMISTRY OF PHOSPHORUS AND OF THE HEAVIER ELEMENTS OF GROUP Va"

An EUCHEM Conference on "Organic Chemistry of Phosphorus and of the heavier Elements of Group Va" will take place from March 29 to April 3, 1971, at Schloss Elmau near Mittenwald, Germany. Professor L. Horner, Mainz, is Chairman of the Conference. The following topics will be dealt with:

1. Synthesis of organic phosphorus compounds with elementary phosphorus
2. Phosphorus and arsenic organic compounds as aids for organic synthesis
3. Stereochemistry of four-, five- and six-binding phosphorus and arsenic compounds
4. Stereochemical factors and kinetics of reactions with phosphorus
5. Aromatic systems with participation of phosphorus or arsenic
6. π- and σ-alternating effects in phosphorus compounds

The provisional program as well as preliminary registration forms may be obtained from Dr. W. Fritsche, Gesellschaft Deutscher Chemiker, D-6000 Frankfurt (M), Postfach 119075, Germany.

Analytica Chimica Acta
Elsevier Publishing Company, Amsterdam
Printed in The Netherlands

BOOK REVIEWS

William Rieman and Harold F. Walton, *Ion Exchange in Analytical Chemistry*, International Series of Monographs, Vol. 38, Pergamon Press, Oxford, 1970, xiii+ 295 pp., price 130 s.

There are not many books that have given me such pleasure to review as this one, and there are at least two reasons why this is so. Firstly, the use of ion exchange, especially in analytical chemistry, is an obvious and timely choice of subject for detailed coverage. Secondly, treatment of the subject, ranging from *General Properties of Ion-Exchange Resins*, in Chapter 2, to a *Study of Complex Ions* in the last of the book's 11 chapters, bears the hallmark of writers skilled in the art of making reading matter unequivocal and interesting. The chapters are dealt with in such a way as to make sequential reading unnecessary, but all are inter-related and highlight the characteristics and properties of ion exchangers as reagents in quantitative separation processes. A random selection of other chapter headings includes: *Ion-Exchange Kinetics, Nonchromatographic Applications, Technique of Ion-Exchange Chromatography, Applications of Ion-Exchange Chromatography*, and *Less Common Ion Exchangers.*

The book emphasises the plate-equilibrium theory of chromatography, and although this is less rigorous, theoretically, than the mass-transfer theory, it is, perhaps, more helpful to the analyst, *e.g.* in calculating the concentration and pH of an eluent to provide the best separation, based on data obtained from a minimum number of elutions.

Throughout the book, considerable space is devoted to the preparation, structure and properties of ion exchangers, pertinent not only to the well-known resins, but also to inorganic, cellulosic, and liquid ion exchangers. Although the analyst will not find within its pages detailed procedural instructions to meet specific requirements, the essential facts are there for sensible interpretation.

Summarising: a splendid book, comprehensive, up-to-date, well consolidated with about 800 supporting references, and well worth purchasing.

W. T. Elwell (Birmingham)

Methods of Biochemical Analysis, Edited by David Glick, Vol. 18, Interscience Publishers – J. Wiley & Sons, Inc., New York, 1970, vi + 421 pp., price £8.00.

Once again the Editor has arranged for the presentation of a series of well documented articles which will be of interest and practical assistance to workers in a number of fields in which biochemical techniques are applied.

P. Andrews writes on the estimation of molecular size and molecular weights of biological compounds by gel filtration using column or thin-layer techniques with cross-linked dextran, polyacrylamide and agarose gels. S. Hjerten deals concisely with the theory of and equipment for free zone electrophoresis and its application to low molecular weight compounds, proteins, nucleic acids, viruses and whole cells.

I. Tinoco, Jr. and C. R. Cantor contribute a detailed account of the application of optical rotatory dispersion and circular dichroism to the study of biopolymers. R. T. Jones deals with automated peptide chromatography and gives a wealth of practical information which will be of great value to the reader wishing to embark on the technique. The use of the Dansyl reaction in biochemical analysis is described by N. Seiler in a chapter which deals systematically with all aspects of the application of this increasingly widely-used technique. Finally H. H. Wotiz and S. J. Clark give an account of newer developments in the analysis of steroids by gas chromatography.

H. G. Bray (Birmingham)

Wolfgang Nebe, *Analytische Interferometrie*, Akademische Verlagsgesellschaft, Geest & Portig K.G., Leipzig, 1970, 170 pp., DM 35,—.

This very useful book appeared in the East-German series of monographs entitled *Technisch-Physikalische Monographien*. The author works in the Karl Zeiss factory, Jena, where some of the instruments dealt with in the book are manufactured. The book comprises 8 chapters. In the first the theoretical principles of analytical interferometry are described, starting from scratch, so that any chemist or student, who knows little about the technique, can familiarise himself with it easily. In the next chapter analytical interferometers are dealt with. The third chapter provides general guidance about setting up an interferometric laboratory, purification of chemicals, and in general, hints about experimentation. These basic chapters are followed by various applications. First, analyses of binary gas mixtures are discussed (Chapter 4), then, as an extension of the previous topic, the analyses of multicomponent gas mixtures are described (5). Under the title "Special gas analyses" (6), various important applications are dealt with, such as the analysis of explosive gases, poisonous gases and clinical gas analysis. The analysis of liquids is treated in a separate chapter (7). A very interesting part of the book is the last chapter (8), where the historical development of interferometry is described, naming the English scientist Thomas Young as the discoverer of the phenomenon of light interference. A very useful set of 15 tables appears as an appendix of the book, which is meant for the practical analyst. The comprehensive bibliographic section lists 337 references with their full titles (in German translation). Author and subject indices conclude the book, and there is a table of contents at the beginning.

The book is a definite gain for the literature of analytical chemistry. A shortened English version of the book will appear in the Wilson–Wilson: *Comprehensive Analytical Chemistry* series as an extended chapter in Volume IV.

G. Švehla (Belfast)

Anal. Chim. Acta, 54 (1971) 379–380

B. I. Ionin and B. A. Ershov, *NMR Spectroscopy in Organic Chemistry*, Plenum Press, New York, 1970, x+382 pp., price $ 25.—.

The present text, a translation of the Russian version published in 1967, is the first of a series of monographs on Physical Methods in Organic Chemistry. The book begins with three, quite readable chapters dealing with the theory of n.m.r., chemical shifts and spin–spin coupling. Another chapter is concerned with the analysis of complex spectra, which is followed by a description of the use of n.m.r. in elucidating the structure of organic compounds. Finally, the value of n.m.r. for studying intermediates, molecular complexes and solvates, in elucidating the kinetics and mechanisms of reactions, and in establishing the structure of isomers is demonstrated. An appendix contains the spectra of 55 compounds of various types.

The wide range of examples quoted in the book emphasizes the great value of n.m.r. to organic and structural chemistry, but no consideration of the use of the technique for the analysis of organic compounds is presented. Thus, it is of little direct value to the organic analyst, although the analytical potentialities of n.m.r. spectroscopy can readily be inferred.

A. Townshend (Birmingham)

Anal. Chim. Acta, 54 (1971) 380

CONTENTS

Short Communications

(continued on page 4 of cover)

Continued from inside page of cover

PRINTED IN THE NETHERLANDS